THE UNIVERSITY
of EDINBURGH

Development of circulating microRNA in drug-induced liver injury: studies in humans and zebrafish

Bastiaan Vliegenthart

Thesis submitted in fulfilment of the requirements for the degree

Doctor of Philosophy

2017

DECLARATION

I declare that the work contained within has been composed by me, and I have made a substantial contribution which is clearly indicated in each results chapter. No part of this thesis has been submitted for any other degree or professional qualification. In the event that parts of the work have been published before, this information has been added to each chapter.

Adriaan Daniël Bastiaan Vliegenthart

ABSTRACT

The aim of these studies was to identify circulating miRNAs that can be used as biomarkers in patients with paracetamol-induced liver injury. Whether the miRNAs discovered in humans could be back-translated to zebrafish with the aim of developing a liver toxicity model to replace rodent use was also investigated.

First, the miRNA signature of DILI induced by paracetamol was defined. Plasma miRNAs were quantified in paracetamol overdose patients. A signature of 16 miRNAs was discovered that best separated patients with liver injury from those without liver injury. This signature was tested in a second cohort and resulted in the detection of paracetamol-induced liver injury with high specificity and sensitivity. At first presentation to hospital miR-122-5p was the most sensitive single miRNA and superior to ALT activity in predicting liver injury.

In order to further qualify miR-122-5p, three detailed studies relevant to possible clinical scenarios were performed. The effect of acute alcohol ingestion (commonly co-ingested with paracetamol overdose) on circulating concentrations of miR-122-5p in healthy volunteers was investigated. Alcohol ingestion induced a small, non-clinically relevant, increase in miR-122-5p. The effect of chronic kidney disease (CKD) and haemodialysis (HD) on circulating miR-122-5p concentrations was explored because kidney dysfunction has been associated with a reduction in the concentration of circulating miRNAs. HD patients had lower concentrations of miR-122-5p compared to healthy volunteers and CKD patients. To facilitate miRNA measurement outwith hospitals, miR-122-5p was measured in a blood drop from a finger prick. miR-122-5p was readily measurable in finger prick samples and concentrations were significantly higher in the blood drop from DILI patients compared with healthy volunteers.

To complement miR-122-5p as a marker of toxicity, circulating paracetamol metabolites were measured in plasma samples from paracetamol overdose patients. A higher percentage of circulating metabolites formed by cytochrome P450 enzymes

were present in patients with liver injury and these metabolites were superior to both ALT and paracetamol concentration with regard to early patient stratification.

To reduce need for rodent studies, miRNAs were back-translated into zebrafish. In order to study circulating miR-122-5p in adult zebrafish, a bloodletting method by collecting blood retro-orbitally was developed. After studying different dosing regimens of paracetamol in adult and larvae zebrafish the model was determined to be too variable with regard to liver injury. A new drug, triptolide, originating from traditional Chinese medicine and responsible for DILI in China, was tested as an alternative model for drug-induced liver injury in zebrafish larvae. miRNA-122-5p decreased in zebrafish larvae after triptolide treatment and triptolide-induced liver injury could be tracked by fluorescent microscopy. Selective plane illumination microscopy was able to track the decrease in liver volume during triptolide exposure. In order to identify the toxic pathways involved in triptolide-induced liver injury, RNA-sequencing was performed. This identified KEGG pathways including ribosome, spliceosome and notch signalling as pathways affected by triptolide.

In summary, miRNAs can be used as highly sensitive biomarkers to detect acute liver injury in patients and zebrafish. Zebrafish may represent an alternative model species to study DILI, further work is needed.

LAY SUMMARY

Liver injury is a disease that can be caused by using drugs and can be life-threatening. A common cause of liver injury is paracetamol overdose. In this study, molecules called microRNAs were measured in the blood from patients after paracetamol overdose. It was discovered that a specific microRNA (miR-122) is released from the injured liver into the blood in massive amounts. Subsequently, miR-122 was measured in 3 common clinical scenarios. The first scenario was acute alcohol consumption that increased the concentration of miR-122 in the blood by a small amount. The second scenario was the effect of kidney injury, a common event during paracetamol overdose. It was found that patients on hemodialysis had a lower concentration of miR-122 before dialysis compared to healthy volunteers, chronic kidney disease patients and patients that previously had received a kidney transplant. To be able to measure miR-122 outside the hospital, miR-122 was measured in a blood drop from a finger prick. The concentration of miR-122 in the blood drops from patients was higher compared to healthy volunteers. To reduce the need for rodents, miR122 were measured in zebrafish. In adult zebrafish exposed to paracetamol, miR-122 was increased in the circulation. After studying different concentrations of paracetamol in adult and larvae zebrafish, the model was too variable.

A new molecule, triptolide, originating from traditional Chinese medicine and responsible for liver injury in China, was tested. In zebrafish larvae triptolide induced reproducible liver injury. miR-122 decreased in zebrafish larvae after triptolide treatment and triptolide-induced liver injury could be seen with microscopy. In order to find out how triptolide toxicity works, we studied gene expression and found that the expression of many genes was changed after triptolide treatment. In summary, miR-122 can be used as highly sensitive blood measures to detect acute liver injury in patients and fish. Zebrafish represent an alternative experimental model species to study liver injury.

ACKNOWLEDGEMENTS

I would like to thank my family, friends, supervisors and colleagues, who have supported me throughout my studies. I would specifically like to name:

- Struan Stark, also known as Starkey, for his hospitality and for showing me how to live like an 'Scotsman'
- Caroline, for all her love and support
- My Dutch friends Bart, Olaf and Thomas for visiting me in Edinburgh and supporting me
- The Dutch visiting students Laura Peeters, Carmelita de Potter and Cécile Berends, who have helped me with various projects
- Dr Carl Tucker and staff from the Zebrafish facility
- Dr Chunmin Wei for her excellent work, introducing triptolide and her world famous Chinese food
- Dr Charlotte Buckley for her help with the selective plane illumination microscopy
- Dr Jonathan Shaffer and Dr Eric Lader from Qiagen for performing the miRNA profiling and answering all technical questions about PCR
- Dr Matthew Bailey, Dr Andrea Caporali, and Professor David Webb, members of my PhD committee, for their guidance throughout my PhD
- And finally, Dr James Dear, my primary supervisor, for his excellent guidance, optimism, patience, motivational talks and continuous offering of opportunities.

This work would not have been possible without the generous funding of the NC3Rs.

TABLE OF CONTENTS

LIST OF TABLES

LIST OF FIGURES

LIST OF ABBREVIATIONS

ABC	ATP binding cassette
ADRs	Adverse drug reactions
Ago2	Argonaute 2
AHR2	Aryl hydrocarbon receptor 2
ALDH3A1	Aldehyde dehydrogenase 3A1
ALI	Acute liver injury
ALT	Alanine amino transferase
APAP	Acetaminophen (Paracetamol)
Paracetamol-CYS	Paracetamol-cysteine
APAP-no TOX	Paracetamol overdose without toxicity
Paracetamol-Sul	Paracetamol-sulfate
APAP-TOX	Paracetamol overdose with toxicity
BD	Bile duct
CA	Canaliculi
CKD	Chronic kidney disease
Ct	Cycle threshold
CV	Central vein
CYP	Cytochrome P450
DAMP	Damage-associated molecular pattern
DILI	Drug induced liver injury
dpf	Days post fertilisation
DsRed	*Discosoma* sp. Red fluorescent protein
ECV	Extra cellular vesicle
EMA	European Medicines Agency
ESRD	End-stage renal disease
fabp10a	*Fatty acid binding protein 10a*
FDA	US Food and Drug Administration
GFP	Green fluorescent protein
GLDH	Glutamate dehydrogenase

GSNOR	*S*-nitrosoglutathione reductase
HA	Hepatic artery
HD	Haemodialysis
HLA	Human leukocyte antigen
HMGB1	High-mobility-group box-1
HP	Hepatocyte plate
hpf	Hours post fertilisation
HPLC-ECD	High-performance liquid chromatography with electrochemical detection
HT	Hepatocyte tubule
IMI	Innovative Medicines Initiative
INR	International normalised ratio
K18	Keratin 18
KCC	King's College Criteria
KIM-1	Kidney Injury Molecule-1
LI	Lateral incision
MAPP	Markers and Paracetamol Poisoning study
MHRA	Medicines & Healthcare products Regulatory Agency
miRNAs	MicroRNAs
mRNA	Messenger RNA
mtDNA	Mitochondrial DNA
NAC	Acetylcysteine
NAPQI	*N*-acetyl-*p*-benzoquinone imine
NOS	Nitric oxide synthase
NOS2b	Nitric oxide synthase 2b
NPV	Negative predictive value
NQO1	NAD(P)H dehydrogenase quinone 1
PACT	protein activator of PKR
PCR	Polymerase chain reaction
PKR	Protein kinase RNA-activated
POC	Point-of-care

PPV	Positive predictive value
Pre-miRNA	Precursor microRNA
pri-miRNA	Primary microRNA transcript
PSTC	Predictive Safety Testing Consortium
PT	Portal tract
PV	Portal vein
RAGE	Receptor for advanced glycation end products
RISC	RNA-induced silencing complex
RNA	Ribonucleic acid
RO	Retro orbital
ROC-AUC	Area under the receiver operator curve
SAFE-T	Safer And Faster Evidence-based Translation
SNAP	Scottish and Newcastle Antiemetic pretreatment for Paracetamol Poisoning study
SPIM	Selective plane illumination microscopy
STA2	Glutathione *S*-transferase α1
TBP	Target biomarker profile
TLRs	Toll-like receptors
TP	Triptolide
TRBP	The double-stranded RNA binding protein
UGT1A2	UDP glucuronosyltransferase 1A2
VAST	Vertebrate Automated Screening Technology

PUBLICATIONS

Papers accepted for publication

Vliegenthart AD, Berends C, de Potter CM, Kersaudy-Kerhoas M, Dear JW. Capillary miR-122 represents a sensitive and specific biomarker for human drug-induced liver injury. British Journal of Clinical Pharmacology. 2017;3.

Vliegenthart AD, Shaffer JM, Clarke JI, Peeters LE, Caporali A, Bateman DN, Wood DM, Dargan PI, Craig DG, Moore JK, Thompson AI, Henderson NC, Webb DJ, Sharkey J, Antoine DJ, Park BK, Bailey MA, Lader E, Simpson KJ, Dear JW. Comprehensive microRNA profiling in acetaminophen toxicity identifies novel circulating biomarkers for human liver and kidney injury. Scientific Reports. 2015;5:15501.

McCrae JC, Sharkey N, Webb DJ, Vliegenthart AD, Dear JW. Ethanol consumption produces a small increase in circulating miR-122 in healthy individuals. The Journal of Clinical Toxicology. 2016;54:53-55.

Rivoli L*, Vliegenthart AD*, de Potter CM, van Bragt JJ, Tzoumas N, Gallacher P, Farrah TE, Dhaun N, Dear JW. The effect of renal dysfunction and haemodialysis on circulating liver specific miR-122. British Journal of Clinical Pharmacology. 2017 Mar;83(3):584-592 *co-first authors.

Vliegenthart ADB, Kimmitt RA, Seymour JH, Homer NZ, Eddleston M, Gray A, Webb DJ, Lewis SC, Bateman DN, Dear JW. Circulating Acetaminophen Metabolites Accurately Predict Hepatotoxicity And Represent New Clinical Toxicokinetic Biomarkers. Clinical Pharmacology and Therapeutics. 2017 Apr;101(4):531-540.

Vliegenthart AD, Starkey Lewis P, Tucker CS, Del Pozo J, Rider S, Antoine DJ, Dubost V, Westphal M, Moulin P, Bailey MA, Moggs JG, Goldring CE, Park BK, Dear DN. Retro-orbital blood acquisition facilitates circulating microRNA measurement in zebrafish with paracetamol hepatotoxicity. Zebrafish 2014;11:219-226.

Vliegenthart AD, Antoine DJ, Dear JW. Target biomarker profile for the clinical management of paracetamol overdose. British Journal of Clinical Pharmacology. 2015;80:351-362.

Liga A, Vliegenthart AD, Oosthuyzen W, Dear JW, Kersaudy-Kerhoas M. Exosome isolation: a microfluidic road-map. Lab on a Chip. 2015;15:2388-2394.

Bateman DN, Dear JW, Thanacoody HK, Thomas SH, Eddleston M, Sandilands EA, Coyle J, Cooper JG, Rodriguez A, Butcher I, Lewis SC, Vliegenthart AD, Veiraiah A, Webb DJ, Gray A. Reduction of adverse effects from intravenous acetylcysteine treatment for paracetamol poisoning: a randomised controlled trial. Lancet 2014;383:697-704.

Vliegenthart AD, Tucker CS, Del Pozo J, Dear JW. Zebrafish as model organisms for studying drug-induced liver injury. British Journal of Clinical Pharmacology. 2014;78:1217-1227.

Chapter 1: Introduction

1.1 Acute liver failure

Fulminant hepatic failure was first described in 1970 as “a severe liver injury, potentially reversible in nature and with onset of hepatic encephalopathy within 8 weeks of the first symptoms in the absence of pre-existing liver disease” (1). Today, the main elements of this description remain relevant, but the classifications have changed. Modern classification systems for acute liver failure (ALF) recognize distinct disease phenotypes (2). The classification developed by O’Grady and colleagues classifies ALF into hyperacute, acute or subacute. The determinants for these classifications are time from jaundice to encephalopathy, severity of coagulopathy, severity of jaundice and the degree of intracranial hypertension (3). The classification developed by Bernuau and colleagues divides the disorder into fulminant and subfulminant classes, depending on the jaundice to encephalopathy interval (4).

These classifications are clinically useful and can help to indicate the probable cause and prognosis of the disease. In the Western world, the incidence of ALF is less than ten cases per million people every year (5-7). Historically, the mortality has been over 80% (8). However, in the recent years, the possibility of liver transplantation and improvement in multidisciplinary intensive care support has reduced the mortality rate. Currently, the short-term survival post transplantation is more than 65% (9). Early identification of patients that will not survive without transplantation is of great importance. Various prognostic evaluation systems, developed from analyses of historical patient cohorts, have been introduced. Of these evaluation systems, the King’s College Criteria (KCC), using age, cause, encephalopathy, bilirubin level and coagulopathy as risk factors, is most commonly used (10). The results from a meta-analysis from 18 studies with data from 1105 patients indicates that the KCC has a sensitivity of 68 (57-79)%, specificity 81 (72-90)% which indicates that there is a lot of room for improvement (11).

The two main causes of ALF are viral infections and drug-induced liver injury (DILI) (12, 13). In the developing world, the main cause of ALF are hepatitis A, B and E, whereas DILI is the most common cause of ALF in the US and the UK (13).

1.2 Drug-induced liver injury

DILI is a frequent cause of liver injury that presents with a broad spectrum of clinical manifestations that can vary from acute hepatitis, cholestasis, nodular regenerative hyperplasia and sinusoidal obstruction syndromes with each pathology being able to occur in acute or chronic patterns (14). Many drugs that cause DILI can be categorised as either intrinsic liver toxins, with dose-dependent and predictable adverse effects, or idiosyncratic (15).

Idiosyncratic reactions are non-predictable and occur at therapeutic doses in only one per 1000 to 100 000 patients who take the medication (16). The latency of idiosyncratic DILI varies from 5 days to 90 days after the start of drug therapy and the severity can vary from mild asymptomatic injury to ALF. Idiosyncratic liver toxicity is usually identified in late stages of drug development or after a new drug has already been released to the marketplace, making it the most frequent reason for the withdrawal from the market of an approved drug (15, 17). Some drugs cause idiosyncratic DILI more often than other drugs. Notorious for causing DILI are some antibiotics including amoxicillin, isoniazid, trimetroprim, fluoroquinolones, macrolides and minocycline. Other drugs that are relatively common causes of idiosyncratic DILI are non-steroid anti-inflammatory agents, valproate, methotrexate and anabolic steroids (18). Partly because of its rarity, the pathogenesis of idiosyncratic DILI is incompletely understood which makes it hard to predict in earlier drug development stages (19).

The most widely used drug causing intrinsic DILI is Paracetamol (Acetaminophen - APAP). Paracetamol is used by millions of people worldwide as a safe analgesic drug at therapeutic doses. In overdose, it is well known to be toxic to the liver. Indeed, in the Western world, paracetamol is the commonest cause of acute liver injury (ALI)

with being responsible for 57% of ALF cases in the UK (20) and close to 50% in the US (9, 21). Paracetamol overdose is a very common reason for hospital attendance (around 100,000 UK patients each year) (22). In terms of UK hospital admission, the number of patients per year (around 50,000) is comparable to other 'giants' of emergency medicine such as heart failure and hip fracture (23).

To improve patient care and reduce pressure on already stretched health care providers, new biomarkers are needed that identify or exclude liver toxicity soon after the drug is ingested. This introduction highlights the current state of paracetamol poisoning management and how novel biomarkers could improve patient care and save healthcare providers money.

1.3 Mechanism of paracetamol-induced acute liver injury

At therapeutic doses, the major route of paracetamol metabolism is through conjugation. Cellular injury is due to the reactive metabolite *N*-acetyl-*p*-benzoquinone imine (NAPQI) that is produced by the cytochrome P450 enzymes CYP2E1, CYP1A2 and CYP3A4 (24-26). At therapeutic paracetamol doses, only low concentrations of NAPQI are formed and this metabolite is efficiently detoxified by conjugation with glutathione. At toxic doses, the paracetamol conjugation reaction becomes saturated and more paracetamol becomes oxidised by cytochrome P450 into NAPQI. The cellular stores of glutathione become exhausted, which results in NAPQI covalently binding to sulfhydryl (SH-) groups in structural proteins, forming protein adducts leading to oxidative stress, mitochondrial injury, hepatocyte cell death by either apoptosis (minor pathway) or necrosis (major pathway), multi-organ failure and potentially patient death **(Figure 1)** (27). Antidote treatment with acetylcysteine (NAC) restores cellular glutathione concentrations. When administered soon after drug overdose (within about 8 hours), NAC is highly effective in preventing liver injury (28, 29). However, when NAC treatment is delayed, its efficacy is substantially reduced (28).

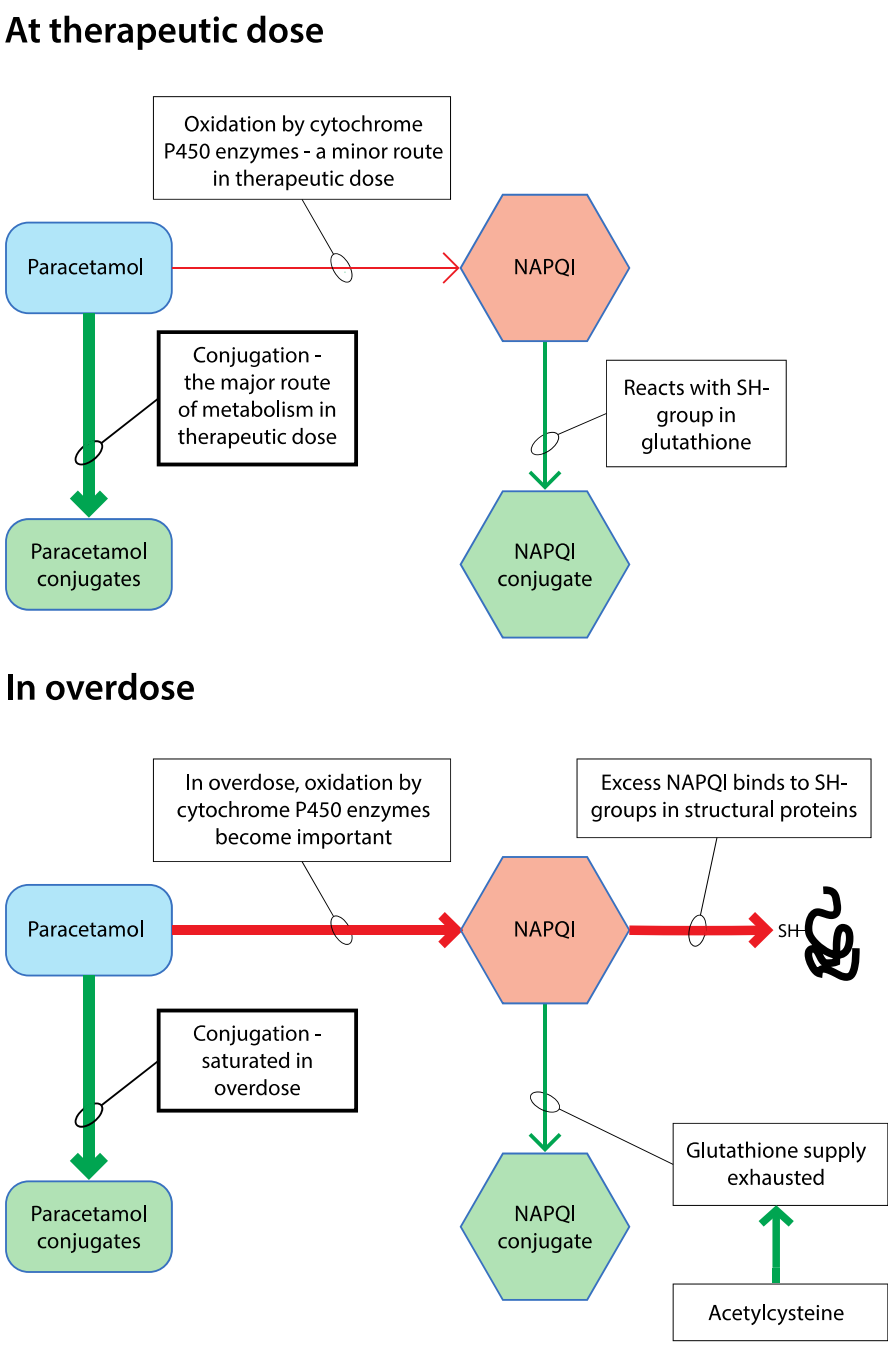

Figure 1. Paracetamol metabolism. At therapeutic doses conjugation is the major route for paracetamol metabolism. Oxidation of paracetamol by cytochrome P450 is a minor route at therapeutic doses of paracetamol, forming N-acetyl-p-benzoquinone imine (NAPQI) that quickly reacts with glutathione. When an overdose of paracetamol is taken, conjugation becomes saturated and more NAPQI is formed by oxidation. When the glutathione supply is exhausted, NAPQI binds to sulfhydryl (SH-) groups in structural proteins, resulting in cell injury.

1.4 Use of ALT to assess risk of hepatocyte injury after paracetamol overdose

Serum alanine amino transferase (ALT) activity is the current, widely used, biomarker for hepatocyte injury after paracetamol overdose (and in many other settings). Although ALT has never been formally qualified against liver histology as a biomarker for drug-induced liver injury in humans, its utility has been qualified by decades of clinical experience (30). However, the majority of patients present to the emergency department soon after overdose with only around 10% presenting later than 12 hours post drug ingestion (31). To confidently exclude the development of liver injury, patients require an ALT measurement at least 24 hours after the overdose was ingested (32). This limits patient stratification in emergency care settings and potentially increases length of hospital stay. Apart from these time/kinetic issues, there are other important limitations of using ALT as a biomarker of liver injury. Changes in ALT activity do not only occur in paracetamol-induced ALI, but with a wide range of acute and chronic liver pathologies such as fatty liver disease, viral hepatitis and liver cancer which decreases the confidence in its utility for causality assessment of paracetamol induced liver injury (33). Increases in serum ALT activity can also be a result of myocardial damage or extreme exercise (34), which may generate false-positive results. Because paracetamol-induced ALI cannot be confidently confirmed or excluded by using serum ALT activity as a biomarker at the hospital 'front-door', the decision to treat with NAC following an overdose is primarily based on the blood paracetamol concentration (35). To stratify patients as being 'at-risk' for hepatotoxicity after a single overdose (total ingestion of paracetamol taking less than around 1-2 hours) a nomogram is used that plots blood paracetamol concentration against time after overdose. This nomogram can only be confidently applied 4 hours after overdose ingestion, when absorption is believed to be complete (36). The utilisation of the blood paracetamol nomogram after overdose depends on the correct reporting of the time of overdose, small errors in timing can result in an incorrect treatment (27). When the paracetamol overdose is ingested over a longer time period (staggered overdose) or if the patient was exposed to a modified release or intravenous formulation (37) the nomogram cannot be used and the treatment

decision is based on the reported dose of paracetamol and the serum ALT activity. There is an unmet clinical need for new biomarkers that can guide treatment to patients at high-risk of paracetamol-induced ALI and identify patients with low-risk of liver injury that may require shorter, lower doses of NAC or even no treatment at all. To decrease the risk of developing ALI, the MHRA lowered the utility threshold of NAC by using a single '100 mg l^{-1}' treatment line, treating all staggered/uncertain ingestions, ceasing risk assessment and increasing the duration of the initial NAC infusion from 15 to 60 minutes (38). Recent health economic calculations have estimated that this change resulted in an increase of around £8M in the annual spend by UK healthcare providers (22), which further strengthens the case for new biomarkers that improve stratification of patients with paracetamol overdose.

1.5 Target Biomarker Profile

In order to identify new biomarkers that could add real value to the management of paracetamol poisoning *desirable* and *acceptable* properties – the target biomarker profile (TBP - **table 1)** are proposed.

Table 1. Desired and acceptable biomarker attributes.

Attribute	**Desired**	**Acceptable**
Specific for paracetamol overdose	Exclusively elevated by paracetamol-induced injury	Liver injury
Sensitivity for ruling out injury	ROC-AUC 1	AUC ≥ 0.90
Rapidly assayed	At point of care	<60 minutes turnaround time
Feasibility of assay	Feasible in settings where resources are sparse (developing countries)	Feasible in standard clinical labs (developed countries)
Invasiveness / sample preparation time	Whole blood	Plasma/serum
Conserved (translational) across in vitro models, in vivo models and humans	Fully conserved between *in vitro* models, *in vivo* models and humans	Conserved between rodent models and humans
Time after overdose at which it is able to predict the onset of liver injury	4h	8h
Signal to noise	Single measure required to differentiate between healthy reference value and disease	Requires measurement at two time points
Quantitative relationship with disease severity	Quantitative	Qualitative
Distinguish benign and clinical relevant increase in ALT	Predicts liver failure	Predicts ALT rise
Mediator of liver injury	Has existing therapeutic intervention	Potential drug target

This approach is widely used in biomarker development to set criteria that will be used to define future success. For further background the US Food and Drug Administration have produced guidance (39). The suggested biomarker properties specifically relate to the clinical management of paracetamol overdose, what is desirable or acceptable in other settings may be different. For all biomarkers their diagnostic performance may change when they are measured on different validated assay platforms (for example, a new point-of-care platform in contrast with the laboratory gold standard), so the TBP could need to be re-assessed when new clinical assays become available and rigorously validated. It is also important to note that defined *desirable* and *acceptable* properties can assist with the development of prospective qualification studies in man to define the context of use for a putative biomarker (40).

A biomarker specific for paracetamol toxicity is *desired,* as this test could not be misinterpreted due to a signal produced by other causes of liver injury. A biomarker diagnostic for paracetamol toxicity would be valuable when the aetiology of liver injury cannot be identified, reported to be the case in 17% of patients with ALI (9). However, a marker that reports liver injury due to any cause is *acceptable,* since in most cases it is known that the patient has ingested an overdose (proven by blood paracetamol measurement).

Ideally, a new biomarker would differentiate disease from non-disease with 100% sensitivity and specificity (area under the receiver operator curve (ROC-AUC) of 1), but an *acceptable* performance as a ROC-AUC of 0.90 is proposed. This is a comparable accuracy to troponin T assays when they were first introduced into clinical medicine for acute myocardial infarction stratification (41). In real clinical practice the biomarker's context of use, derived from prognostic qualification studies in man, may prioritise sensitivity or specificity and the *acceptable* criterion is a starting point for development.

If the biomarker could be assayed rapidly at point-of-care it could be used outside of standard hospital laboratories, for example, in an ambulance, phase 1 clinical trial unit or in the developing world. An *acceptable* level of performance would be a

turnaround time of 60 minutes in a standard hospital laboratory, as per the guidance of the clinical biochemists/chemical pathologists and clinical biochemistry services regarding the measurement of commonly requested routine clinical biochemistry and haematology tests in emergency departments (42). Ideally, the assay would be performed on a drop of whole blood obtained from the fingertip, resulting in a minimally invasive test with short sample preparation time. *Acceptable* would be measuring the biomarker in plasma or serum. The biomarker assay is *desired* to be measurable in settings where resources are sparse, such as in developing countries. But *acceptable* would be the ability to perform the assay in standard hospital labs. Recently, data suggest that ALT can be measured using a robust point-of-care, finger stick test with a rapid turn around time (43). Despite the drawbacks of ALT, this technology might provide the clinician with a signal that triggers an improved sensitive and specific liver safety assessment. Furthermore, advances in these technologies also point to a pathway of development and validation of such methodologies to assess potential biomarkers with improved characteristics at the point-of-care.

If the biomarker can report liver injury as early as 4 hours after paracetamol ingestion, it would complement the paracetamol blood concentration nomogram for making treatment decisions in patients presenting early after overdose. *Acceptable* would be the ability to predict liver injury at 8 hours after paracetamol ingestion, the time point after which NAC treatment loses efficacy (28, 44).

A biomarker that is fully translational between *in vitro* models, animals and humans would aid the detection of hepatotoxic compounds in drug development. However, a biomarker being translational between rodents and humans would be *acceptable.*

A biomarker with a high signal-to-noise ratio that only requires a single measurement is *desirable.* Serial measurement would be *acceptable,* as is the case with troponin for acute myocardial infarction (45).

Ideally, the biomarker could distinguish between a benign ALT rise, the development of serious liver injury and imminent liver failure with higher sensitivity and specificity than “Hy’s Law”, the most commonly method for indicating the risk of a drug to

induce sever liver injury (46). Hy's Law has been developed by clinical observations of Dr. Hyman Zimmerman(47) and later specified by Dr. Robert Temple of the U.S. Food and Drug Administration based on ALT or AST and total bilirubin (48).Acceptable would be the prediction of an ALT rise. The ability of a biomarker to have a quantitative relationship with the severity of the paracetamol toxicity would allow for different treatment strategies in patients with different severities of liver injury. Acceptable would be a biomarker that qualitatively discriminates injury from non-injury.

Should a biomarker also be a mediator of liver injury then the marker could represent a companion diagnostic that identifies patients for a novel therapeutic. *Desirable* criterion would be a marker that has a drug already approved for human use, *acceptable* would be a marker that mediates the disease process and has potential therapeutics in development.

1.6 New biomarker candidates for paracetamol-induced liver injury and their performance compared with the target biomarker profile

Currently there is huge investment into the development and qualification of novel biomarkers to improve the prediction and monitoring of drug-induced liver injury in preclinical species and in man (**Figure 2**). A number of public-private consortia exist such as the IMI (Innovative Medicine Initiative) funded SAFE-T (Safer And Faster Evidence-based Translation) project and the Critical Path institute supported PSTC (Predictive Safety Testing Consortium) with these objectives as specific goals. Although the efforts and achievements of these consortia have been previously reported, here the case for the TBP to improve treatment and to aid the understanding of the mechanistic basis of paracetamol overdose is presented. In the next section microRNAs, a selection of protein markers (Keratin-18, High-mobility group box-1 and glutamate dehydrogenase), mitochondrial DNA fragments, Kidney Injury Molecule-1 and paracetamol protein adducts will be introduced and its key properties regarding the TBP will be listed.

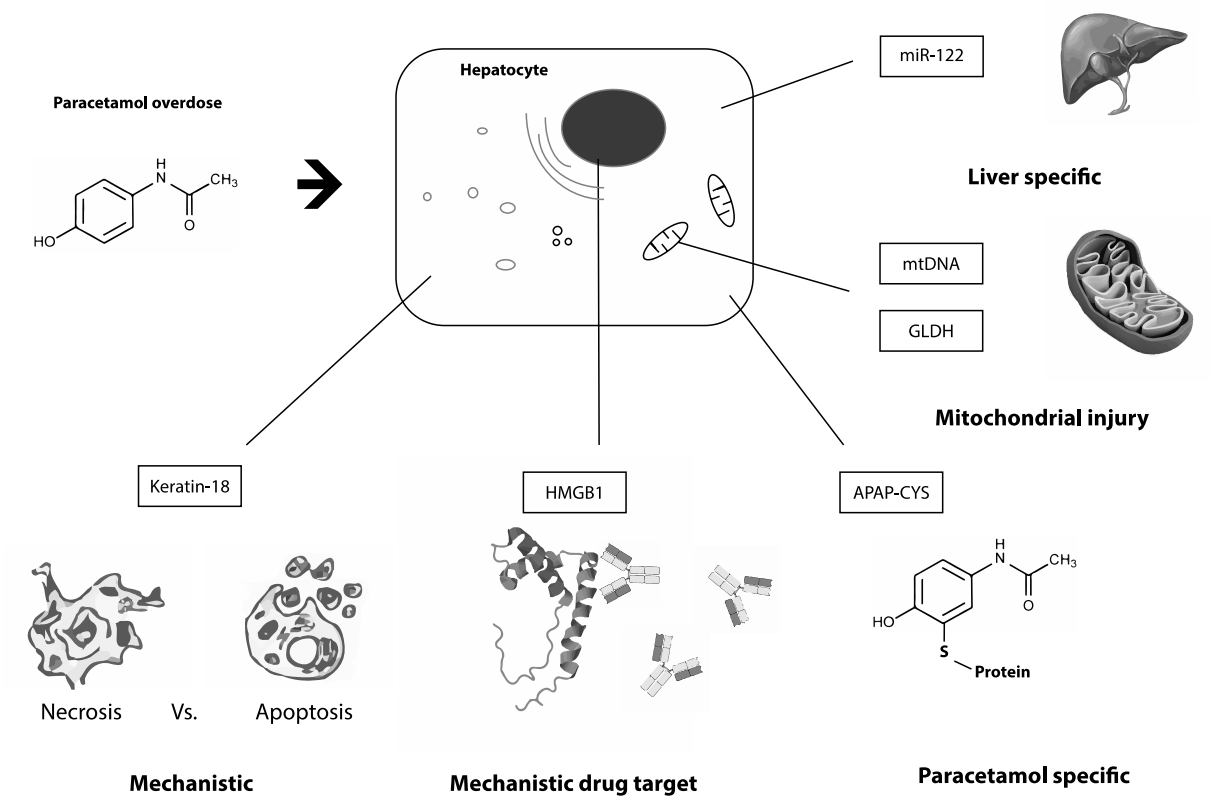

.

Figure 2. Key properties of novel biomarkers for paracetamol-induced liver injury. From Vliegenthart et al, 2015 (49).

1.6.1 microRNAs

Key properties:

- Specific for liver injury
- Fully conserved (translational) across in vitro models, *in vivo* models and humans
- Early marker for ALI with a ROC-AUC of >.90
- Predicts ALT rise

MicroRNAs (miRNAs) are small (~22 nucleotides long) non-protein coding RNA species involved in post-transcriptional gene product regulation found in viruses, plants and mammals. miRNAs affect many cellular pathways including development, differentiation, metabolism, haemostasis and apoptosis (50). Besides playing an important role in health, many miRNAs have been implicated in human diseases (50). The most recent release of mirBase annotated 2588 mature human miRNA species (51).

The genomic sequences for miRNAs are distributed throughout the genome including exonic and intronic regions, as well as intergenic regions (52). The first step in miRNA biogenesis is the transcription by RNA polymerase II or RNA polymerase III resulting in a primary transcript known as pri-miRNA (53, 54). A pri-miRNA contains a ~80 nucleotide stem-loop, a terminal loop and a single stranded sequence of a few hundred bases which is capped at the 5' end and polyadenylated at the 3' end (55).

The pri-miRNA is next processed by the microprocessor complex existing out of Drosha (an RNase III enzyme) and (DiGeorge critical region 8) DGCR8. Drosha contains two RNAse domains that cleave the 5'and 3' arms of the pri-miRNA hairpin (56). DGCR8 determines the precise cleavage site by stably interacting with the pri-miRNA molecule (57). The resulting pre-miRNA is transported out of the cell nucleus into the cytoplasm by Exportin-5-Ran-GTP (58).

In the cytoplasm, the RNA-induced silencing complex (RISC) loading complex, including the RNAse III Dicer, the double-stranded RNA-binding protein (TRBP),

protein activator of PKR (PACT) and Argonaute-2 (Ago2), cleaves the pre-miRNA into its mature length (59-61). After cleavage, the mature miRNA, attached to Ago2 forms the active RISC **(Figure 3)**.

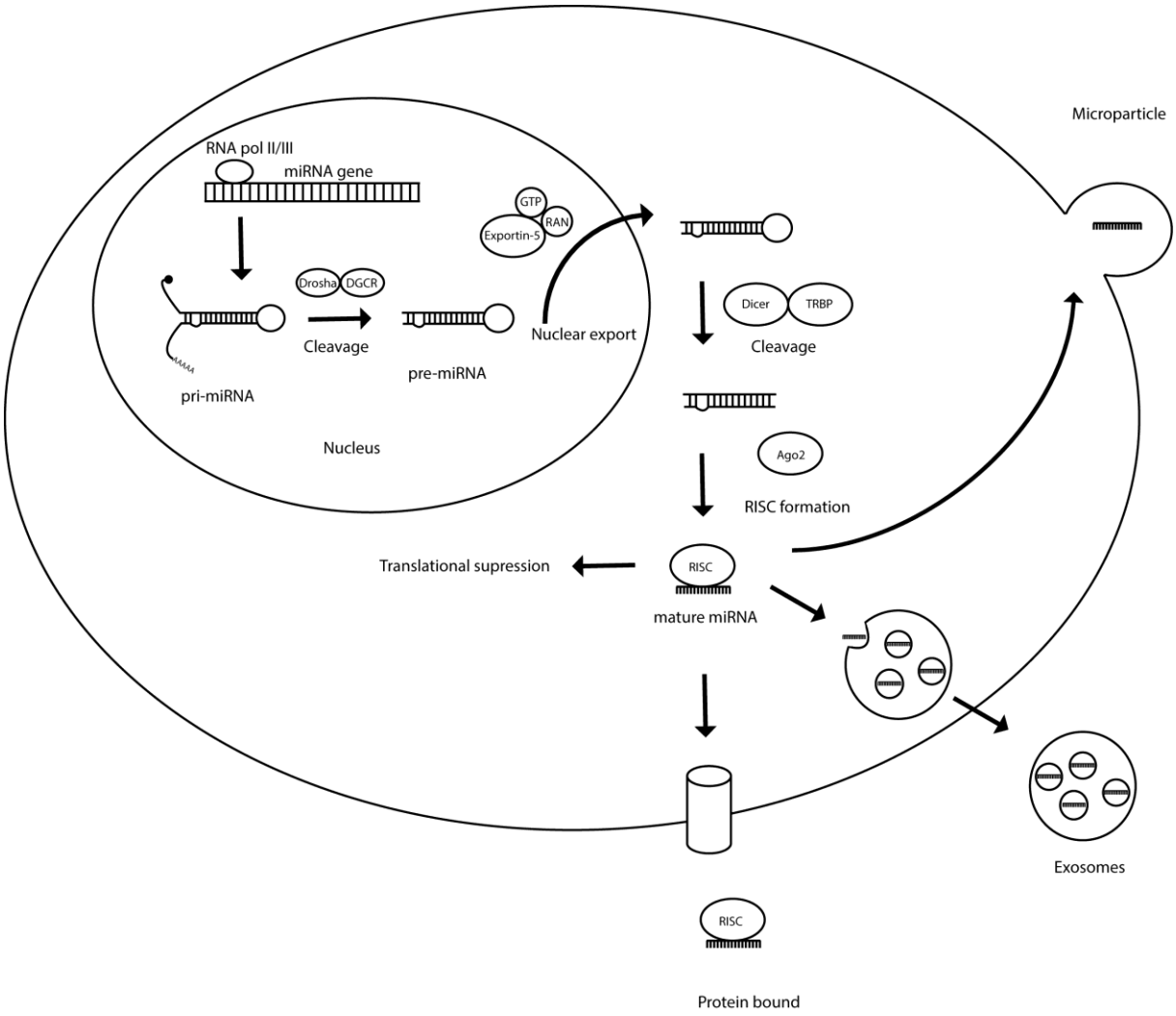

Figure 3. The miRNA biosynthesis pathway and modes of export out of the cell.

Complementary base-pairing of the miRNA guides RISC to its target mRNA. In plants, the miRNAs usually have perfect or near perfect base paring with its target mRNA which promotes cleavage by RISC and subsequent degradation of the mRNA (62). In mammals, inhibition of protein translation occurs by partial complementary pairing between miRNAs and mRNAs. In this case miRNAs are complementary for 6-8 nucleotides at the 5'end of the miRNA which is called the seed sequence (63). Many

alternative detours and crossroads have been found in the biogenesis of miRNAs which are comprehensively described by Winter and colleagues (64).

Although miRNAs fulfil their biological functions inside cells, miRNAs are transported out of cells where they are very stable due to protection from RNAses by being encapsulated in exosomes, microparticles (65) and protein complexes **(Figure 3)** (66). Although most miRNAs are expressed in many tissues, certain miRNAs appear to be highly organ specific (67). Liver tissue expresses a number of distinct miRNAs, especially miR-122-5p, the most abundant hepatic miRNA that has very low to no expression in other healthy tissues, which makes this marker highly liver specific (67). miR-122-5p is a multifunctional RNA species that modulates multiple pathways involved in stress response (68), fatty-acid metabolism (69), cholesterol synthesis (70) and hepatocellular carcinoma (71).

The potential of circulating miRNAs to serve as biomarkers for ALI was first reported in mice treated with a toxic dose of paracetamol (72). miR-122-5p was the miRNA species that had the largest fold change between control and paracetamol treated mice (72). Subsequently circulating miR-122-5p has been reported as a marker for ALI in rats (73), dogs (74), zebrafish (75) and pigs (76).

In patients with established ALI circulating miR-122-5p is around 100 fold higher compared to healthy controls and overdose patients without ALI (77). Furthermore, miR-122-5p has also been shown to provide utility at reporting liver injury in paediatric populations of paracetamol overdose (78). ***At first presentation to hospital,*** in a UK cohort of 129 patients from Edinburgh and Newcastle Upon-Tyne, miR-122-5p was measured at a median of 8 hours post-overdose in patients requiring subsequent NAC therapy ('Edinburgh and Newcastle study') (79). In this first sample miR-122-5p correlated significantly with peak hospital stay ALT activity and INR. miR-122-5p was significantly higher in those patients that developed subsequent ALI. ROC analysis revealed that miR-122-5p had an AUC value (sensitivity at 90% specificity, 95% CI) of 0.93 (0.83, 0.86-1.0, $P < 0.0001$) suggesting that miR-122-5p could accurately separate patients with and without ALI at an early time when ALT activity was still normal.

1.6.2 Protein markers

1.6.2.1 Keratin-18

Key properties:

- Conserved between rodent models and humans.
- Mechanism-based (apoptosis vs necrosis)
- Early marker for ALI with a ROC-AUC of >.90
- Predicts ALT rise
- Prognostic marker

Keratins are intermediate filament proteins, expressed by epithelial cells, that are responsible for cell structure, differentiation, mitosis and apoptosis (80, 81). Keratin 18 (K18) is abundantly expressed in the liver and other digestive epithelial cells (82). During apoptosis, phosphorylation and cleavage of K18 results in cellular rearrangement. Full-length K18 is passively released from necrotic cells whereas cleaved K18 fragments are released from apoptotic cells once membrane integrity is lost (83). Circulating cleaved K18 (apoptosis) and full-length K18 (necrosis) can be measured using ELISA-based assays to report apoptosis and necrosis (84, 85).

Cleaved K18 and full-length K18 have been reported to be circulating mechanistic biomarkers for apoptosis and necrosis in mouse models of paracetamol-induced ALI (86, 87). Full-length and cleaved K18 were measured in a mixed UK and US cohort of paracetamol-induced ALI patients - they were increased in the circulation of paracetamol-induced ALI patients compared to paracetamol overdose patients without ALI and healthy controls.

In patients with established ALI full-length and cleaved K18 were significantly higher in patients that subsequently reached the King's College Criteria (KCC) for liver transplant (10). Further analysis revealed that the percentage of total circulating K18 derived from cleaved K18 (from apoptotic cells) was relatively lower in patients that

reached the KCC compared to those that did not (87). ROC analysis confirmed that full-length K18 had a higher AUC than ALT for predicting patients that met KCC and for the outcome of liver transplant/death (87). Another research group has recently confirmed the ability of circulating cleaved and full-length K18 to report liver injury after paracetamol overdose (88). In this study both cleaved and full-length K18 correlated with poor outcome (death or liver transplant).

At first presentation to hospital - In the Edinburgh and Newcastle first presentation study - cleaved and full-length K18, measured in the first sample, correlated with peak ALT activity and INR during hospital stay. ROC analysis revealed that full-length K18 had an AUC value (sensitivity at 90% specificity, 95% CI) of 0.94 (0.9, 0.87-1.0, $P < 0.0001$) suggesting that this form of K18 could accurately separate patients with and without ALI at an early time when ALT activity was still normal. The performance of the cleaved form of K18 was less accurate with regard to reporting ALI at first presentation to hospital (AUC: 0.77; sensitivity at 90% specificity 0.21) (79). This is consistent with necrosis being more prominent than apoptosis in the pathophysiology of paracetamol-induced acute liver injury (89).

1.6.2.2 HMGB1

Key properties:

- Prognostic marker
- Mechanism-based (DAMP – inflammatory mediator)
- Early marker for ALI with a ROC-AUC of >.90
- Predicts ALT rise
- Conserved between rodent models and humans
- Potential drug target

High-mobility group box-1 (HMGB1) is an evolutionary conserved chromatin-binding protein expressed in the nucleus of virtually all cells. HMGB1 is passively released into the extracellular space by cells that are undergoing necrosis and plays a key role in

alerting the immune system to dying cells and thus works as a damage-associated molecular pattern (DAMP) molecule (90-92). HMGB1 stimulates an immune response by activating toll-like receptors (TLRs) and the receptor for advanced glycation end products (RAGE) (93-95). Besides being passively released, HMGB1 is actively released as a cytokine in a hyper-acetylated form by various immune cells such as monocytes and macrophages after activation by inflammatory stimuli (96). Whether the extracellular cytokine activity of HMGB1 functions as a chemo attractant or pro-inflammatory mediator depends on the redox state of three key cysteine residues (95, 97). HMGB1 can be measured in the circulation and increased levels are related to increased disease activity in sepsis (98), pancreatitis (99) and rheumatoid arthritis (100). In a mouse model of paracetamol toxicity circulating total and acetylated forms of HMGB1 displayed temporal kinetics that correlated with the onset of necrosis and inflammation respectively, confirming the potential of HMGB1 as an indicator of cell death processes (101). HMGB1 is a potential mediator of paracetamol-induced hepatotoxicity – anti-HMGB1 antibodies and knocking out HMGB1 in the liver reduced hepatic inflammation and liver injury in mouse models of paracetamol poisoning (90, 102, 103). A partly humanized chimeric antibody targeting HMGB1 was reported to be successful in reducing paracetamol induced ALI in mice. This confirms progress in the endeavour to bring HMGB1 specific therapy to future clinical development (104).

In patients with established ALI total and acetylated HMGB1 was increased in the circulation compared to paracetamol overdose patients without ALI and healthy controls (87). Acetylated HMGB1 was significantly increased in patients that reached KCC compared to patients that did not. ROC analysis demonstrated that HMGB1 (both total and acetylated) had a higher AUC than ALT for predicting patients that will reach KCC and predicting liver transplant/death (87).

At first presentation to hospital HMGB1 had an AUC value (sensitivity at 90% specificity, 95% CI) of 0.97 (0.91, 0.91-1.0, $P < 0.0001$), suggesting that HMGB1 could accurately identify patients with ALI at the time when ALT activity was still normal (79). Comparing ROC curves suggests that HMGB1 may be the most accurate biomarker at first presentation, but this needs to be tested in larger studies.

1.6.2.3 Glutamate dehydrogenase

Key properties:

- Conserved between rodent models and humans.
- Predicts ALT rise

Glutamate dehydrogenase (GLDH) is a mitochondrial enzyme that catalyses the reversible deamination of glutamate to α-ketoglutarate plus free ammonia by using NAD or NADP as a co-factor (105). Circulating GLDH has been suggested to be a specific mechanistic marker for mitochondrial damage. Mitochondrial damage releases GLDH into the cytosol from where it can be leaked into the circulation with cell necrosis. When the cellular content is released from necrotic cells into the circulation, intact injured mitochondria are released. For this reason, freshly drawn blood needs to be centrifuged at > 14,000 x *g* for 20 min to pellet the intact mitochondria (106). It was reported that mice treated with furosemide, a loop diuretic deemed to cause centrilobular liver necrosis without affecting mitochondrial function (107), produced a significant increase in serum ALT activity with only a non-significant increase in serum GLDH activity (108). By contrast, paracetamol treated mice had a substantial increase in GLDH along with ALT suggesting that the increase of circulating GLDH is indicative of paracetamol-induced mitochondrial damage and not simply caused by leakage of the enzyme from necrotic cells (108).

In patients with established ALI circulating GLDH is elevated. ***At first presentation to hospital*** GLDH is less accurate than miR-122-5p, K18 and HMGB1 with regard to identifying patients with subsequent ALI despite NAC with an AUC value (sensitivity at 90% specificity, 95% CI) of 0.80 (0.19, 0.68-0.93, *P* = 0.0003) (79).

1.6.3 Mitochondrial DNA fragments

Circulating mitochondrial DNA (mtDNA) has been reported to act as a DAMP molecule via TLR mediated activation of inflammatory cells (109, 110). Increased

concentrations of circulating mtDNA have been associated with the systemic inflammatory response syndrome, multiple organ dysfunction syndrome and mortality in patients admitted to intensive care (111, 112).

In patients with established ALI circulating mtDNA was increased as measured by absolute quantification of mtDNA encoding NADH dehydrogenase and cytochrome c oxidase. The plasma concentration of mtDNA in patients with abnormal liver function increased over time and peak levels correlated with peak ALT (108). As is the case with GLDH, circulating mtDNA may be a mechanistic marker for paracetamol-induced mitochondrial injury (108).

1.6.4 Kidney Injury Molecule-1

Key properties:

- Prognostic
- Translational between humans and rodents
- Point of care tested developed with rapid turn around
- Formally qualified by regulatory authorities for the investigation of drug-induced renal injury in preclinical drug development

Kidney Injury Molecule-1 (KIM-1) is a transmembrane glycoprotein that confers phagocytic activity on the proximal tubule cells of the kidney. During AKI, KIM-1 is rapidly up-regulated and its ecto-domain is shed into urine and blood where it is a sensitive and specific biomarker of acute kidney injury. Furthermore, KIM-1 has been formally qualified by regulatory authorities for its use to monitor acute kidney injury in the preclinical setting (113). In patients with paracetamol overdose, secondary injury to the kidney and specifically the proximal tubule epithelia is a major determinate of mortality. Indeed, biomarkers such as serum creatinine are often incorporated into prognostic algorithms. However, serum creatinine is delayed in its onset and data from animal models and in humans has repeatedly demonstrated the ability of KIM-1 to increase earlier following acute kidney injury (114, 115). ***In patients***

with established ALI circulating KIM-1 has been reported to be elevated, particularly in those patients who subsequently died or required a liver transplant compared to spontaneous survivors (116). The fold change in KIM-1 in this poor prognostic group was higher than creatinine and KIM-1 outperformed creatinine in a ROC analysis. Furthermore, circulating KIM-1 was an independent predictor of outcome in a logistic regression model (116).

1.7 Paracetamol protein adducts

Key properties:

- Conserved between rodent models and humans.
- Exclusively selective for paracetamol overdose
- Reflective of the initial molecular initiating event (MIE)
- Point of care tested developed with rapid turn around

When NAPQI is formed during paracetamol metabolism it covalently binds with proteins forming paracetamol-protein adducts, of which cysteine adducts are the most common (117). After the binding of NAPQI with cysteine, the structure of NAPQI reverts to that of paracetamol resulting in paracetamol-cysteine (paracetamol-CYS). In mouse models of paracetamol-induced ALI, immunohistochemical methods report that paracetamol-CYS adducts are formed in the liver in a temporally progressive, central to peripheral pattern (118). Experiments in mice also report paracetamol-CYS adducts in serum, suggesting that injured liver cells release paracetamol-CYS adducts into the circulation. Notably, serum paracetamol-CYS adducts were only detectable after toxic doses of paracetamol (119).

More recently, a high-performance liquid chromatography with electrochemical detection (HPLC-ECD) assay has been developed. This assay has been used to detect paracetamol -CYS adducts in liver and serum after hepatotoxic dosing of paracetamol to mice (120) and in both adult and paediatric human serum samples with paracetamol-induced ALI (121-123). In the sample preparation for this assay, dialysis

is performed to remove potential contaminating free paracetamol-CYS metabolites so that only the protein bound paracetamol-CYS adducts are measured. The protein fraction is then isolated for analysis (120). Due to the relatively long plasma half time of 1.7±0.3 days in adults (124) and 1.5 ± 0.3 days in children and adolescents (125), paracetamol-CYS adducts can be detected up to 7 days after a large overdose (121). By contrast, the plasma half-life for paracetamol is 1.5-2.5h (126). The longer half-life of paracetamol-CYS adducts could potentially allow risk assessment/diagnosis in patients who present when paracetamol has been cleared from the circulation. When the aetiology of ALI is known, paracetamol-CYS adducts have no defined advantage over ALT because kinetic changes in paracetamol-CYS adducts track ALT activity (121). A point-of-care immunoassay for measuring paracetamol-CYS adducts, AcetaSTAT, is currently in early clinical development and it was reported that it identified patients with established paracetamol-induced ALI with a positive predictive value (PPV) of 89.2% and negative predictive value (NPV) of 100% (127).

1.8 Current biomarker performances and future challenges

Table 2 gives an overview of the characteristics of each marker. Each of the characteristics has at least one biomarker that meets the *acceptable* or *desired* specifications. However, all these biomarkers have only been measured in a relatively small numbers of patients and large multi-centre trials are required to qualify current findings and further explore and confirm the attributes of these biomarkers. These studies should confirm at which time after paracetamol overdose the biomarker is able to predict liver injury and the sensitivity for ruling out injury. These studies should also determine the signal-to-noise ratio of each marker, identify which markers (if any) can distinguish between a benign and clinically relevant increases in ALT, and establish if there is a quantitative relationship between biomarker level and outcome. There is considerable scope for improvement in the “rapidly assayed” and “feasibility of assay” characteristics in the TBP. At the time of writing, only the calorimetric assay for GLDH fulfils the characteristic “feasibility of assay” as it has been validated in automated modern clinical chemistry labs within a turnaround time

of less than 1 hour. The point of care test, AcetaSTAT, is the only test in clinical development that could potentially be “rapidly assayed” (127). Large validation studies are required to test its performance. All other biomarkers are typically measured manually in research laboratories with time consuming and expensive kits. There is an urgent need for standardized and validated commercial assays that can be used at point-of-care to stratify paracetamol overdose patients for entry into trials of new therapeutic approaches. In order to have the driver for introducing one or more of these biomarkers into clinical practice their measurement must add value to patient care (128). In the setting of paracetamol overdose, a normal test result might add value by giving the treating clinician more confidence in discharging a patient. Given the large number of patients, this could reduce the pressure on acute hospital beds and save the health provider money. Conversely, an abnormal test result might trigger entry into a stratified clinical trial, indicate need for different treatment with a new therapy or referral for specialist care. To further fill the ‘toolbox’ of markers in the TBP, the large pool of circulating miRNAs and advances in sensitive profiling technologies, offer a promising opportunity (51). When miR-122-5p was discovered to be a sensitive marker for liver injury in mice the technology used to profile miRNAs in the circulation only resulted in 53 unique miRNA species in treated mice versus 43 miRNAs in control mice (72). There is a need for comprehensive profiling of all circulating miRNA species in humans with paracetamol overdose to identify a panel of the most sensitive miRNAs that can detect paracetamol induced liver injury in humans which is one of the aims of this thesis.

Table 2. Comparative biomarker profiles.

Attribute	Desired	Acceptable
Specific for paracetamol overdose	paracetamol-CYS adducts	miR-122-5p, GLDH
Sensitivity for ruling out injury	-	miR-122-5p, Keratin-18, HMGB1,
Rapidly assayed	paracetamol-CYS adducts	GLDH, KIM-1
Feasibility of assay	GLDH?	GLDH
Invasiveness / sample preparation time	-	miR-122-5p, Keratin-18, HMGB1, GLDH, mtDNA
Conserved (translational) across in vitro models, in vivo models and humans	miR-122-5p	Keratin-18, HMGB1, GLDH, mtDNA, KIM-1
Time after overdose at which it is able to predict the onset of liver injury	-	miR-122-5p, Keratin-18, HMGB1, GLDH
Signal to noise	miR-122-5p, Keratin-18, paracetamol-CYS adducts, HMGB1, GLDH, KIM-1	-
Quantitative relationship with disease severity	-	miR-122-5p, HMGB1
Distinguish benign and clinical relevant increase in ALT	Keratin-18, HMGB1	miR-122-5p, GLDH
Mediator of liver injury	-	HMGB1

1.9 Test systems for studying drug induced liver injury

In order to better understand DILI and find new biomarkers, the establishment of a reliable research model remains a key challenge.

1.9.1 *In vivo* models

In 1991 Terblanche and Hickman introduced the requirements of an ideal animal model for studying acute liver failure (129). Up until today, no ideal animal model exists that fulfils all these requirements. Even though each animal model has limitations, they play a fundamental role in current and future studies. Most widely used models related to DILI use paracetamol due to its clinical significance (130). Other frequently used drugs in animal models are D-galactosamine and thioacetamide (131).

Due to high costs and low throughput, animal models are not ideally suited for early phase drug screens. Large animals such as pigs and dogs are usually only used for the development of new therapeutic approaches for ALF (129). In most cases the preclinical species of choice are rats and mice. Rats are still required for standard safety evaluation of new drugs, however in the case of paracetamol-induced liver injury, the rat is unsuitable since they do not develop mitochondrial oxidant stress or JNK activation resulting in minimal liver injury (132).

The mouse model for paracetamol induced liver injury has been used since the 1970s (133). This model has had great importance in understanding the mechanism of paracetamol induced liver injury (134). Due to mechanistic similarities with humans, mice are currently the most widely used model species (108). Another advantage of mice are the well-established transgenic and knock out lines that can be used to study DILI.

1.9.2 *In vitro* test systems

To reduce animal usage, cost and the ability to test a high number of compounds in a short time, numerous *in vitro* test systems have been developed and applied (135). The use of these *in vitro* systems have multiple advantages compared to using animal models including the reduced cost of animal maintenance and care, and the ability to test small amounts of compound in a high throughput fashion.

Immortalised liver cell lines, primary hepatocytes and precision cut liver slices have remained the main models for toxicity testing with each having advantages and disadvantages (136).

1.9.2.1 Immortalised liver cell lines

The most common immortalised liver cell lines include HepG2, Fa2N-4, Hep3B, HBG and HepaRG (137, 138). Immortalised liver cell lines mainly originate from tumours and have to advantage of indefinite proliferative capacity (139).

The human hepatoma HepG2 line stems back from the 1970s. It retained the expression of many liver specific genes, however it lacks the expression of important genes including cytochrome P450 genes, membrane transporters, phase II enzymes and nuclear receptors (137). The human hepatoma HepaRG line appears to be a good alternative with high proliferative capacity, the ability to differentiate into hepatocytes and biliary cells and the much greater expression of the major P450 enzymes as well as other liver-specific functions (139).

1.9.2.2 Primary hepatocytes

Primary hepatocytes isolated from humans have the advantage of expressing the typical hepatic biochemical functions and containing the entire hepatic drug-metabolizing enzyme system (140). However, as soon as 24 hours after isolation,

there is significant down regulation of many important enzymes involved in drug metabolism (141). This decline in metabolic capacity can be reduced by culturing hepatocytes in a sandwich format in which the hepatocytes form a monolayer inbetween two collagen layers mimicking the extracellular layer (142, 143). Another strategy for partially preventing the decline in CYP activity is by introducing a mixture of CYP inducers to the cell medium (144).

A major disadvantage of these cell systems is that only one cell type is present. This makes these systems unsuitable for detecting toxicities in which non-hepatocyte cell functions are involved. DILI is often a complex multi-cellular process in which not just hepatocytes but many other cell types can play a role and have an important contribution to the toxicity (145, 146).

1.9.2.3 Precision cut liver slices

A multicellular approach is the use of precision cut liver slices. Precision cut liver slices present small slices of liver with all the different cell types, cell-cell contacts and extracellular matrix of the liver present in its natural architecture (147). Precision cut liver slices could be prepared from multiple organs, allowing for multi organ incubations enabling studies on the gut-liver axis (148).

In human precision cut liver slices, gene expression changes after culturing for 24h, however these changes mainly reflect extracellular matrix and cytoskeletal remodelling. Importantly, genes involved in stress, toxicity, drug metabolism and transport hardly change (135). Although precision cut liver slices can be cultured for up to 7 days, some important functions, such as metabolic capacity, decline after 3 days (149). In order to perform longitudinal studies, culture conditions of precision cut liver slices need to be further improved.

Precision cut liver slices are a promising model for studying DILI, but the main disadvantage of human precision cut liver slices is that the supply of intact human tissue is limited (140).

Another promising model organism with many *in vitro* model advantages but the complexity of *in vivo* models are zebrafish.

1.10 Zebrafish as model organisms for studying drug induced liver injury

The zebrafish is a promising animal for assessing drug-induced toxicity in a variety of organ systems (150). Well-established zebrafish assays have frequently been utilised for measurement of cardiac function, CNS assessment, gastrointestinal function and developmental toxicity (151, 152). The zebrafish liver can also be used to study drug toxicity, however in comparison to other organs, the zebrafish model of liver toxicity has been utilised less frequently.

The use of this model has the potential to identify new biomarkers, drug targets for the treatment of DILI and play a role in pre-clinical drug development. Also, the use of zebrafish is in line with the 3R's (reduce, refine, and replace) approach of animal use for scientific purposes by replacing higher order animals with lower order zebrafish (particularly zebrafish embryos).

1.11 Potential advantages of zebrafish as a model for studying DILI

Histopathology and clinical chemistry have been traditionally used to report liver toxicity in established animal models. To decrease the cost and time of toxicity studies, alternative test systems have been developed. These include liver slices (153), cultured primary hepatocytes (154), immortal hepatic cell lines such as the human hepatoblastoma-derived HepG2 line (155) and the recently derived human hepatocyte HepaRG line (139). The advantage of these *ex vivo* and *in vitro* approaches is that they can be used efficiently for high throughput screening. However, the usefulness of these approaches for toxicological testing of compounds can be questioned based on differences in gene expression between the different systems (156) and the low sensitivity of the cytotoxicity assays, which can be less than 25% for the detection of hepatotoxic agents (157).

In order to perform liver toxicity testing with a higher degree of sensitivity, *in vivo* assessment is necessary. This allows study of the dose-dependent toxicity of a drug within the complex physiology of a whole organism. Higher vertebrate organisms (e.g. rodents and pigs) are physiologically similar to humans and have been used for this approach. However, smaller, lower-order vertebrates, such as the zebrafish, have similar molecular and cellular processes that can accurately model human physiology (150). In addition, the zebrafish offers significant advantages in comparison to rodents (**Table 3**) and other larger animals. The zebrafish embryo is optically transparent and grows outside the uterus. This makes it possible to detect and monitor developmental changes easily from the single-cell stage. For example, the zebrafish embryo has allowed researchers to study embryonic lethal phenotypes; something that was not possible with mammalian models(158). Additionally, an early zebrafish embryo, at 3 days post fertilisation (dpf), is ~3.5 mm long. This allows zebrafish embryos to be grown at high stocking densities in multi-well plates. The high fecundity of the zebrafish (each female can lay ~200 eggs per week) can generate hundreds of embryos for screening, each of which has very rapid development. This reduces the cost of zebrafish husbandry significantly, when compared with larger laboratory animals. Furthermore, the Wellcome Trust Sanger Institute has sequenced the genome of the zebrafish, and many of these sequences have been annotated (http://vega.sanger.ac.uk/Danio_rerio/Info/Index) (159). Further advantages of the zebrafish have been described elsewhere in literature (152, 160-162).

Table 3**. Comparative advantages of using zebrafish and mice to model DILI.**

Zebrafish vs Mouse	
Advantages of zebrafish	**Advantages of mice**
Optically large and transparent embryos	Characterized inbred strains, including knock-out and knock-in strains
Ex utero development	More complementary with mammalian organs and closer physiological similarity to humans
Similar cellular and sub-cellular processes to humans	Easier to draw blood
Rapid development of liver ~72-96 hpf	Feasible to perform pharmaco/toxico kinetic studies
High fecundity (~200 eggs/female/week)	Genome duplication of fish results in multiple copies of genes
Large numbers of fish can be easily maintained	
Embryonic fish can survive up to 7 days without a Cardiovascular system	
Low overall cost	
Easy drug delivery by dissolving in the tank water, with possibility of drug delivery by microinjection	
Feasibility of high throughput screens	
N numbers available per study, allowing improved statistical analysis	
Lower order mammal (in line with 3R principle)	

1.12 Zebrafish liver anatomy is different to rodents and humans

Studies examining the zebrafish organs, specifically the liver, have revealed multiple similarities with higher vertebrates (163). When liver budding starts at 28 hours post fertilisation (hpf), growth factor and gene expression similar to those of humans and rodents has been reported in zebrafish (164). When hepatic organogenesis is completed at 72 hpf, the liver is perfused with blood and is functional (165). At 120 hpf, the zebrafish is actively seeking food and the yolk sac reserves have become exhausted. By this time, larvae already have a fully functional liver. In comparison, in the embryonic mouse the primary liver bud starts to grow around embryonic day 8.5–9 and the liver is mature at embryonic day 18.5, just before birth (166). The tri-lobed

liver of the zebrafish is similar to the liver of mammals with regard to biological function; this includes processing of lipids, vitamins, proteins and carbohydrates and the synthesis of serum proteins (163). The main difference between the mammalian and zebrafish liver is the structural organisation of the liver tissue. Instead of having the large bile ducts, portal veins and hepatic arteries organised in portal tracts, these are randomly allocated throughout the liver parenchyma in the zebrafish. Hepatocytes in the mammal liver are arranged in plates, whereas in the zebrafish liver they are arranged in tubules. In zebrafish, the bile canaliculi radiate centripetally between hepatocytes to anastomose with a single ductular cell, forming a ductule at the centre of the tubule. These ductules form a network that transports the bile secreted by hepatocytes. Downstream, these ductules merge into intrahepatic bile ducts, converging at the cystic duct, which exits the liver at the hilum to connect with the gallbladder. Subsequently, the gallbladder empties into the intestine through the common bile duct (**Figure 4**) (164, 167). The above-mentioned lack of lobular arrangement impairs morphological differentiation between venules from the portal and hepatic veins, because these vessels are histologically identical.

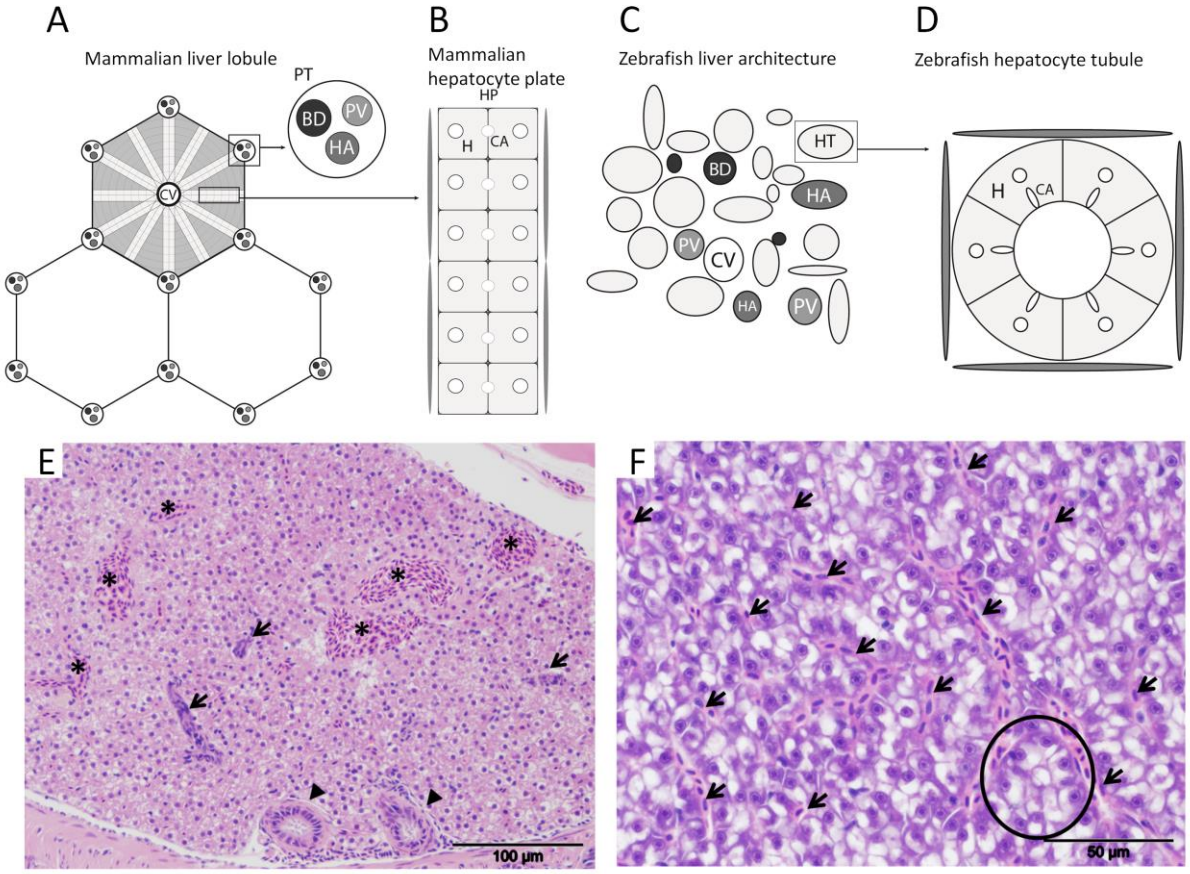

Figure 4. Schematic transverse representations of mammalian and zebrafish liver architecture. (A) The mammalian liver lobule, arranged with plates of hepatocytes radiating outward from a central vein (CV). At the corners of each lobule are portal tracts (PT), containing a portal vein (PV), a hepatic artery (HA) and a bile duct (BD). (B) Mammalian bilayered hepatocyte plate. Bicellular canaliculi (CA) are located adjacent to the hepatocytes (H) in the hepatocyte plate (HP). A basal hepatocyte membrane allows transport of oxygen, proteins and different macromolecules to the hepatocytes. Blood enters the liver through the portal vein and hepatic artery, after which it enters the central vein through sinusoid vessels, located between the plates. (C) The zebrafish liver architecture. The portal vein (PV), hepatic artery (HA), bile duct (BD), hepatocyte tubule (HT) and the central vein (CV) are scattered throughout the parenchyma. (D) Zebrafish hepatocytes (H) are arranged in tubules around small bile ducts, which receive bile from the hepatocyte canaliculi (CA). Sinusoids are located at the periphery of these tubules. (E) Histological image of male zebrafish liver (haematoxylin and eosin staining at ×200 magnification). Note

the presence of several biliary ducts (arrows), bile ductules (arrowheads) and blood vessels (*), with lack of lobular arrangement. (F) Histological image of female zebrafish liver (haematoxylin and eosin staining at ×400 magnification). This high-power image displays sinusoidal spaces between hepatocytes (arrows) and an instance of the tubular arrangement of hepatocytes (encircled), which is frequently not visible histologically. Note the difference in staining of male and female zebrafish liver. From Vliegenthart et al, 2014. (75).

1.13 Zebrafish drug metabolism is similar to rodents and humans

One of the key physiological functions of the liver is oxidative catalytic transformation, which leads to activation or inactivation of many endogenous and exogenous compounds. This metabolism is mainly performed by the cytochrome P450 (CYP) enzymes, which are predominantly localized in the liver. The metabolic reactions performed by the CYP enzymes include oxidation, reduction and hydrolysis. The CYP enzymes can be divided into two major groups. The first group of enzymes, with generally narrow substrate specificity, are predominantly involved in synthesis, activation or inactivation of endogenous regulatory molecules. The second group predominantly metabolize xenobiotics, but may also metabolize endogenous compounds (168, 169).

These reactions are divided in two phases. In phase I, the metabolized compound is oxidized, reduced or hydrolysed. These phase I reactions are predominantly mediated by CYP enzymes. In phase II, conjugation takes place (not CYP enzyme mediated). The rate of these reactions is controlled by expression levels and activity of the specific enzymes (170).

When selecting an animal model for toxicity testing, characterization of the metabolic properties of the selected species is very important. These properties influence DILI, for example, by creating reactive metabolites, and this will determine whether a compound is toxic (171).

Therefore, the application of zebrafish as a model of human (hepatic) endogenous and exogenous compound metabolism requires the full range of *CYP* genes; these have been identified in zebrafish and annotated with regard to their phylogenetic relationships to human CYP enzymes. This essential study was reported by Goldstone and colleagues, who characterised a total of 94 *CYP* genes in the zebrafish genome (168). Based on homologous amino-acid sequences, they reported that these genes fitted into 18 *CYP* gene families that are also present in humans and other mammals. The CYP enzyme families 1–4, which predominantly metabolize exogenous compounds, are more diverse in zebrafish than in humans. However, analysis of shared synteny demonstrates an evolutionary relationship between human and zebrafish *CYP* genes. In the *CYP* families 5–51, zebrafish have single genes like humans, and there is a high degree of conservation between human and zebrafish sequences (168).

Metabolic experiments demonstrate that drugs are metabolized when exposed to zebrafish embryos by similar reactions to those in humans. An overview of reported metabolic experiments is presented in **Table 4**. The metabolic degradation of the widely used nonsteroidal anti-inflammatory drug ibuprofen is well studied in different mammals (172, 173). The compound is metabolized by different reactions, including oxidation of the parent compound to hydroxyl-ibuprofen and carboxy-ibuprofen, as well as glucuronic acid conjugation of both parent and metabolite compounds (174). In humans, the oxidation of ibuprofen is catalysed by the CYP2C8/9 isoforms (175). When ibuprofen is exposed to zebrafish embryos, hydroxylated ibuprofen can be detected in the zebrafish extracts and water samples, suggesting that zebrafish have an analogous metabolic system to the human CYP2C8/9 (176).

Following exposure to high dose paracetamol, in humans, rat and mice, the reactive metabolite NAPQI is formed by phase I metabolism of paracetamol by predominately CYP3A4 (177-179). Recently, Chng and colleagues used a glutathione trapping assay for NAPQI to determine that zebrafish generate the same reactive metabolite as humans. The same authors reported that the zebrafish CYP3A65, orthologue for the human CYP3A4, contributed to the formation of NAPQI, as well as the phase I hydroxylation of testosterone (180).

Table 4. Specific metabolic drug reactions reported in zebrafish compared with humans.

Drug metabolism in zebrafish				
Compound	**Reaction observed in zebrafish**	**Similar to human**	**Human P450 isoform**	**Ref**
Ibuprofen	Hydroxylation	Yes	CYP2C8/9	(174)
Paracetamol	Hydroxylation	Yes	CYP3A4	(180)
Testosterone	Hydroxylation	Yes	CYP3A4	(180)
Cisapride	Sulfate conjugation	No	CYP3A4	(181)
Verapamil	N-dealkylation and Hydroxylation	Yes	CYP3A4, CYP2C8/9, CYP1A2	(181)
Chlorpromazine	Hydroxylation, Oxidation, N-Demethylation, Glucuronidation and Sulfation	Yes	CYP1A2, CYP2D6	(181)
Phenacetin	De-ethylation	Yes	CYP1A2	(181)
Dextromethorphan	Demethylate	Yes	CYP2D6	(181)
Bupropion	Hydroxylation	Yes	CYP2B6	(181)
Ethanol	Oxidation	Yes	CYP2E1	(182)

Alderton and colleagues (181) confirmed that zebrafish embryos are able to perform the metabolic phase I reactions, oxidation, *N*-demethylation, *O*-demethylation and *N*-dealkylation, as well as the metabolic phase II metabolic reactions, sulfation and glucuronidation. The metabolites of three compounds, namely cisapride, verapamil and chlorpromazine, were profiled. With cisapride, the mammalian phase I reactions (piperidine *N*-delakylation and fluorophenyl ring oxidation) and phase II reactions (glucuronidation, resulting in glucuronide conjugates) were not observed in zebrafish (183). However, following exposure of zebrafish to verapamil, a number of metabolites were formed by N-dealkylation and hydroxylation; these reactions are also present in mammals (184). Three major metabolites of chlorpromazine, which are excreted in human urine, were also excreted by zebrafish; these metabolites were formed by hydroxylation, oxidation, *N*-demethylation, glucuronidation and sulfation. Alderton and colleagues also reported that zebrafish embryos were able to de-

ethylate phenacetin, demethylate dextromethorphan and hydroxylate bupropion (181).

The nuclear receptor, pregnane X receptor (PXR), is involved in the transcriptional regulation of cytochrome P4503A (CYP3A) and the multidrug resistance 1 transporter (MDR1) (185, 186). Studies have confirmed that CYP enzymes can be induced and inhibited in zebrafish as reported in mammals. Bresolin and colleagues (187) studied the *in vivo* expression of *PXR*, *CYP3A* and *MDR1* genes in the liver of zebrafish treated with the synthetic steroid pregnenolone 16α-carboninitrile, a potent PXR agonist (188). The liver of the fish treated with pregnenolone 16α-carboninitrile had a 1.9-fold increase in *PXR*, followed by a 1.8-fold increase of *CYP3A* and 1.6-fold increase in *MDR1*. This suggests that the regulation of PXR, CYP3A and MDR1 is conserved in zebrafish and similar to mammals (187).

Tseng and colleagues (189) found that CYP3A65 expression was upregulated in the embryo (84 hpf) intestine by rifampicin and dexamethasone. In addition to the PXR pathway, the aryl hydrocarbon receptor 2 (AHR2) has a role in the pathway that regulates gene expression and is activated by endogenous and exogenous compounds, such as drugs and xenobiotics (190). Orthologues genes of the aryl hydrocarbon receptor are present in different mammals, such as humans, mice and rats, and regulates expression levels of enzymes involved in phase I metabolism, including CYP1A2, CYP1B1 and aldehyde dehydrogenase 3A1 (ALDH3A1), as well as phase II metabolism, including NAD(P)H dehydrogenase quinone 1 (NQO1), UDP glucuronosyltransferase 1A2 (UGT1A2) and glutathione *S*-transferase α1 (STA1) (191). Expression of CYP3A65 was increased by exposing fish to 2,3,7,8-tetrachloro-dibenzo-*p*-dioxin, a AHR2 ligand (192), during early embryonic stages, and inhibition of AHR2 translation by antisense morpholino oligonucleotides inhibited both normal and 2,3,7,8-tetrachloro-dibenzo-*p*-dioxin-stimulated CYP3A65 transcription in embryonic intestine. These data suggest that AHR2 regulates CYP3A65 expression in zebrafish (189).

In summary, the zebrafish liver contains enzymes that metabolize a variety of endogenous and exogenous compounds in a similar manner to human liver.

Additionally, these enzymes are subject to similar regulation mechanisms to those reported in humans. These findings support the potential of the zebrafish as an animal model for DILI.

1.14 The zebrafish immune system is similar to rodents and humans

Hepatic inflammation is commonly reported in various liver diseases, including DILI. Liver toxic drugs can have a direct effect on liver cells to release DAMPS that stimulate immune cell secretion of chemokines and cytokines. Various immune cells such as lymphocytes, neutrophils and macrophages can subsequently infiltrate the liver. This complex immune response has been widely described by several authors (193-195). Additionally, specific genetic backgrounds can be a risk factor for idiosyncratic DILI in humans (196, 197). For example, a variety of leukocyte antigen (HLA) haplotypes are associated with immunological drug hypersensitivity (e.g. amoxicillin/clavulanate and abacavir) (198-201).

Many similarities exist between the zebrafish and the mammalian immune systems. Different studies of haematopoiesis in zebrafish have demonstrated that most, if not all, cell types of the human immune system have zebrafish counterparts, although the sites of origin differ (202). There is a variation in the repertoire of chemokine receptors in different species, regardless of the specific evolutionary position. Despite this, the expression and function of orthologous chemokine receptors in lower and higher vertebrates are highly similar (203). While the zebrafish metabolizes drugs using similar pathways to humans, whether a similar immune response takes place with DILI in zebrafish is yet to be confirmed.

1.15 A range of drugs induce liver toxicity in zebrafish

Different methods have been used to assess liver toxicity in zebrafish, for example, visual assessment of gross and microscopic morphological changes, serum enzyme

and biomarker tests, hepatic excretory tests, and assessment of alterations in chemical constituents of the liver.

1.15.1 Gross/subgross visual phenotypic assessment

The ability to perform assays for liver toxicity with visually assessable phenotypic end-points enables transparent zebrafish larvae to be used in high-throughput screening.

A comparative toxic screen of 50 different compounds classified to be hepatotoxic by the US FDA, and non-toxic controls, was performed in zebrafish embryos. The compounds were screened in a researcher-blinded fashion for evaluation of three specific phenotypic end-points of liver toxicity, i.e. change in liver size, liver morphological abnormality and yolk-sac retention. A sensitivity for hepatotoxic drugs of 86% and specificity for nonhepatotoxic drugs of 77% was reported, which resulted in an overall correlation of 84% with mammalian *in vivo* data (204). However, when four compounds were excluded from the analysis because of low uptake into the embryo from the tank water, an increased sensitivity, specificity and overall predictability of 97, 77 and 91%, respectively, was reported (205).

He and colleagues (206), exposed zebrafish embryos at 120 hpf to six known mammalian hepatotoxic drugs (paracetamol, aspirin, tetracycline hydrochloride, sodium valproate, cyclophosphamide and erythromycin) and two nontoxic compounds (sucrose and biotin), after which three phenotypic visual end-points of liver toxicity were assessed quantitatively. These end-points were liver degeneration score, changes in liver size and shape and yolk-sac retention. These end-points were easily measured under a light microscope without the need for dissection. All six hepatotoxic compounds induced liver degeneration, reduced liver size and led to yolk-sac retention, which suggested that this assay could be predictive for liver toxicity. Zhang and colleagues (207) have developed a transgenic zebrafish line (LiPan) that expresses a liver-specific fluorescent protein (DsRed) under the *fabp10a* promoter. They reported that the LiPan line could identify hepatotoxic drugs by detecting changes in both liver red fluorescence and liver size in a dosage-dependent

fashion. This was demonstrated by exposing the LiPan line to the hepatotoxic drugs paracetamol, aspirin, isoniazid and phenylbutazone.

Nadanaciva and colleagues (208), exposed 72 hpf zebrafish embryos to a panel of 11 NSAIDs (flufenamic acid, tolfenamic acid, mefenamic acid, diclofenac, meloxicam, sudoxicam, piroxicam, diflunisal, acetylsalicylic acid, nimesulide, and sulindac). At 120 hpf all fish were assessed for lethality and morphology. The effects on fish were compared to the effects of the NSAIDs on the respiration of rat liver mitochondria and other mechanistic endpoints in rat hepatocytes. It was found that all three assays were complementary and able to correctly identify “toxic”from “non-toxic” drugs in accordance to the safety profile in human.

1.15.2 Liver histopathology

Specific changes in zebrafish liver histology have been reported: North and colleagues reported widespread necrosis and sinusoidal haemorrhage after adult zebrafish were exposed to 10 mM paracetamol for 12 hours. Paracetamol exposure (10 mM) to fish concurrently to NAC (10 µM) improved survival, serum ALT activity and histology (209). As described in other mammals, exposing zebrafish to hexachlorocyclohexane results in specific histological changes such as hepatic macrovesicular triglyceride droplets, glycogen depletion and the presence of club-shaped mitochondria (210). Exposure of zebrafish to thioacetamide induces steatohepatitis, which is accompanied by the accumulation of fatty droplets and apoptosis (211). Zebrafish exposed to ethanol display histological changes such as steatosis, as seen in alcoholic liver disease in human (212). In conclusion, both embryonic and adult zebrafish are amenable to study of the histological changes that accompany different liver pathologies, such as steatosis, apoptosis and necrosis.

1.15.3 Circulating biomarkers

Whilst zebrafish embryos offer a range of advantages that facilitate high throughput screening, adult zebrafish are needed if circulating biomarkers are to be measured.

Murtha and colleagues determined multiple serum biochemical values in zebrafish (±1 year old), such as total bilirubin concentration (mean ± SD, 0.38 ± 0.1 mg dl^{-1}; range, 0.2–0.6 mg dl^{-1}) and serum alanine transaminase (ALT) activity (mean ± SD, 376 ± 25.3 U l^{-1}; range, 343–410 U l^{-1}) (213). In a paracetamol-induced liver toxicity model in adult zebrafish, North and colleagues demonstrated that ALT activity increased in zebrafish in a dose- and time-dependent fashion (209). Injury was reduced by acetylcysteine treatment of paracetamol exposed zebrafish, as is the case in humans (214). Cox and colleagues reported that after paracetamol exposure, inhibition of the enzymic regulator *S*-nitrosoglutathione reductase (GSNOR) minimized liver toxicity in zebrafish. A GSNOR-specific inhibitor improved survival and histology and lowered ALT activity through the cytoprotective Nrf2 pathway. Paracetamol toxicity studies in GSNOR-deficient mice confirmed conservation of the hepatoprotective properties of *S*-nitrosothiol signalling across vertebrates (215). This supports use of the zebrafish as a translational model of human paracetamol toxicity and biomarker research.

1.16 Challenges in using zebrafish as a new model for DILI

Although a substantial amount of research demonstrates the potential of zebrafish as a model of liver toxicity, there are a number of challenges.

Zebrafish are often exposed to a drug by dissolving the drug in the water, which enables easy and fast drug administration. This is an advantage of the model that allows for high-throughput phenotypic screening, especially if transgenic lines are used (216). The problem with this method of drug administration is that, although the concentration of drug in water is known, the amount taken up by the fish is imprecise and variable, which limits the study of toxicokinetics. Berghmans and

colleagues (217) studied the uptake of nine compounds in zebrafish embryos by dissolving the compounds in the water and found a large variability in the bioavailability of the different compounds. This was because the physiochemical properties of different compounds determine the absorption of the compounds into the fish through the gills and intestine, rather than simply their aqueous concentration. If required, drugs can be injected into the yolk sac of embryonic fish, and this method can therefore quantify the administered dose at the expense of being time consuming (218).

The relationship between the drug's lipophilicity and the amount of compound penetrating the zebrafish has been determined (217) however no single physiochemical property can accurately predict the uptake of different types of compounds (219). Therefore, bioanalysis should be performed to correlate the amount of drug in the fish (the real body burden) and the observed toxic effects (220). For instance, sodium valproate, a potential liver toxic drug in humans did not cause liver toxic effects in zebrafish embryos, possibly due to poor uptake of this drug. In contrast, valproic acid did cause liver toxicity in zebrafish embryos with higher blood concentrations, indicating increased uptake (204). To overcome the possible problem of absorption, the amount of drug taken up by the fish can be determined by using radio-labelled compound and liquid scintillation counting or radio high-performance liquid chromatography. Other methods that determine the uptake of drug into fish include lysing embryos and then using liquid chromatography–tandem mass spectrometry (LC-MS) analysis (221). Recently this approach was able to determine the pharmacokinetics of paracetamol in zebrafish larvae. It was reported that the larvae had an uptake of 0.290 pmole/min and clearance of 2.96 x 10^7 L/h that scaled reasonably well with clearance rates in higher vertebrates (222).

In adult zebrafish, the uptake of compounds can be determined by drawing blood from adult zebrafish and measuring the concentration of the compound in blood plasma. However, because of the low blood yields obtained from zebrafish, typically 3–20 µl of whole blood (223-227), 10–20 fish may have to be pooled. Zang and colleagues (227) described a recovery method that allows for serial blood sampling from adult zebrafish, but it takes 1–2 weeks for fish to recover normal haemoglobin

values after taking a small blood sample of 2 µl. This delayed recovery may limit the application to toxicity studies.

Goldstone and colleagues (168) demonstrated that 66 of the 88 studied *CYP* genes in zebrafish embryos have a differential level of expression during development between 3 and 48 hpf. This stresses the importance of age on toxicity when zebrafish embryos are used. In liver toxicity studies, embryos must be >3 dpf (168). Circadian rhythms will influence an organism's susceptibility and responses to xenobiotic exposure. It is established that ATP binding cassette (ABC) transporters have a significant impact on bio-availability, metabolism and excretion of drugs. The gene expression of some transporters, including P-glycoprotein, could be under circadian transcriptional regulation in zebrafish, as reported in mice (228). Therefore, age-related and circadian-related gene expression profiles will impact on the relative higher amount of toxic metabolite, which might influence susceptibility. It is for this reason that standardization of protocols when using embryonic stages is an important consideration in high-throughput screens.

Early identification of hepatotoxic compounds would accelerate the process of drug discovery and development and reduce the enormous costs. The zebrafish appears to be a model that may complement established models. However, before the model can be applied on wider scale more validation is needed to confirm the translatability of the model to humans. This may include testing established human hepatotoxic and nonhepatotoxic compounds, comparing dose responses between fish and humans and developing translational biomarkers that bridge between fish, rodents and humans. Furthermore, the immunological response observed with DILI in humans has to be studied in zebrafish to confirm mechanistic similarity. Ultimately, use of the zebrafish as a model for DILI is promising and may enable better decision making in the early stages of drug discovery, before a compound is tested in higher mammals.

Hypothesis and Aims

The hypotheses investigated in this study are:

1) miRNAs can be used as specific markers for hepatotoxicity in humans.
2) Zebrafish can be used as a pre-clinical model for drug induced liver injury.

In order to test these hypotheses, the aims of the studies described in this thesis are:

- Identify the circulating miRNAs that are most sensitive to detect paracetamol induced liver injury in humans.
- Develop the leading miRNA candidate by determining the effect of alcohol consumption and renal dysfunction. Furthermore, determine whether microRNA measured in capillary blood obtained from a finger prick could be used as biomarker for DILI.
- Explore the toxicokinetics of circulating paracetamol metabolites.Develop a blood letting method in adult zebrafish and test if circulating miRNA is increased with paracetamol induced liver injury in zebrafish.Develop a hepatotoxicity model in zebrafish larvae.

Chapter 2: Comprehensive microRNA profiling in paracetamol toxicity identifies novel circulating biomarkers for human liver and kidney injury

2.1 Introduction

In humans, a miRNome subset of 372 miRNAs has been quantified in 49 patients with paracetamol hepatotoxicity or ischemic hepatitis (229). This study confirmed that miRNAs were increased and decreased and suggested that certain species could distinguish between these distinct aetiologies of liver injury (229). Changes in circulating miRNAs have also been reported in small numbers of hepatotoxicity patients analysed by high-throughput sequencing (78, 230). These studies did not address the unmet clinical need for improved patient stratification, back translate to pre-clinical models or identify signals of kidney toxicity. In the present study we recruited over 200 patients and assayed all miRNAs annotated in miRBase (version 18), a biological database that acts as an archive of miRNA sequences and annotations (51), to identify which miRNAs were differentially expressed in plasma from overdose patients with and without paracetamol toxicity. Selected miRNA candidate biomarkers were tested for liver and kidney specificity in humans and mice, and sensitivity with regard to patient stratification at first presentation to hospital.

The results of this chapter were published as:

Vliegenthart AD, Shaffer JM, Clarke JI, Peeters LE, Caporali A, Bateman DN, Wood DM, Dargan PI, Craig DG, Moore JK, Thompson AI, Henderson NC, Webb DJ, Sharkey J, Antoine DJ, Park BK, Bailey MA, Lader E, Simpson KJ, Dear JW. Comprehensive microRNA profiling in acetaminophen toxicity identifies novel circulating biomarkers for human liver and kidney injury. Sci Rep 2015;5:15501. (231)

Paper 1

SCIENTIFIC REPORTS

OPEN

Comprehensive microRNA profiling in acetaminophen toxicity identifies novel circulating biomarkers for human liver and kidney injury

Received: 18 June 2015
Accepted: 22 September 2015
Published: 22 October 2015

A. D. B. Vliegenthart[1], J. M. Shaffer[2], J. I. Clarke[3], L. E. J. Peeters[1], A. Caporali[1], D. N. Bateman[1], D. M. Wood[4,5], P. I. Dargan[4,5], D. G. Craig[6], J. K. Moore[6], A. I. Thompson[7], N. C. Henderson[7], D. J. Webb[1], J. Sharkey[3], D. J. Antoine[3], B. K. Park[3], M. A. Bailey[1], E. Lader[2], K. J. Simpson[6] & J. W. Dear[1]

Our objective was to identify microRNA (miRNA) biomarkers of drug-induced liver and kidney injury by profiling the circulating miRNome in patients with acetaminophen overdose. Plasma miRNAs were quantified in age- and sex-matched overdose patients with (N = 27) and without (N = 27) organ injury (APAP-TOX and APAP-no TOX, respectively). Classifier miRNAs were tested in a separate cohort (N = 81). miRNA specificity was determined in non-acetaminophen liver injury and murine models. Sensitivity was tested by stratification of patients at hospital presentation (N = 67). From 1809 miRNAs, 75 were 3-fold or more increased and 46 were 3-fold or more decreased with APAP-TOX. A 16 miRNA classifier model accurately diagnosed APAP-TOX in the test cohort. In humans, the miRNAs with the largest increase (miR-122-5p, miR-885-5p, miR-151a-3p) and the highest rank in the classifier model (miR-382-5p) accurately reported non-acetaminophen liver injury and were unaffected by kidney injury. miR-122-5p was more sensitive than ALT for reporting liver injury at hospital presentation, especially combined with miR-483-3p. A miRNA panel was associated with human kidney dysfunction. In mice, miR-122-5p, miR-151a-3p and miR-382-5p specifically reported APAP toxicity - being unaffected by drug-induced kidney injury. Profiling of acetaminophen toxicity identified multiple miRNAs that report acute liver injury and potential biomarkers of drug-induced kidney injury.

Acetaminophen (paracetamol) is a safe analgesic drug when taken at therapeutic doses. However, in overdose acetaminophen is hepatotoxic and is the most common cause of acute liver failure in the United States and Europe[1,2]. After overdose, the reactive metabolite N-acetyl-p-benzoquinone imine (NAPQI) is generated in excess, depleting cellular glutathione (GSH) then binding covalently to cellular proteins resulting in oxidative stress and hepatocyte death, predominately by necrosis[3]. Cell death releases

[1]Pharmacology, Toxicology and Therapeutics, University/BHF Centre for Cardiovascular Science, Edinburgh University, UK. [2]Qiagen, Fredrick, Maryland, USA. [3]MRC Centre for Drug Safety Science, Department of Molecular & Clinical Pharmacology, Institute of Translational Medicine, University of Liverpool, Liverpool, UK. [4]Clinical Toxicology, Guy's and St Thomas' NHS Foundation Trust, London, UK. [5]King's College London, London, UK. [6]Scottish Liver Transplantation Unit, Royal Infirmary of Edinburgh, Edinburgh, UK. [7]MRC Centre for Inflammation Research, University of Edinburgh, The Queen's Medical Research Institute, 47 Little France Crescent, Edinburgh. Correspondence and requests for materials should be addressed to J.W.D. (email: james.dear@ed.ac.uk)

intra-cellular molecules into the extra-cellular milieu and this is reflected by changes in circulating protein and RNA[4]. The current antidote, acetylcysteine (NAC), replenishes cellular GSH and is highly effective at preventing liver injury if administered soon after overdose[5]. However, NAC treatment takes at least 21 hours to complete so resulting in substantial hospital bed occupancy and commonly producing adverse drug reactions; 65% of NAC-treated patients vomited, retched or needed antiemetic therapy in a recent randomised controlled trial[6]. To selectively target treatment to those who stand to benefit and facilitate early safe hospital discharge of low risk patients there is an unmet need for new biomarkers that stratify patients by their risk of liver injury at first presentation to hospital, soon after overdose, an early time point when current markers such as serum alanine transaminase (ALT) activity lack sensitivity and specificity[7].

Acetaminophen can also induce kidney tubular cell death resulting in acute kidney injury (AKI)[8] and, in the presence of liver injury, AKI is one of the key predictors of need for urgent liver transplantation to avoid death. Kidney injury is currently quantified by serum creatinine. However, patients with AKI are not in steady-state with regard to kidney function and serum creatinine is slow to report cellular damage. Serum creatinine also lacks specificity, becoming elevated by non-renal pathologies such as dehydration and muscle injury[9]. New biomarkers are needed to report drug-induced kidney injury with enhanced sensitivity and specificity.

MicroRNAs (miRNAs) are small (~22 nucleotide-long) non-protein coding RNA species involved in post-transcriptional gene-product regulation[10]. In blood, miRNAs are stable because they are protected from degradation by extra-cellular vesicles (such as exosomes), RNA binding protein complexes (such as argonaute 2 – Ago2) and high-density lipoproteins[11,12]. The different circulating carriers for miRNA may reflect different pathways of release from cells; exosomal miRNAs may represent physiological release whereas miRNAs bound to Ago2 are increased with cell necrosis. As they are amplifiable and some are tissue restricted, miRNAs represent a reservoir for biomarker discovery. Liver-enriched miR-122-5p is released by injured hepatocytes and is a circulating biomarker for liver toxicity in zebrafish[13], rodents[14] and humans[15]. In patients with acetaminophen-induced liver injury circulating miR-122-5p has been reported to be increased around 100-fold compared to controls[15,16]. However, it is not known whether other miRNAs can out-perform miR-122-5p with regard to patient stratification.

The field of profiling multiple circulating miRNAs to discover signatures of toxicity is relatively new. In rodent models of acetaminophen toxicity there have been profiling studies of relatively small numbers of circulating miRNAs - these studies demonstrate that multiple miRNA species change with liver injury[17,18]. In humans, a miRNome subset of 372 miRNAs was quantified in 49 patients with acetaminophen hepatotoxicity or ischemic hepatitis[17]. This study confirmed that miRNAs were increased and decreased and suggested that certain species could distinguish between these distinct aetiologies of liver injury[17]. Changes in circulating miRNAs have also been reported in small numbers of hepatotoxicity patients analysed by high-throughput sequencing[18,19]. These studies did not address the unmet clinical need for improved patient stratification, back translate to pre-clinical models or identify signals of kidney toxicity. In the present study we recruited over 200 patients and assayed miRBase version 18 to identify which miRNAs were differentially expressed in plasma from overdose patients with and without acetaminophen toxicity (APAP-TOX and APAP-no TOX, respectively). Selected miRNA candidate biomarkers were tested for liver and kidney specificity in humans and mice, and sensitivity with regard to patient stratification at first presentation to hospital.

Results

Circulating miRNAs that were differentially expressed with acute liver injury. The experimental design used to identify differentially expressed miRNAs is presented in Fig. 1. In phase 1 of this discovery study, randomly selected APAP-TOX and APAP-no TOX samples were pooled and expressed miRNAs were identified. From 1809 miRNA species, 359 miRNAs fulfilled our criteria of expression (Ct value < 35 with a single, sharp melt peak) in at least one of the 4 sample pools (2 x APAP-TOX and 2 x APAP-no TOX). The patient demographics and clinical chemistry results from APAP-TOX and APAP-no TOX patients in the training set and test set are presented in supplementary Table 1. In Phase II, these 359 miRNAs were quantified in each of the 54 patient samples of the training set using a bespoke PCR array. The PCR results from phase II for each microRNA are presented in supplementary file 1. The PCR results from 1 sample in the APAP-TOX group did not have any amplification curves and this sample was excluded from further analyses. The phase II PCR profiling results: 75 miRNAs were 3-fold or more increased in the APAP-TOX patient group compared to the age- and sex-matched APAP-no TOX group. 46 miRNAs were 3-fold or more decreased in the APAP-TOX patient group. These data are presented in Fig. 2A as a volcano plot. The largest median (IQR) increased circulating miRNAs were miR-122-5p 68 (11–277), miR-885-5p 57 (17–372) and miR-151a-3p 57 (16–360) (Fig. 2B). A heatmap with cluster analysis of >3-fold increased/decreased circulating miRNAs in the APAP-no TOX and APAP-TOX patients from the training set is displayed in supplementary Figure 1. This heatmap demonstrates that APAP-TOX patients can be clustered into sub-groups based on the expression of miRNA panels. There was a group of patients with lower miR-30b-5p, miR-186-5p, miR-382-5p, miR-27a-3p, miR-15a-3p and miR15a-5p. These APAP-TOX patients were more unwell (INR 2.0 (16-3.4) v 1.4 (1.2–1.5) in rest of APAP-Tox group $P = 0.003$; serum creatinine 152 mg/dl (64–289) v 61 mg/dl (58–67) $P = 0.01$). The largest fold increase miRNAs (miR-122-5p and miR-885-5p) were highly correlated across patients in the

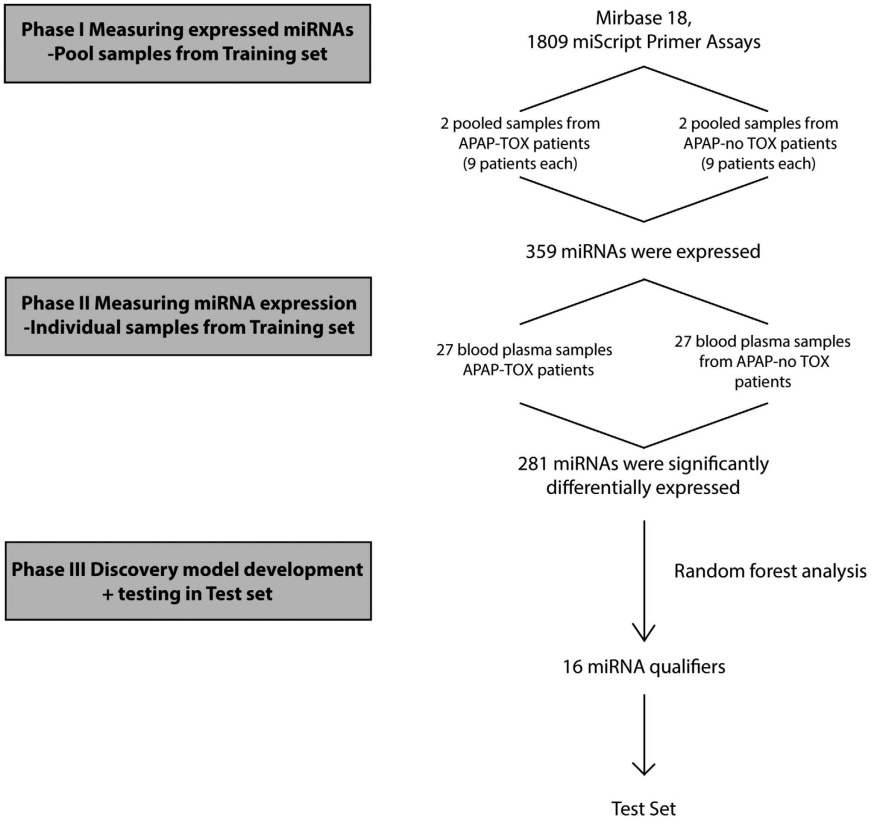

Figure 1. Study design. Phase I identified the expressed microRNAs (miRNAs) in pooled samples from acetaminophen toxicity (APAP-TOX) patients and acetaminophen overdose with no toxicity (APAP-no TOX) patients. In Phase II, expressed miRNAs were quantified in 27 APAP-TOX and 27 APAP-no TOX patients. For data processing, C_t values were calibrated for RNA recovery using the cel-miR-39-3p assay (which detects a synthetic miRNA spiked in to each sample during sample prep). In Phase III, random forest analysis was performed to develop the classifier model that was subsequently tested in the test set.

training set (Fig. 3A). miR-122-5p has been reported to circulate in a protein fraction of plasma rather than in extra-cellular vesicles although this has not been characterized in humans. After antibody-mediated pull down of Ago2 (corrected by IgG control), acetaminophen toxicity induced a significant increase in the amount of miR-122-5p and miR-885-5p specifically bound to Ago2 (Fig. 3B,C), consistent with both miRNAs being released bound to this protein. Interestingly there was no increase in miR-151a-3p, which suggests different mechanisms of release across miRNA species (Fig. 3D). *In situ* hybridization for miR-122-5p and miR-885-5p was performed on liver explants removed following acetaminophen overdose. Both these miRNAs localised to hepatocytes and their expression was reduced in the areas of centrilobular necrosis, consistent with release from injured cells (Fig. 3E).

Development and testing of miRNA diagnostic panels. In Phase III random forest statistics were used to identify which miRNAs separate APAP-TOX from APAP-no TOX. The analysis demonstrated that 16 miRNAs ('classifier model') had the lowest prediction error - the largest marginal decrease in prediction accuracy when their values are randomly permuted (Fig. 4A). This classifier model was tested in an independent test set of 81 patient samples (Fig. 4B). The probability of a sample being correctly classified by the miRNA model as APAP-TOX was significantly higher when the true classification was APAP-TOX (median percent probability (IQR): 75 (63–77) for true APAP-TOX; 44 (43–47) for true APAP-no TOX; $P < 0.0001$). For an APAP-TOX classification probability cut-off of 50% (i.e. higher probability of APAP-TOX than APAP-no TOX) the classifier series sensitivity was 90% (95% CI: 76 to 97) and specificity was 90% (77 to 97) (Fig. 4B).

Specificity of candidate miRNA biomarkers. The 3 largest fold increase miRNAs (miR-122-5p, miR-885-5p and miR-151a-3p) and the miRNA with the lowest prediction error from the classifier model (miR-382-5p) were taken forward and tested for specificity and sensitivity.

Human specificity studies. In patients with acute liver injury (ALI) due to a diverse range of non-acetaminophen causes, all 4 miRNA species were significantly changed in their circulating

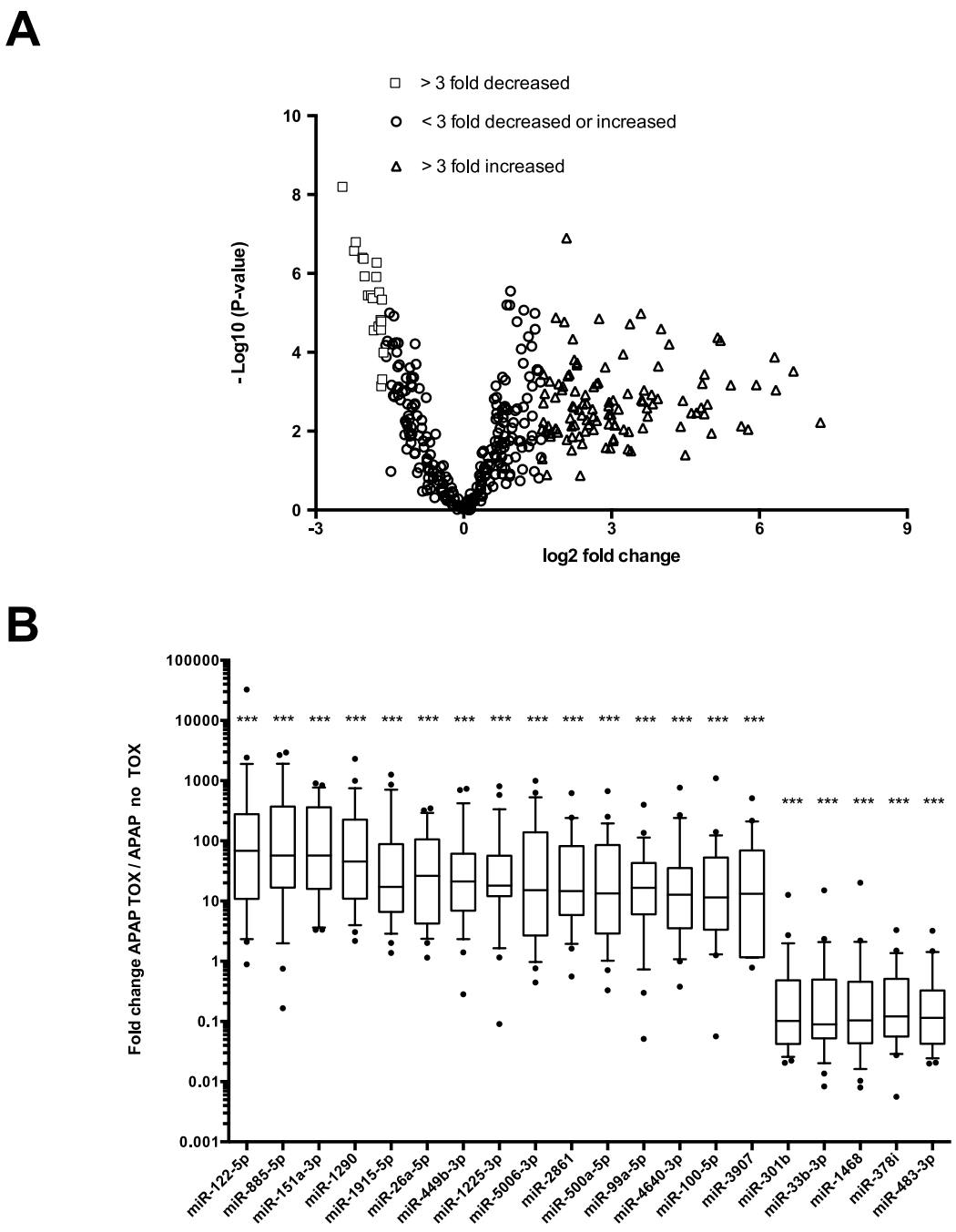

Figure 2. Differentially expressed circulating microRNAs (miRNAs) with toxicity. (**A**) Volcano plot of miRNA data when acetaminophen toxicity (APAP-TOX) patients were compared with age and sex matched acetaminophen no toxicity (APAP-no TOX) patients. The negative logarithm base 10 of the P-value is plotted against log 2 difference in estimated relative expression values. Respectively, the triangles and squares correspond to miRNAs that were more than 3 fold increased or decreased in the APAP-TOX patients relative to the APAP-no TOX patients. (**B**) Box-and-whisker plots displaying the top 15 highest fold increase miRNAs and 5 highest fold decrease miRNAs. The fold regulation was calculated using the $2^{-\Delta\Delta Ct}$ method. Statistically significant differences were determined by Wilcoxon matched-pairs signed rank test using $2^{-\Delta Ct}$. Ct values were normalized using global Ct mean. Statistically significant differences were determined by Mann Whitney Test using ΔCt values. ***$P < 0.001$; **$P < 0.01$; *$P < 0.05$.

concentration to levels comparable with the APAP-TOX group (Fig. 5A–D). The kidney is commonly injured in the setting of ALI so could be the tissue of origin for circulating miRNAs and kidney dysfunction could affect the circulating concentration of liver-derived miRNAs by altering their clearance. Two complementary approaches were used to determine miRNA liver specificity in the presence of kidney

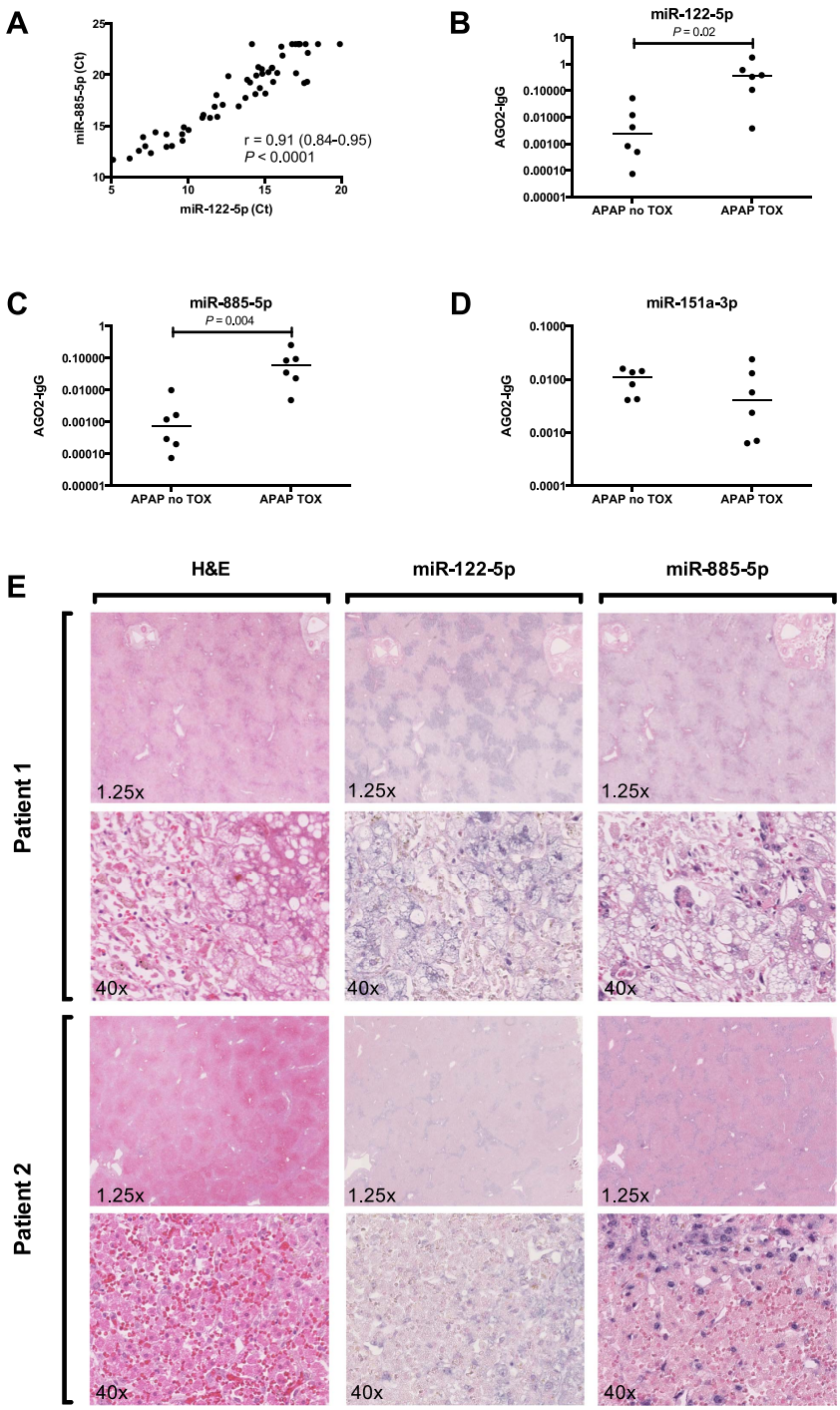

Figure 3. miR-122-5p and miR-885-5p are released from human hepatocytes bound to the carrier protein Ago2. Figure (**A**) Pearson correlation plot of circulating miR-885-5p and miR-122-5p across APAP-TOX and APAP-no TOX patients. Figure (**B**–**D**) represent the relative Ago2 fraction for miR-122-5p, miR-885-5p and miR-151a-5p respectively in APAP-TOX (N = 6) and APAP-no TOX (N = 6) patients. The Y axis represents the $2^{-\Delta Ct}$ value obtained from the Ago2 pull-down minus the $2^{-\Delta Ct}$ value obtained from the IgG pull-down from the same sample, both normalised by spiked-in synthetic miR-39. Statistically significant differences were determined by Mann Whitney Test. Figure (**E**) presents liver tissue from 2 patients whom underwent liver transplantation for severe acute liver failure due to acetaminophen overdose. Images from hematoxylin and eosin (H&E) and *in situ* hybridization for miR-122-5p and miR-885-5p are presented.

injury. APAP-TOX patients without and with kidney dysfunction (serum creatinine concentration >110 μmol/L) were compared across the training and test sets (supplementary Table 2). There was an increase in the median PCR-array Ct value with kidney dysfunction, consistent with a overall reduction

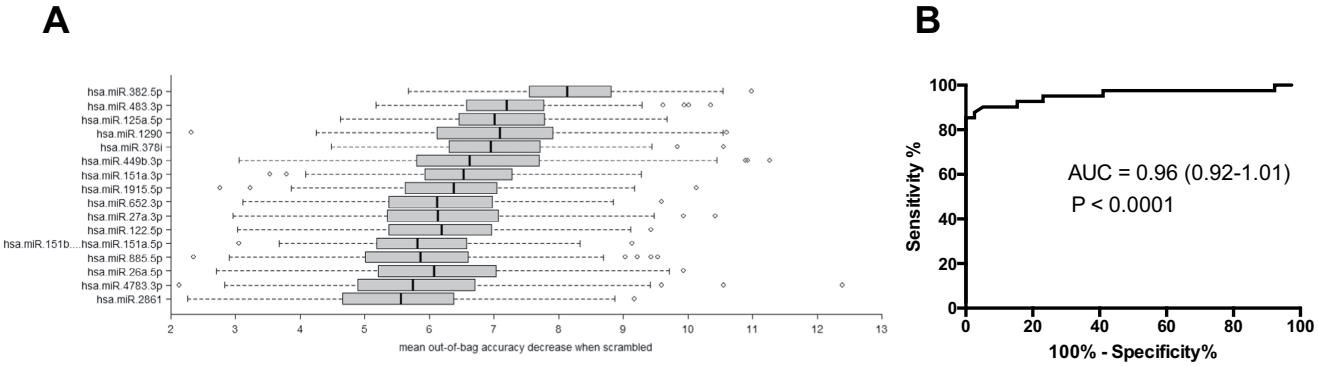

Figure 4. Random forest statistics analysis. Figure (**A**) presents the top 16 miRNAs that separate APAP-TOX from APAP-no TOX in the training set. miRNAs were ranked according to the marginal decrease in out-of-bag prediction accuracy when the gene's expression measurements are scrambled. Figure (**B**) Receiver operator characteristic curve displaying the performance of the top 16 miRNAs from the training set with regard to distinguishing APAP-TOX from APAP- no TOX in the test set.

in circulating miRNAs (APAP-TOX no AKI: 16.55 (15.78–17.49); APAP-TOX AKI: 18.01 (16.84–19.02). P = 0.0007). However, there was no difference in miR-122-5p, miR-885-5p, miR-151a-3p or miR-382-5p (Table 1). The miRNAs that were significantly changed with kidney dysfunction are presented in Table 1.

Mouse specificity studies. Mouse models of acetaminophen and cisplatin toxicity were compared with regard to miRNA circulating concentrations, cisplatin toxicity being a well-established model of drug-induced AKI. Acetaminophen induced liver injury was confirmed by a median (IQR) serum ALT activity of 7230IU/L (5355–23615, N = 8) and histologically by centrilobular hepatic necrosis. By contrast with vehicle treated controls (N = 7), acetaminophen toxicity in mice resulted in increased miR-122-5p and miR-151a-3p, and decreased miR-382-5p, in line with our human data (Fig. 5E–H). However, miR-885-5p was not translatable across species and did not change. Cisplatin-induced AKI was demonstrated by significant elevations in urinary KIM-1 concentration (control: 1322 pg/mgUCr (766–1460); cisplatin 10,964 pg/mgUCr (4493–16003). N = 7, P = 0.0003) and histologically, there were apoptotic proximal tubular cells, sloughing and an overall reduced number of epithelial cells. Cisplatin had no effect on miR-122-5p, miR-885-5p, miR-151a-3p or miR-382-5p (Fig. 5E–H).

Human case report. To further define temporal changes, miRNA candidate biomarkers were measured in serial samples from a 49 year-old man who presented to hospital soon after a large overdose (4 hour acetaminophen concentration: 405 mg/L) with initially normal serum ALT activity (28 U/L) and kidney function (serum creatinine: 83 μmol/L). Despite prompt NAC treatment (started 6 hours after overdose), the patient subsequently developed significant liver injury (peak ALT: 12,353 U/L) with coagulopathy (peak INR: 2.8) and kidney injury (peak creatinine: 151 μmol/L) (Fig. 6F–H). The patient's liver injury recovered with continued NAC treatment, providing an opportunity to track miRNA concentrations from no apparent injury, into significant organ injury and through to liver recovery. The temporal profiles of the individual miRNAs were different; miR-122-5p concentration was elevated but decreased earlier than ALT (Fig. 6A). miR-885-5p remained elevated longer than miR-122-5p (Fig. 6B). In line with the array data, both miR-382-5p and miR-19a substantially decreased in concentration and, interestingly, they remained below the hospital admission level (Fig. 6C,D). miR-34a initially increased but then fell to below the admission concentration, a decrease which corresponded temporally with increased serum creatinine concentration (Fig. 6E).

Identification of endogenous miRNA normalizers. To identify which miRNAs were most stably expressed across APAP-TOX and APAP-no TOX patients NormFinder analysis was performed on the training set data. miR-1287 was the most stably expressed with a stability value of 1.22*10−5. All results from the NormFinder assessment are reported in supplementary Table 3. miR-1913, miR-671, miR-1287, Let-7d, miR-1260 and miR-324 were taken forward and measured in the APAP-early patient samples using RT-PCR. The demographics and standard clinical chemistry for this patient cohort are presented in supplementary Table 4. In accordance with the NormFinder assessment, miR-1287 was most stably expressed across the different samples with a coefficient of variation (CV) of 1.71% (supplementary Figure 2).

Sensitivity - comparison of leading microRNA discriminators with ALT as a diagnostic of early ALI. In the 67 APAP-early patients, miR-122-5p identified subsequent liver injury when normalized by

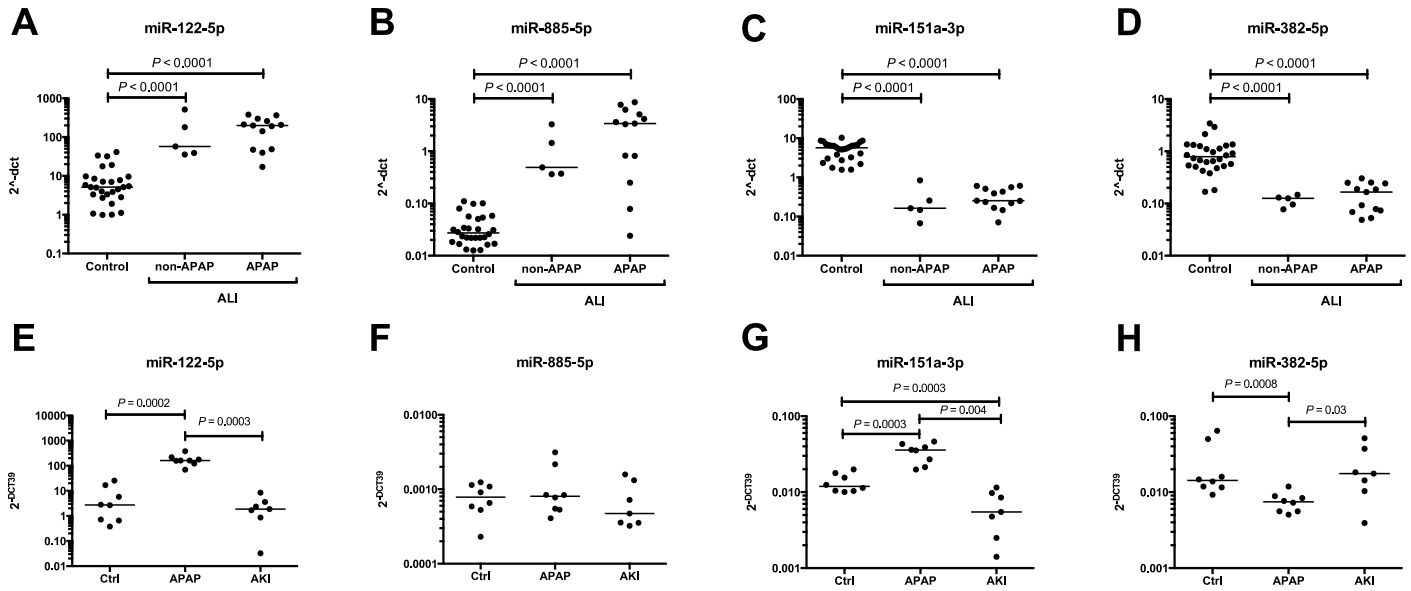

Figure 5. Biomarker specificity for liver injury. Figure (**A**–**D**) present circulating miR-122-5p, miR-885-5p, miR-151a-3p and miR-382-5p in APAP-no TOX patients and patients with acute liver injury (ALI) induced by APAP overdose or another aetiology (non-APAP). Figure (**E**–**H**) present miR-122-5p, miR-885-5p, miR-151a-3p and miR-382-5p in control mice, APAP overdose mice and cisplatin-induced acute kidney injury (AKI) mice. Values represent $2^{-\Delta Ct}$ normalised by miR-1287 in human samples and spiked in synthetic miR-39 in mice samples. Statistically significant differences were determined by Wilcoxon matched-pairs signed rank test.

miRNA	Fold change	*P* value	ROC-AUC (95% CI)	*P* value	SENS (95% CI)
miR-19a-3p	−3.76	**<0.0001**	0.76 (0.66–0.86)	**<0.0001**	0.51 (0.35–0.67)
miR-19b-3p	−4.10	**0.001**	0.73 (0.61–0.85)	**0.001**	0.27 (0.12–0.46)
miR-192-5p	−1.66	**0.001**	0.73 (0.61–0.85)	**0.001**	0.20 (0.08–0.39)
miR-34a-5p	−5.71	**0.003**	0.71 (0.58–0.83)	**0.003**	0.20 (0.08–0.39)
miR-3187-3p	−5.30	**0.005**	0.70 (0.58–0.83)	**0.005**	0.47 (0.28–0.66)
miR-122-5p	1.28	0.92	0.51 (0.36–0.65)	0.92	0.27 (0.12–0.46)
miR-885-5p	1.25	0.73	0.53 (0.38–0.67)	0.72	0.33 (0.17–0.53)
miR-151a-3p	1.28	0.27	0.58 (0.44–0.72)	0.27	0.10 (0.02–0.27)
miR-382-5p	1.46	0.67	0.53 (0.39–0.68)	0.67	0.17 (0.06–0.35)

Table 1. Comparison of circulating miRNAs in acetaminophen-induced acute liver injury patients with and without kidney dysfunction. ROC-AUC (area under the curve with 95% CI), sensitivity (SENS with 95% CI) at 90% specificity and statistical significance are given. Negative fold change means lower with kidney dysfunction.

any of the 6 endogenous miRNA normalizers described above (miR-122-5p area under ROC curve normalized by miR-1913, 0.97 (95% CI 0.92–1.01); miR-671, 0.96 (0.92–1.01); miR-1287, 0.95 (0.90–1.00); let7-d, 0.94 (0.89–1.00); miR-1260, 0.93 (0.88–1.00); miR-324, 0.93 (0.87–1.00) miR-122-5p ROC-AUC significantly larger than all other miRNAs – $P < 0.05$). miR-885-5p, miR-151a-5p and miR-382-5p were inferior to ALT for early prediction of liver injury (Fig. 7). When the largest fold increase and decrease phase II miRNAs were combined (miR-122-5p and miR-483-3p, respectively) there was a modest increase in the area under the ROC curve compared with miR-122-5p alone. No other miRNA combination improved predictive accuracy (data not shown).

Discussion

To date, this is the largest and most comprehensive study of the circulating miRNome in humans with acetaminophen toxicity. We identified multiple miRNA species that separated APAP-TOX from APAP-no TOX in a training set of patients, then tested the panels in a separate patient cohort. The large number of

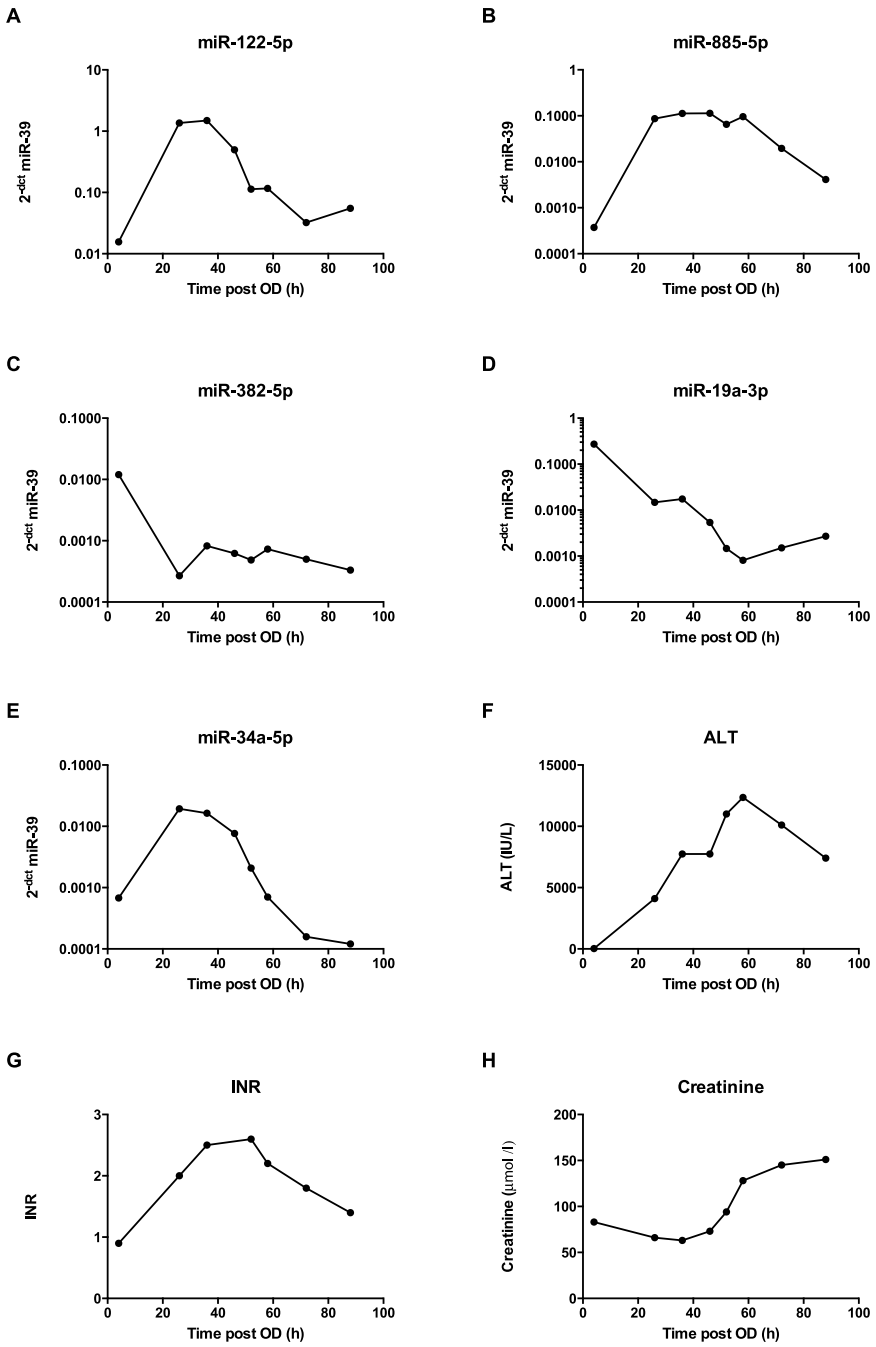

Figure 6. Timeline of current and novel miRNA biomarkers following a large acetaminophen overdose in a 49 year-old male. Values for miRNA represent $2^{-\Delta Ct}$ normalised by spiked-in synthetic miR-39.

miRNAs that were screened in this study (1809) allowed the identification of novel miRNA species that report toxicity. The largest fold change miRNAs (miR-122-5p, miR-885-5p and miR-151-3p) and the best discriminating miRNA (miR-382-5p) were taken forward and tested for specificity. Although variable, they report acute liver injury across patients and mouse models, even in the presence of kidney injury. Kidney injury resulted in significantly decreased miRNAs that represent new circulating biomarker candidates. The most stable internal miRNA normalizers were discovered and used to normalize miRNAs to compare with ALT activity with regard to sensitivity (the stratification of patients at first presentation to hospital). miR-122-5p very accurately predicted liver injury at first presentation to hospital, especially when combined with the largest decrease miRNA.

This study reported that 75 circulating miRNA species were more than 3-fold increased with acute liver injury, demonstrating the potential of multiple miRNA species as biomarkers. miRNAs identified in the training set of patients were validated in a separate patient cohort from a separate clinical unit. This 16-miRNA 'signature' of acute liver injury accurately identified toxicity. The most abundant miRNA

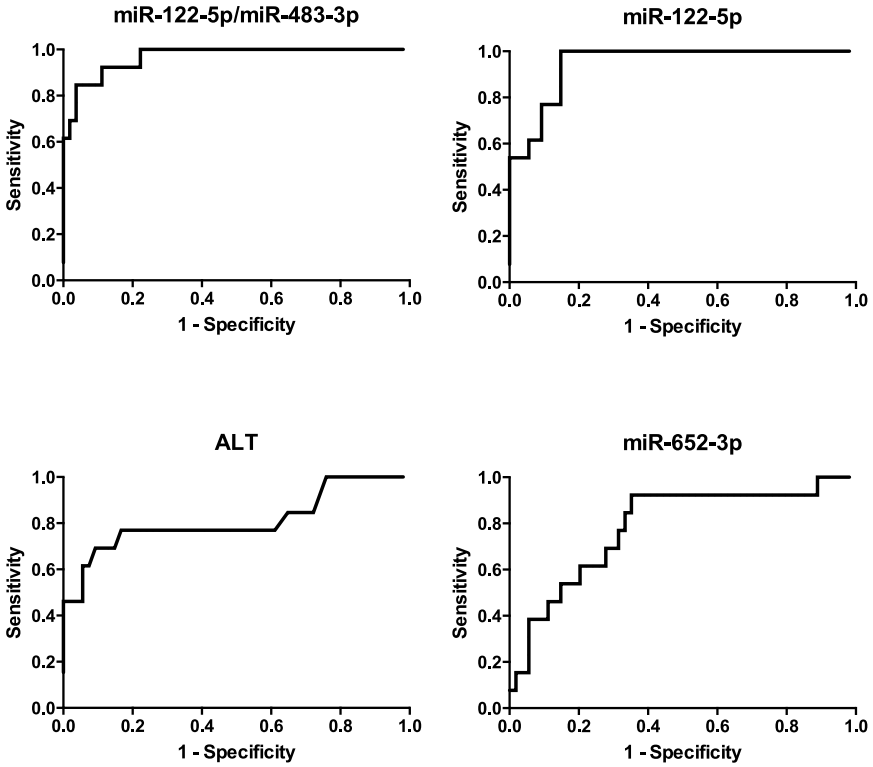

Biomarker	ROC-AUC (95% CI)	SENS (95% C.I.)	PPV (%)	NPV (%)	P Value
miR-122-5p/miR-483-3p	0.97 (0.93-1.01)	0.85 (0.55-0.98)	69	96	< 0.0001
miR-122-5p	0.95 (0.90-1.00)	0.62 (0.32-0.86)	62	91	< 0.0001
ALT	0.81 (0.65-0.97)	0.69 (0.39-0.91)	64	92	0.0006
miR-652-3p	0.78 (0.64-0.92)	0.38 (0.14-0.68)	50	86	0.002
miR-151a-3p	0.71 (0.57-0.85)	0.61 (0.47-0.74)	62	91	0.02
miR-483-3p	0.70 (0.55-0.84)	0.23 (0.05-0.54)	38	83	0.03
miR-885-5p	0.66 (0.50-0.83)	0.41 (0.28-0.55)	50	86	0.07
miR-125a-5p	0.65 (0.29-0.77)	0.43 (0.29-0.77)	55	88	0.01
miR-382-5p	0.59 (0.42-0.76)	0.26 (0.15-0.40)	38	83	0.32
miR-449b	0.56 (0.40-0.73)	0.23 (0.05-0.54)	38	83	0.48

Figure 7. Biomarker sensitivity - ROC curve analysis supports the potential for miR-122-5p to predict the development of ALI. ROC analysis was calculated to determine the potential for plasma miRNAs and serum ALT activity to predict the development of TOX at first presentation to hospital following acetaminophen overdose. TOX was defined as >3xULN ALT activity during hospital admission. The ROC curves of the 4 most accurate predictors are presented. AUC (area under the curve with 95% CI), sensitivity (SENS at 90% specificity) with 95% CI, positive and negative predictive values (PPV and NPV) and statistical significance for AUC value is presented in table. The miRNAs are normalized by miR-1287.

species in the liver[20], miR-122-5p, was the highest increased circulating miRNA but other species were elevated to comparable degrees (miR-885-5p, miR-151-3p) or were ranked higher by random forest analysis in terms of ability to report injury (miR-382-5p). Circulating miRNAs are stable because they are either bound to proteins or encapsulated in extra-cellular vesicles (or both). The presence of miRNA in vesicles such as exosomes is controversial, with some studies reporting very low amounts in the exosomal cargo[21]. Also extra-cellular vesicles contain Ago2 suggesting there is not a clear division between the two circulating fractions. For the first time we demonstrate that human miR-122-5p circulates bound to the protein Ago2 and this fraction increases with liver injury. Ago2-bound miR-885-5p also increases with injury and both these miRNAs were localised to hepatocytes by *in situ* hybridization on human liver explants removed at transplantation for acetaminophen toxicity. These data suggest release of miR-122 and miR-885 from the same cells attached to the same carrier protein.

The 3 highest fold increase miRNAs and the leading discriminator in our model were tested for specificity. Across all our human array studies and in mice models miR-382-5p decreased in circulating

concentration with liver injury. The mechanism of this circulating decrease of miR-382-5p is unknown, but conceptually could be either a decrease in production (such as reduced gene transcription in the injured liver) or increased clearance. Given that more miRNAs increase than decrease in the circulation with acute liver injury it would require a highly selective process of altered clearance to explain the specific decrease in miR-382-5p and decreased tissue expression seems more plausible. miR-122-5p, miR-885-5p, miR-151-3p and miR-382-5p reported acute liver injury due to causes other than acetaminophen, which is consistent with them being liver specific and demonstrates that this panel has utility in the diagnosis of acute liver injury due to multiple causes. Furthermore, none of this panel changed with kidney injury in humans or mice, which also supports liver specificity and validates their use in patients with liver and kidney injury, which commonly co-exist in life-threatening acute liver failure. There were miRNA species that changed with kidney dysfunction and they consistently decreased in circulating concentration. A general fall in circulating miRNA concentrations has been reported in chronic kidney disease and suggested to be due increased blood RNAase activity[22]. Our data would suggest AKI also reduces most, but not all, circulating miRNAs. In the present study the performance of the leading miRNA, miR-19a, was modest with regard to separating liver injury from liver and kidney injury (ROC-AUC 0.76). However, human diagnostic performance may be improved when multiple time points post-drug exposure are analysed in larger studies. This is supported by the case reported in this paper, which demonstrated a decrease in miR-19a before serum creatinine was elevated. By definition, the patients with kidney dysfunction had more severe acetaminophen toxicity and differences in circulating miRNAs could reflect more severe liver injury rather than kidney injury *per se*. Whether miRNA species such as miR-19a are truly kidney specific or represent liver toxicity prognosis markers is an important area for further development.

It is widely reported that miRNAs translate across species; for example, we have reported that miR-122-5p reports liver injury in cell models, zebrafish, rodents and humans. Our array data are consistent with smaller acetaminophen studies performed in rodents: 586 miRNA species were measured in mice[14] and 750 miRNA species were measured in rats[23]. In addition to miR-122-5p, the miRNA species miR-22, miR-29b, miR-29c, miR-130a and miR-193 were increased in both mice and humans. In rats, in addition to miR-122-5p, the increase of miR-22, miR-193 and miR-194 was in accordance with our human data[23]. This demonstrates the translational potential of miRNAs across rodents and humans. However, the data presented in this study clearly demonstrate that miR-885-5p does not increase with acetaminophen toxicity in mice, an important limitation. Comparative biomarker profiles for miR-122-5p, miR-885-5p, miR-151-3p and miR-382-5p are summarized in supplementary Table 5.

Although miR-122-5p had the highest fold increase in APAP-TOX patients, it was ranked 11th place in the miRNA panel, suggesting that other microRNA species may have greater clinical utility. As a first step in determining the clinical utility of our miRNA panel, the performance of selected members was compared with ALT with regard to patient stratification at first presentation to the ED. These patients were recruited from a different hospital to the training and test patient sets (London as compared to Edinburgh). ROC analysis revealed that miR-122-5p was superior to ALT activity with regard to predicting APAP-TOX in early APAP patients. This observation confirms our previous investigation, in which miR-122-5p displayed superior predictive value over ALT activity at the hospital 'front door', in a separate cohort of patients from a different hospital[16]. miRNA species were identified which were stable across patients with and without organ injury. These internal normalizers can be used to report sample degradation and failed miRNA extraction from plasma. Therefore, they are of value for future studies of acute liver injury providing their stability is confirmed in each specific clinical study. When normalized by any of the stable miRNAs, miR-122-5p was superior to ALT. At first presentation, miR-122-5p was also superior to other miRNAs with regard to prediction of subsequent liver injury. This important result may reflect the high abundance of miR-122-5p within the hepatocyte compared to other miRNAs, its high degree of tissue selectivity, potential different pathways of release from injured cells (although miR-885-5p is also bound to same protein), different stability in the circulation or miR-122-5p having a higher baseline circulating concentration. Interestingly, combining miR-122-5p with miR-483-3p resulted in an increase in predictive accuracy (as judged by the largest area under the ROC curve). While this is hypothesis generating, it may be that combining miRNAs that increase and decrease represents the optimal biomarker qualification strategy.

In conclusion, miRNA panels are associated with liver and kidney toxicity in patients with acetaminophen overdose. These panels include novel miRNAs not previously described as toxicology biomarkers. For patient stratification at first presentation to hospital miR-122-5p is the lead miRNA candidate for clinical development, possibly in combination with miR-483-3p. Use of miRNA biomarkers could allow earlier prediction of patients at risk of organ injury and enable targeted intervention in these patients; furthermore they could allow earlier prediction of patients at low risk and enable shorter antidotal treatment regimens and reduce length of hospital stay.

Patients and Methods

Patient Cohorts. The local research ethics committee approved the study and informed consent was obtained from all patients before entry into the study. The study was carried out in accordance with the approved relevant guidelines.

Acetaminophen toxicity (APAP-TOX) patients. A total of 68 adult patients (aged 16 years and above) admitted to the Royal Infirmary of Edinburgh (RIE), UK with ALI, secondary to acetaminophen ingestion, were entered into the study. ALI was defined as a sudden deterioration in liver function in the absence of a history of chronic liver disease with a clear history of excess acetaminophen ingestion. All patients received intravenous NAC treatment.

There were two separate cohorts within this APAP-TOX group. First, patients admitted to the Clinical Toxicology Unit at RIE with a peak serum ALT activity greater than 3 x upper limit of normal (>150 U/L) formed the training set (N = 27). Second, patients admitted to the Scottish Liver Transplantation Unit at RIE with peak ALT > 150 U/L formed the test set (N = 41). There was no patient overlap between training and test sets. Blood samples with peak hospital stay ALT activity were analysed in both training and test sets.

Acetaminophen no toxicity (APAP-no TOX) patients. 67 patients were recruited from RIE. The entry criterion was a history of acetaminophen ingestion in overdose that required treatment with NAC as per UK guidelines at the time of hospital admission[24]. All patients had a plasma acetaminophen concentration above the Prescott nomogram, which confirmed potentially toxic exposure. Blood was collected at the end of the intravenous NAC infusion for measurement of serum ALT activity and absence of liver injury was confirmed by a normal serum ALT activity (<50 U/L). APAP-no TOX patients were age- and sex-matched with the training and test set APAP-TOX patients. There was no patient overlap between training and test set. Blood from the end of NAC treatment was used in this study.

Acute liver injury not due to acetaminophen (Non-APAP ALI). Samples from 5 subjects with ALI not due to acetaminophen were recruited to this study. The causes of injury were autoimmune hepatitis, primary graft non-function, small-for-size syndrome, malignancy and clarithromycin-induced liver injury.

First presentation to hospital patients (APAP-early). These patients (total N = 67) were all recruited from St Thomas' Hospital, London UK. Inclusion criteria were: adult with a clear history of excess acetaminophen ingestion and a timed blood acetaminophen concentration that was judged by the treating physician to necessitate hospital admission for intravenous NAC therapy, as per UK guidelines at the time of study. All patients completed the full course of NAC treatment. For all study participants, demographic data and blood results were recorded. ALI was defined as peak serum ALT activity greater than 3x the upper limit of the normal range (>150 IU/L), the UK indication for continuing NAC therapy after completion of the initial regimen. The first blood sample at presentation to hospital was collected for the APAP-early cohort.

In all groups, blood samples were centrifuged at 1000 × g for 15 minutes at 4 °C. The supernatant was then separated into aliquots and stored at −80 °C until analysis.

MicroRNA profiling of training set. In the training set 27 APAP-TOX samples were compared with 27 APAP-no TOX samples. The methods for profiling are described in the supplemental methods.

MicroRNA profiling of test set. In the test set 41 APAP-TOX samples were compared with 40 APAP-no TOX samples. miRNA species were selected based on fold change from the training set results. Sample processing was as described for the training set and real-time PCR was again performed on a Fluidigm BioMark HD.

Ago2-associated miRNA isolation. Magna Bind goat anti-mouse IgG magnetic bead slurry, 100 μL, (Thermo Scientific, Waltham, USA) was incubated with 10 μg of mouse monoclonal anti-Ago2 (Abcam, Cambridge, UK) or mouse normal IgG (Santa Cruz Biotechnology, Dallas, US) antibodies for 2 h at 4 °C. The antibody-coated beads were then added to plasma and incubated overnight at 4 °C with rotation. Beads were washed and each sample then eluted in RNAse free water before QIAzol was added for RNA isolation. Ago2 isolation was determined by western blot analysis.

Targeted miRNA measurement. Selected miRNAs were quantified in plasma samples by RT-qPCR as described in the supplemental methods. *In situ* hybridisation was performed on human liver removed at the time of transplantation (explant) using methods described in our previous study[13]. The patients had severe acute liver failure secondary to acetaminophen overdose.

Mouse models of liver and kidney toxicity. Mouse studies were in accordance the Animals (Scientific Procedures) Act 1986 and approved by the local Animal Ethics Committee. In brief, male CD1 mice (28–33 g) were treated with either 0.9% saline, cisplatin (20 mg/kg) or acetaminophen (350 mg/kg) IP. At 24–72 hours after treatment, blood was collected via cardiac puncture and allowed to clot before isolation of serum which was stored at −80 °C. Tissue samples were collected and either snap frozen or fixed in neutral buffered formalin (10%).

Statistical analysis. Data are presented as median and range or interquartile range (IQR). Each dataset was analysed for normality using a Shapiro-Wilk test. For nonparametric datasets, comparisons were made using the Mann-Whitney U test or Wilcoxon matched-pairs signed rank test. All calculations and receiver operator characteristic (ROC) curves were performed using GraphPad Prism software (GraphPad Software, La Jolla, CA). Profiling data were analysed by random forests to give an estimate of how well we can classify individuals in a new data set into each group. Random forests create a set of classification trees based on continual sampling of the experimental units and compounds. Each observation is then classified based on the majority votes from all of the classification trees. Details of random forest analysis can be found in the supplemental methods.

References

1. Larson, A. M. *et al.* Acetaminophen-induced acute liver failure: results of a United States multicenter, prospective study. *Hepatology (Baltimore, Md.)* **42,** 1364–1372, doi: 10.1002/hep.20948 (2005).
2. Bernal, W., Auzinger, G., Dhawan, A. & Wendon, J. Acute liver failure. *Lancet* **376,** 190–201, doi: 10.1016/s0140-6736(10)60274-7 (2010).
3. Hinson, J. A., Roberts, D. W. & James, L. P. Mechanisms of acetaminophen-induced liver necrosis. *Handbook of experimental pharmacology*. 369–405, doi: 10.1007/978-3-642-00663-0_12 (2010).
4. Antoine, D. J. *et al.* Molecular forms of HMGB1 and keratin-18 as mechanistic biomarkers for mode of cell death and prognosis during clinical acetaminophen hepatotoxicity. *Journal of hepatology* **56,** 1070–1079, doi: 10.1016/j.jhep.2011.12.019 (2012).
5. Smilkstein, M. J., Knapp, G. L., Kulig, K. W. & Rumack, B. H. Efficacy of oral N-acetylcysteine in the treatment of acetaminophen overdose. Analysis of the national multicenter study (1976 to 1985). *The New England journal of medicine* **319,** 1557–1562, doi: 10.1056/nejm198812153192401 (1988).
6. Bateman, D. N. *et al.* Reduction of adverse effects from intravenous acetylcysteine treatment for paracetamol poisoning: a randomised controlled trial. *Lancet* **383,** 697–704, doi: 10.1016/s0140-6736(13)62062-0 (2014).
7. Dear, J. W. & Antoine, D. J. Stratification of paracetamol overdose patients using new toxicity biomarkers: current candidates and future challenges. *Expert review of clinical pharmacology* **7,** 181–189, doi: 10.1586/17512433.2014.880650 (2014).
8. Blakely, P. & McDonald, B. R. Acute renal failure due to acetaminophen ingestion: a case report and review of the literature. *Journal of the American Society of Nephrology: JASN* **6,** 48–53 (1995).
9. Star, R. A. Treatment of acute renal failure. *Kidney international* **54,** 1817–1831, doi: 10.1046/j.1523-1755.1998.00210.x (1998).
10. Bartel, D. P. MicroRNAs: target recognition and regulatory functions. *Cell* **136,** 215–233, doi: 10.1016/j.cell.2009.01.002 (2009).
11. Mitchell, P. S. *et al.* Circulating microRNAs as stable blood-based markers for cancer detection. *Proceedings of the National Academy of Sciences of the United States of America* **105,** 10513–10518, doi: 10.1073/pnas.0804549105 (2008).
12. Vickers, K. C., Palmisano, B. T., Shoucri, B. M., Shamburek, R. D. & Remaley, A. T. MicroRNAs are transported in plasma and delivered to recipient cells by high-density lipoproteins. *Nature cell biology* **13,** 423–433, doi: 10.1038/ncb2210 (2011).
13. Vliegenthart, A. D. *et al.* Retro-orbital blood acquisition facilitates circulating microRNA measurement in zebrafish with paracetamol hepatotoxicity. *Zebrafish* **11,** 219–226, doi: 10.1089/zeb.2013.0912 (2014).
14. Wang, K. *et al.* Circulating microRNAs, potential biomarkers for drug-induced liver injury. *Proceedings of the National Academy of Sciences of the United States of America* **106,** 4402–4407, doi: 10.1073/pnas.0813371106 (2009).
15. Starkey Lewis, P. J. *et al.* Circulating microRNAs as potential markers of human drug-induced liver injury. *Hepatology (Baltimore, Md.)* **54,** 1767–1776, doi: 10.1002/hep.24538 (2011).
16. Antoine, D. J. *et al.* Mechanistic biomarkers provide early and sensitive detection of acetaminophen-induced acute liver injury at first presentation to hospital. *Hepatology (Baltimore, Md.)* **58,** 777–787, doi: 10.1002/hep.26294 (2013).
17. Ward, J. *et al.* Circulating microRNA profiles in human patients with acetaminophen hepatotoxicity or ischemic hepatitis. *Proceedings of the National Academy of Sciences of the United States of America* **111,** 12169–12174, doi: 10.1073/pnas.1412608111 (2014).
18. Krauskopf, J. *et al.* Application of high-throughput sequencing to circulating microRNAs reveals novel biomarkers for drug-induced liver injury. *Toxicological sciences: an official journal of the Society of Toxicology* **143,** 268–276, doi: 10.1093/toxsci/kfu232 (2015).
19. Yang, X. *et al.* Potential of extracellular microRNAs as biomarkers of acetaminophen toxicity in children. *Toxicology and applied pharmacology*. doi: 10.1016/j.taap.2015.02.013 (2015).
20. Chang, J. *et al.* miR-122, a mammalian liver-specific microRNA, is processed from hcr mRNA and may downregulate the high affinity cationic amino acid transporter CAT-1. *RNA biology* **1,** 106–113 (2004).
21. Chevillet, J. R. *et al.* Quantitative and stoichiometric analysis of the microRNA content of exosomes. *Proceedings of the National Academy of Sciences of the United States of America* **111,** 14888–14893, doi: 10.1073/pnas.1408301111 (2014).
22. Neal, C. S. *et al.* Circulating microRNA expression is reduced in chronic kidney disease. *Nephrology, dialysis, transplantation: official publication of the European Dialysis and Transplant Association - European Renal Association* **26,** 3794–3802, doi: 10.1093/ndt/gfr485 (2011).
23. Su, Y. W. *et al.* A panel of serum microRNAs as specific biomarkers for diagnosis of compound- and herb-induced liver injury in rats. *PloS one* **7,** e37395, doi: 10.1371/journal.pone.0037395 (2012).
24. Thanacoody, H. K. *et al.* Scottish and Newcastle antiemetic pre-treatment for paracetamol poisoning study (SNAP). *BMC pharmacology & toxicology* **14,** 20, doi: 10.1186/2050-6511-14-20 (2013).

Acknowledgements

Author ADBV was supported by an NC3Rs PhD Studentship (NC/K001485/1). Author JWD acknowledges the support of an NHS Research Scotland (NRS) Career Research Fellowship through NHS Lothian and the UK Regenerative Medicine Platform Niche Hub. Author KJS acknowledges the support from the Chief Scientist Office, Scotland (ETM/191).

Author Contributions

The authors have contributed to the manuscript by planning the study (A.D.B.V., J.M.S., E.L. and J.W.D.), collecting the data (A.D.B.V., J.M.S., L.E.J.P., J.I.C., A.T. and J.S.), patient identification and recruitment (D.N.B., D.M.W., P.I.D., D.C. and J.K.M.) analysis of data (A.D.B.V., J.M.S., L.E.J.P., J.K.M. and J.W.D.), and preparation and revision of the manuscript (all authors).

Additional Information

Supplementary information accompanies this paper at http://www.nature.com/srep

Competing financial interests: The authors declare no competing financial interests.

How to cite this article: Vliegenthart, A. D. B. *et al.* Comprehensive microRNA profiling in acetaminophen toxicity identifies novel circulating biomarkers for human liver and kidney injury. *Sci. Rep.* **5**, 15501; doi: 10.1038/srep15501 (2015).

2.2 Contributions by the candidate

Measurement of the miRNA panel and 6 endogenous miRNA normalisers in the 67 Paracetamol overdose patient samples collected directly after presenting to the hospital; Argonaut pulldown with subsequent miRNA measurements in a selection of patient samples; Measurement of miRNAs in samples from the case report for producing the timeline; miRNA measurements in the mouse samples from Paracetamol overdose mice and cisplatin-induced kidney injury mice; All statistical analyses apart from the Random forest analysis; Producing all figures apart from figure 4A; Writing and revising the manuscript.

2.3 Discussion

To date, this is the largest and most comprehensive study of the circulating miRNome in humans with paracetamol toxicity. We identified multiple miRNA species that separated APAP-TOX from APAP-no TOX in a training set of patients, then tested the panels in a separate patient cohort. The large number of miRNAs that were screened in this study (1809) allowed the identification of novel miRNA species that report toxicity. The largest fold change miRNAs (miR-122-5p, miR-885-5p and miR-151-3p) and the best discriminating miRNA (miR-382-5p) were taken forward and tested for specificity. Although variable, they reported acute liver injury across patients and mouse models, even in the presence of kidney injury. Kidney injury resulted in significantly decreased miRNAs that represent new circulating biomarker candidates. The most stable internal miRNA normalizers were discovered and used to normalize miRNAs to compare with ALT activity with regard to sensitivity (the stratification of patients at first presentation to hospital). miR-122-5p very accurately predicted liver injury at first presentation to hospital, especially when combined with the largest decrease miRNA.

2.4 Copyright

Chatper 3: Further qualification of miR-122-5p as a marker of hepatotoxicity in humans

3.1 Introduction

Because miR-122-5p was the most sensitive miRNA for predicting ALI in the previous study, it was chosen to further qualify and explore this marker in three clinically-relevant scenarios.

Since co-ingestion of ethanol is common in overdose patients (232, 233), the effect of acute ethanol ingestion had to be defined. For this reason, healthy volunteers were recruited and blood was collected up to 48 hours before they intended to drink ethanol, and again 3-5h after the participants had consumed ethanol in order to measure circulating miR-122-5p concentration.

The results from this study are published as:

McCrae JC, Sharkey N, Webb DJ, Vliegenthart AD, Dear JW. Ethanol consumption produces a small increase in circulating miR-122 in healthy individuals. Clin Toxicol (Phila) 2016;54:53-55. (234)

Kidney dysfunction is one of the key predictors of death and need for urgent liver transplantation in the presence of significant liver injury, with serum creatinine concentration being a component of the King's College Criteria (KCC) (10). Renal dysfunction has been reported to affect the circulating concentration of microRNAs. In patients with chronic kidney disease (CKD) Neal et al. reported significantly reduced total plasma microRNA and reductions in certain specific species (miR-16, -21, -210, -638) (235). In the previous chapter, the patients with acute liver injury also had a global reduction in circulating miRNA (231). Patients with ALI may need short-term haemodialysis (HD), for example, as a bridge to possible liver transplantation. For this reason, the effect of HD in patients with end-stage renal disease (ESRD) on

circulating miR-122-5p was determined and compared with healthy controls, patients with CKD and patients with successful renal transplant.

Findings from this study are published as:

Rivoli L*, Vliegenthart AD*, de Potter CM, van Bragt JJ, Tzoumas N, Gallacher P, Farrah TE, Dhaun N, Dear JW. The effect of renal dysfunction and haemodialysis on circulating liver specific miR-122. Br J Clin Pharmacol 2016. (236) *co-first authors.

Up until now, all studies involving miR-122-5p serum or plasma venous samples have been analysed in specialist laboratories with time-consuming and expensive kits. There is an unmet need for assays that can rapidly and accurately measure miRNA at the point-of-care (POC). Ideally, a POC assay would measure miR-122-5p in a single blood drop from a finger prick, be affordable for use in resource-limited settings and suitable for use near, or actually in, a patient's home (43). Such an assay could provide an early signal of DILI in patients at elevated risk, for instance, following prescription of antimicrobials with a significant DILI liability (7, 9, 237). With development, serial monitoring of miR-122-5p could improve patient safety by allowing medication change before life-threatening liver failure develops and by supporting safe reintroduction of treatment after interruption. In commercial drug development, measurement of miR-122-5p using a finger prick could reduce the need for venepuncture, which is especially advantageous in certain groups such as children and when multiple serial measurements in the same person are required. For this reason, in this project it was determined if miR-122-5p could be measured in a capillary blood drop from a finger prick and to compare the concentration to venous blood and plasma; to assess the intra-individual variability of capillary miR-122-5p concentration and to establish whether capillary miR-122-5p can report DILI in patients.

Findings from this study are published as:

Vligenthart AD, Berends C, Potter CMJ, Kersaudy-Kerhoas M, Dear JW. Capillary miR-122 represents a sensitive and specific biomarker for human drug-induced liver injury. Br J Clin Pharmacol (238)

3.2 Contributions by the candidate

Paper 2: Recruiting the volunteers; Measurement of miRNAs in all samples; The statistical analysis of data; Producing the figures; Preparation and revision of the manuscript.

Paper 3: miRNA measurements in plasma samples from the healthy volunteers, CKD patients, ESRD patients and kidney transplant patients; Performing the Argonaut pulldown and isolating the exosomes with subsequent miRNA measurements; Statistical analysis of the data; Producing the figures; Preparation and revision of the manuscript.

Paper 4: miRNA measurements in the blood samples and blood drops; Statistical analysis of the data; Preparation and revision of the manuscript.

Paper 2

CLINICAL TOXICOLOGY, 2016
VOL. 54, NO. 1, 53–55
http://dx.doi.org/10.3109/15563650.2015.1112015

Taylor & Francis
Taylor & Francis Group

BRIEF COMMUNICATION

Ethanol consumption produces a small increase in circulating miR-122 in healthy individuals

Jame C. McCrae[a], Noel Sharkey[b], David J. Webb[c], A. D. Bastiaan Vliegenthart[c] and James W. Dear[c]

[a]Ashworth Laboratories, University of Edinburgh, Edinburgh, UK; [b]Edinburgh Medical School, University of Edinburgh, Edinburgh, UK; [c]Department of Pharmacology, Toxicology & Therapeutics, BHF Centre for Cardiovascular Science, The Queen's Medical Research Institute, University of Edinburgh, Edinburgh, UK

ABSTRACT

Introduction: MicroRNA 122 (miR-122) is a new circulating biomarker for liver injury, which increases earlier than conventional markers in patients with acetaminophen hepatotoxicity. However, as co-ingestion of ethanol is common with drug overdose, a confounding effect of acute ethanol consumption on serum miR-122 must be examined. *Methods*: Blood was collected from healthy volunteers before and after recreational consumption of ethanol. Routine biochemistry and haematology measurements were performed, and serum miR-122 was measured by qPCR. The primary outcome was the difference in serum miR-122 with ethanol consumption. *Results*: We recruited 18 participants (72% male). Their mean serum ethanol concentration was 113 mg/dl (95% confidence interval [CI] 91–135 mg/dl) after consuming ethanol. Serum miR-122 increased from a mean of 71.3 million (95% CI 29.3–113.2 million) to 139.1 million (95% CI 62.6–215.7 million) copies/ml (2.2-fold increase). There was no significant difference in serum alanine aminotransferase activity before and after ethanol consumption. *Conclusion*: miR-122 increased with moderate ethanol consumption, but the fold change was modest. As increases with acetaminophen toxicity are 100- to 10 000-fold, moderate ethanol intoxication is unlikely to confound the use of this biomarker of hepatotoxicity.

ARTICLE HISTORY
Received 1 September 2015
Revised 19 October 2015
Accepted 19 October 2015
Published online
16 November 2015

KEYWORDS
Biomarkers; ethanol; toxicity; microRNA

Introduction

MicroRNAs are short (~22 nt) RNA species that do not code for proteins, but affect gene expression via binding to messenger RNA (mRNA) and blocking translation to protein.[1,2] Some are tissue-specific and stable in the circulation which has led to microRNAs being developed as organ injury biomarkers.[3–5]

miR-122 is abundant and liver-specific, representing over 70% of all hepatocyte microRNA.[2] It has been implicated in liver pathologies, such as viral hepatitis, hepatocellular carcinoma, drug-induced liver injury and alcoholic liver disease.[2–4] Recently, we reported that miR-122 is a biomarker of liver injury in paracetamol (acetaminophen – APAP) poisoning. In patients requiring acetylcysteine (NAC) treatment for APAP overdose, circulating miR-122 rose more quickly than alanine aminotransferase (ALT), and could accurately predict subsequent liver injury at first presentation to hospital.[6]

If miR-122 is going to have clinical utility as a marker for acute liver injury in APAP poisoning, the effect of acute ethanol ingestion needs to be defined, as co-ingestion of ethanol is common in overdose patients.[7] This study is an examination of circulating miR-122 before and after ethanol ingestion in healthy volunteers.

Methods

We prospectively recruited healthy volunteers in the age group of 18–65 years, with pre-existing plans to consume ethanol recreationally. Ethical approval was obtained from the South East Scotland research ethics committee and informed consent obtained from all participants. Exclusion criteria were: previous liver disease or hepatobiliary surgery; previous viral hepatitis; recent viral infection; recent strenuous exercise; consumption of cytochrome P450-inducing medication; past medical history of epilepsy, cancer, diabetes mellitus or alcoholism; psychiatric disease; pregnancy or the possibility of pregnancy and direct connection to clinical staff involved in the study.

We collected blood up to 48 h before, and again 3–5 h after the participants had consumed ethanol. The amount of ethanol to be consumed was not specified in advance. In serum the following parameters were measured: full blood count, urea and electrolytes, bilirubin, ALT, alkaline phosphatase, gamma-glutamyl transferase, coagulation profile, ethanol and miR-122. Samples were refrigerated immediately and prepared for analysis within 24 h.

miR-122 was measured by PCR as previously described.[8] Absolute quantification of miR-122 was achieved by generating a standard curve using synthetic target. All other analyses were

CONTACT Jame C. McCrae jcmccrae@gmail.com Room 3.08, Ashworth Laboratories, King's Buildings, University of Edinburgh, West Mains Road, Edinburgh EH9 3JT, Scotland, UK

performed by laboratory services at the Royal Infirmary of Edinburgh.

The primary outcome was difference in serum miR-122 before and after ethanol consumption. We calculated the sample size as follows: alpha-level 0.05; beta-level 0.9; standard deviation 0.203 (calculated from the first five participants' pre-consumption serum miR-122); we estimated that to determine a minimal difference in miR-122 delta-Ct of 0.165 (corresponding to a 2-fold increase in copy number per millilitre) we would require 18 participants. Statistical analysis was performed using Graphpad Prism (GraphPad Software, La Jolla, CA).

Results

Eighteen healthy subjects were recruited to the study as per the power calculation, of whom 13 (72%) were male. Table 1 summarises the clinical parameters at baseline and after ethanol consumption. Notably, there was no significant difference between ALT measurements, which were all in the normal range. Several blood parameters were significantly different after alcohol consumption. There were small but statistically significant changes in the leucocyte count, creatinine, urea, potassium and bilirubin.

At baseline no participants had a detectable serum ethanol. After consuming ethanol, their mean serum ethanol concentration was 113 mg/dl (range 20–175). There was a 2.2-fold increase of miR-122 from a mean value of 71.3 (95% confidence interval [CI] 29.3–113.2 million) to 139.1 million (95% CI 62.6–215.7 million) copies/ml (Fig. 1; $p = 0.006$).

Discussion

ALT is a serum marker used to detect hepatocellular injury that has been in common practice for several decades.[9] Despite this, there are several issues with its use: low-level insults may not affect ALT, and there is a considerable delay between the insult to the liver and a subsequent rise in serum. miR-122 is one of a panel of new biomarkers that appear to have increased sensitivity and specificity compared with ALT with regard to detecting liver injury.[5,6]

Table 1. Clinical parameters before and after ethanol consumption.

Clinical parameter	Before Mean (SD)	After Mean (SD)	p Value
Haemoglobin (g/l)	148 (7)	146 (8)	0.17
Leucocyte count (x10^9/l)	7.2 (2.9)	8.4 (1.7)	**0.04**
Platelets (x10^9/l)	261 (51)	261 (44)	0.98
INR	1.0 (0.1)	1.0 (0.1)	0.07
APTT Ratio	1.0 (0.1)	1.0 (0.1)	0.72
C-fibrinogen (g/l)	2.3 (0.3)	2.2 (0.3)	0.22
Urea (mmol/l)	5.0 (1.4)	4.6 (0.9)	**0.04**
Creatinine (micromol/l)	74.9 (6.4)	79.9 (12.3)	**0.03**
Sodium (mmol/l)	140 (1)	141 (3)	0.08
Potassium (mmol/l)	4.5 (0.5)	4.1 (0.2)	**0.01**
Bilirubin (micromol/l)	15.6 (12.0)	11.3 (10.0)	**0.00**
ALT (U/ml)	31.9 (25.0)	31.4 (23.7)	0.56
ALP (U/ml)	70.8 (13.2)	73.7 (14.2)	0.06
GGT (U/ml)	22.2 (16.8)	22.2 (17.0)	0.87
Ethanol (mg/dl)	0 (0)	113.4 (44.1)	**<0.001**

Statistically significantly different parameters are highlighted in bold. ALP, alkaline phosphatase; APTT, activated partial thromboplastin time; GGT, gamma-glutamyl transpeptidase; INR, international normalized ratio; SD, standard deviation.

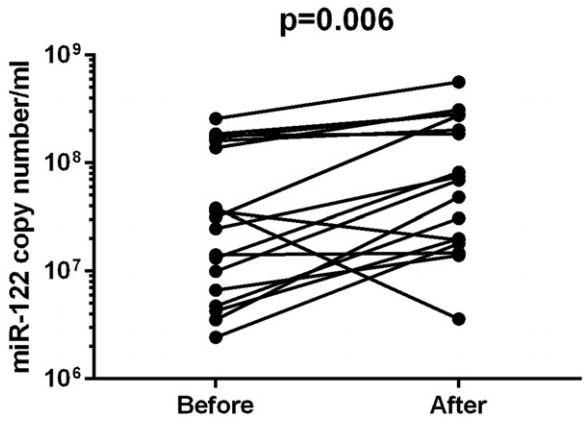

Fig 1. Serum miR-122 before and after ethanol consumption.

Co-ingestion of ethanol is common in overdose,[7,10] and so its effects on new biomarkers must be determined. We have identified a small but statistically significant increase in miR-122 after consumption of recreational levels of ethanol by healthy young adults. The mean increase in serum ethanol in this study (113 mg/dl) represents a moderate level of inebriation, but well above the drink–drive limit in many countries (e.g. 80 mg/dl in USA, England, Wales; 50 mg/dl in Scotland).

In previous studies miR-122 has increased 100- to 10 000-fold in response to hepatocellular injury.[5,8] It is doubtful, therefore, in mixed overdoses of APAP and ethanol that elevations of miR-122 above around 2-fold could be due to ethanol ingestion alone. These data indicate that ethanol co-ingestion is unlikely to be a significant contributor to the massive increases in miR-122 seen after APAP overdose. This is essential information for the further development of miR-122 as a biomarker of APAP-mediated hepatocellular injury.

Our study has a few limitations: first, though the data set is sufficient to address our primary outcome, it does not have sufficient power to determine any relationship between level of ethanol ingestion and miR-122 level. Furthermore, patients taking mixed ethanol/APAP overdoses can present with serum ethanol levels greater than the range covered by our study and we cannot fully exclude the possibility that these might increase mir-122 more substantially. This will need further research in the clinical setting.

The participant groups had some differences in their blood parameters before and after ethanol consumption. Although statistically significant, the authors feel that these changes would not be considered clinically important as they were all modest and within their respective normal ranges. Finally, our participants were healthy individuals with no history of liver disease; it is unknown how applicable our findings are to patients with pre-existing hepatic illness, and further exploration in this patient group is required.

Conclusion

Acute ethanol ingestion leads to a significant rise in miR-122. This increase is small compared with the biomarker signal with APAP-mediated liver injury.[6] This study contributes to the

ongoing clinical development of miR-122 as a liver injury biomarker for use in clinical toxicology.

Declaration of interest

The authors wish to thank the Myre Sim Fund and the Dowager Countess Eleanor Peel Trust for their support.

The authors report no conflicts of interest. The authors alone are responsible for the content and writing of this article.

References

1. McDaniel K, Herrera L, Zhou T, et al. The functional role of microRNAs in alcoholic liver injury. J Cell Mol Med. 2014;18:197–207.
2. Su T-H, Liu C-H, Liu C-J, et al. Serum microRNA-122 level correlates with virologic responses to pegylated interferon therapy in chronic hepatitis C. Proc Natl Acad Sci. 2013;110:7844–7849.
3. Zhang Y, Jia Y, Zheng R, et al. Plasma microRNA-122 as a biomarker for viral-, alcohol-, and chemical-related hepatic diseases. Clin Chem. 2010;56:1830–1838.
4. Wang K, Zhang S, Marzolf B, et al. Circulating microRNAs, potential biomarkers for drug-induced liver injury. Proc Natl Acad Sci. 2009;106:4402–4407.
5. Vliegenthart ADB, Antoine DJ, Dear JW. Target biomarker profile for the clinical management of paracetamol overdose: biomarkers for paracetamol-induced liver injury. Br J Clin Pharmacol. 2015;80:351–362.
6. Antoine DJ, Dear JW, Lewis PS, et al. Mechanistic biomarkers provide early and sensitive detection of acetaminophen-induced acute liver injury at first presentation to hospital. Hepatology. 2013;58:777–787.
7. Waring WS, Stephen AF, Malkowska AM, et al. Acute ethanol coingestion confers a lower risk of hepatotoxicity after deliberate acetaminophen overdose. Acad Emerg Med. 2008;15:54–58.
8. Starkey Lewis PJ, Dear J, Platt V, et al. Circulating microRNAs as potential markers of human drug-induced liver injury. Hepatology. 2011;54:1767–1776.
9. Senior JR. Alanine aminotransferase: a clinical and regulatory tool for detecting liver injury-past, present, and future. Clin Pharmacol Ther. 2012;92:332–339.
10. Teo AIC, Cooper JG. The epidemiology and management of adult poisonings admitted to the short-stay ward of a large Scottish emergency department. Scott Med J. 2013;58:149–153.

British Journal of Clinical Pharmacology

Paper 3

Br J Clin Pharmacol (2016) •• ••–•• 1

HUMAN TOXICOLOGY

The effect of renal dysfunction and haemodialysis on circulating liver specific miR-122

Correspondence James W. Dear, University/BHF Centre for Cardiovascular Science, University of Edinburgh, The Queen's Medical Research Institute, 47 Little France Crescent, Edinburgh EH16 4TJ, UK. Tel.: +44 013 1242 9216; Fax: +44 013 1242 9214; E-mail: james.dear@ed.ac.uk

Received 21 March 2016; **Revised** 26 August 2016; **Accepted** 16 September 2016

Laura Rivoli, A. D. Bastiaan Vliegenthart, Carmelita M. J. de Potter, Job J. M. H. van Bragt, Nikolaos Tzoumas, Peter Gallacher, Tariq E. Farrah, Neeraj Dhaun and James W. Dear

Edinburgh University/BHF Centre for Cardiovascular Science, The Queen's Medical Research Institute, Edinburgh

Keywords chronic kidney disease, dialysis, hepatotoxicity, microRNA, miR-122

AIMS

microRNA-122 (miR-122) is a hepatotoxicity biomarker with utility in the management of paracetamol overdose and in drug development. Renal dysfunction and haemodialysis have been associated with a reduction in circulating microRNA. The objective of this study was to determine their effect on miR-122.

METHODS

Blood samples were collected from 17 patients with end-stage renal disease (ESRD) on haemodialysis, 22 healthy controls, 30 patients with chronic kidney disease (CKD) and 15 patients post-kidney transplantation. All had normal standard liver function tests. Samples from ESRD patients were collected immediately pre- and post-haemodialysis. Serum alanine transaminase activity (ALT), miR-122 and miR-885 (liver enriched) were compared.

RESULTS

Circulating miR-122 was substantially reduced in ESRD patients pre-haemodialysis compared with the other groups (19.0-fold lower than healthy controls; 21.7-fold lower than CKD). Haemodialysis increased miR-122 from a median value of 6.7×10^3 (2.3×10^3–1.4×10^4) to 1.6×10^4 (5.4×10^3–3.2×10^4) copies ml^{-1}. The increase in miR-122 did not correlate with dialysis adequacy. miR-122 was reduced in the argonaute 2 bound fraction pre-haemodialysis; this fraction was increased post-dialysis. There was no change in miR-122 associated with extracellular vesicles. miR-885 was also reduced in ESRD patients (4-fold compared to healthy subjects) and increased by haemodialysis.

CONCLUSION

miR-122 is substantially lower in ESRD compared to healthy controls, patients with CKD and transplanted patients. Haemodialysis increases the concentration of miR-122. These data need to be considered when interpreting liver injury using miR-122 in patients with ESRD on dialysis, and specific reference ranges that define normal in this setting may need to be developed.

DOI:10.1111/bcp.13136

WHAT IS ALREADY KNOWN ABOUT THIS SUBJECT

- microRNA-122 (miR-122) is a sensitive and specific biomarker for drug-induced liver injury that is being qualified for use in clinical medicine and drug development.
- Renal dysfunction and haemodialysis can affect circulating microRNA concentrations.

WHAT THIS STUDY ADDS

- miR-122 is substantially lower in the circulation of patients with end-stage renal disease on haemodialysis.
- This decrease is specifically in the miR-122 fraction bound to the microRNA carrier protein argonaute 2.
- Haemodialysis increases the circulating concentration of miR-122.
- Reference ranges that define normality may need to take into account renal function.

Introduction

MicroRNAs are small (~22 nucleotide-long) non-protein coding RNA species involved in post-transcriptional gene-product regulation [1]. In blood, microRNAs are stable because they are protected from degradation by extracellular vesicles (ECVs), such as exosomes, RNA binding protein complexes, such as argonaute 2 (Ago2), and high-density lipoproteins [2, 3]. As they are amplifiable and some are tissue restricted, circulating microRNAs represent a reservoir for biomarker discovery. Liver-enriched miR-122 is released by injured hepatocytes, primarily bound to Ago2, and is a translational circulating biomarker for liver injury in zebrafish [4], rodents [5] and humans [6]. In patients with drug-induced liver injury (DILI), circulating miR-122 is increased around 100-fold [6, 7] and accurately predicts hepatotoxicity when all current hepatotoxicity biomarkers are still normal [7]. In the context of DILI there is a strong correlation between circulating concentrations of miR-122 and miR-885, another microRNA with a large fold increase following DILI. miR-885 is released directly from hepatocytes as reported by *in situ* hybridization studies of human liver DILI explants [8]. miR-122 is currently undergoing qualification as a clinical biomarker for stratification of patients at risk of paracetamol-induced liver injury and as a translational safety biomarker for use in preclinical and clinical drug development.

In the presence of liver injury, kidney function is one of the key predictors of death and need for urgent liver transplantation, with serum creatinine concentration being a component of the King's College Criteria [9] and the Model for End-Stage Liver Disease [10] scoring systems that are used for prognostic stratification. Circulating kidney injury molecule-1 (KIM-1) is a marker of kidney tubular injury that predicts outcome in patients with acute liver injury with higher sensitivity than creatinine and other common prognostic tools [11]. Renal dysfunction has been reported to affect the circulating concentration of microRNAs. Neal *et al.* reported significantly reduced total plasma microRNA and reductions in certain specific species (miR-16, -21, -210, -638) in patients with chronic kidney disease (CKD) [12]. We recently profiled the circulating miRNome in patients with paracetamol-induced acute liver injury and also demonstrated a global reduction in circulating microRNA with renal dysfunction [8]. In our profiling study there was no change in miR-122; however, an effect of renal dysfunction may have been undetectable given the high plasma miR-122 concentrations that accompany acute liver injury.

Patients with DILI may need short-term haemodialysis (HD), for example, as a bridge to possible liver transplantation. The effect of HD on circulating microRNAs depends on the species studied, with no effect being reported for some species (miR-21, -210) [13] but a significant decrease after HD being reported for miR-499 [14]. In the current study we measured circulating miR-122 concentrations in patients with end-stage renal disease (ESRD) before and after HD and compared them with healthy controls, patients with CKD and patients with a successful renal transplant. These data were compared with standard liver injury markers, dialysis parameters and miR-885.

Methods

Patients

In total, 84 subjects were recruited to this study, 17 with stable ESRD on maintenance HD from the outpatient dialysis unit at the Royal Infirmary of Edinburgh, UK (numbers as per power calculation), 22 healthy volunteers, 30 with CKD and 15 patients post-transplantation. Healthy controls and patients with ESRD and kidney transplantation were prospectively recruited for this study. Samples from patients with CKD were taken from a previously published study [15]. The study was approved by the local research ethics committee (Tayside Committee on Medical Research Ethics B) and performed in accordance with the Declaration of Helsinki. Informed consent was obtained from all participants.

ESRD patients

Inclusion criteria were: age 18 or over, treated with HD for over 3 months. Patients affected by liver disease or with a history of hepato-biliary surgery were excluded; other exclusion criteria were consumption of cytochrome P450-inducing medications, past medical history of epilepsy, cancer, alcoholism and/or psychiatric disease.

All patients were treated with HD for 4–5 hours per session, three times per week. Data collected included demographic characteristics, cause of ESRD, dialysis age and current medications. All patients were dialysed without heparin to prevent inhibition of polymerase chain reaction (PCR).

CKD patients

Patients with CKD stages I–V (estimated glomerular filtration rate 6–91 ml min^{-1}/1.73 m^2 calculated using the MDRD

equation) were matched with ESRD patients for age, gender, body mass index (BMI) and blood pressure (BP). In brief, subjects were recruited from the renal outpatient clinic at the Royal Infirmary of Edinburgh. The inclusion criteria were: male or female CKD patients, 18–65 years old and clinic BP ≤ 160/100 mmHg, whether or not on anti-hypertensive medication. We excluded patients with a renal transplant or on dialysis, patients with systemic vasculitis or connective tissue disease, those with a history of established cardiovascular disease, peripheral vascular disease, diabetes mellitus, respiratory disease, or neurological disease, and those with current alcohol abuse or pregnancy.

Renal transplantation patients

Patients entered the study if their transplant was performed six or more months prior, their renal function was stable and their estimated glomerular filtration rate (eGFR) was greater than 60 ml $min^{-1}/1.73m^2$. Patients with abnormal liver functions tests or a history of liver disease were excluded.

Healthy volunteers

Age, gender, BMI and BP matched adults with no medical complaints and no medication use were recruited.

Blood collection

In healthy subjects blood was collected into three EDTA plasma tubes (2.7 ml) and processed without delay – centrifugation at 1200 *g* for 10 min at 4°C. Then one sample was immediately frozen at −80°C. To test miR-122 stability, the remaining plasma samples were left unprocessed at room temperature or 4°C for 24 h or 7 days.

Two blood plasma samples were collected from each HD patient, one immediately before and one after a single dialysis session, directly from dialysis needles. For CKD and transplant patients, samples were collected on the study day. ESRD, CKD and transplant patient blood plasma samples were immediately processed by centrifugation at 1200*g* for 10 min at 4°C and then supernatant frozen at −80°C.

Biochemical analysis

The following parameters were measured: full blood count, urea and electrolytes, creatinine, bilirubin, alanine aminotransferase (ALT), alkaline phosphatise (ALP) and gamma-glutamyl transferase (GGT).

MicroRNAs were measured by PCR using SYBR green-based detection as previously described [8]. RNA was isolated from 50 µl plasma samples using the miRNeasy Serum/Plasma Kit (Qiagen, Venlo, Netherlands). RNA was eluted in a fixed volume of 14 µl, after which 2.5 µl of each eluate was reverse transcribed into cDNA using the miScript II RT Kit (Qiagen, Venlo, Netherlands) following manufacturer's instructions. The synthesized cDNA was ten-fold diluted and used for cDNA template in combination with the miScript SYBR Green PCR Kit (Qiagen, Venlo, Netherlands) using the specific miScript assays (Qiagen, Venlo, Netherlands). Real-time PCR was performed on a Light Cycler 480 (Roche, Basel, Switzerland) using the recommended miScript cycling parameters.

Where indicated, results were confirmed by TaqMan-based PCR. The small RNA eluate was reverse transcribed using the Taqman assay containing specific stem-loop reverse-transcription RT primers (Applied Biosystems, Foster City, CA, USA) for each target miRNA species, following the manufacturer's instructions. In the reverse transcription reaction, 1 µl of RNA was used to produce the complementary DNA (cDNA) template. Then, 1 µl of cDNA was used in the PCR mixture with specific PCR primers (Applied Biosystems, Foster City, CA) in a total volume of 10 µl. Levels of miRNA were measured using the Light Cycler 480 (Roche, Basel, Switzerland).

Absolute quantification of microRNA was achieved by generating a standard curve using synthetic target. Standard curves were generated by reverse transcribing known concentrations of miScript miRNA mimics (Qiagen, Venlo, The Netherlands) in 0.1X TE buffer spiked with 10 ng μl^{-1} Poly-C (Sigma-Aldirch, Gillingham, UK). The resulting cDNA was measured using serial dilutions on three different plates to demonstrate minimal variability.

The Agilent 2100 Bioanalyzer Small RNA kit was used according to the manufacturer's instructions to quantify RNAs in the 6–150 nucleotide size range.

Extra-cellular vesicle isolation

Human plasma was fractionated by differential centrifugation to isolate microRNA containing ECVs. Plasma (1 ml) was centrifuged at 2000*g* for 30 min then 12 000*g* for 45 min. The supernatant was then ultracentrifuged at 110 000*g* for 1.5 h to pellet ECVs. The pellet was resuspended in 2 ml PBS, after which an additional ultracentrifugation step of 110 000*g* for 1.5 h was performed. The vesicles were re-suspended for miRNA analysis. ECV presence and number was quantified by nanoparticle tracking analysis as previously described [16].

Ago2 isolation

Magna Bind goat anti-mouse IgG magnetic bead slurry, 100 µl (Thermo Scientific, Waltham, USA), was incubated with 10 µg of mouse monoclonal anti-Ago2 (Abcam, Cambridge, UK) or mouse normal IgG (Santa Cruz Biotechnology, Dallas, US) antibodies for 2 h at 4°C. The antibody-coated beads were then added to plasma and incubated overnight at 4°C with rotation. Beads were washed three times and each sample then eluted in RNAse-free water before QIAzol was added for RNA isolation.

Statistical analysis

The primary outcome was difference in serum miR-122 before and after HD. Out of five microRNA species, the smallest difference between ESRD and control that was reported by Neal *et al.* was a two-fold reduction [12]. Therefore, this cutoff was used as the minimal effect size for the power calculation. We calculated the sample size as follows: alpha-level 0.05; beta-level 0.8; standard deviation 0.203; we estimated that to determine a minimal difference in miR-122 ΔCt of 0.165 (corresponding to a two-fold change in copy number/ml) we would require 17 participants. All data are presented as median with interquartile range as D'Agostino & Pearson omnibus normality test failed to demonstrate a normal

distribution for the data. Statistical analysis was performed using Graphpad Prism (GraphPad Software, La Jolla, California, USA). Nominal statistical significance was set at $P < 0.05$.

Results

Firstly, the stability of miR-122 was determined. After processing human blood into plasma, storage at room temperature or 4°C for 24 h or 7 days had no significant effect on miR-122 concentration (Figure 1). Subject demographics and medications are shown in Table 1. As expected, the patient groups had significantly lower haemoglobin concentrations and were prescribed multiple medications. Erythropoietin, iron, 1α-calcidol, phosphate binders and calcimimetics were more commonly used in the ESRD group. The aetiologies of CKD were polycystic kidney disease (n = 8), glomerulonephritis (n = 6), obstructive uropathy (n = 5), Alport Disease (n = 1), with one unknown cause. The aetiologies of ESRD were obstructive uropathy (n = 5), diabetic nephropathy (n = 4), glomerulonephritis (n = 3), polycystic kidney disease (n = 1), pyelonephritis (n = 1), hypertensive nephropathy (n = 1), interstitial nephritis (n = 1) and one unknown cause. The diseases that resulted in need for transplantation were IgA nephropathy (n = 3), hypertensive nephropathy (n = 1), interstitial nephritis (n = 1), nephrolithiasis (n = 2), adult polycystic kidney disease (n = 1), Alport syndrome (n = 2), reflux nephropathy (n = 3), diabetic nephropathy (n = 1) and focal segmental glomerulosclerosis (n = 1). In the transplanted patient group the median eGFR was 80 ml min^{-1}/1.73m^2 (IQR: 67–95; range: 60–97), as calculated by the MDRD equation.

Total circulating microRNA was lower in patients with CKD (Figure 2). Serum ALT activity was lower in CKD and ESRD compared with healthy controls and transplanted patients (healthy ALT: median 18 IU l^{-1} (IQR16–30); CKD 11 IU l^{-1} (6–13); ESRD 12 IU l^{-1} (9–19); transplant 23 IU l^{-1} (14–38)). (Figure 3A). Haemodialysis induced a statistically significant, but clinically insignificant, increase in ALT from 12 (9–19) to 13 (11–21) IU l^{-1}. By contrast with ALT, miR-122 was not different when healthy controls were compared with CKD (Figure 3B). Pre-HD miR-122 circulating concentration was 19-fold lower compared with healthy controls (pre-HD median value of 6.7×10^3 (2.3×10^3–1.4×10^4); healthy controls 1.3×10^5 (7.6×10^4–3.8×10^5) copies ml^{-1}; $P < 0.0001$). Compared with healthy subjects, miR-122 was 5.0-fold lower pre-HD when PCR was performed using Taqman (Supplementary Figure S1). HD induced a 2.4-fold increase in miR-122 (post-HD: 1.6×10^4 (5.4×10^3–3.2×10^4) copies ml^{-1}). In patients with renal transplantation, miR-122 was comparable to the healthy controls (post-transplant: 4.7×10^4 (2×10^4–2.3×10^5) copies ml^{-1}). miR-885 was also reduced in ESRD patients (4-fold compared to healthy subjects) and increased by haemodialysis (from a median value of 5 (2–14) to 10 (5–18) copies ml^{-1}) and renal transplantation (294 (224–436) copies ml^{-1}) (Figure 3C). In the 30 patients with CKD, there was no significant correlation between eGFR and miR-122 (Figure 4). In ESRD there was no correlation between change in miR-122 and fluid removed by HD, urea reduction ratio (URR) or change in ALT. There was a significant correlation with change in miR-885 (Figure 5).

miR-122 circulates bound to Ago2 and encapsulated in ECVs. ECVs were isolated from plasma (Figure 6); there was no difference in miR-122 when ESRD patient samples were compared to healthy controls (Figure 6). By contrast, when Ago2 was isolated from plasma, the miR-122 fraction bound to this protein was significantly lower in ESRD patients pre-HD compared to healthy controls and post-HD samples (Figure 6).

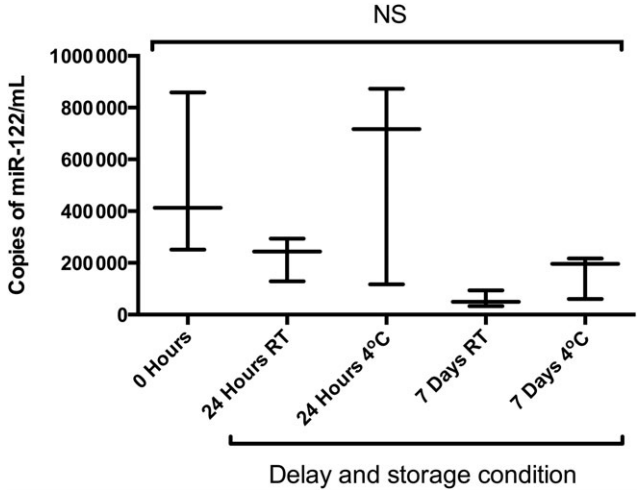

Figure 1

miR-122 is stable in plasma. Plasma samples were collected from healthy volunteers (n = 3) and immediately centrifuged to isolate plasma. One plasma sample was stored at −80°C without delay and the remaining tubes were left at room temperature (RT) or 4°C for 24 h or 7 days. Data presented as a Tukey plot

Discussion

An essential part of biomarker development is the definition of normal reference ranges that allows patients with disease to be identified with a level of accuracy that is fit for purpose given the biomarker's context of use. In this paper we demonstrate that Ago2-bound miR-122 is substantially reduced in patients with ESRD on HD who have standard liver function tests (such as ALT) within the normal range. Furthermore, HD increases miR-122, which may reflect hepatocyte injury given the concomitant increase in ALT and miR-885 and the lack of correlation with measures of dialysis adequacy. These data need to be considered when interpreting miR-122 concentrations in patients with ESRD on dialysis, and specific reference ranges that define normal in this setting may need to be developed.

Before commencing recruitment into this study, we confirmed that miR-122 was stable in plasma. This is consistent with the general view in the literature that microRNAs are stable in the circulation, a property that makes them attractive biomarker candidates. This stability is believed to be due to their binding to carrier proteins or encapsulation in vesicles. In the specific case of miR-122 we have recently

Table 1

Subject characteristics

	Healthy controls	CKD	Haemodialysis	Post-transplant
Number of patients	22	30	17	15
Age (years)	55 ± 10	48 ± 10	58 ± 13	43 ± 10
Sex M, % (*n*)	55 (12)	50 (15)	47 (8)	73 (11)
BMI (kg m^{-2})	26 ± 5	26 ± 6	27 ± 6	25 ± 4
SBP (mmHg)	128 ± 13	123 ± 14	129 ± 19	129 ± 15
ALT (U l^{-1})	22 ± 10	11 ± 7	15 ± 8	37 ± 44
Bil (μmol l^{-1})	9 ± 4	9 ± 3	9 ± 3	13 ± 6
CRP (mg dl^{-1})	1 ± 2	2 ± 2	10 ± 15	6 ± 6
Haemoglobin mg dl^{-1})	146 ± 13	134 ± 16	115 ± 12	135 ± 16
Medications, *n* (%)				
ACE-I		12 (40)	4 (20)	5 (33)
ARB		5 (17)	1 (6)	0 (0)
Beta-blockers		13 (43)	8 (47)	4 (27)
Statins		9 (30)	8 (47)	2 (13)
Antiplatelets		6 (20)	6 (35)	1 (7)
Warfarin		1 (3)	3 (18)	0 (0)
CCBs		14 (47)	4 (20)	7 (47)
Diuretics		1 (3)	0 (0)	0 (0)
Corticosteroids		0 (0)	0 (0)	10 (67)
Calcineurin inhibitor		0 (0)	0 (0)	15 (100)
Mycophenolate mofetil		0 (0)	0 (0)	12 (80)
Erythropoietin		2 (7)	17 (100)	0 (0)
Oral iron supplement		8 (27)	16 (99)	0 (0)
1-α calcidol		8 (27)	16 (99)	9 (60)
Phosphate binders		4 (13)	11(65)	4 (27)
Calcimimetics		0 (0)	3 (18)	0 (0)
alpha blockers		0 (0)	0 (0)	2 (13)

Age, gender; haemoglobin and medications of the 84 enrolled subjects (Healthy Controls, Chronic Kidney Disease (CKD) Haemodialysis and Post-transplant) are shown. ACE-I, ACE inhibitors; ARB, angiotensin receptor blockers; ALT, alanine aminotransferase; Bil, bilirubin; BMI, body mass index; CCB, calcium channel blockers; CRP, C-reactive protein; SBP, systolic blood pressure. Values are expressed as mean ± SD.

demonstrated that this microRNA species circulates predominantly bound to the carrier protein Ago2 [8].

The total circulating microRNA concentration was reduced in patients with CKD. This is consistent with data from Neal *et al*. who also reported a significant decrease [12]. Neal *et al*. presented data supporting a possible mechanism for this global reduction: patients with CKD have increased RNAse activity in their blood. The primary objective of our study was to explore miR-122 concentrations in patients with impaired kidney function. This liver-specific biomarker was reduced in the group with the worst kidney function, patients with ESRD. This is clinically important, as normal reference ranges may need to take into account the patient's GFR. Patients with CKD had miR-122 concentrations that were no different to controls. This is consistent with our previous published data that demonstrated no reduction in miR-122 in patients with CKD [6]. However, in the present study patients with CKD had lower serum ALT activity. This demonstrates a disconnect between ALT and miR-122 (which typically track each other, albeit with miR-122 having more rapid kinetics), and possibly reflects differences in the effect of renal dysfunction on mechanisms of ALT cellular release and clearance. Our published data demonstrate that miR-122 and miR-885 are related; both species are released from injured hepatocytes and their circulating concentrations are tightly positively correlated [8]. When compared with healthy controls, miR-885 was also substantially lower in patients with ESRD but not those patients with CKD.

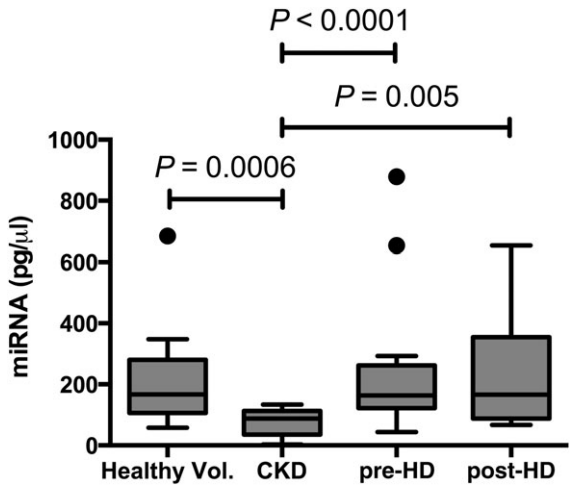

Figure 2

Total circulating microRNA is lower in chronic kidney disease (CKD) stage IV. microRNA in plasma was quantified by Agilent 2100 Bioanalyzer. Patient groups were healthy controls (n = 17), CKD (n = 20), and end-stage renal disease immediately before and after haemodialysis (pre-HD and post-HD, respectively, both n = 17)

HD has been reported to reduce the circulating concentration of certain microRNA species, which could relate to their being cleared in the dialysate fluid [14]. The data presented in this article are the first to demonstrate an increase in microRNA after HD. The increase in miR-122 did not correlate with parameters of dialysis adequacy or fluid removal, which argues against volume changes being the explanation for the increase. Serum ALT activity and miR-885 also increased after HD, which suggests that there is mild hepatocyte injury during the HD session.

In the field of drug-induced liver injury, miR-122 has significant promise as a new sensitive and specific biomarker of hepatocyte injury. More broadly, across a wide range of disease areas, circulating microRNAs are being proposed as biomarkers. However, their kinetics in the circulation are poorly defined, specifically their clearance. Following acute liver injury miR-122 is elevated in concentration earlier than ALT and decreases before ALT. However, this kinetic profile is not consistent across all microRNAs that change significantly following liver injury, with some changing later and having longer 'half-lives' in the circulation [8]. Future studies should investigate the clearance mechanisms of microRNA when combined with their different circulating carriers. Such studies would include defining the contribution of the kidney. The present study clearly demonstrates that the Ago2-bound form of miR-122 is substantially reduced in patients with ESRD. Mechanisms that underlie this are yet to be defined but may include reduced production of microRNA. However, if this were the case, the ECV-bound fraction would also be expected to fall. Neal *et al.* have reported that ESRD is associated with increased circulating RNAse activity [12]. The Ago2-bound form of miR-122 may be more sensitive to enzymatic digestion compared with ECV-encapsulated miR-122. *A priori* it could be hypothesized that the ECV fraction would differ between patients with ESRD and healthy controls because work by our group [17], and others [18], has clearly

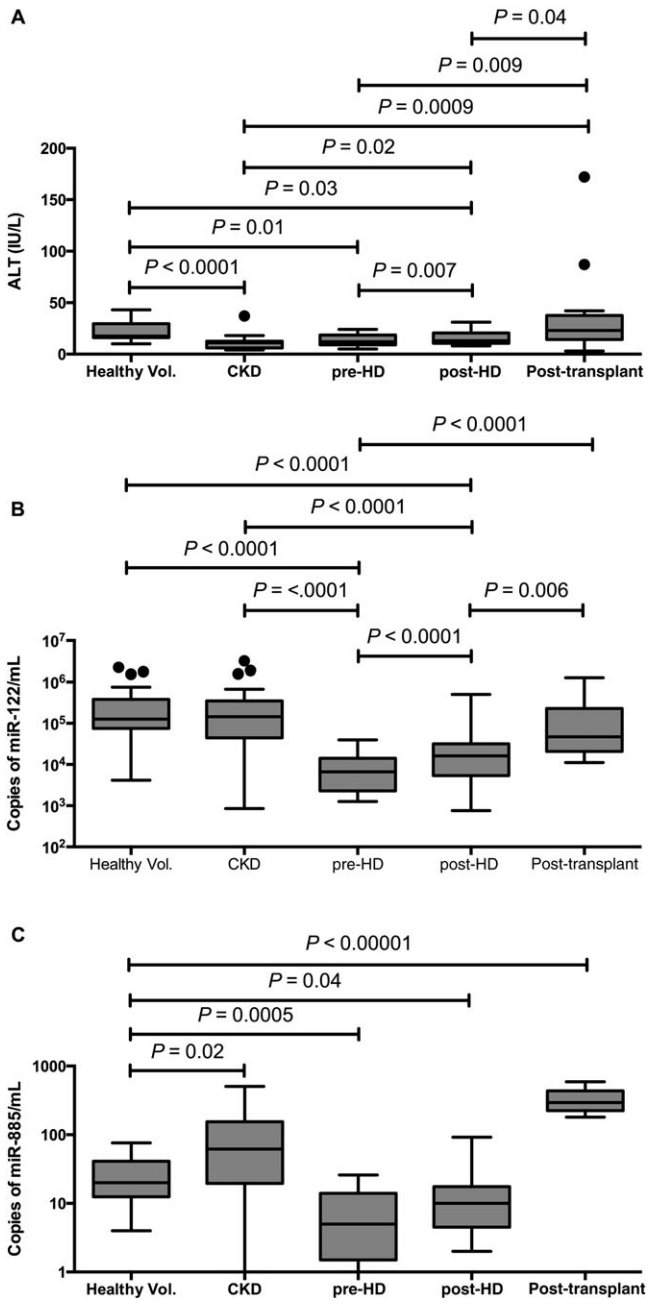

Figure 3

miR-122 is lower in end-stage renal disease and is increased by haemodialysis. Plasma was isolated from healthy controls (n = 22), chronic kidney disease (CKD) stage IV (n = 30), end-stage renal disease immediately before and after haemodialysis (pre-HD and post-HD, respectively, both n = 17) and patients with renal transplantation (n = 15). Serum ALT activity (A), miR-122 (B) and miR-885 (C) were measured. Data are presented as Tukey plots

demonstrated that systemically injected ECVs are excreted in urine. This would suggest that their clearance may be altered in ESRD. However, the miR-122 concentration in this fraction did not change. Defining the kinetics of miR-122 will be a priority if it is to be adopted into clinical practice and drug development.

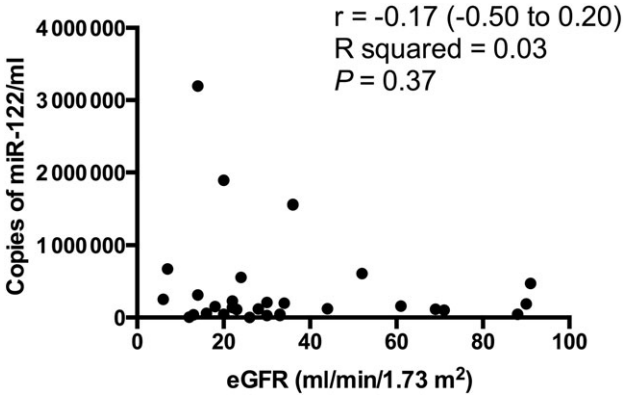

Figure 4

Circulating miR-122 is not related to the estimated glomerular filtration rate (eGFR) in patients with CKD. Each point represents a patient with CKD. eGFR calculated by the MDRD equation. Pearson correlation data are presented

miR-122 is being qualified as a biomarker for a range of diseases. In patients with established paracetamol-induced acute liver injury, miR-122 is increased on average around 100-fold [6]. In patients with ESRD, our study demonstrates a reduction in miR-122 of 19-fold compared with matched healthy controls. Therefore, the miR-122 signal associated with established ALI may still be appreciable even if the patient's baseline miR-122 concentration were lower than normal due to ESRD. An important future clinical application of miR-122 may be the stratification of patients at first presentation to hospital after paracetamol overdose with regard to their risk of subsequent ALI. In this 'pre-injury' context of use, the fold difference in miR-122 between high- and low-risk groups is smaller (around 17-fold) [7]. Therefore, pre-existing severe renal impairment may have a significant impact on the interpretation of miR-122. We propose that future qualification should include defining reference ranges in patients with reduced renal function.

There are some limitations to our study. Although recruitment was based on our pre-study power calculation, this is a discovery study that needs to be built on in larger patient cohorts. As is to be expected, patients with ESRD were prescribed multiple medications, which could potentially affect circulating microRNA concentrations. Such confounding by medication has been demonstrated for platelet-derived microRNAs and anti-platelet agents [19]. There are no data regarding the effect of anti-hypertensives on miR-122. Liver toxicity with ACE inhibitors, angiotensin receptor blockers and beta blockers is rare and all the patients in this study had normal standard liver function tests. Furthermore, our study included a CKD group who were prescribed similar

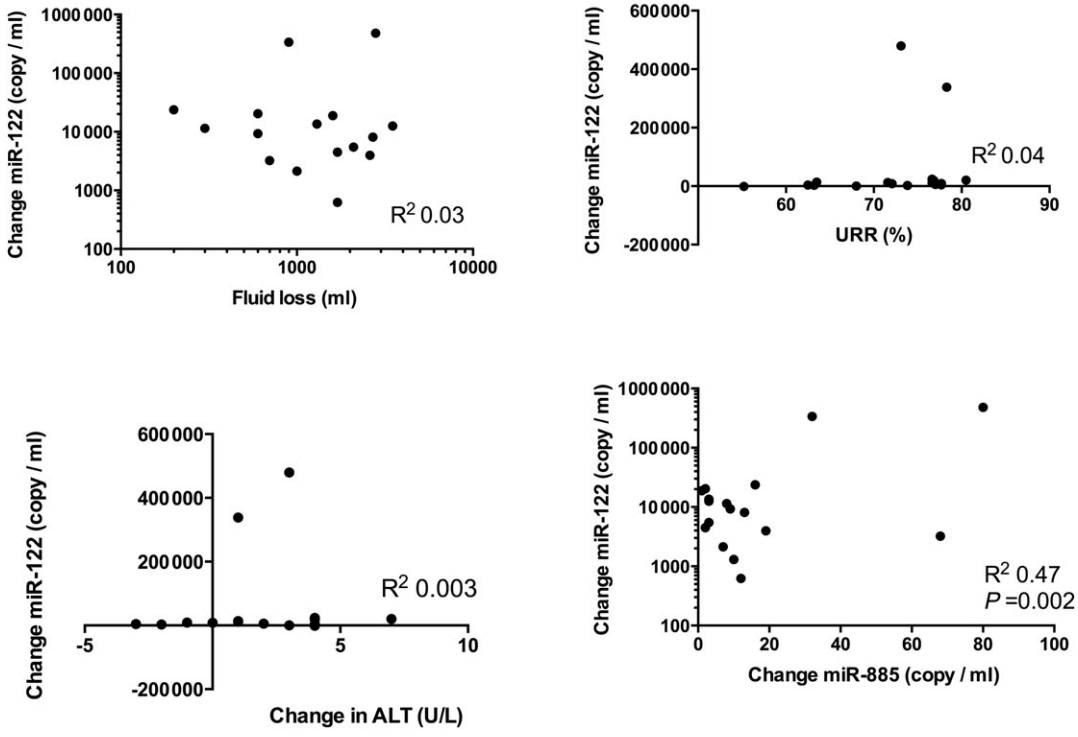

Figure 5

Haemodialysis-induced change in circulating miR-122 correlates with change in miR-885. In patients with end-stage renal disease, haemodialysis increased plasma miR-122. This increase did not have a significant relationship with volume of fluid removed during dialysis (A), urea reduction ratio (URR) (B) or change in ALT (C). There was a significant relationship with the dialysis-induced increase in plasma miR-885 (D)

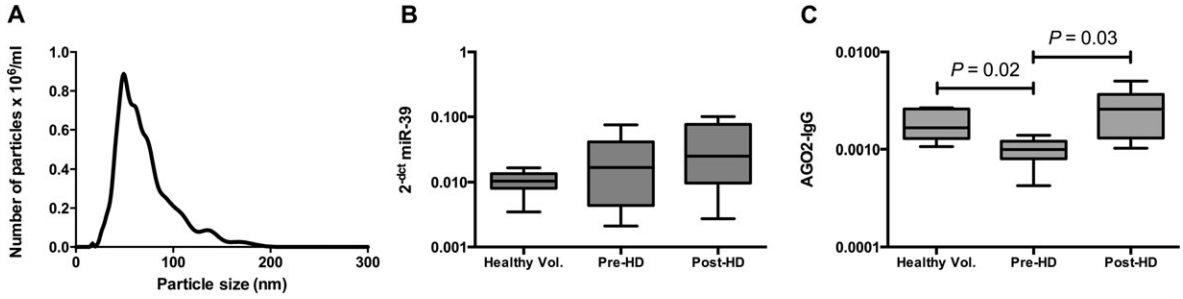

Figure 6

miR-122-5p in the extracellular vesicle fraction and Ago2 bound fraction. (A) size and number of particles measured by nanoparticle tracking analysis (NTA) following isolation of extracellular vesicles from human plasma by differential centrifugation. (B) Tukey boxplot of miR-122-5p measured in the extracellular vesicle pellet after ultracentrifugation of plasma samples from healthy volunteers and end-stage renal disease immediately before and after haemodialysis (pre-HD and post-HD). (C) Tukey boxplot of miR-122-5p measured in the antibody-isolated Ago2 fraction from healthy volunteers, pre-HD and post-HD. The *y*-axis represents the 2-Δ*Ct* value obtained from the Ago2 pull-down minus the 2-Δ*Ct* value obtained from IgG control pull-down from the same sample. All miR-122-5p measurements were normalized to spiked-in synthetic miR-39

cardiovascular medications but had substantially higher circulating miR-122 in comparison with ESRD patients. There is no evidence in the literature to suggest that the medications used more in the ESRD group (erythropoietin, iron, 1α-calcidol, phosphate binders and calcimimetics) have any effect on the liver or microRNA, at least in therapeutic doses.

In summary, miR-122 is lower in ESRD and haemodialysis restores the concentration of circulating miR-122 to healthy levels, which may reflect dialysis-induced hepatocyte injury given the concomitant increase in ALT and miR-885. These data need to be considered when interpreting liver injury using miR-122 in patients with ESRD on dialysis, and specific reference ranges that define normal in this setting may need to be developed.

Competing Interests

All authors have completed the Unified Competing Interest form at http://www.icmje.org/coi_disclosure.pdf (available on request from the corresponding author) and declare: no support from any organization for the submitted work; no financial relationships with any organizations that might have an interest in the submitted work in the previous 3 years; no other relationships or activities that could appear to have influenced the submitted work.

LR acknowledges the support of Società Italiana di Nefrologia (SIN). JWD acknowledges the support of NHS Research Scotland (NRS) through NHS Lothian and a BHF Centre of Research Excellence Award. ADBV was supported by an NC3Rs PhD Studentship (NC/K001485/1). ND is supported by a British Heart Foundation Intermediate Clinical Research Fellowship (FS/13/30/29994).

Contributors

L.R. and A.D.B.V. contributed equally to this article.

References

1 Bartel DP. MicroRNAs: target recognition and regulatory functions. Cell 2009; 136: 215–33.

2 Mitchell PS, Parkin RK, Kroh EM, Fritz BR, Wyman SK, Pogosova-Agadjanyan EL, *et al*. Circulating microRNAs as stable blood-based markers for cancer detection. Proc Natl Acad Sci U S A 2008; 105: 10513–8.

3 Vickers KC, Palmisano BT, Shoucri BM, Shamburek RD, Remaley AT. MicroRNAs are transported in plasma and delivered to recipient cells by high-density lipoproteins. Nat Cell Biol 2011; 13: 423–33.

4 Vliegenthart AD, Starkey Lewis P, Tucker CS, Del Pozo J, Rider S, Antoine DJ, *et al*. Retro-orbital blood acquisition facilitates circulating microRNA measurement in zebrafish with paracetamol hepatotoxicity. Zebrafish 2014; 11: 219–26.

5 Wang K, Zhang S, Marzolf B, Troisch P, Brightman A, Hu Z, *et al*. Circulating microRNAs, potential biomarkers for drug-induced liver injury. Proc Natl Acad Sci U S A 2009; 106: 4402–7.

6 Starkey Lewis PJ, Dear J, Platt V, Simpson KJ, Craig DG, Antoine DJ, *et al*. Circulating microRNAs as potential markers of human drug-induced liver injury. Hepatology (Baltimore, Md) 2011; 54: 1767–76.

7 Antoine DJ, Dear JW, Lewis PS, Platt V, Coyle J, Masson M, *et al*. Mechanistic biomarkers provide early and sensitive detection of acetaminophen-induced acute liver injury at first presentation to hospital. Hepatology (Baltimore, Md) 2013; 58: 777–87.

8 Vliegenthart AD, Shaffer JM, Clarke JI, Peeters LE, Caporali A, Bateman DN, *et al*. Comprehensive microRNA profiling in acetaminophen toxicity identifies novel circulating biomarkers for human liver and kidney injury. Sci Rep 2015; 5: 15501.

9 O'Grady JG, Alexander GJ, Hayllar KM, Williams R. Early indicators of prognosis in fulminant hepatic failure. Gastroenterology 1989; 97: 439–45.

10 Schmidt LE, Larsen FS. MELD score as a predictor of liver failure and death in patients with acetaminophen-induced liver injury. Hepatology 2007; 45: 789–96.

11 Antoine D, Sabbisetti V, Craig D, Simpson K, Bonventre J, Park B, *et al*. Circulating kidney injury molecule-1 predicts prognosis and poor outcome in patients with acetaminophen-induced liver injury. Hepatology 2015; 62: 591–9.

12 Neal CS, Michael MZ, Pimlott LK, Yong TY, Li JY, Gleadle JM. Circulating microRNA expression is reduced in chronic kidney disease. Nephrol Dial Transplant 2011; 26: 3794–802.

13 Martino F, Lorenzen J, Schmidt J, Schmidt M, Broll M, Gorzig Y, *et al*. Circulating microRNAs are not eliminated by hemodialysis. PLoS One 2012; 7: e38269.

14 Emilian C, Goretti E, Prospert F, Pouthier D, Duhoux P, Gilson G, *et al*. MicroRNAs in patients on chronic hemodialysis (MINOS study). Clin J Am Soc Nephrol 2012; 7: 619–23.

15 Lilitkarntakul P, Dhaun N, Melville V, Blackwell S, Talwar DK, Liebman B, *et al*. Blood pressure and not uraemia is the major determinant of arterial stiffness and endothelial dysfunction in patients with chronic kidney disease and minimal co-morbidity. Atherosclerosis 2011; 216: 217–25.

16 Oosthuyzen W, Sime NE, Ivy JR, Turtle EJ, Street JM, Pound J, *et al*. Quantification of human urinary exosomes by nanoparticle tracking analysis. J Physiol 2013; 591: 5833–42.

17 Oosthuyzen W, Scullion K, Ivy JR, Morrison EE, Hunter RW, Starkey Lewis P, *et al*. Vasopressin regulates extracellular vesicle uptake by kidney collecting duct cells. J Am Soc Nephrol 2016. doi:10.1681/ASN.2015050568.

18 Cheng Y, Wang X, Yang J, Duan X, Yao Y, Shi X, *et al*. A translational study of urine miRNAs in acute myocardial infarction. J Mol Cell Cardiol 2012; 53: 668–76.

19 Willeit P, Zampetaki A, Dudek K, Kaudewitz D, King A, Kirkby NS, *et al*. Circulating microRNAs as novel biomarkers for platelet activation. Circ Res 2013; 112: 595–600.

Supporting Information

Additional Supporting Information may be found in the online version of this article at the publisher's web-site:

http://onlinelibrary.wiley.com/doi/10.1111/bcp.13136/suppinfo.

Figure S1 Circulating miR-122 is lower in patients with end-stage renal disease pre-haemodialysis (pre-HD) compared with healthy volunteers. miR-122 was measured by TaqMan PCR. Data are presented as Tukey plots. n = 17 per group.

British Journal of Clinical Pharmacology

Paper 4

Br J Clin Pharmacol (2017) •• ••–•• 1

HUMAN TOXICOLOGY

MicroRNA-122 can be measured in capillary blood which facilitates point-of-care testing for drug-induced liver injury

Correspondence James W. Dear, University/BHF Centre for Cardiovascular Science, University of Edinburgh, The Queen's Medical Research Institute, 47 Little France Crescent, Edinburgh, EH16 4TJ, UK. Tel.: +44 0131 242 9216; E-mail: james.dear@ed.ac.uk

Received 6 October 2016; **Revised** 3 February 2017; **Accepted** 18 February 2017

A. D. Bastiaan Vliegenthart[1], Cécile Berends[1], Carmelita M. J. Potter[1], Maiwenn Kersaudy-Kerhoas[2,3] and James W. Dear[1]

[1]Pharmacology, Toxicology and Therapeutics, University/BHF Centre for Cardiovascular Science, Edinburgh University, UK, [2]Institute of Biological Chemistry, Biophysics and Bioengineering, School of Engineering and Physical Science, Heriot-Watt University, UK, and [3]Division of Infection and Pathway Medicine, University of Edinburgh, UK

Keywords finger prick, liver toxicity, microRNA, miR-122, point-of-care

AIMS

Liver-enriched microRNA-122 (miR-122) is a novel circulating biomarker for drug-induced liver injury (DILI). To date, miR-122 has been measured in serum or plasma venous samples. If miR-122 could be measured in capillary blood obtained from a finger prick it would facilitate point-of-care testing, such as in resource-limited settings that have a high burden of DILI.

METHODS

In this study, in healthy subjects, miR-122 was measured by polymerase chain reaction in three capillary blood drops taken from different fingers and in venous blood and plasma ($n = 20$). miR-122 was also measured in capillary blood obtained from patients with DILI ($n = 8$).

RESULTS

Circulating miR-122 could be readily measured in a capillary blood drop in healthy volunteers with a median (interquartile range) cycle threshold (Ct) of 32.6 (31.1–34.2). The coefficient of variation for intraindividual variability across replicate blood drops was 49.9%. Capillary miR-122 faithfully reflected the concentration in venous blood and plasma (Pearson $R = 0.89$, $P < 0.0001$; 0.88, $P < 0.0001$, respectively). miR-122 was 86-fold higher in DILI patients [median value 1.0×10^8 (interquartile range 1.89×10^7–3.04×10^9) copies/blood drop] compared to healthy subjects [1.85×10^6 (4.92×10^5–5.88×10^6) copies/blood drop]. Receiver operator characteristic analysis demonstrated that capillary miR-122 sensitively and specifically reported DILI (area under the curve: 0.96, $P = 0.0002$).

CONCLUSION

This work supports the potential use of miR-122 as biomarker of human DILI when measured in a capillary blood drop. With development across DILI aetiologies, this could be used by novel point-of-care technologies to produce a minimally invasive, near-patient, diagnostic test.

DOI:10.1111/bcp.13282

WHAT IS ALREADY KNOWN ABOUT THIS SUBJECT

- Drug-induced liver injury (DILI) is a major healthcare challenge in western countries and in resource-limited settings.
- microRNA-122 (miR-122) has substantial promise as a sensitive and specific biomarker of hepatocyte injury when measured in venous samples.

WHAT THIS STUDY ADDS

- miR-122 can be quantified reliably in a capillary blood drop from a finger prick.
- Capillary miR-122 faithfully reflects the plasma and venous whole blood concentration.
- Capillary miR-122 can identify patients with DILI with high sensitivity and specificity.
- If combined with a novel point-of-care detection platform, capillary miR-122 could allow near patient testing for DILI.

Introduction

Drug-induced liver injury (DILI) presents a major burden to clinical medicine and is a common cause of drug failure during clinical development [1]. In western clinical medicine, about half of the cases of acute liver failure are caused by DILI [2]. In the developing world, cotreatment of human immunodeficiency virus (HIV) and tuberculosis (TB) is a major cause of DILI. Globally, an estimated 37 million people are HIV-positive, with eastern and southern Africa carrying the highest burden with an estimated 19 million people infected [3]. The South African, TB incidence is particularly high; new diagnoses being 834 per 100 000 *per annum* [4]. TB prevalence is high in people coinfected with HIV, with 42% of HIV-positive TB cases receiving both TB and antiretroviral treatment [5]. DILI complicates TB treatment in up to 33% of cases [6], and in South Africa the in-hospital mortality from DILI has been reported to be around 30% [5].

MicroRNAs (miRNAs) are small (~22 nucleotides long) nonprotein-coding RNAs involved in post-transcriptional gene regulation [7]. In the circulation, miRNAs are protected from degradation by binding to RNA protein complexes (such as argonaute 2) and high-density lipoproteins, and being encapsulated in extracellular vesicles such as exosomes [8, 9]. As miRNAs are amplifiable and some are tissue enriched [10], they have emerged as a reservoir for the discovery of biomarkers that report organ injury [11].

The liver enriched miRNA-122 (miR-122) is a circulating biomarker of DILI. miR-122 is released into the circulation when hepatocytes are injured and is a translational safety biomarker across zebrafish [12], rodents [13] and humans [14–16]. In humans, miR-122 is around 100-fold higher in paracetamol overdose patients with DILI compared to those patients without liver injury [17] and is able to report DILI soon after overdose when serum alanine transaminase (ALT) activity is still in the normal range [14, 15, 18]. Circulating miR-122 is not DILI specific but is specific for hepatocyte injury. It is also increased in patients with cholestyramine-induced liver injury [19], ischemic hepatitis [20], viral hepatitis [21] and cholestatic liver injury [22]. In these published studies serum or plasma venous samples have been analysed in specialist laboratories with time-consuming and expensive kits. There is an unmet need for assays that can rapidly and accurately measure miRNA at the point-of-care (POC) [23]. Ideally, a POC assay would measure miR-122 in a single blood drop from a finger prick, be affordable for use in resource-limited settings and suitable for use near, or actually in, a patient's home [24]. Such an assay could provide an early signal of DILI in patients at elevated risk, for instance, following prescription of antimicrobials with a significant DILI liability [25–27]. With development, serial monitoring of miR-122 could improve patient safety by allowing medication change before life-threatening liver failure develops and by supporting safe reintroduction of treatment after interruption. In commercial drug development, measurement of miR-122 using a finger prick could reduce the need for venepuncture, which is especially advantageous in certain groups such as children and when multiple serial measurements in the same person are required.

The aims of this study were to determine if miR-122 can be measured in a capillary blood drop from a finger prick and to compare the concentration with venous blood and plasma; to assess the intraindividual variability of capillary miR-122 concentration and to establish proof of concept as to whether capillary miR-122 can report DILI in patients.

Material and methods

The study was approved by the research ethics committee (East Midlands – Nottingham 1 Research Ethics Committee) and performed in accordance with the Declaration of Helsinki. Informed consent was obtained from all participants.

Healthy volunteers

Healthy volunteers were eligible if they had no history of liver disease, were taking no medications and were willing to give blood samples by venepuncture and finger prick.

Drug-induced liver injury patients

A total of eight adult patients (age 24–82 years) admitted to the Royal Infirmary of Edinburgh, UK with DILI were entered into the study. In each patient, causality of liver injury was scored as *definitive* by the Roussel Uclaf Causality Assessment Method [28].

Blood collection

Blood was collected in EDTA tubes by venepuncture. Immediately, a 50 μL aliquot was collected in 1 mL of Qiazol (Qiagen, Venlo, Netherlands) for whole blood analysis. The remaining blood was centrifuged at 11 000 × *g* for 15 min at 4°C after which the supernatant was separated into aliquots and frozen at –80°C until miRNA extraction.

Table 1

Copy numbers of capillary miR-122 per blood drop (BD1: index finger; BD2: middle finger; BD3: ring finger) in healthy volunteers. The coefficient of variation (CV) across the three blood drops is presented

Healthy volunteer number	BD1 (copy/drop)	BD2 (copy/drop)	BD3 (copy/drop)	CV (%)
1	0.45×10^6	0.40×10^6	1.53×10^6	81.13
2	3.39×10^6	11.5×10^6	4.11×10^6	71.14
3	0.29×10^6	0.41×10^6	0.11×10^6	54.52
4	0.24×10^6	0.11×10^5	0.20×10^6	37.15
5	0.59×10^6	0.17×10^6	0.42×10^6	54.17
6	1.25×10^6	0.91×10^6	0.69×10^6	29.85
7	0.11×10^6	0.20×10^6	0.28×10^6	43.24
8	2.85×10^6	5.20×10^6	1.18×10^6	65.70
9	1.53×10^6	0.89×10^6	0.69×10^6	42.28
10	0.29×10^6	0.23×10^6	4.45×10^6	146.1
11	0.13×10^6	0.14×10^6	0.19×10^6	20.47
12	1.37×10^6	2.81×10^6	1.93×10^6	35.53
13	2.09×10^6	0.64×10^6	1.20×10^6	56.18
14	1.53×10^6	6.40×10^6	5.52×10^6	57.85
15	5.06×10^6	9.52×10^6	8.79×10^6	30.74
16	10.6×10^6	9.07×10^6	10.3×10^6	8.00
17	7.61×10^6	9.37×10^6	5.70×10^6	24.26
18	1.81×10^6	3.00×10^6	5.18×10^6	51.21
19	4.70×10^6	2.69×10^6	2.79×10^6	33.44
20	36.6×10^6	36.3×10^6	10.3×10^6	54.38
Mean	4.12×10^6	5.00×10^6	3.28×10^6	49.87

Three finger-prick blood drops (BD1: index finger, BD2: middle finger, BD3: ring finger) per healthy volunteer were obtained using disposable lancets that are used in routine clinical practice for glucose measurement (Accu-Chek, Roche, Basel, Switzerland – adjustable depth settings 1.8 mm). In DILI patients, one blood drop from the index finger was collected. After blood drop collection, Qiazol (1 ml) was added to each sample. All samples were stored at –80°C until analysis.

MicroRNA extraction

MicroRNA was extracted using miRNeasy Serum/Plasma kit (Qiagen), following the manufacturer's instructions. For venous blood and plasma, 50 µl of sample was used in combination with 150 µl nuclease free water. For capillary blood, 200 µl nuclease free water was added to the Qiazol containing each blood drop.

Real-time polymerase chain reaction

From each sample, 2.5 µl of RNA eluate was reverse transcribed into cDNA using the miScript II RT Kit (Qiagen) following manufacturer's instructions. The synthesized cDNA was 5-fold diluted and used for cDNA template in combination with the miScript SYBR Green polymerase chain reaction (PCR) Kit (Qiagen) using the specific miScript assays (Qiagen). Real-time PCR was performed in duplicate on a Light Cycler 480 (Roche) using the recommended miScript cycling parameters.

Absolute quantitation of miRNA was achieved by generating a standard curve using synthetic target. Standard curves were generated by reverse transcribing known concentrations of miScript miRNA mimics (Qiagen, Venlo, The Netherlands) in 0.1X TE buffer spiked with 10 ng μl^{-1} Poly-C (Sigma–Aldrich, Gillingham, UK). The resulting cDNA was measured using serial dilutions on three different plates on 3 different days to demonstrate minimal variability [interassay coefficient of variation (CV): 3.4%]. The calibration curve was linear in the cycle threshold (Ct) range of 20.0–36.1. A Ct value of 37.1 was obtained in water control.

Statistical analysis

Statistical differences, correlations and receiver operator characteristic (ROC) curve analyses were performed using Graphpad Prism (GraphPad Software, La Jolla California, USA). Nominal statistical significance was set at $P < 0.05$.

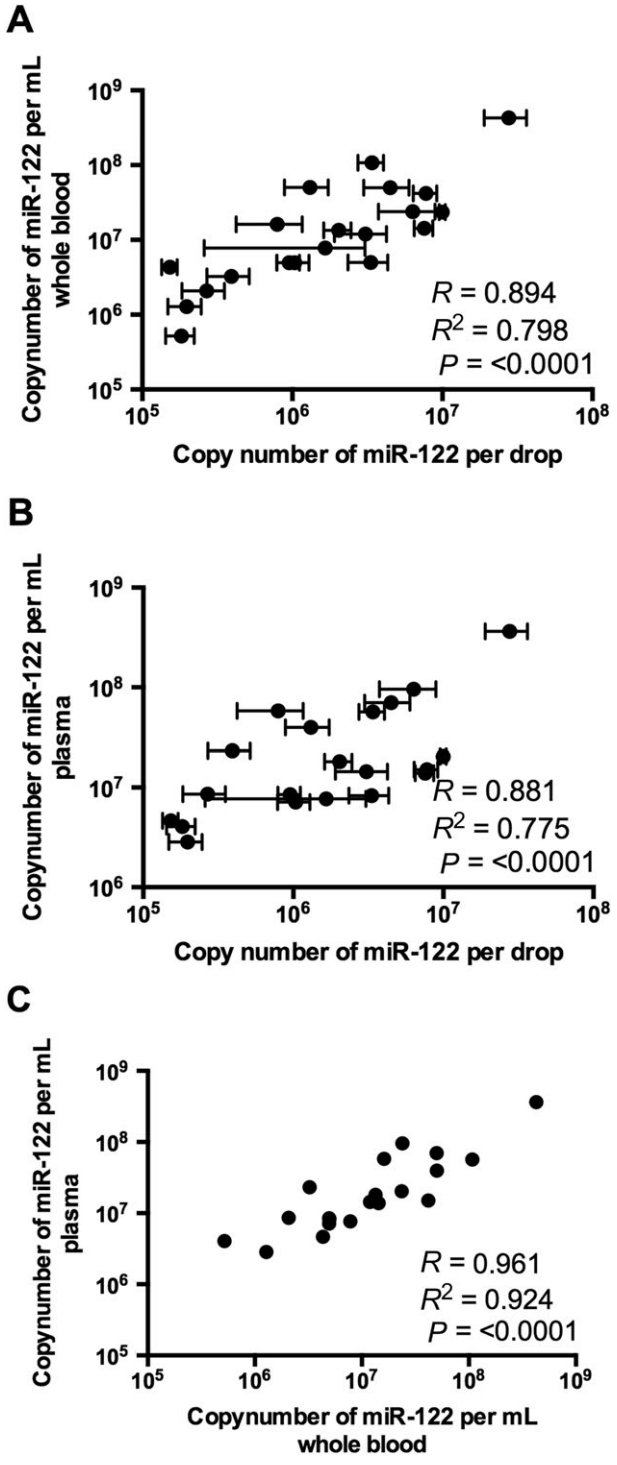

Figure 1

Scatter graphs. Correlation between copy numbers of miR-122 per mL (A) venous blood or (B) plasma and copy numbers of miR-122 per capillary blood drop. (C) correlation between copy numbers of miR-122 per mL venous blood and plasma in each healthy volunteer (n = 20). Pearson R values are 0.89 ($P < 0.0001$), 0.88 ($P < 0.0001$) and 0.92 ($P < 0.0001$), respectively (Pearson's correlation test). Blood drop values represent the mean copy number measured in three drops, error bars represent standard errors of the mean

Results

Capillary miR-122 can be measured in a finger prick blood drop

A total of 20 adults (14 females, median age 24 years; range 21–31 years) were recruited to this study. First it was determined whether a capillary blood drop yields sufficient miR-122 for robust quantification. Capillary blood Ct values (obtained by quantitative PCR) were all within the linear range of the calibration curve [mean (range) 32.6 (29.1–35.4)]. Copy numbers of miR-122 per blood drop in the healthy controls are presented in Table 1. Across the replicate drops from different fingers the mean CV (± standard deviation) was 49.9 ± 28.9%. The CV ± standard deviation of duplicate PCR measurements of the same blood drop was 0.94 ± 1.29%.

Capillary miR-122 correlates with venous blood and plasma

Across the healthy volunteers, the relationship between copy numbers of miR-122 per blood drop and copy numbers of miR-122 per mL of venous blood and plasma was determined. Copy number of miR-122 per blood drop significantly correlated with miR-122 measured in venous blood and plasma ($P < 0.0001$, Figure 1A, B). The correlation coefficients (R^2) were 0.80 and 0.78 and the Pearson R values [95% confidence interval (CI)] were 0.89 (0.75–0.96) and 0.88 (0.72–0.95), both $P < 0.0001$, in venous blood and plasma, respectively. As would be expected there was a significant correlation between venous blood and plasma miR122 (Figure 1C).

Liver-enriched miRNA-122 is higher in ALI patients

Capillary miR-122 was measured in blood drop samples obtained from patients with DILI (n = 8) and compared with healthy volunteers (n = 20). Clinical parameters of the DILI patient cohort are summarized in Table 2, along with their capillary miR-122 concentrations. In the single case of nonparacetamol DILI (induced by nitrofurantion) other causes of liver disease such as viral hepatitis (A–E) were excluded. miR-122 was increased 86 fold in DILI patients [median 1.58×10^8 (interquartile range 4.67×10^6–4.51×10^9) copies/blood drop] compared to healthy volunteers [1.85×10^6 (1.53×10^5–2.77×10^7) copies/blood drop] P = 0.004 (Figure 2). ROC analysis was performed to determine the sensitivity and specificity of miR-122 for detecting DILI (Figure 3). Capillary miR-122 had high sensitivity and specificity (area under the curve; 0.96 (95%CI 0.89–1.04), P = 0.0002, sensitivity: 86% at 90% specificity).

Discussion

This study has demonstrated, for the first time, that capillary miR-122 can be measured in a single blood drop to report DILI. This facilitates point-of-care measurement out with hospital, such as in the developing world where the burden of DILI is substantial.

Table 2

Clinical parameters of the patient cohort with drug-induced liver injury (DILI).

Patient	Age (years)	Sex	ALT activity ($U\ l^{-1}$)	INR	Serum creatinine ($\mu mol\ l^{-1}$)	ALP activity (U/L)	Bilirubin ($\mu mol\ dl^{-1}$)	Aetiology	Copies miR-122/ drop
1	82	F	3475	2	50	74	29	Paracetamol	1.58×10^8
2	44	F	10 543	6.9	47	101	106	Paracetamol	4.51×10^9
3	54	F	1210	8.9	66	236	162	Nitrofurantoin	4.09×10^7
4	24	F	1608	1.4	79	239	224	Paracetamol	1.58×10^8
5	29	M	1143	1.7	52	43	17	Paracetamol	5.64×10^7
6	25	M	1653	1.9	72	147	58	Paracetamol	1.66×10^9
7	45	M	1131	1.5	65	79	34	Paracetamol	3.50×10^9
8	35	M	1101	1.8	57	141	32	Paracetamol	1.16×10^7

ALT, alanine aminotransferase; INR, international normalized ratio; serum creatinine; ALP, alkaline phosphatise; bilirubin and aetiology of DILI are presented

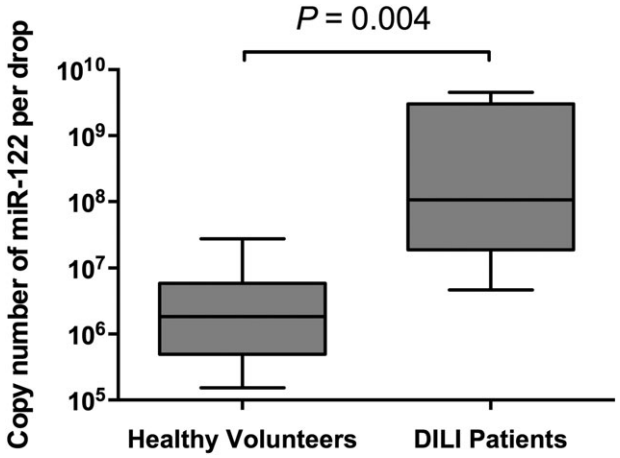

Figure 2

Copy number of miR-122 per blood drop from healthy volunteers (n = 20) and drug-induced liver injury patients (n = 8). Data are presented as a Tukey plot. In healthy volunteers, the mean copy number measured in three drops was used

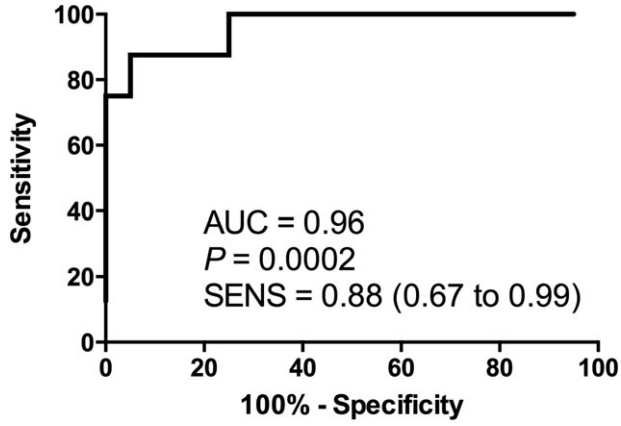

Figure 3

Receiver operator characteristic curve analysis with respect to blood drop miR-122 as a discriminator of drug-induced liver injury patients from healthy volunteers. Area under the curve (AUC), statistical significance and sensitivity (SENS) at 90% specificity (95%CI) are presented

When measured in capillary blood, the miR-122 Ct values were all within the quantifiable range of the PCR assay that had a linear calibration curve up to a Ct of 36. Intraindividual variability was tested by comparing three different blood drops taken from the same volunteer and resulted in an average CV of around 50%. Respectively, the intra-assay and interassay CVs of the PCR assay were only 0.94% and 3.4%, therefore the CV across the blood drops probably represents the variable volumes of the blood drops obtained during the collection procedure. The intraindividual CV of blood drop volume obtained from a finger has been reported to be 83% [29]. This is comparable to the intraindividual CV of miR-122 measured in our study. In a future POC assay, the variability of sample volume could be reduced by automated microchip sample processing technologies [30, 31] as already applied in test strips for international normalized ratio (INR) POC testing in the context of warfarin dosing [32]. Furthermore, as the circulating concentration of miR-122 increases up to a 100 fold in DILI patients [14], a CV of 50% would be expected to have little effect on the detection of DILI.

The concentration of capillary miR-122 measured in blood drops strongly correlated with blood and plasma obtained from venepuncture. This provides reassurance that our data reflect circulating concentrations. Furthermore, capillary miR-122 was significantly higher in blood drops from patients with DILI compared to healthy volunteers with a median fold increase of 86 and a ROC curve area under the curve of 0.96. These data confirm that the dynamic changes and the sensitivity to report DILI is similar between blood drops and earlier reported results from serum/plasma venous samples [14, 15]. A challenge in using circulating miRNAs as

biomarkers for human pathology is that the contribution of different tissues to the circulating pool is often unknown. Most miRNAs are expressed in multiple cell types, by contrast miR-122 is highly specific for the liver [33, 34]. miR-122 is not expressed in platelets, T-cells, B-cells, granulocytes or erythrocytes, which contain a wide variety of other miRNA species [35]. This makes miR-122 suitable for accurate measurement in whole blood without need for plasma or serum isolation.

There is an urgent need for improved DILI monitoring in the developing world where cotreatment of HIV and TB is a common cause [5]. However, despite the need, DILI monitoring in resource-limited settings is often restricted by practical concerns. The requirement for expensive tools and highly trained technicians can mean testing is only done in centralized or regional laboratories [24]. Moreover, many patients undergoing TB treatment in resource-limited settings have a negative association with venepuncture itself, do not have a primary care physician and do not value regular visits to a health care professional for health maintenance, which reduces potential participation in DILI monitoring [36]. A rapid POC test for measuring miR-122 from a single blood drop would mean that the patient undergoing TB and/or HIV treatment could use the assay at home (or near home). This study has demonstrated that a blood drop can be used as the matrix to measure miR-122. Recently, substantial effort has been spent in developing highly sensitive, rapid, reliable and low-cost methods for measuring miRNAs in minimal sample volumes. Electrochemical DNA hybridization sensors have potential as detection techniques in a POC test because this technology can detect specific miRNAs in the attomolar range without PCR amplification [37]. Other promising miRNA detection methods include nanoparticle-based optical technologies [38], surface plasmon resonance [39, 40] and amplification-free fluorescence-based assays [41, 42]. As miR-122 is a relatively high-concentration, organ-specific, circulating miRNA with a large dynamic range in disease it represents an ideal target for assay development with line of sight on a commercial product tackling a global health need.

This is an early phase proof of concept study that predominately used paracetamol toxicity as the model of DILI (seven of eight patients). Work is now required to determine whether capillary miR-122 has clinical utility in DILI caused by other drugs, especially antimicrobials. In conclusion, this work supports the potential use of miR-122 as biomarker of human DILI when measured in a blood drop from a finger prick. This could be used by novel POC technologies to produce a minimally invasive, near patient, diagnostic for DILI that has enhanced sensitivity and specificity compared to current tests.

Competing Interests

All authors have completed the Unified Competing Interest form at http://www.icmje.org/coi_disclosure.pdf (available on request from the corresponding author) and declare: no support from any organization for the submitted work; no financial relationships with any organizations that might have an interest in the submitted work in the previous 3 years; no other relationships or activities that could appear to have influenced the submitted work.

Author ADBV was supported by an National Centre for the Replacement Refinement & Reduction of Animals in Research (NC3Rs) PhD Studentship (NC/K001485/1). Author JWD acknowledges the support of an NHS Research Scotland (NRS) Career Research Fellowship through NHS Lothian and the UK Regenerative Medicine Platform Niche Hub.

Contributors

The experiments were performed by A.D.B.V., C.B. and C.P. Analysis was by M.K.K. and the study was co-ordinated by J.W.D.

References

1 Giacomini KM, Krauss RM, Roden DM, Eichelbaum M, Hayden MR, Nakamura Y. When good drugs go bad. Nature 2007; 446: 975–7.

2 Kaplowitz N. Idiosyncratic drug hepatotoxicity. Nat Rev Drug Discov 2005; 4: 489–99.

3 UNAIDS. Fact sheet 2016, 2016.

4 WHO. Global tuberclosis report, 2015.

5 Schutz C, Ismail Z, Proxenos CJ, Marais S, Burton R, Kenyon C, *et al*. Burden of antituberculosis and antiretroviral drug-induced liver injury at a secondary hospital in South Africa. S Afr Med J 2012; 102: 506–11.

6 Saukkonen JJ, Cohn DL, Jasmer RM, Schenker S, Jereb JA, Nolan CM, *et al*. An official ATS statement: hepatotoxicity of antituberculosis therapy. Am J Respir Crit Care Med 2006; 174: 935–52.

7 Bartel DP. MicroRNAs: target recognition and regulatory functions. Cell 2009; 136: 215–33.

8 Mitchell PS, Parkin RK, Kroh EM, Fritz BR, Wyman SK, Pogosova-Agadjanyan EL, *et al*. Circulating microRNAs as stable blood-based markers for cancer detection. Proc Natl Acad Sci U S A 2008; 105: 10513–8.

9 Vickers KC, Palmisano BT, Shoucri BM, Shamburek RD, Remaley AT. MicroRNAs are transported in plasma and delivered to recipient cells by high-density lipoproteins. Nat Cell Biol 2011; 13: 423–33.

10 Liang Y, Ridzon D, Wong L, Chen C. Characterization of microRNA expression profiles in normal human tissues. BMC Genomics 2007; 8: 166.

11 Szabo G, Bala S. MicroRNAs in liver disease. Nat Rev Gastroenterol Hepatol 2013; 10: 542–52.

12 Vliegenthart AD, Starkey Lewis P, Tucker CS, Del Pozo J, Rider S, Antoine DJ, *et al*. Retro-orbital blood acquisition facilitates circulating microRNA measurement in zebrafish with paracetamol hepatotoxicity. Zebrafish 2014; 11: 219–26.

13 Wang K, Zhang S, Marzolf B, Troisch P, Brightman A, Hu Z, *et al*. Circulating microRNAs, potential biomarkers for drug-induced liver injury. Proc Natl Acad Sci U S A 2009; 106: 4402–7.

14 Vliegenthart AD, Shaffer JM, Clarke JI, Peeters LE, Caporali A, Bateman DN, *et al*. Comprehensive microRNA profiling in acetaminophen toxicity identifies novel circulating biomarkers for human liver and kidney injury. Sci Rep 2015; 5: 15501.

15 Antoine DJ, Dear JW, Lewis PS, Platt V, Coyle J, Masson M, *et al*. Mechanistic biomarkers provide early and sensitive detection of acetaminophen-induced acute liver injury at first presentation to hospital. Hepatology (Baltimore, Md)2013; 58: 777–87.

16 Krauskopf J, Caiment F, Claessen SM, Johnson KJ, Warner RL, Schomaker SJ, *et al*. Application of high-throughput sequencing to circulating microRNAs reveals novel biomarkers for drug-induced liver injury. Toxicol Sci 2015; 143: 268–76.

17 Starkey Lewis PJ, Dear J, Platt V, Simpson KJ, Craig DG, Antoine DJ, *et al*. Circulating microRNAs as potential markers of human drug-induced liver injury. Hepatology (Baltimore, Md)2011; 54: 1767–76.

18 Dear JW, Antoine DJ, Starkey-Lewis P, Goldring CE, Park BK. Early detection of paracetamol toxicity using circulating liver microRNA and markers of cell necrosis. Br J Clin Pharmacol 2014; 77: 904–5.

19 Singhal R, Harrill AH, Menguy-Vacheron F, Jayyosi Z, Benzerdjeb H, Watkins PB. Benign elevations in serum aminotransferases and biomarkers of hepatotoxicity in healthy volunteers treated with cholestyramine. BMC Pharmacol Toxicol 2014; 15: 42.

20 Ward J, Kanchagar C, Veksler-Lublinsky I, Lee RC, McGill MR, Jaeschke H, *et al*. Circulating microRNA profiles in human patients with acetaminophen hepatotoxicity or ischemic hepatitis. Proc Natl Acad Sci U S A 2014; 111: 12169–74.

21 Zhang Y, Jia Y, Zheng R, Guo Y, Wang Y, Guo H, *et al*. Plasma microRNA-122 as a biomarker for viral-, alcohol-, and chemical-related hepatic diseases. Clin Chem 2010; 56: 1830–8.

22 Shifeng H, Danni W, Pu C, Ping Y, Ju C, Liping Z. Circulating liver-specific miR-122 as a novel potential biomarker for diagnosis of cholestatic liver injury. PLoS One 2013; 8: e73133.

23 Vliegenthart AD, Antoine DJ, Dear JW. Target biomarker profile for the clinical management of paracetamol overdose. Br J Clin Pharmacol 2015; 80: 351–62.

24 Pollock NR, Rolland JP, Kumar S, Beattie PD, Jain S, Noubary F, *et al*. A paper-based multiplexed transaminase test for low-cost, point-of-care liver function testing. Sci Transl Med 2012; 4: 152ra29.

25 Ostapowicz G, Fontana RJ, Schiodt FV, Larson A, Davern TJ, Han SH, *et al*. Results of a prospective study of acute liver failure at 17 tertiary care centers in the United States. Ann Intern Med 2002; 137: 947–54.

26 Kumar R, Bhatia V, Khanal S, Sreenivas V, Gupta SD, Panda SK, *et al*. Antituberculosis therapy-induced acute liver failure: magnitude, profile, prognosis, and predictors of outcome. Hepatology (Baltimore, Md)2010; 51: 1665–74.

27 Jones M, Nunez M. Liver toxicity of antiretroviral drugs. Semin Liver Dis 2012; 32: 167–76.

28 Danan G, Teschke R. RUCAM in drug and herb induced liver injury: the update. Int J Mol Sci 2016; 17.

29 Grady M, Pineau M, Pynes MK, Katz LB, Ginsberg B. A clinical evaluation of routine blood sampling practices in patients with diabetes: impact on fingerstick blood volume and pain. J Diabetes Sci Technol 2014; 8: 691–8.

30 Song Y, Huang YY, Liu X, Zhang X, Ferrari M, Qin L. Point-of-care technologies for molecular diagnostics using a drop of blood. Trends Biotechnol 2014; 32: 132–9.

31 Cui F, Rhee M, Singh A, Tripathi A. Microfluidic sample preparation for medical diagnostics. Annu Rev Biomed Eng 2015; 17: 267–86.

32 Pluddemann A, Thompson M, Wolstenholme J, Price CP, Heneghan C. Point-of-care INR coagulometers for self-management of oral anticoagulation: primary care diagnostic technology update. Br J Gen Pract 2012; 62: e798–800.

33 Ludwig N, Leidinger P, Becker K, Backes C, Fehlmann T, Pallasch C, *et al*. Distribution of miRNA expression across human tissues. Nucleic Acids Res 2016; 44: 3865–77.

34 Landgraf P, Rusu M, Sheridan R, Sewer A, Iovino N, Aravin A, *et al*. A mammalian microRNA expression atlas based on small RNA library sequencing. Cell 2007; 129: 1401–14.

35 Teruel-Montoya R, Kong X, Abraham S, Ma L, Kunapuli SP, Holinstat M, *et al*. MicroRNA expression differences in human hematopoietic cell lineages enable regulated transgene expression. PLoS One 2014; 9: e102259.

36 Shieh FK, Snyder G, Horsburgh CR, Bernardo J, Murphy C, Saukkonen JJ. Predicting non-completion of treatment for latent tuberculous infection: a prospective survey. Am J Respir Crit Care Med 2006; 174: 717–21.

37 Campuzano S, Pedrero M, Pingarron JM. Electrochemical genosensors for the detection of cancer-related miRNAs. Anal Bioanal Chem 2014; 406: 27–33.

38 Zhang J, Cui D. Nanoparticle-based optical detection of MicroRNA. Nano Biomed Eng 2013; 5: 1–0.

39 Ding X, Yan Y, Li S, Zhang Y, Cheng W, Cheng Q, *et al*. Surface plasmon resonance biosensor for highly sensitive detection of microRNA based on DNA super-sandwich assemblies and streptavidin signal amplification. Anal Chim Acta 2015; 874: 59–65.

40 Li X, Cheng W, Li D, Wu J, Ding X, Cheng Q, *et al*. A novel surface plasmon resonance biosensor for enzyme-free and highly sensitive detection of microRNA based on multi component nucleic acid enzyme (MNAzyme)-mediated catalyzed hairpin assembly. Biosens Bioelectron 2016; 80: 98–104.

41 Arata H, Hosokawa K, Maeda M. Rapid sub-attomole microRNA detection on a portable microfluidic chip. Anal Sci 2014; 30: 129–35.

42 Ishihara R, Hasegawa K, Hosokawa K, Maeda M. Multiplex microRNA detection on a power-free microfluidic Chip with laminar flow-assisted dendritic amplification. Anal Sci 2015; 31: 573–6.

3.3 Discussion

Co-ingestion of ethanol is common in patients presenting to hospital after a deliberate overdose (232, 233), and so its effects on new biomarkers must be determined. In order to test the effect of acute ethanol ingestion on miR-122-5p, 18 healthy volunteers were recruited and a small but significant increase in miR-122-5p was found after consumption of recreational levels of ethanol (2.2-fold increase). In previous studies miR-122-5p increased 100- to 1000 fold in response to hepatocellular injury (77, 231). It is doubtful, therefore, in mixed overdoses of APAP and ethanol that elevations of miR-122-5p above around 2-fold could be due to ethanol ingestion alone. These data indicate that ethanol co-ingestion is unlikely to be a significant contributor to the massive increases in miR-122-5p seen after APAP overdose. This is essential information for the further development of miR-122-5p as a biomarker of APAP-mediated hepatocellular injury.

An essential part of biomarker development is the definition of normal reference ranges that allows patients with disease to be identified with a level of accuracy that is fit for purpose given the biomarker's context of use. In this project it was demonstrated that Ago2-bound miR-122-5p is substantially reduced in patients with ESRD on HD who have standard liver function tests (such as ALT) within the normal range. Furthermore, HD increases miR-122-5p, which may reflect hepatocyte injury given the concomitant increase in ALT and miR-885-5p and the lack of correlation with measures of dialysis adequacy. These data need to be considered when interpreting miR-122-5p concentrations in patients with ESRD on dialysis.

The third scenario studied in this chapter demonstrated, for the first time, that capillary miR-122-5p can be measured in a single blood drop and can be used as sensitive and specific biomarker of DILI. This facilitates point-of-care measurement out with hospital, such as in the developing world where the burden of DILI is substantial. Recently, substantial effort has been spent in developing highly sensitive, rapid, reliable and low cost methods for measuring miRNAs in minimal sample volumes. Electrochemical DNA hybridization sensors have potential as detection

techniques in a POC test because this technology can detect specific miRNAs in the attomolar range without PCR amplification (239). Other promising miRNA detection methods include nanoparticle-based optical technologies (240), surface plasmon resonance (241, 242) and amplication-free fluorescence-based assays (243, 244). As miR-122-5p is a relatively high concentration, organ specific circulating miRNA with a large dynamic range in disease it represents an ideal target for proof-of-concept assay development with line of sight on a commercial product tackling a global health need.

3.4 Copyright

Paper 2: http://www.tandfonline.com/page/help/permissions

Paper 3 ϑ Π: http://onlinelibrary.wiley.com/journal/10.1111/(ISSN)1365-2125/homepage/Permissions.html

Chapter 4: Circulating paracetamol metabolites are toxicokinetic early biomarkers of acute liver injury

4.1 Introduction

miR-122-5p is a highly sensitive and specific marker that enables early stratification of patients by hepatocyte injury. To further improve risk assessment of patients presenting with a paracetamol overdose improved quantification of the toxic burden is required. Paracetamol concentration itself is a sub-optimal predictor of toxic NAPQI formation due to inter individual differences in pharmacology (245, 246). Therefore, circulating paracetamol metabolites were studied.

The primary objective of this study was to define the relationship between circulating paracetamol metabolites and ALI using serial samples collected in The Scottish and Newcastle Antiemetic Pretreatment for Paracetamol Poisoning study (SNAP) (247) (the discovery cohort). There was subsequent validation in samples taken at first presentation in two non-SNAP hospitals as part of the Markers and Paracetamol Poisoning (MAPP) study (the validation cohort). The secondary objective was to explore the effect of ondansetron on paracetamol metabolism to provide a mechanistic explanation for the increase in liver injury with this commonly used anti-emetic.

The results of this study are published as:

Vliegenthart, ADB, Kimmitt, RA, Seymour, JH, Homer, NZ, Eddleston, M, Gray, A, Webb, DJ, Lewis, SC, Bateman, DN, Dear, JW. Circulating Acetaminophen Metabolites Accurately Predict Hepatotoxicity And Represent New Clinical Toxicokinetic Biomarkers. Clinical Pharmacology and Therapeutics. 2016

4.2 Contributions by the candidate

Producing and validating the dataset; Performing all data analysis apart from the post hoc logistic regression modelling presented in table 4; Producing the figures; Preparation and revision of the manuscript.

Circulating Acetaminophen Metabolites Are Toxicokinetic Biomarkers of Acute Liver Injury

ADB Vliegenthart[1], RA Kimmitt[1], JH Seymour[1], NZ Homer[1], JI Clarke[2], M Eddleston[1], A Gray[3], DM Wood[4,5], PI Dargan[4,5], JG Cooper[6], DJ Antoine[2], DJ Webb[1], SC Lewis[7], DN Bateman[1] and JW Dear[1]

Acetaminophen (paracetamol-APAP) is the most common cause of drug-induced liver injury in the Western world. Reactive metabolite production by cytochrome P450 enzymes (CYP-metabolites) causes hepatotoxicity. We explored the toxicokinetics of human circulating APAP metabolites following overdose. Plasma from patients treated with acetylcysteine (NAC) for a single APAP overdose was analyzed from discovery ($n = 116$) and validation ($n = 150$) patient cohorts. In the discovery cohort, patients who developed acute liver injury (ALI) had higher CYP-metabolites than those without ALI. Receiver operator curve (ROC) analysis demonstrated that at hospital presentation CYP-metabolites were more sensitive/specific for ALI than alanine aminotransferase (ALT) activity and APAP concentration (optimal CYP-metabolite receiver operating characteristic area under the curve (ROC-AUC): 0.91 (95% confidence interval (CI) 0.83–0.98); ALT ROC-AUC: 0.67 (0.50–0.84); APAP ROC-AUC: 0.50 (0.33–0.67)). This enhanced sensitivity/specificity was replicated in the validation cohort. Circulating CYP-metabolites stratify patients by risk of liver injury prior to starting NAC. With development, APAP metabolites have potential utility in stratified trials and for refinement of clinical decision-making.

Study Highlights

WHAT IS THE CURRENT KNOWLEDGE ON THE TOPIC?

☑ Acetaminophen overdose is common. Decisions regarding the need for treatment are frequently based on measurement of the blood acetaminophen concentration. However, acetaminophen must be metabolized to cause liver injury. Acetaminophen metabolites are present in the circulation after therapeutic dosing and overdose.

WHAT QUESTION DID THIS STUDY ADDRESS?

☑ Are circulating acetaminophen metabolites elevated with acute liver injury and can they predict injury better than acetaminophen parent drug concentration?

WHAT THIS STUDY ADDS TO OUR KNOWLEDGE

☑ Patients who developed acute liver injury had higher acetaminophen metabolites derived from the cytochrome P450 pathway that mediates toxicity. Hospital presentation metabolites were more sensitive and specific for liver injury compared with the parent drug.

HOW THIS MIGHT CHANGE CLINICAL PHARMACOLOGY OR TRANSLATIONAL SCIENCE

☑ Acetaminophen metabolites can predict liver injury and have potential utility in stratified trials and for refinement of clinical decision-making.

Acetaminophen (paracetamol, APAP) overdose is a common reason for attending the hospital and the leading cause of acute liver failure in the Western world.[1] In the United States, over 400,000 Emergency Department visits relating to APAP overdose were recorded between 2006 and 2010.[2] Annually in the UK, APAP overdose results in ~100,000 Emergency Department presentations and 50,000 hospital admissions,[3] and is the direct cause of death in around 150 people.[4]

The mechanism of acute liver injury (ALI) after APAP overdose is well defined and can be translated from rodents to humans using mechanistic biomarkers.[5] APAP is predominantly metabolized into nontoxic glucuronide (APAP-Glu) and sulfate (APAP-Sul) conjugates. A small fraction is metabolized by cytochrome P450 (CYP) enzymes into the reactive metabolite *N*-acetyl-p-benzoquinone imine (NAPQI). When NAPQI is formed it reacts with the cysteine sulfhydryl group on glutathione (GSH). Most APAP-GSH is subsequently converted into APAP-cysteine (APAP-Cys) and APAP-mercapturate (APAP-Mer) conjugates.[6] APAP metabolites are detectable in plasma from healthy volunteers after therapeutic doses and in patients after APAP overdose.[7–10] They rapidly increase after ingestion of a therapeutic dose, with APAP-Glu having a higher concentration than the

[1]Pharmacology, Toxicology and Therapeutics, University/BHF Centre for Cardiovascular Science, University of Edinburgh, UK; [2]MRC Centre for Drug Safety Science, Department of Molecular & Clinical Pharmacology, Institute of Translational Medicine, University of Liverpool, Liverpool, UK; [3]Emergency Medicine Research Group, Department of Emergency Medicine, Royal Infirmary of Edinburgh, Edinburgh, UK; [4]Clinical Toxicology, Guy's and St Thomas' NHS Foundation Trust, London, UK; [5]King's College London, London, UK; [6]Emergency Department, Aberdeen Royal Infirmary, Aberdeen, UK; [7]Centre for Population Health Sciences, University of Edinburgh, Edinburgh, UK. Correspondence: J Dear (james.dear@ed.ac.uk)

Received 27 June 2016; accepted 17 October 2016; advance online publication 00 Month 2016. doi:10.1002/cpt.541

parent drug from 1–2 hours after ingestion.[6] Urinary metabolites of APAP can identify subjects with liver injury in the context of therapeutic dosing.[11]

In overdose, glutathione can become depleted and NAPQI can then bind to sulfhydryl groups in cellular proteins.[6] This may lead to oxidative stress, mitochondrial injury, hepatocyte necrosis, and acute liver failure. The protein binding of NAPQI results in APAP protein adducts that can be quantified by measurement of APAP-Cys that is released from the protein fraction of serum or plasma following protease enzyme treatment.[12] This is a distinct pool of APAP-Cys to the *in vivo* glutathione-derived metabolite that is present in the nonprotein fraction of the circulation. Glutathione-derived APAP-Cys is removed by dialysis in studies designed to quantify circulating APAP protein adducts.[13–15] APAP protein adducts are released from necrotic hepatocytes, although this remains controversial.[16] The focus of the present study was the metabolism of APAP as opposed to quantification of cell death. Therefore, we measured APAP-Cys in the nonadduct fraction of plasma.

The current antidote, acetylcysteine (NAC), replenishes cellular GSH and is effective at preventing liver injury if administered soon after overdose.[17,18] NAC could also directly bind to NAPQI, although this is not a significant pathway in rodents.[19] The decision to start treatment with NAC is commonly based on the dose ingested and a timed blood APAP measurement, which is interpreted using a binary treat/no treat nomogram with the threshold for treatment at a level of low risk. Current clinical practice, therefore, treats a number of patients who would not come to harm if they did not receive NAC.[20] Despite this conservative approach there are still patients who develop acute liver injury (ALI). Targeted therapies that reduce cell death and aid tissue regeneration are in development.[21,22] To facilitate stratified clinical trials there is an unmet need for new biomarkers of liver injury. These need to be accurate at early timepoints, when current markers lack sensitivity and specificity.[23]

Although the efficacy of NAC has been established for over 35 years, the optimal dosing regimen is still undetermined. The Scottish and Newcastle Antiemetic Pretreatment for Paracetamol Poisoning study (SNAP) compared the conventional intravenous NAC regimen with an identical NAC dose given in a modified (shorter) regimen.[24] Patients who had ingested a single acute overdose were randomized to one of four treatment arms: modified NAC regimen pretreated with the intravenous antiemetic ondansetron (ondansetron-modified) or pretreated with placebo (saline) (placebo-modified); or the conventional NAC regimen with or without ondansetron (ondansetron-conventional and placebo-conventional). The primary finding of the SNAP study was that the modified regimen resulted in substantially reduced vomiting, anaphylactoid reactions, and treatment interruptions. Although that study was not powered for efficacy, there was no significant difference in liver injury between modified and conventional regimens. However, unexpectedly, significantly more ondansetron-treated patients developed an elevation in serum alanine aminotransferase (ALT) activity compared to placebo. Given that APAP overdose and NAC therapy are commonly accompanied by nausea and vomiting, it is important to understand whether ondansetron worsens liver toxicity as even small increases in ALT could result in extra NAC treatment and avoidable increases in length of hospital stay.

The primary objective of this study was to define the relationship between circulating APAP metabolites and ALI. The secondary objective was to explore the effect of ondansetron on APAP metabolism to provide a mechanistic explanation for the increase in liver injury with this commonly used antiemetic.

RESULTS

The relationship between APAP metabolites and ALI (defined as an increased serum ALT activity of 50% or more) was investigated using serial samples collected in the SNAP trial (the discovery cohort). There was subsequent validation in samples taken at first presentation to two hospitals as part of the Markers and Paracetamol Poisoning (MAPP) study (the validation cohort). An overview of APAP metabolism is presented in **Figure 1**, with the metabolites measured in this study indicated. Patient screening and recruitment to the original SNAP trial, and the current discovery cohort, is presented in **Figure 2**. The characteristics of those patients with blood samples available for this study were similar across SNAP treatment groups aside from the higher incidence of liver injury in ondansetron-treated patients **(Supplementary Table 1)**, which mirrors the whole SNAP trial cohort.

Patients with and without ALI in the SNAP "discovery" cohort and the MAPP "validation" cohort are compared in **Tables 1 and 2**, respectively. In the time window of this study all patients in the discovery cohort received the same total dose of NAC, given either by the conventional or modified protocol. In both cohorts the increase in ALT was modest in those patients with ALI, with a median peak serum ALT activity of 154 U/L (65–909) and a median peak International Normalized Ratio (INR) of 1.4 (1.3–1.6) in the discovery cohort and 252 U/L (22–1256) and 1.2 (1.1–1.6) in the validation cohort. This increase in INR may reflect APAP inhibition of vitamin K-dependent activation of clotting factors rather than liver synthetic dysfunction.[25] There was no change in kidney function with ALI in either cohort as reported by change in serum creatinine concentration.

APAP metabolite kinetics

APAP parent drug concentration measured by liquid chromatography, tandem mass spectrometry (LC-MS/MS) correlated significantly with the value from the clinical laboratory APAP assay. The Pearson r value (95% confidence interval (CI)) was 0.88 (0.84–0.92), $P < 0.0001$ with a correlation coefficient (R^2) of 0.78 **(Supplementary Figure 1A)**. In the discovery cohort, the plasma APAP and metabolite concentrations at pretreatment and at 12 h and 20.25 h after the start of NAC treatment are presented in **Supplementary Figure 1B**. APAP-Glu was the metabolite with the highest concentration followed by APAP-Sul, APAP-Cys, APAP-Mer, and APAP-GSH. All metabolites decreased after the start of treatment, and only APAP-Glu was higher in concentration than APAP parent drug.

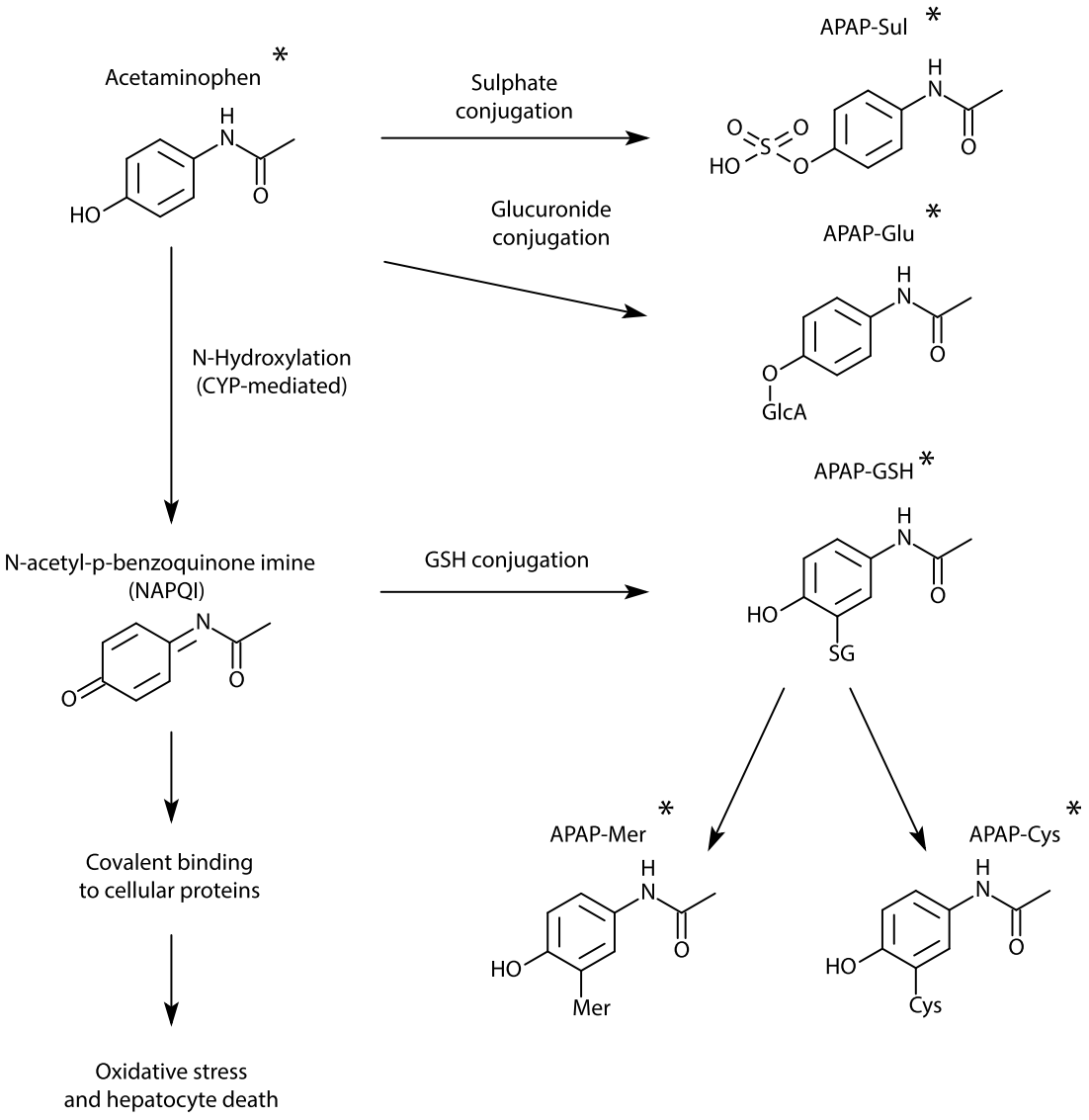

Figure 1 Pathways of acetaminophen (APAP) metabolism. APAP-sulphate (APAP-Sul); APAP-glucuronide (APAP-Glu); glutathione (GSH); APAP-glutathione (APAP-GSH); APAP-cysteine; (APAP-Cys); APAP-mercapturate (APAP-Mer). *Measured in this study.

Relationship between APAP metabolites and acute liver injury

Discovery cohort (SNAP). APAP half-life was longer in patients who developed liver injury compared to those with no injury: 3.11 h (2.38–4.38) vs. 2.36 h (2.02–2.68), $P = 0.004$ (**Figure 3a**). The concentrations of the APAP metabolites in patients without and with ALI are presented in **Supplementary Figure 2**. To compare the relative amount of metabolites formed by CYP activity compared to non-CYP conjugation, the $AUC_{(0\text{-}20.25h)}$ of CYP metabolites (APAP-Cys, APAP-Mer, APAP-GSH) was expressed as a fraction of the total $AUC_{(0\text{-}20.25h)}$ (CYP/total(%)). Patients who developed liver injury had a significantly higher $AUC_{(0\text{-}20.25h)}$ (CYP/total(%)) compared to those without liver injury (74 (58–746) vs. 47 (30–77), $P = 0.003$) (**Figure 3b**). $AUC_{(0\text{-}20.25h)}$ (CYP/total(%)) had a significant correlation with peak hospital stay ALT (**Figure 3c**).

APAP parent drug is used in clinical practice to stratify patients at hospital presentation. To explore the prognostic potential of metabolites formed by CYP activity the plasma concentration of the CYP metabolites (APAP-Cys, APAP-Mer, APAP-GSH) at pretreatment (0 h) were expressed as a fraction of the total metabolites (CYP/total (%)). Patients who developed liver injury had a significantly higher CYP/total (%) at pretreatment compared to those who did not develop liver injury, 2.21% (1.05–4.50) vs. 0.87% (0.58–1.43), $P = 0.0004$ (**Figure 3d**). The absolute concentration of APAP-Cys was significantly higher pretreatment with NAC in those patients with subsequent ALI (**Supplementary Figure 2**). Pretreatment CYP/total (%) remained higher in those patients who developed liver injury when the discovery cohort was censored by time from overdose to blood sampling (<8 h: ALI 3.12% (1.00–8.11) vs. no ALI 0.91% (0.59–1.40), $P = 0.006$; >8 h: ALI 2.16% (1.18–4.43) vs. no ALI 0.75% (0.50–1.70), $P = 0.05$).

The performance of each metabolite in the discovery cohort, alone and combined, was compared with regard to predicting

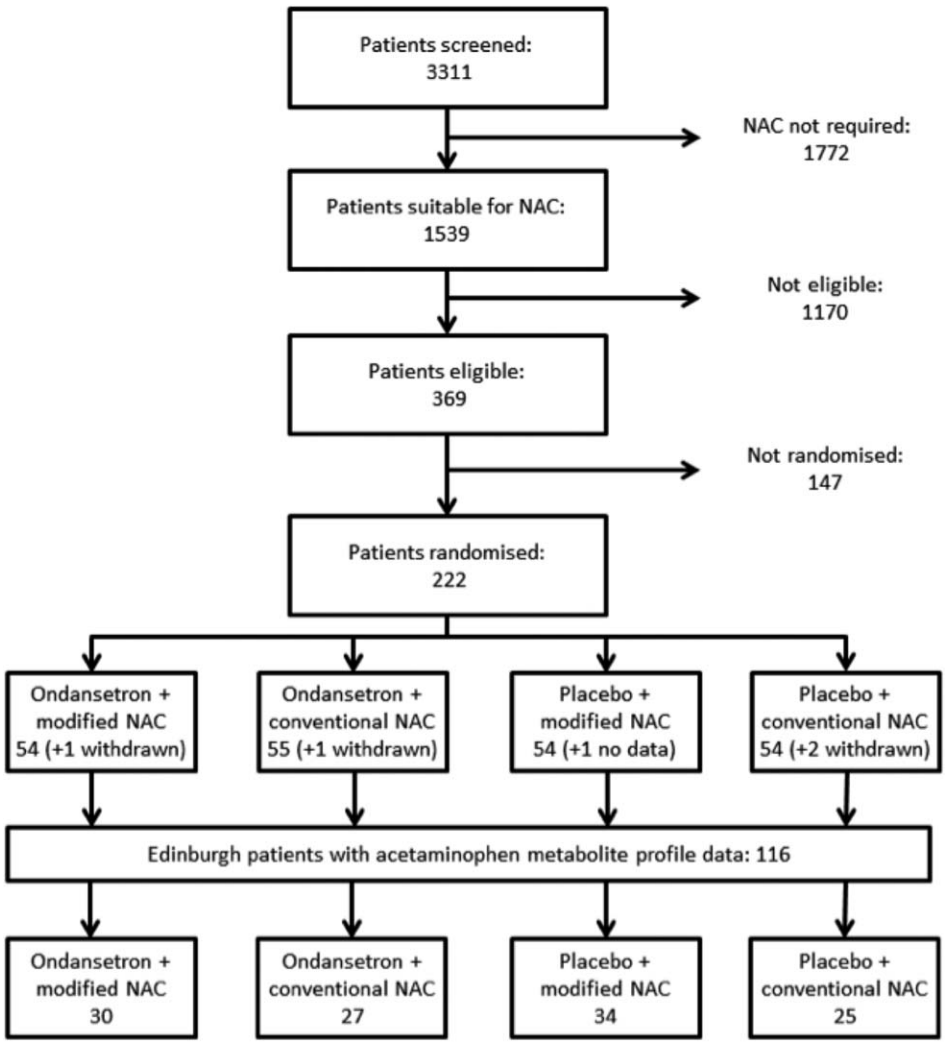

Figure 2 Study profile. The number of patients screened, suitable for NAC, eligible, and randomized into the original SNAP trial together with the number of patients (116) and their respective treatment arms in whom APAP metabolites were measured.

ALI at pretreatment using receiver operator characteristic analysis (ROC) (**Table 3**). The CYP metabolites had a superior predictive performance in comparison with the current markers (ALT and APAP parent drug had ROC-AUC of 0.67 (0.50–0.84) and 0.50 (0.33–0.67), respectively) **(Supplementary Figure 3a–d)**. In this discovery cohort the optimal metabolite combination was the ratio of APAP-Cys (CYP mediated) and APAP-Sul (non-CYP mediated), with an ROC-AUC of 0.91 (0.83–0.98). This metabolite combination at presentation had a significant correlation with peak ALT activity **(Supplementary Figure 3e)**.

Validation cohort (MAPP). The validation cohort consisted of 150 patients recruited from two geographically distinct hospitals, different from the site of recruitment for the discovery cohort. In blood samples collected at first presentation to hospital after single APAP overdose (before NAC was commenced), CYP/total (%) in those patients who developed liver injury was significantly higher compared to those who did not develop liver injury (0.95% (0.46–1.78) vs. 0.53% (0.34–0.84), $P = 0.02$) **(Supplementary Figure 3f)**. APAP-Cys and APAP-Mer were significantly higher in those patients with subsequent ALI **(Supplementary Figure 2)**.

Consistent with the results from the discovery cohort, CYP metabolites had superior predictive performance in comparison with the current standard markers (**Table 3**). In the validation cohort the sum of all the CYP metabolites had the largest ROC-AUC (0.83 (0.71–0.94)). As in the discovery cohort, APAP and ALT had no predictive value as assessed by ROC analysis (APAP ROC-AUC 0.57 (0.41–0.73); ALT ROC-AUC 0.51 (0.35–0.67)).

Effect of ondansetron on APAP metabolism

In the SNAP trial, patients pretreated with ondansetron had a higher incidence of liver injury that may reflect an effect on APAP metabolism. However, when liver injury patients were excluded, there was no difference in APAP half-life with ondansetron treatment compared to placebo, 2.48 h (2.07–2.97) vs. 2.23 h (1.97–2.56), $P = 0.10$. There was also no difference in $AUC_{(0\text{-}20.25h)}$ (CYP/total (%)) when ondansetron was compared to placebo (ondansetron: 54 (34–93) vs. placebo 43 (25–70), $P = 0.15$).

Table 1 Patient characteristics of the discovery cohort divided by absence or presence of acute liver injury according to the British National Formulary 2009[37]

	>50% ALT rise	No > 50% ALT rise	*P*-value
Number	14	102	
Median (IQR) age (years)	28 (21-32)	37 (26-48)	**0.03**
Median (IQR) weight (kg)	62 (56-71)	70 (59-80)	0.27
Number of females	11 (79%)	61 (55%)	0.17
Median (IQR) time from ingestion to treatment (h)	6.7 (7.8-10.7)	7.2 (8.0-10.0)	0.63
Number with ingestion to treatment <8hr	8 (57%)	65 (64%)	0.63
Median (IQR) ingested acetaminophen (mg/kg)	332 (190-393)	222 (165-313)	0.06
Number who ingested acetaminophen ≥16g	9 (64%)	44 (43%)	0.14
Median (IQR) admission alanine aminotransferase (U/L)	24 (18-82)	18 (13-26)	**0.04**
Median (IQR) peak alanine aminotransferase (U/L)	154 (65-909)	18 (14-27)	**< 0.0001**
Median (IQR) admission INR	1.0 (1.0-1.2)	1.0 (0.9-1.0)	**0.01**
Median (IQR) peak INR	1.4 (1.3-1.6)	1.1 (1.0-1.2)	**< 0.0001**
Median (IQR) admission billirubin (μmol/l)	12 (7-17)	7 (5-9)	**0.009**
Median (IQR) admission GGT (U/l)	19 (12-42)	25 (16-42)	0.25
Median (IQR) admission creatinine (μmol/l)	69 (59-81)	65 (59-74)	0.44
Median (IQR) peak creatinine (μmol/l)	70 (59-81)	67 (60-79)	0.68
Median (IQR) change in creatinine (%)	-5.4 (-22.8-3.1)	-6.0 (-12.6-1.7)	0.46
Alcohol ingested	1 (7%)	59 (58%)	**< 0.0001**
Other drugs ingested	9 (64%)	67 (66%)	0.92
Nutritional deficiency	2 (14%)	17 (17%)	0.82
Debilitating disease	0 (0%)	2 (2%)	0.60
Chronic alcohol use	0 (0%)	44 (43%)	**0.002**
Identified as high risk	2 (14%)	57 (56%)	**0.004**
Number who received ondansetron	11 (79%)	46 (45%)	**0.02**
Number who received modified NAC	7 (50%)	57 (56%)	0.68

P-value for difference between groups was determined by Mann-Whitney test or chi-square test.

APAP-Cys/APAP-Sul was higher in the pretreatment blood sample from patients randomized to ondansetron compare to placebo. *Post hoc* analysis of the SNAP trial by logistic regression modeling demonstrated that when APAP-Cys/APAP-Sul was added to the stratified randomization process the incidence of ALI in the ondansetron treated patients was not different from placebo (**Table 4**).

Effect of modified NAC regimen on APAP metabolism

There was no difference in APAP half-life or $AUC_{(0\text{-}20.25h)}$ (CYP/total(%)) between SNAP trial conventional and modified NAC treatment (half-life: 2.19 h (1.97–2.54) vs. 2.44 h (2.08–2.84), $P = 0.08$. $AUC_{(0\text{-}20.25h)}$ (CYP/total (%)) 42 (32–89) vs. 53 (26–76), $P = 0.95$).

DISCUSSION

This study demonstrates that the cytochrome P450 enzyme-mediated mechanism of APAP toxicity described in rodent models translates to humans. The key novel findings were that a higher percentage of circulating metabolites formed by cytochrome P450 enzymes (CYP metabolites) were present in patients with liver injury and these metabolites were superior to both ALT and APAP with regard to early ALI risk stratification. The potential value of CYP metabolites to future clinical trials was demonstrated by their incorporation *post-hoc* into the SNAP trial. This showed that the reported increase in ALI with ondansetron was no different than placebo. This work has the potential to be built on and produce an important change in the management of APAP overdose—a very common medical emergency with suboptimal tools for patient stratification.

We measured five APAP metabolites (two non-CYP-mediated and three CYP-mediated) alongside APAP parent drug. APAP half-life was 2–2.5 h in patients who did not develop ALI and was prolonged to over 3 h in people with ALI. The prolongation of APAP half-life was smaller than reported in previous studies

Table 2 Patient characteristics of the validation cohort divided by absence or presence of acute liver injury (>50% increase in ALT)

	>50% ALT rise	No. >50% ALT rise	*P*-value
Number	19	131	
Median (IQR) age (years)	41 (19-65)	36 (22-48)	0.60
Number of females	12 (63%)	86 (72%)	0.83
Median (IQR) time from ingestion to sampling (h)	5.0 (4.0-8.0)	5.5 (4.0-13.25)	0.65
Number with ingestion to treatment <8hr	13 (57%)	94 (64%)	0.76
Median (IQR) ingested acetaminophen (gram)	13 (22-35)	15 (9-21)	**0.01**
Number who ingested acetaminophen ≥16g	11 (58%)	58 (44%)	0.27
Median (IQR) admission alanine aminotransferase (U/L)	18 (12-34)	18 (13-28)	0.86
Median (IQR) peak alanine aminotransferase (U/L)	252 (22-1256)	19 (14-28)	**< 0.0001**
Median (IQR) admission INR	1.0 (1.0-1.0)	1.1 (1.0-1.2)	**0.0004**
Median (IQR) peak INR	1.1 (1.0-1.1)	1.2 (1.1-1.6)	**< 0.0001**
Median (IQR) admission billirubin (μmol/l)	8 (6-15)	5 (5-9)	**0.04**
Median (IQR) admission GGT (U/l)	26 (15-40)	17 (13-47)	0.88
Median (IQR) admission creatinine (μmol/l)	59 (48-68)	57 (51-68)	0.99
Median (IQR) peak creatinine (μmol/l)	64 (55-78)	61 (55-70)	0.70
Median (IQR) change in creatinine since admission (%)	2.3 (-5.9-16.7)	-2.0 (-12.6-8.2)	0.14

P-value for difference between groups was determined by Mann-Whitney test or chi-square test.

(half-life up to 6.9 h), which is likely due to their patients having more severe ALI, as indicated by an ALT activity of ≥1,000 U/l.[6] The present study suggests that mild ALI is associated with a reduction in the capacity to metabolize APAP. This increase in half-life might reflect an intrinsic lower capacity to metabolize APAP that results in liver injury after overdose due to increased production of NAPQI. Alternatively, liver injury may cause a lower metabolic capacity. In this study there was no evidence of a difference in renal function between those patients with and without ALI, which otherwise could have affected metabolite clearance. APAP-Glu and APAP-Sul (formed through phase II non-CYP metabolism) were the highest concentration APAP metabolites in the circulation.[6,26,27] In previously published studies, about one-third of APAP was metabolized into APAP-Sul and two-thirds into APAP-Glu. The APAP-Sul pathway becomes saturated even at therapeutic doses[26,27] and the higher capacity of the APAP-Glu pathway is likely to explain the higher circulating concentration of APAP-Glu, which is in agreement with earlier reports.[6,7]

Current practice worldwide is to measure plasma or serum APAP as a central part of risk stratification after overdose. However, APAP *per se* is relatively nontoxic without CYP-mediated metabolism.[28,29] The CYP generated reactive metabolite, NAPQI, mediates ALI following APAP overdose.[30] Therefore, biomarkers that report activity of CYP-mediated APAP metabolism may, theoretically, refine patient care pathways. *A priori*, it could be hypothesized that APAP-GSH, APAP-Cys, and/or APAP-Mer would be either higher in those with liver injury because of increased CYP metabolism or lower because of reduced glutathione bioinactivation of NAPQI. This study demonstrates that patients with ALI have a relatively higher circulating fraction of CYP metabolites compared to phase II metabolites. Importantly, from a clinical perspective, prior to NAC treatment the fraction of CYP-mediated metabolites was higher in people who subsequently developed ALI. Although all patients included in this study received NAC treatment following measurement of their plasma APAP concentration, the absolute value of APAP had no predictive value for the development of subsequent ALI. We chose not to interpret APAP with regard to time from overdose—such as by creating multiple nomogram lines[31]—to facilitate head-to-head comparison with metabolites measured in the same sample. By contrast with APAP, the CYP metabolite APAP-Cys was able to predict the onset of ALI with an ROC-AUC of 0.75 in the discovery cohort and an ROC-AUC of 0.82 in the validation cohort. APAP-Cys is commonly used as a surrogate measure of circulating APAP-protein adducts. In this study the protein fraction was removed prior to mass spectrometry, which distinguishes it from the protocol used for adduct measurement. Therefore, the data presented in this article are likely to accurately reflect APAP-Cys derived from glutathione conjugation with NAPQI. When the ratio of APAP-Cys and APAP-Sul was calculated, prediction accuracy was further increased to an ROC-AUC of 0.91 in the discovery cohort. The optimal measure of CYP metabolism remains to be determined by future larger studies.

Multiple new biomarkers of hepatocyte injury,[5] inflammation,[32] tissue regeneration,[21] and kidney injury[33] have recently been identified. These markers have high sensitivity and specificity for reporting injury or assessing prognosis (depending on the

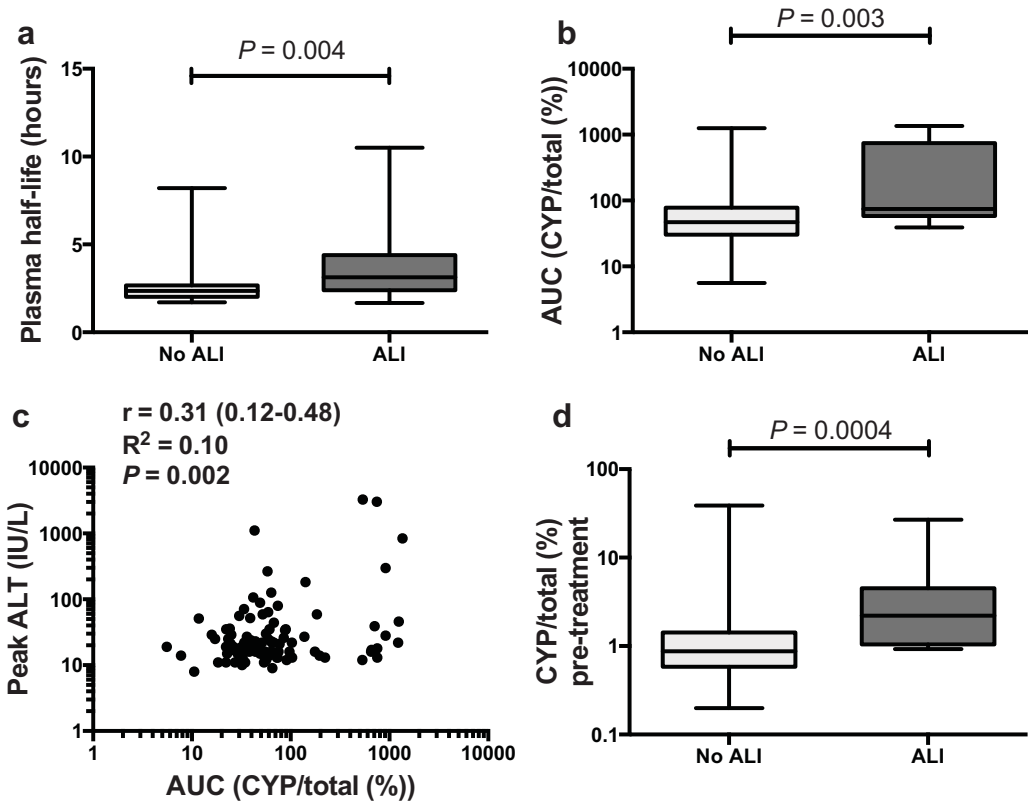

Figure 3 Discovery cohort. (**a**) APAP half-life in patients developing acute liver injury (ALI, as defined by >50% ALT increase) (n = 14) and those with no injury (no ALI) (n = 102). (**b**) Area under the curve (AUC) for the proportion of total metabolites formed by CYP enzyme activity (CYP/Total(%)) from time 0 to 20.25 h after starting NAC in liver injury (ALI) (n = 14) and nonliver injury (No ALI) patients (n = 102). (**c**) Correlation between the AUC for the proportion of total metabolites formed by CYP enzyme activity (CYP/Total(%)) from time 0 to 20.25 h after starting NAC and peak hospital stay serum alanine transaminase (ALT) activity (n = 116). (**c**) At pretreatment before NAC and ondansetron or placebo. Metabolites formed by CYP enzyme activity are expressed as a proportion of total circulating metabolites (CYP/total (%)) in liver injury (n = 14) and nonliver injury patients (n = 102). In (**a,b,d**): boxes show median ± IQR, whiskers represent range.

context of use). CYP metabolites complement these markers by offering potential refinement of risk stratification beyond the measurement of APAP parent drug. It has been proposed that the product of the APAP concentration and serum ALT activity can determine the risk of liver injury independent of time from drug ingestion.[34] A combination of CYP metabolites and one or more highly sensitive liver injury markers (such as miR-122) promises to more accurately identify patients at risk of liver injury despite NAC treatment. Using this new combination in routine clinical practice still requires development. However, in the context of clinical trials these markers may offer value in the near future. The potential for refinement of clinical trials was demonstrated when the SNAP trial results were reanalyzed with the pre-ondansetron treatment ratio of APAP-Cys/APAP-Sul included. In this refined analysis the apparent increase in ALI reported with ondansetron was not different from placebo. This is because the more sensitive CYP pathway biomarker demonstrated that, by chance, more patients with a toxic metabolite profile were randomized to ondansetron compared to placebo. Future clinical trials of novel therapeutic strategies could be enhanced by measurement of CYP metabolites that may identify patients who will develop ALI despite treatment with NAC. For both CYP metabolites and other novel biomarkers to be useful in clinical trials, a key roadblock to be overcome is the development and validation of point-of-care assays that can provide measurements within the timeframe for patient identification and trial recruitment.[35]

Our data are from an early-phase discovery study that only included patients treated with NAC (because they had serial blood tests). Future work will include those patients deemed not to require treatment after overdose based on interpretation of the currently used biomarkers. In this study we interpreted the APAP metabolite data at first presentation without regard for time from ingestion. In the future, nomograms may be developed that are analogous to the APAP treatment lines. The increase in ALT used to define our primary outcome of ALI (50% rise) was modest. This was chosen by the SNAP trialists before this randomized clinical trial started and so was also used in this follow-up biomarker discovery study. The incidence of larger increases in ALT (such as >1,000 U/L) was too low in both our discovery and validation cohorts for robust analysis. Therefore, future studies will be needed to define the relationship between CYP metabolites and more severe injury.

In summary, circulating APAP metabolites formed by CYP enzymes are toxicokinetic biomarkers that stratify patients by their risk of subsequent ALI prior to starting NAC. With

Table 3 Predictive accuracy of current and new biomarkers compared to ROC-AUC = 0.5

	Discovery cohort N = 116					Validation cohort N = 150				
Metabolite/ Biomarker	ROC-AUC (95% CI)	P value	SENS (95% CI)	PPV (%)	NPV (%)	ROC-AUC (95% CI)	P value	SENS (95% CI)	PPV (%)	NPV (%)
APAP-CYS/ APAP-Sul	0.91 (0.83-0.98)	**< 0.0001**	0.71 (0.42-0.92)	50	96	0.76 (0.63-0.88)	**0.0003**	0.43 (0.35-0.52)	38	92
CYP%	0.78 (0.67-0.90)	**0.0006**	0.36 (0.13-0.65)	33	91	0.66 (0.51-0.82)	**0.02**	0.11 (0.06-0.17)	14	87
Sum CYP metabolites	0.75 (0.61-0.88)	**0.003**	0.48 (0.38-0.58)	40	93	0.83 (0.71-0.94)	**< 0.0001**	0.44 (0.36-0.53)	39	92
APAP-CYS	0.75 (0.61-0.88)	**0.003**	0.36 (0.13-0.65)	33	91	0.82 (0.71-0.94)	**< 0.0001**	0.44 (0.35-0.52)	39	92
INR	0.70 (0.54-0.86)	**0.03**	0.23 (0.05-0.54)	24	89	0.71 (0.57-0.85)	**0.005**	0.07 (0.03-0.13)	9	87
ALT	0.67 (0.50-0.84)	**0.04**	0.29 (0.08-0.58)	28	90	0.51 (0.35-0.67)	0.86	0.16 (0.03-0.40)	19	88
APAP-Sul	0.65 (0.48-0.82)	0.06	0.50 (0.23-0.77)	41	93	0.53 (0.38-0.67)	0.75	0.11 (0.06-0.17)	14	87
APAP-Glu	0.63 (0.44-0.82)	0.11	0.36 (0.13-0.65)	33	91	0.61 (0.47-0.76)	0.11	0.11 (0.06-0.17)	14	87
APAP-GSH	0.61 (0.46-0.76)	0.19	0.21 (0.05-0.51)	22	89	0.67 (0.61-0.74)	**0.004**	0.41 (0.21-0.64)	37	91
APAP-Mer	0.59 (0.40-0.77)	0.29	0.21 (0.05-0.51)	22	89	0.76 (0.62-0.90)	**0.0003**	0.26 (0.19-0.34)	27	89
APAP LC/MS	0.50 (0.33-0.67)	0.97	0.14 (0.02-0.43)	16	88	0.57 (0.41-0.73)	0.32	0.05 (0.02-0.11)	7	87
APAP hospital lab	0.55 (0.37-0.73)	0.78	0.00 (0.00-0.04)	0	87	0.58 (0.42-0.73)	0.29	0.09 (0.04-0.15)	12	87

The positive and negative predictive values (PPV and NPV, respectively). Table with ROC-AUC (area under the curve with 95% CI), sensitivity (at 90% specificity) with 95% CI, and statistical significance for different metabolites measured at pretreatment in the discovery and hospital presentation in the validation cohort. *P*-value represents significance level are also presented for each metabolite/biomarker.

development, there is the potential for enhanced patient identification for entry into clinical trials of novel treatment pathways and refined clinical decision-making.

METHODS

Patients

All patients were treated with NAC for a single acute APAP overdose. To determine the need for NAC treatment, plasma APAP concentration was measured by the Paracetamol Assay from Cambridge Life Sciences (Cambridgeshire, UK) in the clinical biochemistry laboratories at each center. The APAP concentration was interpreted using the contemporaneous UK APAP treatment nomogram.

Discovery cohort. Patients from the SNAP trial (EudraCT number 2009-017800-10) were recruited at the Royal Infirmary of Edinburgh (RIE), UK. Details of the full SNAP protocol are reported in Thanacoody *et al.*[36] In brief, patients were eligible for entry into the SNAP trial if they presented within 36 h of a single acute APAP overdose and required treatment with NAC, based on standard UK guidance for management. Full informed consent was obtained and the study was approved by the UK Medicines and Healthcare products Regulatory Agency and the Scotland A Research Ethics Committee, UK (ref. no. 10/MRE00/20).

Plasma EDTA blood samples were collected before ("pretreatment"), 12 h and 20.15 h after the start of conventional or modified NAC treatment (with intravenous ondansetron or placebo treatment immediately after the pretreatment blood draw). Plasma was separated and the samples were stored at −80°C until analysis. For all study participants, demographics and blood results were recorded.

Validation cohort. Adult patients (16 and over in Scotland, 18 and over in England) were recruited to the MAPP study if they fulfilled the study inclusion and exclusion criteria. Full informed consent was obtained from every participant and ethical approval for this study was from the South East Scotland Research Ethics Committee and the East of Scotland Research Ethics Committee via the South East Scotland Human Bioresource. Research nurses at each site identified participants on admission to hospital. The inclusion criteria were: a history of APAP overdose that the treating clinician judged to warrant treatment with intravenous NAC as per the contemporaneous UK guidelines; the first blood sample collected within 24 h of last APAP ingestion and the patient had the capacity to consent. Patients were excluded if any of the following applied: patient detained under the Mental Health Act (UK); patient has known cognitive impairment; inability to provide informed consent for any reason or an unreliable history of overdose. Patients having taken a single acute APAP overdose were recruited at St. Thomas Hospital London, UK (n = 59) and Aberdeen Royal Infirmary, UK (n = 91).

Primary endpoint

The primary endpoint was ALI; predefined by SNAP as a rise in serum ALT activity of 50% or more at 20.25 h compared to the hospital admission value.[36]

Table 4 Effect of APAP-Cys/APAP-Sul on acute liver injury in patients treated with ondansetron compared to placebo in SNAP trial

Model	Ondansetron versus placebo Odds ratio (95% CI), *P* value for developing ALI
Full SNAP trial, adjusted[a] as in Lancet paper[21]	0.303 (0.108, 0.851), 0.024
Full SNAP trial, unadjusted[b]	0.332 (0.124, 0.886), 0.028
This study subset of SNAP, unadjusted	0.211 (0.055, 0.801), 0.022
This subset, adjusted for APAP-Cys/APAP-Sul	0.465 (0.097, 2.226), 0.338

[a]Adjusted by the variables in the minimization algorithm, and center. [b]Obtained with a model in which only treatment and regimen were included.

Chemicals and reagents

High-performance liquid chromatography (HPLC)-grade methanol and water were from Fisher Scientific (Loughborough, UK). Acetic acid and formic acid were from Sigma-Aldrich (Gillingham, UK). APAP was from Apollo (Denton, Manchester, UK). APAP-Mer, APAP-GSH, APAP-Sul, APAP-d4 (APAP-d4), and APAP-sulphate-d3 (APAP-SUL-d3) were from Santa Cruz Biotechnology (Heidelberg, Germany). APAP-Cys and APAP-Glu were from CGeneTech (Indianapolis, IN).

Sample preparation and analysis by LC-MS/MS

APAP and metabolites were extracted from plasma by liquid–liquid extraction with acidified methanol. Briefly, 10 μL plasma was enriched with 10 ng APAP-d4 (APAP-d4) and 10 ng APAP-SUL-d3 as internal standards and 0.8 mL methanol (w/0.2% acetic acid) was added, vortexed, and incubated for 20 min on ice. After centrifugation (3000*g*, 10 min, 10°C) to pellet protein in the sample, the supernatant was reduced to dryness under nitrogen at 40°C and reconstituted in mobile phase (200 μL water/methanol (65:35, v/v)) and centrifuged for a second time.

Analysis was carried out by LC-MS/MS. Liquid chromatographic separation was achieved using an Aria CTC autosampler and Allegros pump on an ACE Excel 2 SuperC18 column (150 × 3 mm; 2 μm) protected by a Kinetex KrudKatcher (Phenomenex, UK) at 20°C and detected on a TSQ Quantum Discovery triple quadrupole mass spectrometer (Thermo Fisher Scientific, UK) operated by selective reaction monitoring. The mobile phase consisted of 0.1% formic acid in water and 0.1% formic acid in methanol at a flow rate of 0.3 mL/min. Gradient elution was achieved with a total run time of 9 min from 35% to 5%. The mass spectrometer was operated in polarity switching electrospray mode (300°C, 3 kV). In positive mode, transitions monitored for were m/z 152 → 110.0, 93.1 at 20 and 13 V and m/z 156.1 → 114.1, 97.1 at 15 and 22 V for APAP and APAP-d4, respectively. For the positively ionized APAP metabolites, APAP-Cys, APAP-Mer, and APAP-GSH, m/z 271.1 → 182.0, 207.6 at 8 and 9 V, m/z 313.0 → 140.1, 208.1 at 28 and 16 V and m/z 457.2 → 140 at 33 V were monitored.

For the negatively ionized APAP metabolites APAP-Sul, APAP-Glu, and the internal standard APAP-SUL-d3 m/z 229.8 → 107.0, 150.1 at 36 and 15 V, m/z 326.0 → 113.0, 150.0 at 28 and 16 V and m/z 233.0 → 109.5, 181.4 at 30 and 5 V were monitored.

Statistical analysis

All data are presented as median and interquartile range (IQR), except for ROC data, where 95% CIs are quoted. Comparisons were made using the Mann–Whitney *U*-test. All LC/MS-MS data were transformed from mass to molar concentrations before analyses were performed. APAP plasma half-life was estimated using a nonlinear fit, assuming first-order kinetics. All calculations and ROC analysis were performed using GraphPad Prism software (GraphPad Software, La Jolla, CA). Logistic regression models were run using SAS v. 9.4 (Cary, NC).

Additional Supporting Information may be found in the online version of this article.

ACKNOWLEDGMENTS

A.D.B.V. was supported by an NC3Rs PhD Studentship (NC/K001485/1). Author JWD acknowledges the support of NHS Research Scotland (NRS) through NHS Lothian and a BHF Centre of Research Excellence Award.

CONFLICT OF INTEREST/DISCLOSURE

The authors have no conflicts of interest to disclose.

AUTHOR CONTRIBUTIONS

J.W.D., A.D.B.V., and D.J.W. wrote the article; J.W.D., M.E., A.G., D.J.A., D.J.W., N.B., and D.N.B. designed the research; A.D.B.V., R.A.K., J.H.S., N.Z.H., A.G., D.M.W., P.D., J.G.C., and J.I.C. performed the research; J.W.D., J.I.C., D.J.A., S.C.L., and N.B. analyzed the data.

1. Larson, A.M. *et al*. Acetaminophen-induced acute liver failure: results of a United States multicenter, prospective study. *Hepatology* **42**, 1364–1372 (2005).
2. Altyar, A., Kordi, L. & Skrepnek, G. Clinical and economic characteristics of emergency department visits due to acetaminophen toxicity in the USA. *BMJ Open* **5**, e007368 (2015).
3. Bateman, D.N. *et al*. Effect of the UK's revised paracetamol poisoning management guidelines on admissions, adverse reactions and costs of treatment. *Br. J. Clin. Pharmacol.* **78**, 610–618 (2014).
4. Hawton, K. *et al*. Long term effect of reduced pack sizes of paracetamol on poisoning deaths and liver transplant activity in England and Wales: interrupted time series analyses. *BMJ* **346**, f403 (2013).
5. Antoine, D.J. *et al*. Mechanistic biomarkers provide early and sensitive detection of acetaminophen-induced acute liver injury at first presentation to hospital. *Hepatology* **58**, 777–787 (2013).
6. Prescott, L.F. Kinetics and metabolism of paracetamol and phenacetin. *Br. J. Clin. Pharmacol.* **10**(suppl. 2), 291s–298s (1980).
7. Xie, Y. *et al*. Time course of acetaminophen-protein adducts and acetaminophen metabolites in circulation of overdose patients and in HepaRG cells. *Xenobiotica* **45**, 921–929 (2015).
8. Prescott, L.F., Critchley, J.A., Balali-Mood, M. & Pentland, B. Effects of microsomal enzyme induction on paracetamol metabolism in man. *Br. J. Clin. Pharmacol.* **12**, 149–153 (1981).
9. Lau, G.S. & Critchley, J.A. The estimation of paracetamol and its major metabolites in both plasma and urine by a single high-performance liquid chromatography assay. *J. Pharm. Biomed. Anal.* **12**, 1563–1572 (1994).
10. Heitmeier, S. & Blaschke, G. Direct determination of paracetamol and its metabolites in urine and serum by capillary electrophoresis with ultraviolet and mass spectrometric detection. *J. Chromatogr. B Biomed. Sci. Appl.* **721**, 93–108 (1999).
11. Winnike, J.H., Li, Z., Wright, F.A., Macdonald, J.M., O'Connell, T.M. & Watkins, P.B. Use of pharmaco-metabonomics for early prediction of acetaminophen-induced hepatotoxicity in humans. *Clin. Pharmacol. Ther.* **88**, 45–51 (2010).
12. Muldrew, K.L. *et al*. Determination of acetaminophen-protein adducts in mouse liver and serum and human serum after hepatotoxic doses of acetaminophen using high-performance liquid chromatography with electrochemical detection. *Drug Metab. Dispos.* **30**, 446–451 (2002).
13. Davern, T.J., 2nd *et al*. Measurement of serum acetaminophen-protein adducts in patients with acute liver failure. *Gastroenterology* **130**, 687–694 (2006).
14. James, L. *et al*. Comparison of bile acids and acetaminophen protein adducts in children and adolescents with acetaminophen toxicity. *PLoS One* **10**, e0131010 (2015).
15. James, L.P. *et al*. Pharmacokinetics of acetaminophen-protein adducts in adults with acetaminophen overdose and acute liver failure. *Drug Metab. Dispos.* **37**, 1779–1784 (2009).
16. McGill, M.R. *et al*. Plasma and liver acetaminophen-protein adduct levels in mice after acetaminophen treatment: dose-response, mechanisms, and clinical implications. *Toxicol. Appl. Pharmacol.* **269**, 240–249 (2013).
17. Smilkstein, M.J., Knapp, G.L., Kulig, K.W. & Rumack, B.H. Efficacy of oral N-acetylcysteine in the treatment of acetaminophen overdose. Analysis of the national multicenter study (1976 to 1985). *N. Engl. J. Med.* **319**, 1557–1562 (1988).
18. Prescott, L.F., Park, J., Ballantyne, A., Adriaenssens, P. & Proudfoot, A.T. Treatment of paracetamol (acetaminophen) poisoning with N-acetylcysteine. *Lancet* **2**, 432–434 (1977).
19. Lauterburg, B.H., Corcoran, G.B. & Mitchell, J.R. Mechanism of action of N-acetylcysteine in the protection against the hepatotoxicity of acetaminophen in rats in vivo. *J. Clin. Investig.* **71**, 980–991 (1983).
20. Bateman, D.N. Paracetamol poisoning: beyond the nomogram. *Br. J. Clin. Pharmacol.* **80**, 45–50 (2015).

21. Stutchfield, B.M. *et al*. CSF1 restores innate immunity after liver injury in mice and serum levels indicate outcomes of patients with acute liver failure. *Gastroenterology* **149**, 1896–1909 (2015).
22. Huebener, P. *et al*. The HMGB1/RAGE axis triggers neutrophil-mediated injury amplification following necrosis. *J. Clin. Invest.* **125**, 539–550 (2015).
23. Dear, J.W. & Antoine, D.J. Stratification of paracetamol overdose patients using new toxicity biomarkers: current candidates and future challenges. *Expert Rev. Clin. Pharmacol.* **7**, 181–189 (2014).
24. Bateman, D.N. *et al*. Reduction of adverse effects from intravenous acetylcysteine treatment for paracetamol poisoning: a randomised controlled trial. *Lancet* **383**, 697–704 (2014).
25. Whyte, I.M., Buckley, N.A., Reith, D.M., Goodhew, I., Seldon, M. & Dawson, A.H. Acetaminophen causes an increased International Normalized Ratio by reducing functional factor VII. *Ther. Drug Monit.* **22**, 742–748 (2000).
26. Clements, J.A., Critchley, J.A. & Prescott, L.F. The role of sulphate conjugation in the metabolism and disposition of oral and intravenous paracetamol in man. *Br. J. Clin. Pharmacol.* **18**, 481–485 (1984).
27. Gelotte, C.K., Auiler, J.F., Lynch, J.M., Temple, A.R. & Slattery, J.T. Disposition of acetaminophen at 4, 6, and 8 g/day for 3 days in healthy young adults. *Clin. Pharmacol. Ther.* **81**, 840–848 (2007).
28. Zaher, H. *et al*. Protection against acetaminophen toxicity in CYP1A2 and CYP2E1 double-null mice. *Toxicol. Appl. Pharmacol.* **152**, 193–199 (1998).
29. Gonzalez, F.J. The 2006 Bernard B. Brodie Award Lecture. Cyp2e1. *Drug Metab. Dispos.* **35**, 1–8 (2007).
30. Mitchell, J.R., Jollow, D.J., Potter, W.Z., Davis, D.C., Gillette, J.R. & Brodie, B.B. Acetaminophen-induced hepatic necrosis. I. Role of drug metabolism. *J. Pharmacol. Exp. Ther.* **187**, 185–194 (1973).
31. Cairney, D.G., Beckwith, H.K., Al-Hourani, K., Eddleston, M., Bateman, D.N. & Dear, J.W. Plasma paracetamol concentration at hospital presentation has a dose-dependent relationship with liver injury despite prompt treatment with intravenous acetylcysteine. *Clin. Toxicol. (Phila)* **54**, 405–410 (2016).
32. Antoine, D.J. *et al*. Molecular forms of HMGB1 and Keratin-18 as mechanistic biomarkers for mode of cell death and prognosis during clinical acetaminophen hepatotoxicity. *J. Hepatol.* **56**, 1070–1079 (2012).
33. Antoine, D. *et al*. Circulating kidney injury molecule-1 predicts prognosis and poor outcome in patients with acetaminophen-induced liver injury. *Hepatology* **62**, 591–599 (2015).
34. Sivilotti, M.L., Green, T.J., Langmann, C., Yarema, M., Juurlink, D. & Johnson, D. Multiplying the serum aminotransferase by the acetaminophen concentration to predict toxicity following overdose. *Clin. Toxicol. (Phila)* **48**, 793–799 (2010).
35. Vliegenthart, A.D., Antoine, D.J. & Dear, J.W. Target biomarker profile for the clinical management of paracetamol overdose. *Br. J. Clin. Pharmacol.* **80**, 351–362 (2015).
36. Thanacoody, H.K. *et al*. Scottish and Newcastle antiemetic pretreatment for paracetamol poisoning study (SNAP). *BMC Pharmacol. Toxicol.* **14**, 20 (2013).
37. *British National Formulary*, *58th ed*. (BMJ Group and RPS Publishing: London, 2009).

4.3 Discussion

miR-122-5p is highly sensitive for detecting hepatocyte injury and allows for early stratification of patients. A marker that sensitively quantifies the body's 'toxic burden' with regard to paracetamol metabolites could further improve risk assessment at hospital presentation and during NAC treatment.

This study characterised the toxicokinetics of paracetamol metabolites in a discovery cohort of carefully phenotyped patients from a randomized clinical trial. The key findings were replicated in a separate validation cohort recruited at two different hospital sites. The key novel findings were that a higher percentage of circulating metabolites formed by cytochrome P450 enzymes (CYP metabolites) were present in patients with liver injury and these metabolites were superior to both ALT and paracetamol with regard to early patient stratification. The potential value of CYP metabolites to future clinical trials was demonstrated by their post-hoc incorporation into the SNAP trial. This resulted in the reported increase in ALI with ondansetron being no different to placebo.

Compared to the miRNAs that were able to detect liver injury, paracetamol metabolites are able to quantify the toxic burden. In patients requiring NAC treatment, the circulating paracetamol concentration was not able to predict who is more at risk of liver injury (although the decision to treat with NAC had been made in all patients). Measuring circulating metabolites formed by the toxic pathway allowed prediction of who was at risk of developing liver injury.

This work along with the miRNA work has the potential to be built on in order to improve the management of paracetamol overdose.

4.4 Copyright

Chapter 5: Retro-orbital blood acquisition facilitates circulating microRNA measurement in zebrafish with paracetamol hepatotoxicity.

5.1 Introduction

After identifying microRNAs in human hepatotoxicity, the next step was to develop a translational hepatotoxicity model in zebrafish. Due to the clinical relevance, paracetamol was chosen as first liver toxic compound. In order to measure circulating miRNAs in zebrafish, a method had to be developed for bloodletting. The paper in this chapter describes how a new bloodletting method from zebrafish was developed and compared to the previously described 'tail cut' or 'lateral incision' (LI) bloodletting method. This technique was then used to measure miR-122-5p in adult zebrafish exposed to paracetamol.

The results of this study are published as:

Vliegenthart AD, Starkey Lewis P, Tucker CS, Del Pozo J, Rider S, Antoine DJ, Dubost V, Westphal M, Moulin P, Bailey MA, Moggs JG, Goldring CE, Park BK, Dear JW. Retro-orbital blood acquisition facilitates circulating microRNA measurement in zebrafish with paracetamol hepatotoxicity. Zebrafish 2014;11:219-226. (75)

5.2 Contributions by the candidate

Study design; Execution of all fish experiments; The miRNA measurements; The data collection; All data analysis; Producing all figures; Preparation and revision of the manuscript

ZEBRAFISH
Volume 11, Number 3, 2014

DOI: 10.1089/zeb.2013.0912

Paper 6

Retro-Orbital Blood Acquisition Facilitates Circulating microRNA Measurement in Zebrafish with Paracetamol Hepatotoxicity

Adriaan D.B. Vliegenthart,[1] Philip Starkey Lewis,[2] Carl S. Tucker,[3] Jorge Del Pozo,[4] Sebastein Rider,[1] Daniel J. Antoine,[2] Valérie Dubost,[5] Magdalena Westphal,[5] Pierre Moulin,[5] Matthew A. Bailey,[1] Jonathan G. Moggs,[5] Chris E. Goldring,[2] B. Kevin Park,[2] and James W. Dear[1]

Abstract

Paracetamol is the commonest cause of acute liver failure in the Western world and biomarkers are needed that report early hepatotoxicity. The liver-enriched microRNA (miRNA), miR-122, is a promising biomarker currently being qualified in humans. For biomarker development and drug toxicity screening, the zebrafish has advantages over rodents; however, blood acquisition in this model remains technically challenging. We developed a method for collecting blood from the adult zebrafish by retro-orbital (RO) bleeding and compared it to the commonly used lateral incision method. The RO technique was more reliable in terms of the blood yield and minimum amount per fish. This new RO technique was used in a zebrafish model of paracetamol toxicity. Paracetamol induced dose-dependent increases in liver cell necrosis, serum alanine transaminase activity, and mortality. *In situ* hybridization localized expression of miR-122 to the cytoplasm of zebrafish hepatocytes. After collection by RO bleeding, serum miR-122 could be measured and this miRNA was substantially increased by paracetamol 24 h after exposure, an increase that was prevented by delayed (3 h poststart of paracetamol exposure) treatment with acetylcysteine. In summary, collection of blood by RO bleeding facilitated measurement of miR-122 in a zebrafish model of paracetamol hepatotoxicity. The zebrafish represents a new species for measurement of circulating miRNA biomarkers that are translational and can bridge between fish and humans.

Introduction

At therapeutic doses, paracetamol (acetaminophen) is a safe analgesic drug used by millions of people worldwide. However, in overdose, paracetamol is hepatotoxic, being the most common cause of acute liver failure in the United States and Europe.[1–3] The mechanism of paracetamol hepatotoxicity is well described; in overdose, the reactive metabolite N-acetyl-p-benzoquinone imine (NAPQI) is generated in excess and cellular glutathione (GSH) is depleted, NAPQI then binds covalently to cellular proteins resulting in oxidative stress and consequent hepatocyte necrosis.[4] The current antidote, acetylcysteine (AC), replenishes cellular GSH and is highly effective if administered within 8 h of overdose. However, this treatment is time-consuming and commonly results in adverse drug reactions. Therefore, there is a pressing need for new biomarkers that identify hepatotoxicity soon after overdose to stratify patients and improve the targeting of treatment to those at most risk of adverse outcomes.

microRNAs (miRNAs) are small (~22 nucleotides long) nonprotein coding RNA species involved in post-transcriptional gene product regulation. In the blood, miRNA is protected from degradation by microvesicles[5] and RNA binding protein complexes.[6] As they are amplifiable and tissue restricted, miRNAs represent a new reservoir for biomarker discovery. The liver-enriched miRNA, miR-122, is a circulating biomarker for paracetamol-induced liver toxicity in rodents and humans.[7,8] It has greater specificity for liver injury than serum alanine transaminase (ALT) activity[9] and in humans and

[1]British Heart Foundation Centre for Cardiovascular Science, The Queen's Medical Research Institute, The University of Edinburgh, Edinburgh, United Kingdom.
[2]Department of Molecular and Clinical Pharmacology, MRC Centre for Drug Safety Science, University of Liverpool, Liverpool, United Kingdom.
[3]Biomedical Research Resources, The College of Medicine and Veterinary Medicine, The University of Edinburgh, Edinburgh, United Kingdom.
[4]Easter Bush Pathology, Royal (Dick) School of Veterinary Studies, The University of Edinburgh, Roslin, Midlothian, United Kingdom.
[5]Discovery and Investigative Safety, Preclinical Safety, Novartis Institutes for Biomedical Research (NIBR), Basel, Switzerland.

rodents is elevated soon after overdose when the ALT activity is still normal.[10] miRNAs are highly conserved across species and so represent bridging biomarkers that facilitate translation of toxicity signals from animal models to human clinical trials.

The zebrafish is used to study the drug effects on organ systems such the heart, CNS, and gastrointestinal tract.[11,12] Recent studies have demonstrated that paracetamol exposure induces hepatotoxicity in zebrafish.[13] The zebrafish has many mammalian homologs at multiple loci and several advantages as a vertebrate model compared with rodents and other higher order species. These include lower financial costs, convenient drug delivery, genetically tractable and visually accessible organs.[11,14,15] However, the small size of the adult fish means that the circulating blood volume is low, which makes blood acquisition technically challenging. A number of blood collection techniques exist for zebrafish, such as a lateral incision (LI) in the dorsal aorta; yet, significant limitations remain with regard to the volume of blood that can be collected. For measurement of circulating biomarkers, such as miRNA, there is a need for new approaches to maximize the blood yield. With regard to the clinical translatability of circulating miRNA, it is important to note that the zebrafish liver expresses miR-122, which has an identical nucleotide sequence (UGGAGUGUGACAAUGGU GUUUG) to the rodents and humans.[16]

To date, zebrafish miRNA expression has been studied only in tissues, and no data have been published on circulating miRNA. In this article, we describe a new method for blood collection based on retro-orbital (RO) sinus bleeding, a technique commonly used in rodents.[17] This technique was used to collect blood for measurement of circulating miR-122 in a clinically relevant zebrafish model of paracetamol hepatotoxicity.

Materials and Methods

Ethical approval

All experiments were conducted in accordance with the Animals (Scientific Procedures) Act 1986 in a UK Home Office approved establishment.

Materials

Paracetamol, MS-222 (tricaine methanesulfonate), and ethylenediaminetetraacetic acid (EDTA) were obtained from Sigma-Aldrich (Gillingham, United Kingdom). The MiRNeasy and the MinElute Cleanup kit were obtained from Qiagen Benelux B.V. (Venlo, the Netherlands). Specific reverse transcription (RT) and polymerase chain reaction (PCR) primers were obtained from Applied Biosystems (Foster City, CA) (assay number 002245 for miR-122, 004468_mat for let-7d).

Zebrafish

Fish were 5–24 months old. In all studies, the age of fish was the same across experimental groups. All fish were maintained at 28.5°C, pH 7.2, and conductivity of $\approx$400 μS. Fish were euthanized with 4 mg/mL MS-222 before all blood and tissue collection procedures. All experimental procedures were performed at room temperature (23°C $\pm$ 0.5°C).

Blood collection

To study the relationship between the fish size and blood yield, after euthanasia, each fish was weighed and the total body length (BL) was measured (from the tip of the snout to the origin of the caudal fin). Two methods of blood collection were compared: the established LI technique and a new RO approach. LI was performed as previously described.[18] In brief, after euthanasia, fish were dried and then the tail was cut at the caudal peduncle with a surgical knife. Blood was collected, with the aid of a pipette, into an eppendorf tube containing heparin solution (0.5 μL of 25 mg/mL). For RO bleeding, following euthanasia, fish were quickly dried and then one eye was removed using a pair of fine forceps. The heparin (0.5 μL of 25 mg/mL stock) or EDTA (0.5 μL of 2% stock) solution was pipetted onto the eye socket to prevent the blood from clotting. Once the orbital space had filled with blood, it was pipetted off and collected in an eppendorf tube. After this step, pressure was applied to the fish from the tail toward the head to accumulate more blood into the orbit for collection. This last step was repeated until no more blood could be collected.

Paracetamol toxicity model

Zebrafish were exposed to paracetamol (20–40 mM), dissolved in system water, for 3 h (or system water alone for negative controls). This was followed by a change of system water for 2–21 h with or without AC (3 mM). This brief exposure to high-concentration paracetamol followed by delayed AC treatment was used to replicate a human single, acute overdose. The drug concentrations were based on published data.[13] Experiments were terminated 5–24 h after the start of paracetamol exposure (5–24 hours post exposure [hpe]).

All histology samples were placed in Dietrich's fixative and left to fix for at least 24 h before processing, cutting, and hematoxylin staining using standard protocols. All fish were sectioned sagittally along the midline to allow examination of the hepatic tissue. Hepatic lesions were scored by a boarded pathologist (author J.D.P.), who was blinded to the treatment groups. Zebrafish blood was obtained by the RO technique and pooled as described in the results. Serum was separated by centrifugation and the ALT activity was measured as described by Bergmeyer *et al.*,[19] utilizing a commercial kit (Alpha Laboratories Ltd., Eastleigh, United Kingdom) adapted for use on a Cobas Fara centrifugal analyzer (Roche Diagnostics Ltd., Welwyn Garden City, United Kingdom). The paracetamol concentration was measured by an aryl acylamidase enzymatic assay in the Royal Infirmary of Edinburgh Clinical Biochemistry laboratory.

miR-122 localization by in situ *hybridization*

miR-122 was localized using double-DIG-labeled miRCURY LNA miRNA detection probes (Exiqon A/S, Vedbaek, Denmark) specific for miR-122. The *in situ* hybridization procedure was performed on a fully automated Ventana Discovery Ultra (Roche diagnostics AG, Rotkreuz, Switzerland). All reagents were provided by Roche Diagnostics. Briefly, whole zebrafish sections were deparaffinized at 62°C for 12 min before the proteinase K digestion step (Exiqon A/S, Vedbaek, Denmark) treatment (37°C, 24 min). The anti-miR-122 probe (25 pmoles) was then incubated at 54°C for 3 h with deparaffinized sections. Sections were then washed with 3 $\times$ 8-min cycles of saline sodium citrate at increasing stringency per cycle (2.0 $\times$, 1.0 $\times$, 0.5 $\times$). The secondary antibody (alkaline phosphatase-linked Sheep anti-DIG, dilution 1:500

in antibody diluent) was then incubated at 37°C for 32 min. Chromogenic detection was performed using the BlueMap® kit as per the manufacturer's instructions. The substrate was allowed to develop for 6 h before counterstaining with Red Stain II for 4 min. Slides were manually washed before mounting on laboratory-grade glycerol gelatin (Sigma-Aldrich, Buchs, Switzerland). Slides were scanned using a Nanozoomer 2.0-HT digital slide scanner (Hamamatsu photonics, Hamamatsu, Japan). Images were captured using NDP.view2 software (Hamamatsu photonics).

miRNA measurement

For miRNA analysis, zebrafish blood was obtained by the RO technique and pooled as described in Results. Serum was separated by centrifugation and miRNA was extracted using a miRNeasy kit (Qiagen, Venlo, Netherlands), after which the small RNA fraction was purified using a MinElute kit (Qiagen, Venlo, Netherlands).[8] miRNAs were measured using TaqMan-based quantitative PCR.

The small RNA elute was reverse transcribed using specific stem-loop reverse-transcription RT primers (Applied Biosystems, Foster City, CA) for each target miRNA species, following the manufacturer's instructions. In the reverse-transcription reaction, 2 μL of RNA was used to produce the complementary DNA (cDNA) template in a total volume of 15 μL. Then, 1.33 μL of cDNA was used in the PCR mixture with specific PCR primers (Applied Biosystems) in a total volume of 20 μL. Levels of miRNA were measured using the Light Cycler 480 (Roche, Basel, Switzerland). All samples were assayed in duplicate. miRNA levels were normalized to the levels of let-7d, which has been reported to be an appropriate internal normalizer in humans.[20] At the time of writing, the optimum normalizer for zebrafish was not described.

Statistical analysis

Statistical analysis was performed with GraphPad Prism software (GraphPad Software, Inc., La Jolla, CA). Differences in blood yield between the LI and RO techniques and biomarker differences between the experimental groups were analyzed with the Student's unpaired t test. For correlation analysis, a Pearson's correlation test was used. Nominal statistical significance was set at $p < 0.05$.

Results

Blood yield was higher with the RO technique

The volume of blood obtained by RO ($N = 52$) and LI ($N = 37$) techniques was compared (Fig. 1); the RO technique resulted in significantly higher blood yields than the LI

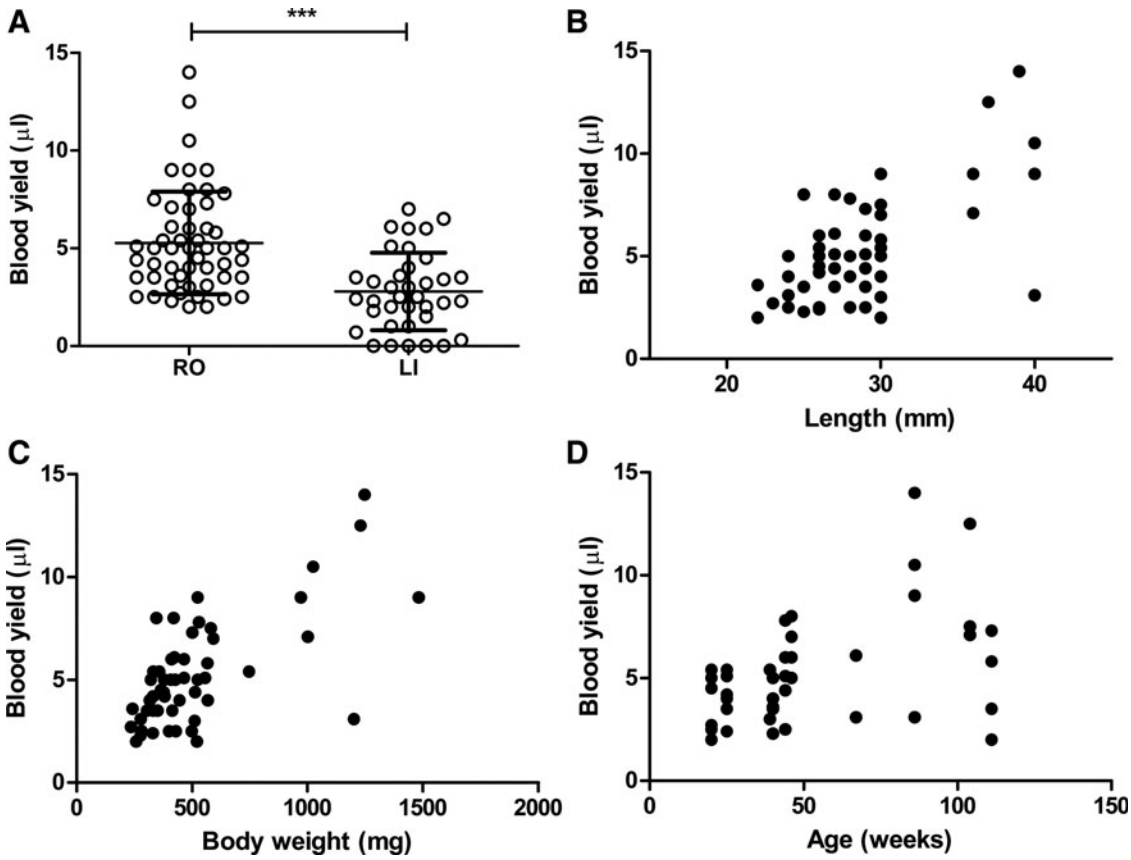

FIG. 1. **(A)** Blood yield for the retro-orbital (RO) technique ($N = 52$) and for the lateral incision (LI) technique ($N = 37$). Each point represents an individual fish. *Horizontal bars* represent the mean. Error bars represent standard deviation. ***$p < 0.0001$. Scatter graphs of RO blood yield in relation to body length **(B)**, body weight **(C)**, and age **(D)**. Each point represents an individual fish. Pearson R values (statistical probabilities) are 0.63 ($p < 0.0001$), 0.67 ($p < 0.0001$), and 0.46 ($p = 0.001$) for length, weight, and age, respectively.

technique (mean per fish ± SD: 5.3 ± 2.6 μL vs. 2.8 ± 2.0 μL, $p < 0.0001$). Furthermore, the LI technique did not result in successful blood collection from every fish, with 6 from 37 providing insufficient or no blood. In comparison, the RO technique resulted in blood collection from every fish, with a minimum yield of 2 μL.

Individual fish age, BL, and body weight (BW) were not significantly different between the RO and LI groups (mean ± SD: age 52.2 ± 30.3 vs. 53.9 ± 32.48 weeks, $p = 0.81$, BL 28.5 ± 4.5 vs. 27.8 ± 3.6 mm, $p = 0.44$, BW 518.6 ± 284.1 vs. 492.7 ± 181.9 mg, $p = 0.62$, for RO vs. LI, respectively). Within the RO group, blood yield correlated significantly with all three parameters. However, BL and BW were more strongly correlated with blood yield than age: BL ($R = 0.63$, $p < 0.0001$), BW ($R = 0.67$, $p < 0.0001$), and age ($R = 0.46$, $p = 0.001$) (Fig. 1).

Paracetamol-induced liver toxicity in adult zebrafish

Next, the RO blood collection technique was applied to a zebrafish model of paracetamol hepatotoxicity. Paracetamol dissolved in the system water entered the zebrafish circulation. In a pooled serum sample from 10 fish, the serum paracetamol concentration was 962 mg/L immediately following a 3-h exposure to paracetamol (30 mM). Exposure to 40 mM paracetamol for 3 h resulted in 4 out of 10 fish dying 3–6 hpe. In the 30 mM group, 1 out of 30 fish died at 2.5 hpe, and 3 out of 30 fish died at 20–23 hpe (Fig. 2). No fish died after 20 mM of paracetamol exposure ($p = 0.02$ for mortality following paracetamol exposure). Exposure to 20 mM and 40 mM paracetamol for 3 h resulted in hepatocyte necrosis at 24 hpe (Fig. 2). There was a dose–response relationship in the mean number of necrotic foci per liver section (mean ± standard error of the mean: control 0.13 ± 0.1, 20 mM 1.5 ± 0.7, 40 mM 2.7 ± 0.7), and both treatment groups induced a significant increase in necrosis compared with control ($p = 0.02$ and $p < 0.001$ for 20 and 40 mM paracetamol, respectively) (Fig. 2). Other histological features included pericapsular macrophage clustering, pigment-laden macrophages, and cytoplasmic granularity of hepatocytes. The former two features were noted in both cases and controls, suggesting these are background findings. Cytoplasmic granularity of hepatocytes appeared to be associated with paracetamol exposure. At 24 hpe, there was a paracetamol-induced dose-dependent increase in the serum ALT activity (Fig. 2).

miR-122 localized to zebrafish hepatocytes

In situ hybridization with the miR-122 probe revealed positive intra-cytoplasmic staining in zebrafish. ISH-positive staining was noted in variable numbers of hepatocytes scattered throughout the hepatic parenchyma, and was characterized by one or more focal deposits within the cytoplasm (Fig. 3).

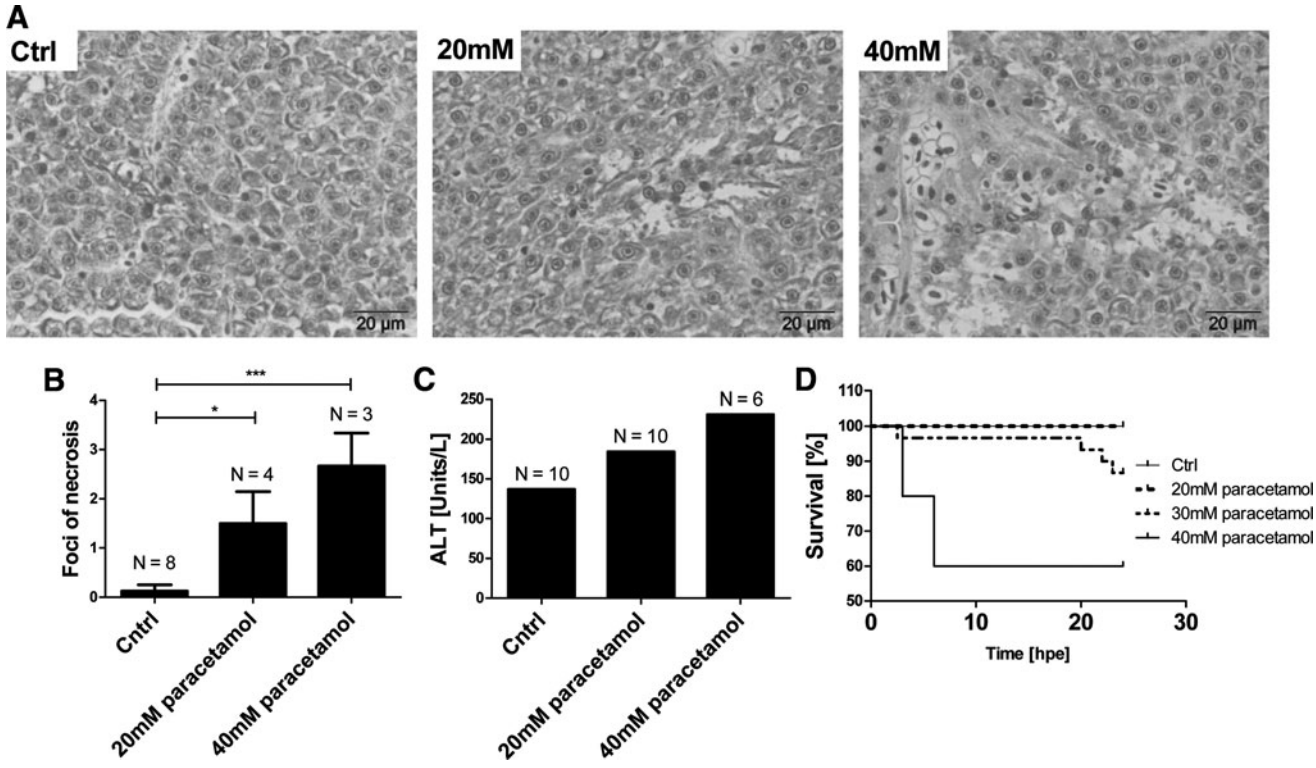

FIG. 2. Effect of paracetamol exposure on adult zebrafish. Paracetamol treatment was for 3 h, all measurements made 24 hpe. **(A)** Histological images of adult zebrafish liver at the indicated paracetamol concentrations; both treatment groups displayed liver necrosis. **(B)** Mean foci of necrosis per liver section at the indicated paracetamol concentrations. N = number of fish per treatment group. Error bars represent SEM, $^*p < 0.05$, $^{***}p < 0.001$. **(C)** Serum ALT activity in pooled samples from each treatment group. N = the number of pooled fish for ALT measurement. **(D)** Survival curves for experimental groups $N = 10$/group. There was a significant difference between treatment groups, $p = 0.02$. ALT, alanine transaminase; hpe, hours post exposure; SEM, standard error of the mean.

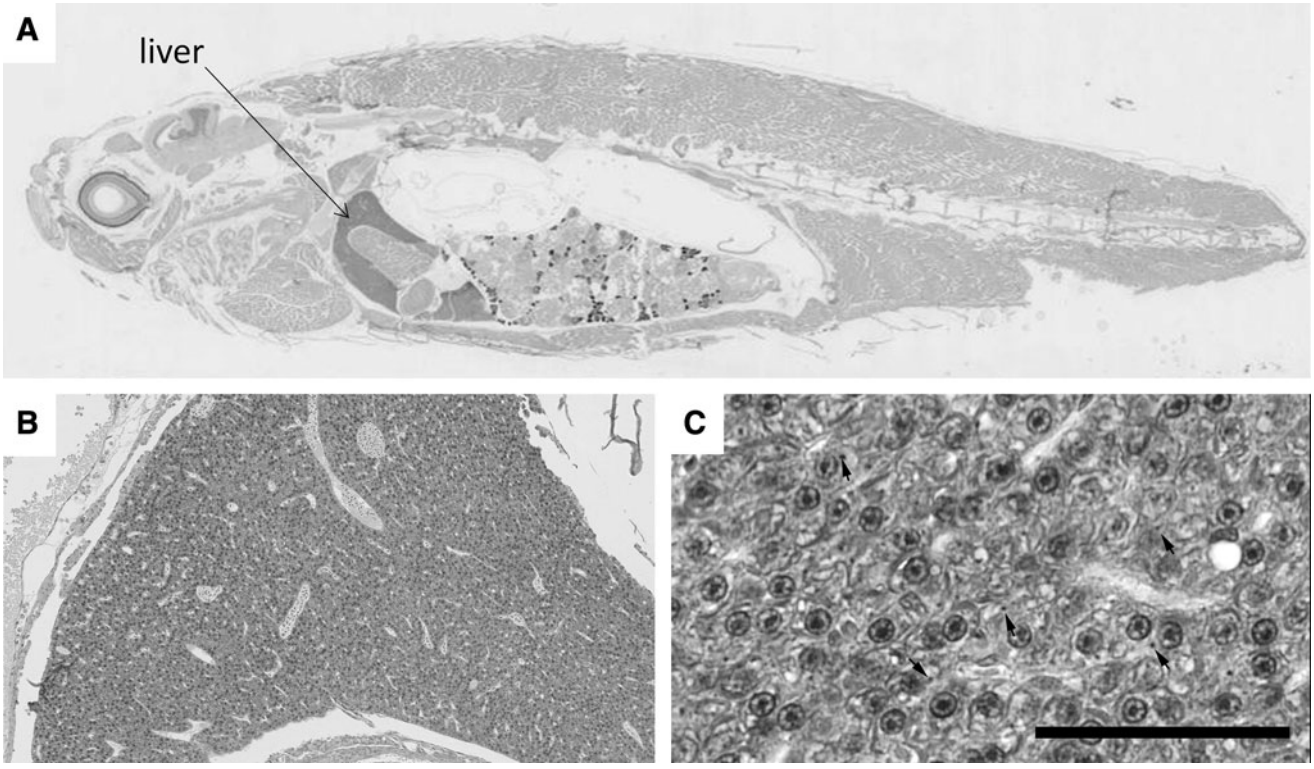

FIG. 3. miR-122 *in-situ* hybridization. **(A)** Whole zebrafish section demonstrates localization to the liver. **(B, C)** Liver microphotographs: widespread intracytoplasmic deposition of ISH substrate in the hepatocytes of a fish (*arrows* indicate focal deposits). Scale bar: 50 μm.

Paracetamol hepatotoxicity was associated with increased circulating miR-122

Measurement of miRNA in pooled serum from adult zebrafish was possible, and this was facilitated by the increased blood yields from RO bleeding. Exposure to paracetamol (20–40 mM for 3 h) resulted in a dose-dependent increase of miR-122 concentration, measured at 24 hpe (Fig. 4). This increase was still apparent when raw ct values were displayed without normalization to the miRNA let-7d (Fig. 4). A paracetamol concentration of 30 mM was chosen to study the effect of AC as this concentration induced a

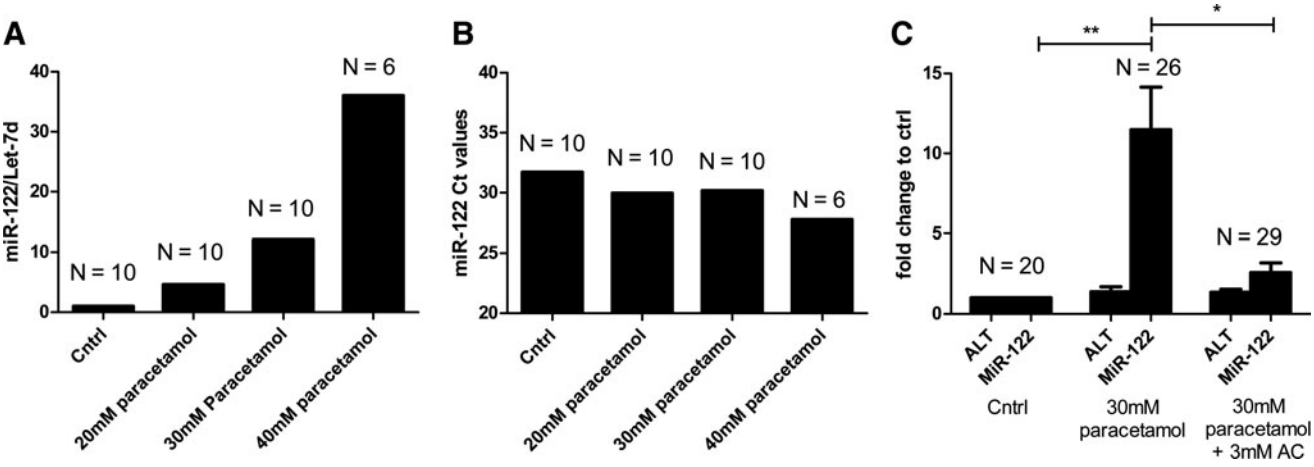

FIG. 4. **(A)** Circulating miR-122 24 hpe to 3 h of paracetamol at the concentrations indicated. miR-122 was normalized to let-7d. *N* = number of fish pooled for microRNA measurement. **(B)** Circulating miR-122 24 hpe to 3 h of paracetamol at the concentrations indicated. Raw ct values are presented without normalization. *N* = number of fish pooled for microRNA measurement. **(C)** Serum ALT activity and miR-122 24 hpe to 3 h of paracetamol (30 mM) followed by 21 h of AC (3 mM) or water. ALT and miR-122 are expressed as fold change compared to control. Values are mean, error bars are SEM. Zebrafish were equally divided across three replicate experiments giving the indicated total numbers per group (*N*). $*p < 0.05$, $**p < 0.001$ for comparison of miR-122/let-7d values between groups indicated. AC, acetylcysteine.

significant increase in circulating miR-122 at 24 hpe (miR-122/let-7d: mean ± SEM, control 0.1 ± 0.005, paracetamol 1.0 ± 0.2. $p = 0.01$) with lower mortality than 40 mM. Zebrafish were divided across 3 replicate experiments giving total numbers per group as presented in Figure 4. Blood was pooled within groups from each experiment. Expressed with reference to each experiment's system water control, there was an eightfold larger increase of miR-122 compared with ALT activity for the same paracetamol dose at 24 hpe (fold change relative to control, 30 mM paracetamol [mean ± SEM]: 1.4 ± 0.3 ALT, 11.5 ± 2.7 miR-122). (Fig. 4). After 3 h of exposure to paracetamol, the fish were treated with AC (3 mM) in the water or water alone for 21 h. With AC, 1 out of 30 fish died (3.3%), whereas 4 out of 30 fish died (13.3%) in the absence of AC. Consistent with delayed AC treatment preventing liver injury, AC prevented the paracetamol-induced increase in circulating miR-122 (miR-122/let-7d: mean ± SEM, paracetamol 1.0 ± 0.2, paracetamol and AC 0.2 ± 0.05. $p = 0.009$). Figure 5 presents the temporal profile of circulating miR-122 and ALT activity at 5–24 hpe to 30 mM paracetamol for 3 h. This demonstrates that miR-122 was not significantly elevated until 24 hpe. With this dose of paracetamol, there was no significant increase in the serum ALT activity.

Discussion

For zebrafish to be useful in circulating biomarker discovery and validation studies, it is vital to maximize the yield of blood from every fish. In this study, we demonstrated that a new RO technique was more efficient than the commonly used LI approach in terms of blood yield. We developed a zebrafish model for paracetamol-induced hepatotoxicity, in which we used the new RO blood draw technique to, for the first time, measure circulating miRNA in zebrafish. We noted that circulating liver-enriched miRNA (miR-122), was elevated in a dose-dependent pattern as a result of paracetamol hepatotoxicity. This is consistent with findings in humans and rodents.

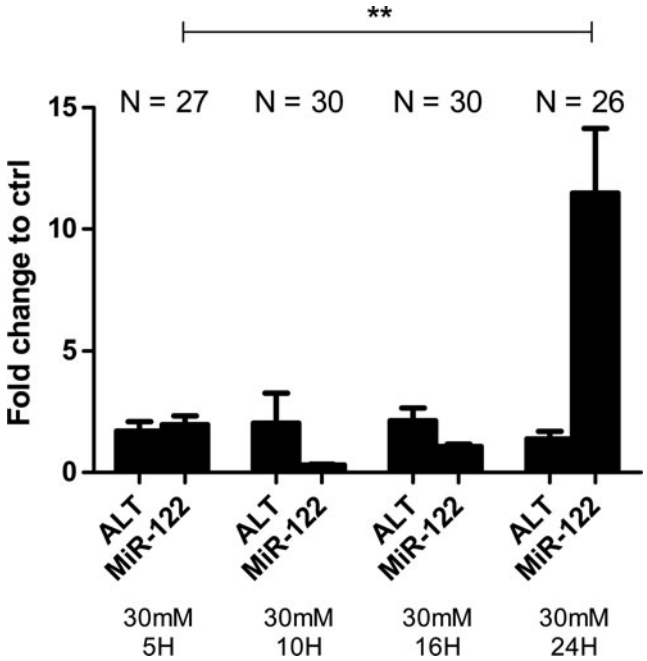

FIG. 5. Serum ALT activity and miR-122 5–24 hpe to 3 h of paracetamol (30 mM). ALT and miR-122 are expressed as fold change compared to controls run at each time point. Values are mean, error bars are SEM. Zebrafish were equally divided across three replicate experiments giving the indicated total numbers per group (*N*). $^{**}p < 0.001$ for comparison of miR-122/let-7d values between groups indicated.

In the present study, the LI blood collection technique yielded a mean of 2.8 μL of blood per fish, but no blood or blood volumes of less than 1 μL were obtained from around 19% of fish. These results are consistent with previous studies.[21,22] The new RO technique yielded a higher mean of 5.3 μL of blood per fish and a maximum of 14 μL. Additionally, the RO technique resulted in a minimum of 2 μL from all fish used in this study. When calculating the number of fish that need to be pooled (with a power of 80%) to ensure a sample of 40 μL of blood, for the RO technique, 13 fish would be needed, whereas 36 fish would be needed if the LI technique is used. Therefore, fewer animals may be needed for a successful experiment if the RO technique is used, which is in compliance with the principle of reduction in the number of experimental animals (www.nc3rs.org.uk).

The fish age, length, and weight correlated significantly with the amount of blood drawn by the RO technique (longer, heavier, and older fish yielded higher volumes of blood). However, the size correlated more strongly with blood yield than fish age, which makes the fish size a more useful predictor of successful blood acquisition. In our study, relatively small fish were mostly used; ~22–30 mm in length. However, a few larger fish, up to 40 mm, were included, which is a size that is rarely exceeded in captivity.[23] These large fish yielded up to 14 μL of blood. The largest reported blood yield was from the study of Pedroso *et al.*,[18] who reported a yield of up to 20 μL; however, the fish size was not disclosed in their report and the anesthetic agent used might have increased the blood yield. Pedroso *et al.*[18] used ice-cold water, which slows fish metabolism,[24,25] however, the UK Animals (Scientific Procedures) Act 1986, does not allow this approach. Jensen,[26] who, like our study, used MS-222 to anesthetize the fish before the LI technique, reported blood yields of 2–8 μL, which is in line with our LI results. Recently, a new technique has been described in which fish were centrifuged in a perforated eppendorf tube after the administration of a LI.[27] They reported comparable blood yields (5.5–11 μL) to the RO approach. However, centrifugation may lead to blood contamination with other body fluids, whereas the RO blood collection approach results in a reduced risk of contamination. Zang *et al.*,[28] described a recovery method that allows for serial blood sampling from adult zebrafish, but it takes 1 to 2 weeks for fish to recover normal hemoglobin values after taking a small blood sample of 2 μL. This delayed recovery may limit the value of serial blood sampling in toxicity studies.

Paracetamol was associated with hepatocyte necrosis in the liver of zebrafish. This is consistent with previous studies in zebrafish that have demonstrated paracetamol-induced formation of NAPQI through the enzymatic action of CYP3A65[29]; hepatic GSH depletion and necrotic cell death.[13] In the present study, the histological evidence of liver injury was accompanied by modestly increased serum ALT activity and clearly increased mortality. The zebrafish

liver expressed miR-122 as detected by ISH. To the best of our knowledge, this is the first study to localize zebrafish miR-122 by *in situ* hybridization and to measure miRNA in zebrafish serum, facilitated by the increased blood volumes collected by the RO technique. In paracetamol-exposed fish, there was a clear, dose–response elevation in circulating miR-122. This is consistent with release from the injured liver as is described in rodents and humans.[7,8] Furthermore, circulating miR-122 is elevated in humans and rodents soon after a paracetamol overdose at a time when ALT is still normal, and therefore, miR-122 appears more sensitive than ALT for reporting hepatotoxicity.[7,10] In the present study, 24 h after paracetamol exposure, when there was histologically proven hepatocyte necrosis, there was an eightfold larger increase of miR-122 than ALT, suggesting a greater sensitivity for reporting tissue injury. More work is needed to fully define the kinetics of circulating miRNA in fish using different dosing regimens for paracetamol and other hepatotoxic drugs. However, this study suggests that miRNA may have significant advantages over ALT measurement in zebrafish.

Delayed AC treatment (administered after paracetamol exposure for 3 h) prevented the increase in circulating miR-122 at 24 hpe. This is, to the authors' knowledge, the first demonstration that effective antidote treatment is reported by a circulating miRNA biomarker. miRNAs are very promising disease biomarkers because they are stable in blood, some display tissue-restricted expression, they rarely undergo postprocessing modification, and they are readily amplifiable signals. Another major strength of miRNA is that they are translational across species, and this study adds zebrafish to the list of species (rodents and humans) that report hepatotoxicity by elevation in circulating miR-122.

The results of this study suggests that with further development, zebrafish may be valuable as a model to identify and explore drug-induced liver injury using miR-122 as a read-out of toxicity that is directly translatable to rodents and humans. The value of such a zebrafish model lies in the simplicity of drug administration, low financial cost, and ease of genetic manipulation. In the present study, we measured the serum paracetamol concentration, which was 962 mg/L immediately following a 3-h exposure to paracetamol (30 mM), a clear evidence that drug in the water enters the fish circulation. This paracetamol concentration is within the range reported in humans and would be expected to produce hepatotoxicity if untreated in clinical practice.

There are limitations to the model that will be a focus of further work. Although RO bleeding increased the blood yield per fish, there was still a need to pool samples to measure biomarkers. Future work will focus on refining techniques to allow miRNA measurement on single fish to produce a significant reduction in numbers needed for experiments. Zebrafish could represent a high-throughput screen, but measurement of miRNA is time-consuming by PCR. There is a need for a rapid point of care assay for miR-122 to speed up the time for results both in preclinical and clinical studies. In this study, we normalized miR-122 using circulating let-7d, as per our published human studies. This is a new field, and further work is needed to determine the optimal normalizing approach for zebrafish blood miRNA.

In summary, collection of blood by RO bleeding facilitated the measurement of circulating miR-122 in a model of paracetamol hepatotoxicity. The adult zebrafish represents a new species for the measurement of circulating miRNA biomarkers that can bridge from fish to humans.

Acknowledgments

All the authors acknowledge the contribution of the British Heart Foundation Centre of Research Excellence Award, and author J.W.D. was supported by the financial support of NHS Research Scotland (NRS), through NHS Lothian. Author A.D.B.V. was supported by the UK NC3Rs Studentship. The authors thank Forbes Howie for analysis of serum ALT activity.

Disclosure Statement

No competing financial interests exist.

References

1. Larson AM, Polson J, Fontana RJ, Davern TJ, Lalani E, Hynan LS, *et al.* Acetaminophen-induced acute liver failure: results of a United States multicenter, prospective study. Hepatology (Baltimore, MD) 2005;42:1364–1372.
2. Møller LR, Nielsen GL, Olsen ML, Thulstrup AM, Mortensen JT, Sørensen HT. Hospital discharges and 30-day case fatality for drug poisoning: a Danish population-based study from 1979 to 2002 with special emphasis on paracetamol. E J Clin Pharmacol 2004;59:911–915.
3. Gunnell D, Murray V, Hawton K. Use of paracetamol (acetaminophen) for suicide and nonfatal poisoning: worldwide patterns of use and misuse. Suicide Life Threat Behav 2000;30:313–326.
4. James LP, Mayeux PR, Hinson JA. Acetaminophen-induced hepatotoxicity. Drug Metab Dispos 2003;31:1499–1506.
5. Hunter MP, Ismail N, Zhang X, Aguda BD, Lee EJ, Yu L, *et al.* Detection of microRNA expression in human peripheral blood microvesicles. PLoS One 2008;3:e3694.
6. Arroyo JD, Chevillet JR, Kroh EM, Ruf IK, Pritchard CC, Gibson DF, *et al.* Argonaute2 complexes carry a population of circulating microRNAs independent of vesicles in human plasma. Proc Natl Acad Sci U S A 2011;108:5003–5008.
7. Wang K, Zhang S, Marzolf B, Troisch P, Brightman A, Hu Z, *et al.* Circulating microRNAs, potential biomarkers for drug-induced liver injury. Proc Natl Acad Sci U S A 2009; 106:4402–4407.
8. Starkey Lewis PJ, Dear J, Platt V, Simpson KJ, Craig DGN, Antoine DJ, *et al.* Circulating microRNAs as potential markers of human drug-induced liver injury. Hepatology (Baltimore, MD) 2011;54:1767–1776.
9. Zhang Y, Jia Y, Zheng R, Guo Y, Wang Y, Guo H, *et al.* Plasma microRNA-122 as a biomarker for viral-, alcohol-, and chemical-related hepatic diseases. Clin Chem 2010;56: 1830–1838.
10. Antoine DJ, Dear JW, Starkey-Lewis P, Platt V, Coyle J, Masson M, *et al.* Mechanistic biomarkers provide early and sensitive detection of acetaminophen-induced acute liver injury at first presentation to hospital. Hepatology (Baltimore, MD) 2013;58:777–787.
11. McGrath P, Li C-Q. Zebrafish: a predictive model for assessing drug-induced toxicity. Drug Discov Today 2008;13: 394–401.
12. Barros TP, Alderton WK, Reynolds HM, Roach AG, Berghmans S. Zebrafish: an emerging technology for

in vivo pharmacological assessment to identify potential safety liabilities in early drug discovery. Br J Pharmacol 2008;154:1400–1413.
13. North TE, Babu IR, Vedder LM, Lord AM, Wishnok JS, Tannenbaum SR, *et al.* PGE2-regulated wnt signaling and N-acetylcysteine are synergistically hepatoprotective in zebrafish acetaminophen injury. Proc Natl Acad Sci U S A 2010;107:17315–17320.
14. Lieschke GJ, Currie PD. Animal models of human disease: zebrafish swim into view. Nat Rev Genet 2007;8:353–367.
15. Zon LI, Peterson RT. *In vivo* drug discovery in the zebrafish. Nat Rev Drug Discov 2005;4:35–44.
16. Wienholds E, Kloosterman WP, Miska E, Alvarez-Saavedra E, Berezikov E, de Bruijn E, *et al.* MicroRNA expression in zebrafish embryonic development. Science (New York, NY) 2005;309:310–311.
17. Hoff J. Methods of blood collection in the mouse. Lab Animal 2000;29:47–53.
18. Pedroso GL, Hammes TO, Escobar TDC, Fracasso LB, Forgiarini LF, da Silveira TR. Blood collection for biochemical analysis in adult zebrafish. J Vis Exp 2012:e3865.
19. Bergmeyer HU, Scheibe P, Wahlefeld AW. Optimization of methods for aspartate aminotransferase and alanine aminotransferase. Clin Chem 1978;24:58–73.
20. Starkey Lewis PJ, Merz M, Couttet P, Grenet O, Dear J, Antoine DJ, *et al.* Serum microRNA biomarkers for drug-induced liver injury. Clin Pharmacol Ther 2012;92:291–293.
21. Eames SC, Philipson LH, Prince VE, Kinkel MD. Blood sugar measurement in zebrafish reveals dynamics of glucose homeostasis. Zebrafish 2010;7:205–213.
22. Murtha JM, Qi W, Keller ET. Hematologic and serum biochemical values for zebrafish (Danio rerio). Comp Med 2003;53:37–41.
23. Spence R, Gerlach G, Lawrence C, Smith C. The behaviour and ecology of the zebrafish, *Danio rerio*. Biol Rev Camb Philos Soc 2008;83:13–34.
24. Johnston IA, Dunn J. Temperature acclimation and metabolism in ectotherms with particular reference to teleost fish. Symp Soc Exp Biol 1987;41:67–93.
25. Denvir MA, Tucker CS, Mullins JJ. Systolic and diastolic ventricular function in zebrafish embryos: influence of norepenephrine, MS-222 and temperature. BMC Biotechnol 2008;8:21.
26. Jensen FB. Nitric oxide formation from nitrite in zebrafish. J Exp Biol 2007;210(Pt 19):3387–3394.
27. Babaei F, Ramalingam R, Tavendale A, Liang Y, Yan LSK, Ajuh P, *et al.* Novel blood collection method allows plasma proteome analysis from single zebrafish. J Proteome Res 2013;12:1580–1590.
28. Zang L, Shimada Y, Nishimura Y, Tanaka T, Nishimura N. A novel, reliable method for repeated blood collection from aquarium fish. Zebrafish 2013;10:425–432.
29. Chng HT, Ho HK, Yap CW, Lam SH, Chan ECY. An investigation of the bioactivation potential and metabolism profile of Zebrafish versus human. J Biomol Screen 2012; 17:974–986.

Address correspondence to:
James W. Dear, PhD, FRCPEdin
British Heart Foundation
Centre for Cardiovascular Science
The Queen's Medical Research Institute
The University of Edinburgh
Room E3.23
47 Little France Crescent
Edinburgh EH16 4TJ
United Kingdom

E-mail: james.dear@ed.ac.uk

5.3 Discussion

For zebrafish to be useful in circulating biomarker discovery and validation studies, it is vital to maximize the yield of blood from every fish. In this study, we demonstrated that a new 'retro orbital' (RO) technique was more efficient than the commonly used LI approach in terms of blood yield. We developed a zebrafish model for paracetamol-induced hepatotoxicity in which we used the new RO blood draw technique to, for the first time, measure circulating miRNA in zebrafish. We noted that circulating liver enriched miRNA (miR-122-5p), was elevated in a dose dependent pattern as a result of paracetamol hepatotoxicity.

This is consistent with findings in humans and rodents. In summary, collection of blood by RO bleeding facilitated measurement of circulating miR-122-5p in a model of paracetamol hepatotoxicity. The adult zebrafish represents a new species for measurement of circulating miRNA biomarkers that can bridge from fish to human.

5.4 Copyright

Chapter 6: Characterization of triptolide-induced hepatotoxicity in zebrafish larvae

6.1 Introduction

After developing a model for hepatotoxicity in adult zebrafish, the next step was to develop a model for hepatotoxicity in zebrafish larvae. Larvae were chosen because they are easier to handle than adult fish, they are optically clear making them suitable for imaging and till 5 dpf they replace controlled animals.

Firstly, liver histology was studied in zebrafish larvae after exposure to paracetamol. Subsequently triptolide (TP), the active compound in *Tripterygium wilfordii* Hook F, a medicinal plant with a long history of use in traditional medicine was used. TP is purported to have multiple pharmacological effects including anti-inflammatory, anti-cancer, neuroprotective and contraceptive activities (248, 249). However, its use is limited by its high incidence of hepatotoxicity (250) and *in vitro* data suggest that inhibition of RNA synthesis may be the mechanism of toxicity (251).

In the study described in this chapter novel imaging tools were used to characterize a new model of DILI due to TP in zebrafish larvae. Histological examination, quantification of miR-122-5p per larva, selective plane illumination microscopy (SPIM) and time-lapse imaging by 2D microscopy to characterise the time course of liver injury were performed. The transcriptional changes induced by TP were investigated by RNA-sequencing and this confirmed mRNA synthesis inhibition and identified nitric oxide production as a protective pathway in the injury pathogenesis.

6.2 Contributions by the candidate

Study design; Execution of paracetamol and triptolide exposure experiments; performing miRNA measurements; time-lapse microscopy; Performing PCR for sequencing validation and measuring inflammatory associated gene expression; Data

collection; Data analysis apart from the sequencing data; Preparation and revision of the manuscript.

6.3 Results

6.3.1 Preliminary studies

First, it was determined whether paracetamol and TP induced liver injury in zebrafish. Larvae were exposed to paracetamol or TP for 48 hours from 3 to 5 dpf. This exposure caused mortality with a dose-response relationship with a 100% death rate reached with 10 mM paracetamol versus 2 µM for TP (**Figure 5A**). Histological examination of larvae revealed injury specifically to the liver. There was a dose response relationship between TP and hepatocyte vacuolation, hepatocyte disarray and oncotic necrosis whereas there was no dose-response relationship with paracetamol (**Figure 5B**). Paracetamol did not induce hepatocyte necrosis despite causing death. Out of 38 zebrafish larvae treated with TP (0.8µM) only 3 did not have histological evidence of liver injury. There was no discernible histological injury to other organs. Because of these results TP was chosen as compound to further characterize its hepatotoxicity in zebrafish larvae.

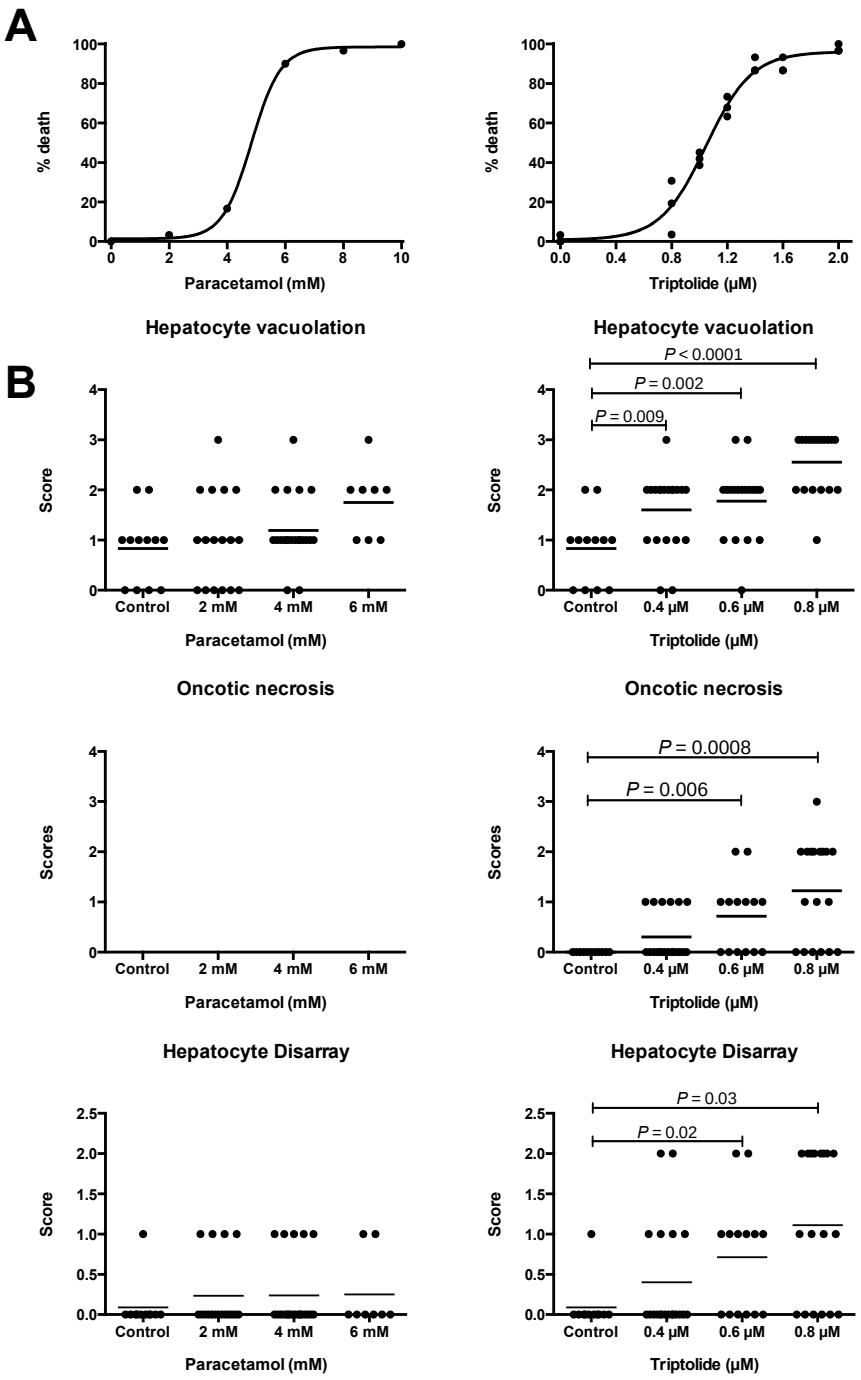

Figure 5. Effect of paracetamol and triptolide on zebrafish larvae after 48 hours (3-5dpf) exposure. (A) Survival of zebrafish larvae after paracetamol or TP exposure at the concentrations indicated. Each dot represents mean mortality of 30 larvae. (B) Scatter plots (mean) of histology scores for hepatocyte vacuolation, hepatocyte disarray and oncotic necrosis after paracetamol or TP exposure at the concentrations indicated (For paracetamol control N = 11, 2 mM N= 17, 4 mM N=21, 6 mM N = 8, For

TP control N=12, 0.4 µM N=20, 0.6 µM N=18 and 0.8 µM N=18). There was no necrosis induced by paracetamol.

6.3.2 Studies with triptolide

The studies with triptolide are being prepared to submit for publication as:

Characterization of triptolide induced hepatotoxicity in zebrafish larvae. AD Bastiaan Vliegenthart, Chunmin Wei, Charlotte Buckley, Cécile Berends, Carmelita MJ de Potter, Jorge Del Pozo, Carl Tucker, Al Ivens, David J Webb and James W Dear.

Paper 7

Title: Characterization of triptolide-induced hepatotoxicity by imaging and transcriptomics in a novel zebrafish model

Running title: Triptolide hepatotoxicity in zebrafish

Authors: AD Bastiaan Vliegenthart[*,¶], (bastiaanvliegenthart@hotmail.com)
Chunmin Wei[*,†,¶], (mini9636@126.com)
Charlotte Buckley[*], (charlotte.b.buckley@gmail.com)
Cécile Berends[*], (cecileberends@gmail.com)
Carmelita MJ de Potter[*], (c.m.j.depotter@students.uu.nl)
Sarah Schneemann[*] (s.a.schneemann@students.uu.nl)
Jorge Del Pozo[‡], (Jorge.Del.Pozo@ed.ac.uk)
Carl Tucker[§], (Carl.Tucker@ed.ac.uk)
John J Mullins[*], (j.mullins@ed.ac.uk)
David J Webb[*], (d.j.webb@ed.ac.uk)
James W Dear[*]. (james.dear@ed.ac.uk)

[¶] these authors contributed equally

Affiliations:

[*] Edinburgh University/BHF Centre for Cardiovascular Science, The Queen's Medical Research Institute, 47 Little France Crescent, Edinburgh, EH16 4TJ, UK.

[†] Center for Drug Evaluation, China Food and Drug Agency, No1 Fuxing Road, Beijing, 100083, China.

[‡] Easter Bush Pathology, Royal (Dick) School of Veterinary Studies, The University of Edinburgh, Easter Bush campus, Roslin, Midlothian EH25 9RG, UK.

[§] Biomedical Research Resources, The College of Medicine and Veterinary Medicine, The University of Edinburgh, 47 Little France Crescent, Edinburgh, EH16 4TJ, UK.

Corresponding author: James W. Dear
University/BHF Centre for Cardiovascular Science, University of Edinburgh, Queen's Medical Research Institute, 47 Little France Crescent, Edinburgh, EH16 4TJ
james.dear@ed.ac.uk
Tel: (+44) 131 242 9214
Fax: (+44) 131 242 9215

Abstract

Triptolide is a vine extract used in traditional Chinese medicines and associated with hepatotoxicity. *In vitro* data suggest that inhibition of RNA synthesis may be the mechanism of toxicity. For studying drug-induced liver injury the zebrafish has experimental, practical and financial advantages compared with rodents. The aim of this study was to explore the mechanism of triptolide toxicity using zebrafish as the model system. The effect of triptolide exposure on zebrafish larvae was determined with regard to mortality, histology, expression of liver specific microRNA-122 and liver volume. Fluorescent microscopy was used to track toxicity in the Tg(-*2.8lfabp*:GFP)^{as3} zebrafish line. Informed by microscopy, RNA-sequencing was used to explore the mechanism of toxicity. Triptolide exposure resulted in dose-dependent mortality, a reduction in the number of copies of microRNA-122 per larva, hepatocyte vacuolation, disarray and oncotic necrosis, and a reduction in liver volume. These findings were consistent across replicate experiments. Time-lapse imaging indicated the onset of injury was 6 hours after the start of exposure, at which point, RNA-sequencing revealed that 88% of genes were downregulated. Immune response associated genes were upregulated in the triptolide-treated larvae including nitric oxide synthase (NOS). Inhibition of NOS increased mortality. Triptolide induces hepatotoxicity in zebrafish larvae. This represents a new model of drug-induced liver injury that complements rodents. RNA sequencing, guided by time-lapse microscopy, revealed early down regulation of genes consistent with previous *in vitro* studies, and facilitated the discovery of mechanistic inflammatory pathways.

Key words: Triptolide, hepatotoxicity, zebrafish, microRNA-122, imaging, nitric oxide synthase

Introduction

Traditional Chinese Medicines (TCMs), including herbal drugs, have been used for thousands of years (Zhang *et al.*, 2012). Currently, TCMs are used around the world with 70-95% of the population in certain developing countries relying on it for their primary medical care (Parveen *et al.*, 2015; Robinson and Zhang, 2011). In the United States, in 2004, around 1 in 5 adults reported taking a herbal product during the past 12 months (Barnes *et al.*, 2004). Despite this high global use of TCM, evidence for efficacy is limited (Bent, 2008; Parveen, Parveen, Parveen and Ahmad, 2015). On the other hand, some TCMs clearly cause toxicity (Bunchorntavakul and Reddy, 2013; Teschke *et al.*, 2012). As there is little evidence of efficacy, it is important to understand safety/toxicity, in order to protect users from unacceptable harms.

An archetypal example of a medicinal plant with a long history of use in TCM is *Tripterygium wilfordii* Hook F, also known as "thunder duke vine" (Kupchan *et al.*, 1972). Its major active ingredient is triptolide (TP), a diterpene triepoxide. TP has been reported to have multiple pharmacological activities, including neuroprotective, anti-inflammatory and contraceptive effects (Chen, 2001; Liu, 2011; Zheng *et al.*, 2013; Ziaei and Halaby, 2016). Unfortunately, the relatively high incidence of toxicity, predominately to the liver, and a narrow therapeutic window, has limited the clinical development of TP (Li *et al.*, 2014). A synthetic pro-drug of TP, F60008, has entered phase 1 clinical trials in patients with advanced solid tumours. However, out of 20 study participants, two died. One subject died without clear cause and the other most likely died from neutropenic sepsis. Further development of F60008 was stopped due to these two deaths and marked variability in its pharmacokinetics (Kitzen *et al.*, 2009).

TP is extensively metabolized, with less than 1% of a single dose being recovered in bile, urine or faeces within 48 hours (Shao *et al.*, 2007). After administration of TP to rats, its concentration was at least 3 fold higher in liver compared to the plasma, kidney, lung, spleen or testicular concentration. This is consistent with unequal tissue distribution (Xue *et al.*, 2012). In rats, the primary phase I metabolic pathway of TP is hydroxylation into mono-hydroxylated triptolides that can subsequently undergo phase II metabolism into glucuronides and sulfates (Du *et al.*, 2014; Li *et al.*, 2008).

CYP3A was identified to be primarily responsible for hydroxylation and dexamethasone, a CYP3A inducer, increased TP metabolism in rat liver microsomes (Ye *et al.*, 2010) and reduced TP-induced hepatotoxic effects (Ye, Li, Yan, Mao, Cai, Xu and Yang, 2010). Conversely, a single dose of TP that caused only mild toxicity in wild-type mice resulted in severe toxicity and death in cytochrome P450 gene deleted mice (Xue *et al.*, 2011). These findings suggest that TP itself is toxic (not dependent on metabolism) and the higher degree of toxicity in the liver may be due to a higher TP distribution to this organ.

TP is a reactive electrophile containing three epoxide groups that can bind to cellular macromolecules (Attia, 2010). It has been reported that TP can covalently bind to a subunit of the transcription factor II human complex (TFIIH) and cause inhibition of its DNA-dependent ATPase activity, which leads to the inhibition of RNA polymerase II mediated transcription (Titov *et al.*, 2011). Another group confirmed that TP inhibited total RNA and mRNA *de novo* synthesis. Up to 98% of genes were down regulated in a human non-small cell lung cancer line after exposure to TP. TP also depleted RPB1, the main RNA polymerase II subunit. These *in vitro* data suggest that inhibition of RNA synthesis may explain the pharmacology and toxicology of TP (Vispe *et al.*, 2009).

In order to better understand drug-induced liver injury (DILI), new tools and models are needed. Zebrafish are a promising animal model for studying DILI with many advantages over rodents (Vliegenthart *et al.*, 2014b). Advantages include convenient drug delivery, high fecundity, lower financial costs, optical clarity of larvae allowing real-time imaging of toxicity and suitability for high-throughput screening that is not possible with other vertebrate systems (Lieschke and Currie, 2007; McGrath and Li, 2008; Zon and Peterson, 2005). Recently, we have established a DILI model in zebrafish using paracetamol as the toxic agent (Vliegenthart *et al.*, 2014a). The main difference between the mammalian and zebrafish liver is the structural organization of the liver tissue. Instead of having the large bile ducts, portal veins and hepatic arteries organised in portal tracts, these are randomly allocated throughout the liver parenchyma in the zebrafish. The tri-lobed liver of the zebrafish is similar to other mammals with regard to biological function. This includes processing of lipids, vitamins, proteins, carbohydrates and the synthesis of serum proteins (Menke et al.,

2011). The metabolic properties of zebrafish regarding xenobiotics, including drugs, also have many similarities with mammals (Vliegenthart et al., 2014b).

In this study we applied novel imaging tools to characterize a new model of DILI due to TP in zebrafish larvae. We performed histological examination, selective plane illumination microscopy (SPIM) and time-lapse imaging by 2D microscopy to characterise the time course of liver injury. The transcriptional changes induced by TP were investigated by RNA-sequencing. The results were consistent with mRNA synthesis inhibition and identified nitric oxide production as a protective pathway in the injury pathogenesis.

Materials and Methods

Fish lines and husbandry

Experiments were conducted in accordance with the United Kingdom Animals (Scientific Procedures) Act 1986 in a United Kingdom Home Office-approved establishment. Zebrafish (*Danio rerio*) were maintained at 28.5^{0}C, as previously described by Westerfield (Westerfield, 2007). Established lines used were WIK and Tg(-*2.8lfabp*:GFP)^{as3} (Her *et al.*, 2003), where GFP is green fluorescent protein.

Chemical exposure

The wild-type WIK line was used for all experiments apart from imaging. Unless otherwise stated larvae were maintained at 28.5°C in 50mL conditioned water (CW). Larvae were exposed to TP (National Institutes for Food and Drug Control, China, >98% pure) dissolved in CW at concentrations described in the results section. For the experiments testing the effect of TP on survival, 30 larvae were treated per 50mL dish for 48 hours (3-5dpf). The concentrations tested were 0 µM (3 dishes), 0.8 µM (3 dishes), 1.0 µM (3 dishes), 1.2 µM (3 dishes), 1.4 µM (2 dishes), 1.6 µM (2 dishes) and 2 µM (2 dishes). For the experiments testing the effect of TP on copies of microRNA-122 (miR-122) per larvae, 30 larvae were treated per 50mL dish for 48 hours (3-5dpf). The concentrations tested were 0 µM (3 dishes), 0.2 µM (3 dishes), 0.4 µM (3 dishes) and 0.8 µM (3 dishes). For the effect of TP on histology 30 larvae were treated per 50mL dish up to 48 hours (3-5dpf). The concentrations tested were 0 µM (3 dishes), 0.2 µM (3 dishes), 0.4 µM (3 dishes) and 0.8 µM (3 dishes), the number of fish of which successful histology scoring could be obtained per treatment are given in the results. For all imaging experiments larvae were treated for 48 hours (3-5dpf) with a concentration of 0, 0.4, 0.8, 1.2 or 1.6 µM in agarose conditions as indicated in the methods of each technique. For the sequencing experiment 5dpf larvae (N=30) were treated per 50mL dish for 6 hours with a TP concentration of 0 µM (8 dishes) or 1.6 µM (8 dishes). For the NOS inhibitor studies 3dpf larvae (N=30) were treated per 50mL dish for 24 hours. With either TP concentration of 0µM, 1.0 µM, or 1.6 µM with or without NOS inhibitor.

Experiments determining the effect of nitric oxide synthase inhibition on TP were blinded such that the investigator scoring larval mortality did not know the treatment groups. When necessary, larvae were anaesthetised with MS-222 (tricaine methanesulfonate - 40 μg ml^{-1}) dissolved in CW. Mortality was assessed in a blinded fashion with no response to stimuli as the measured endpoint.

For adult zebrafish experiments 6 fish (3 treatment and 3 control) aged 12 months were used. Fish were exposed for 10 hours to triptolide (1.6 μM in conditioned water) or conditioned water alone. Then fish were fixed for histopathology. A veterinary pathologist, who was blinded to treatment allocation, assessed the liver sections.

Histology

Larvae were submerged in 10% formalin and left to fix for at least 24 hours at 4°C before processing. Larvae were prepared for histology as described by Sabaliauskas *et al.* (Sabaliauskas *et al.*, 2006) resulting in agarose blocks containing zebrafish larvae. The agarose blocks were then embedded in paraffin blocks using a Thermo Electron Excelsior tissue processor (Thermo, UK). This was achieved by serial immersion in the following: 70% ethanol (1h), 90% ethanol (1h), absolute ethanol (1h x4), xylene (1h x2), wax (1.3h x 3). The blocks were sectioned at 4μm and placed on a glass slide that was then incubated at 52℃ for at least an hour. Tissue sections were then dewaxed and rehydrated using an autostainer (ST5010 Autostainer XL, Leica Microsystems, UK) through three x 5min cycles of xylene, two x 3min cycles of 100% ethanol, one x 2min cycles of 95% ethanol and one x 5min wash of distilled H_2O (dH_2O) and were then left to stand in dH_2O until the next procedure. After rehydration, for haematoxylin and eosin (H&E), slides were stained in the same autostainer by sequential immersion in haematoxylin (5min), dH_2O (5min), Scott's tap water (2min), dH_2O (5min), and eosin (3min). Stained slides were then dehydrated (dH_2O wash (45s), 70% ethanol (30s), 95% ethanol (30s x2), 100% ethanol (1min x2), ethanol/xylene (1min), and xylene (1min x3)), and cover slipped using Pertex Mounting Medium (CellPath Ltd, UK). Fish were sectioned sagittally along the midline to facilitate examination of the liver.

Histology was scored by an accredited (DiplECVP) veterinary pathologist (author JDP), who was blinded to the treatment groups. A semi-quantitative scoring system

was used to grade the pathological changes noted in these livers. Briefly, each feature of interest was ranked as follows: 0=absent; 1=1-25% of total area examined; 2=26-75%; 3=76-100%. The features of interest were hepatocyte vacuolation, hepatocyte swelling, hepatocyte disarray, and oncotic necrosis.

Imaging

Fluorescent microscopy and selective plane illumination microscopy (SPIM) were performed with fluorescent liver reporter zebrafish Tg(−*2.8fabp10*:GFP)^{as3}. Time-lapse recording of zebrafish embryos was performed using an EVOS FL Cell Imaging System (Life Science, USA). Up to 5 larvae (72 days post-fertilisation (dpf)) were oriented in 700 µL agar (0.75%, wt/vol) containing 84 mg/L MS-222. Once the agar was set, 750 µL of CW with TP (concentration as indicated in results) and MS-122 (84 mg/L) was added on top of the agar and the time-lapse recording was started. The incubator was set to 27°C and pictures were taken hourly. ImageJ software (National Institutes of Health, Bethesda, USA) was used to determine maximum GFP intensity in each image.

Selective Plane Illumination Microscopy (SPIM)

A custom built SPIM system was used. This was based on the design previously published (Taylor *et al.*, 2012). A Vortran VersaLase multiple wavelength system with 3 laser diodes (405nm, 488nm and 561nm) was coupled to the SPIM illumination arm using a single mode optical fibre. The appropriate laser power was set using Stradus VersaLase software, and a power meter (Thorlabs Inc, PM100D) was used to verify collimated beam power. The resulting beam was then focused onto the sample (10X 0.3 NA Nikon CFI Fluor water dipping objective) to produce a light sheet. Imaging of the sample was through a 12X 0.8NA Nikon CFI LWD Plan Fluor water dipping objective (N16LWD-PF) and the resulting beam sent to three QI-Click Mono CCD cameras (Q-Imaging Inc) via a series of dichoric filters CFP Em/BW 479/40 nm (MF479-40), GFP Em/BW 525/39 nm (MF525-39), TxRed Em/BW 630/69 nm (MF630-60) (Thorlabs Inc). The entire system was controlled through a written interface operating in the Python language.

SPIM Image Acquisition and Analysis

Fish were age matched and selected from the same batch of eggs. Images were acquired from the same orientation at 1.5µm intervals, at 3, 4 and 5dpf. A Matlab script was written to determine liver volume. Files were automatically segmented based on signal intensity (kept consistent across groups), a mask applied and the signal intensity and area of the mask calculated. This was summed over the volume of the stack and the pixel size used to calculate the volume. Rendering of 3D SPIM image datasets was performed using Amira 3D for Life Sciences v5.5.0; imported fluorescence images were kept consistent throughout time points and treatments and an isosurface was created for liver volume and structure visualisation.

RNA extraction

Total RNA was extracted from pooled zebrafish larvae (30 larvae per sample) for qPCR and RNA-sequencing. Larvae were fixed in Qiazol after which they were disrupted using a tissue disruptor. Subsequently total RNA was extracted using the miRNeasy mini kit (Qiagen, Venlo, Netherlands) eluted in 30 µl RNAse free water.

PCR analysis

For microRNAs 1 µg of total RNA from pooled larvae was reverse transcribed into cDNA using the miScript II RT Kit (Qiagen, Venlo, Netherlands) following manufacturer's instructions. The synthesized cDNA was ten-fold diluted and used for cDNA template in combination with the miScript SYBR Green PCR Kit (Qiagen, Venlo, Netherlands) using the specific miScript assays (Qiagen, Venlo, Netherlands). Absolute quantification of microRNA was achieved by generating a standard curve using synthetic target. Standard curves were generated by reverse transcribing known concentrations of miScript microRNA mimics (Qiagen, Venlo, The Netherlands) in 0.1X TE buffer spiked with 10 ng/µl Poly-C (Sigma-Aldirch, Gillingham, UK). The resulting cDNA was measured using serial dilutions on 3 different plates to demonstrate minimal variability. The final concentration was divided by the number of larvae used within the pooled sample to obtain the average microRNA copy number per larva.

For mRNA, 1 µg of total RNA from pooled larvae was reverse transcribed into cDNA using the QuantiTect Reverse Transcription Kit (Qiagen, Venlo, Netherlands)

following manufacturer's instructions. The synthesized cDNA was ten-fold diluted and used for cDNA template in combination with the QuantiTect SYBR Green PCR Kit (Qiagen, Venlo, Netherlands) using the specific QuantiTect primer assays (Qiagen, Venlo, Netherlands). Real-time PCR was performed on a Light Cycler 480 (Roche, Basel, Switzerland) using the recommended cycling parameters.

RNA-sequencing

For this experiment 5dpf wild type (WIK) zebrafish were used and exposed to triptolide or vehicle control (DMSO). Each treatment group had 8 biological replicates, each replicate consisted of 30 pooled fish. For quality control RIN values were measured on the Agilent Technologies 2100 Bioanalyzer using the Eukaryote Total RNA Nano kit. All samples had a RIN of > 9.5. RNA Sequencing was performed using the Illumina® NextSeq® 550 system with 2x75bp paired end runs. RNA libraries were prepared for each sample with the Truseq® Stranded Total RNA Sample Prep LT Kit. Libraries were checked for size, purity and concentration with a high sensitivity DNA chip on the Agilent Technologies 2100 Bioanalyzer.

The raw sequences were quality assessed using FASTQC. Based on the output of the FASTQC analysis, the raw fastq sequences required no further pre-processing to remove contaminating primers and sequences were not collapsed within each sample. The most recent Ensembl release (Rel84, March 2016) of zebrafish transcript sequences was downloaded using BioMart (Smedley *et al.*, 2015). Alignments (end-to-end, very-sensitive settings) to the reference set were performed using bowtie2 (Langmead and Salzberg, 2012). A requirement for concordant read pair mapping was applied, and all other alignments discarded. Alignments were stored in indexed BAM files. Raw "tag counts" (i.e. sequences aligning) per sample were normalised to the sample with the lowest number of alignments, and counts converted to log2; "abundance normalised" data were not further quantile normalised for linear model fitting purposes.

Gene ontology enrichment analysis

Gene ontology (GO) and Kyoto encyclopaedia of genes and genomes (KEGG) enrichment analysis for over or under representation of GO terms or KEGG pathways were done by using a hypergeometric test for likelihood due to chance, reporting anything more significant than the cut-off *P*-value of 0.001.

Statistical analysis

Statistical differences in copies of microRNA per fish, histology scores, liver volume, difference in gene expression obtained by PCR and death rate were performed using Graphpad Prism (GraphPad Software, La Jolla California, USA). For RNA-seq pairwise comparisons of the two sample groups were performed on the normalised tag counts using linear modelling with the Bioconductor *limma* package (Ritchie *et al.*, 2015). Nominal statistical significance was set at $P < 0.05$, unless an adjusted P value was used (as described with the results).

Results

Triptolide-induced liver toxicity in zebrafish larvae

First, we determined whether TP induced liver injury in zebrafish. Larvae were exposed to TP for 48 hours from 3 to 5 dpf. This exposure caused mortality with a dose-response relationship (Figure 1A). Histological examination of larvae revealed injury specifically to the liver. There was a dose response relationship between TP and hepatocyte vacuolation, oncotic necrosis and hepatocyte disarray subsequent to cell death (Figures 1C-D & Supplementary Figure 1). These histological features were diffusely present throughout the liver tissue. Out of 38 zebrafish larvae treated with TP (0.8μM) only 3 did not have histological evidence of liver injury. There was no discernible histological injury to other organs. To confirm that TP is hepatotoxic in adult zebrafish we exposed fish aged 12 months to TP (1.6 μM) or vehicle control for 10 hours. There was hepatocyte necrosis in TP exposed adult zebrafish (Supplementary Figure 2).

Our previous work has demonstrated that zebrafish release the liver specific microRNA, miR-122, from injured hepatocytes (Vliegenthart, Starkey Lewis, Tucker, Del Pozo, Rider, Antoine, Dubost, Westphal, Moulin, Bailey, Moggs, Goldring, Park and Dear, 2014a). TP exposure resulted in a significant decrease in the number of copies of miR-122 per larva (Figure 1B). Building on these data, SPIM was used to quantify liver volume in the zebrafish line Tg(*-2.8lfabp*:GFP)^{as3} (Figure 2). Images were captured for vehicle control (N=10) and TP-treated fish (N=6) at 5 dpf after 54 hours of drug/vehicle exposure. Control livers increased in size from 3 to 5 dpf and, at 5 dpf, had a higher mean liver volume of 85.4 (SD 0.6) mm^3 compared with no fluorescent signal for TP, $P = 0.0002$ (Figure 2).

Onset of TP -induced hepatotoxicity could be determined by Time-lapse microscopy

Time-lapse microscopy was used to characterise the time course of injury and identify an early time point for RNA sequencing. The fish line Tg*(-2.8lfabp*:GFP)^{as3} enabled quantification of the fluorescence intensity of the liver during TP exposure (Figure 3A). After 6 hours, the fluorescent intensity of TP-treated fish started to

decrease compared to control fish, suggesting that this time may represent the onset of hepatocyte injury (Figure 3B). Histological examination supported the data from time-lapse microscopy. There was statistically significant hepatocyte vacuolation and swelling 6 hours post-exposure to TP (Figure 3C).

RNA-seq revealed pathways involved in triptolide exposure

RNA-seq was performed on 5 dpf larvae after exposure to TP for 6 hours, an early time-point identified by microscopy and histology as being before the onset of fulminant hepatocyte death. A total of 16 sequencing experiments were performed (control N=8 and treatment N=8). Each replicate consisted of 30 pooled larvae, therefore 480 larvae were included in total.

A total of 57,264 transcripts were identified of which 16,926 were statistically significantly differentially expressed with an adjusted *P*-value of 0.01 or less. Of the differentially expressed transcripts, 1995 were upregulated and 14,931 downregulated. Of these significant transcripts, 1433 (12%) were more than 2-fold upregulated and 4675 (88%) were more than 2-fold downregulated (Figure 4A). Unsupervised clustering separated the control group from the TP exposed group (Figure 4B). The top 10 most up- and down-regulated genes based on fold change are presented in table 1.

Gene ontology (GO) enrichment analysis revealed 32 significantly enriched terms in biological process, 16 enriched terms in cellular component and 17 enriched terms in molecular function (Supplementary Table 1). The most significant enriched GO terms were translation ($P = 4.35x10^{-51}$) in the biological process ontology, structure constituent of ribosome ($P = 3.13x10^{-64}$) in the molecular function ontology and ribosome ($P = 9.09x10^{-61}$) in the cellular component ontology. KEGG pathway analysis revealed 6 upregulated pathways of which ribosome ($P = 1.87x10^{-72}$) and cardiac muscle ($P = 8.01x10^{-7}$) pathways were the most significant. Another 18 downregulated KEGG pathways were identified, of which spliceosome ($P = 4.19x10^{-5}$) and notch signaling ($P = 0.0008$) were the most significant (Table 2).

Multiple inflammation associated genes were upregulated and validated by qPCR. Nitric oxide synthase 2b (NOS2b) was 4.0 fold increased ($P<0.0001$) in the TP

treated fish compared to control along with other genes involved in an inflammatory response including TNF-α (32.9 fold, $P<0.0001$), IL-1b (7.6 fold, $P < 0.0001$), IL-6 (4.0 fold, $P < 0.0001$), IL-10 (2.3 fold, $P = 0.01$) and CCR2 (5.6 fold, $P < 0.0001$) (Figure 5A-E).

To further validate the sequencing results, 14 transcripts chosen from differentially regulated pathways and genes involved in the immune response were measured by qPCR. The fold change obtained by RNA-sequencing correlated with the fold change measured by qPCR with a Pearson's r of 0.93, $P < 0.0001$ (Figure 5G).

Nitric oxide synthase is involved in triptolide toxicity

Finally, in order to explore a mechanistic role for NOS2b in TP-induced toxicity, the effect of the non-selective nitric oxide synthase (NOS) inhibitor L-NAME and the selective inducible NOS (iNOS) inhibitor aminoguanidine was determined. Neither compound caused any effect on zebrafish survival when applied alone. Co-treatment with TP and either L-NAME or aminoguanidine significantly increased larval mortality (Figure 6).

Discussion

TP, the primary active compound in *Tripterygium wilfordii*, has a long history of use because of its purported neuroprotective, anti-inflammatory and contraceptive effects (Chen, 2001; Liu, 2011; Zheng, Zhang and Wang, 2013; Ziaei and Halaby, 2016). Due to its high incidence of hepatotoxicity, its utility in clinical medicine is limited (Li, Jiang and Zhang, 2014).

Zebrafish larvae are as proliferative and easily accessible as *in vitro* cell culture models while providing *in vivo* complexity comparable to larger vertebrate models (Vliegenthart, Tucker, Del Pozo and Dear, 2014b). In addition, zebrafish have substantially lower cost and the larvae are optically clear so are suitable for high throughput screening (Lieschke and Currie, 2007; McGrath and Li, 2008; Zon and Peterson, 2005). This unique combination of characteristics makes the zebrafish an attractive model species for studying DILI.

To investigate whether zebrafish larvae could be used as a tool to study TP-induced DILI, larvae were exposed to increasing concentrations of TP. Larvae died with a dose-response relationship in the micromolar range and histological examination revealed that TP induced highly reproducible hepatic necrosis without affecting other organs. The plasma concentration of triptolide in humans (*C*max) is reported to be around 0.15 – 0.4μM.(Yao *et al.*, 2006) In rats, a plasma concentration of 1.5μM has been reported to be associated with histological liver cell necrosis.(Shao, Wang, Xie, Zhu, Sun and A, 2007) These human and rodent studies are consistent with the concentrations that produce hepatotoxicity in our zebrafish larvae, which supports the translational relevance of our fish model. Ours is the first study confirming that TP-induced hepatotoxicity can be modelled in zebrafish larvae. The administration of TP is straightforward and the resultant liver injury is reproducible and tractable. This is in contrast to paracetamol, an archetypal compound used to induce hepatocyte necrosis, which is variable with regard to histological liver injury in larvae and requires millimolar water concentrations for an effect (Vliegenthart, Starkey Lewis, Tucker, Del Pozo, Rider, Antoine, Dubost, Westphal, Moulin, Bailey, Moggs, Goldring, Park and Dear, 2014a). The enhanced ability of TP to induce liver toxicity is likely due to a combination of its pharmacokinetics and its ability to induce injury

without need for metabolism. We believe that the data from these studies with triptolide confirm the benefits of zebrafish as a model organism to screen for DILI.

We previously reported that miR-122 increases in the circulation of patients with DILI with superior sensitivity and specificity compared to the currently used clinical biomarker alanine aminotransferase (ALT) (Vliegenthart *et al.*, 2015). Using *in situ* hybridisation, we reported that miR-122 is specifically expressed in the zebrafish liver and is released into the circulation with DILI. As in humans, in zebrafish miR-122 can be used as a more sensitive and specific biomarker than ALT (Vliegenthart, Starkey Lewis, Tucker, Del Pozo, Rider, Antoine, Dubost, Westphal, Moulin, Bailey, Moggs, Goldring, Park and Dear, 2014a). The present study reports that the number of copies miR-122 per zebrafish larvae is decreased with TP-induced DILI, indicating that miR-122 can also be utilised as a biomarker for DILI in whole zebrafish larvae.

By exploiting the optical transparency of the zebrafish larvae in combination with the liver specific fluorescent reporter transgenic fish line, Tg(-*2.8lfabp*:GFP)^{as3}, we were able to capture 3D images by using SPIM of the fish liver during TP-induced DILI. This confirmed that the liver volume (as reported by fluorescence) is substantially reduced with injury. Because of low bleaching, high acquisition speed and high depth penetration, SPIM is well suited for imaging intact fully functioning zebrafish larvae. These characteristics make SPIM suited for time-lapse imaging of biological processes over long periods of time (Huisken and Stainier, 2009; Weber and Huisken, 2011). This is potentially valuable in studies of development (Kaufmann *et al.*, 2012), functional imaging of multiple brain regions (Panier *et al.*, 2013) and heart function (Mickoleit *et al.*, 2014). This is the first study confirming that SPIM has sufficient depth penetration to image the zebrafish liver from 3 to 5 dpf. SPIM is a tool that could be further exploited in the field of studying liver development and injury in zebrafish.

Fluorescent time-lapse microscopy allowed us to characterise the time course of injury and identified an early time point for RNA sequencing, which demonstrated that TP has similar effects on RNA transcription as *in vitro* models. TP covalently binds to a subunit of TFIIH that leads to inhibition of RNA polymerase II

transcription initiation (Titov, Gilman, He, Bhat, Low, Dang, Smeaton, Demain, Miller, Kugel, Goodrich and Liu, 2011). RNA expression studies using microarrays have shown that both total RNA and mRNA *de novo* synthesis were lowered in a TP treated cancer cell line compared to control. Among the down regulated genes was RPB1, the main RNA polymerase II subunit (Vispe, DeVries, Creancier, Besse, Breand, Hobson, Svejstrup, Annereau, Cussac, Dumontet, Guilbaud, Barret and Bailly, 2009). These *in vitro* data indicate that inhibition of RNA synthesis could explain TP hepatotoxicity. In our study, the RNA-sequencing data also demonstrated that TP leads to a general downregulation of gene expression, with 88% being downregulated in TP treated larvae compared to vehicle control. Notably, this effect on gene expression was measured at an early time-point before fulminant hepatic necrosis had started. Therefore, we propose that inhibition of RNA synthesis may be the mechanism that causes liver toxicity. In line with this hypothesis, gene ontology analysis revealed that, in general, GO terms involved in RNA transcription, such as nucleic acid metabolic processes, transcription, regulation of gene expression and RNA biosynthesis, were significantly reduced. Also KEGG pathways involved in RNA transcription went down, including spliceosome and RNA polymerase. GO terms in biological processes involved in protein synthesis - such as translation, cellular protein metabolic process and protein metabolic process - were increased. We speculate that upregulation of processes involved in protein synthesis might be a response to lower template mRNA; an attempt by the organism to maintain equilibrium.

Other upregulated GO terms were involved in the immune response, defense response, response to other organisms, immune system process, response to viruses and response to lipopolysaccharide. PCR confirmed that multiple inflammatory markers were increased in the TP-treated fish compared to control, with the cytokine TNF-α being increased 32.9 fold. This suggests that, besides a general downregulation of transcription, inflammation potentially has a role in TP-induced DILI. In DILI, the liver injury caused by the drug or its metabolites is often an initiating event for an immune response which determines the extent of liver injury (Ju and Reilly, 2012). Liver necrosis with inflammatory cell infiltration has been reported in TP-induced hepatotoxicity (Fu *et al.*, 2011) and Th17/Treg imbalance has

been associated with the exacerbation of liver inflammation in TP-induced hepatotoxicity (Wang *et al.*, 2014).

Three NOS isoforms have been identified in humans: a neuronal NOS1, an inducible NOS2 and an endothelial NOS3 enzyme. One NOS1 and two NOS2 (NOS2A and NOS2B) genes have been reported to be present in the zebrafish genome. Both liposaccharide stimulation and tail cut injury induces the NOS2 isoforms in zebrafish (Lepiller *et al.*, 2009). Knockdown of NOS2b reduced leukocyte attraction to ventral fin wounds (Wittmann *et al.*, 2015). These data indicate that NOS2b is involved in inflammation. Our results suggest that inhibition of NOS2b in our model increased TP toxicity. This is consistent with a protective role for NOS2b. The protective role of NOS has also been reported in a model of paracetamol liver injury in mice (Hinson *et al.*, 2002). Various other models have also demonstrated that NO protects the liver against oxidative stress induced by ethanol, (Nanji *et al.*, 1995), H_2O_2 (Kim *et al.*, 1995) and CCl_4 (Zhu and Fung, 2000).

In conclusion, TP induces hepatic necrosis in zebrafish larvae and inhibits RNA synthesis in line with previous published data. The hepatocyte necrosis induces an inflammatory response, which partially determines outcome. TP is a model compound for inducing DILI in zebrafish. Zebrafish have experimental properties which complement rodent models of toxicity.

Supplementary Data description

Supplementary Figure 1. Effect of triptolide on zebrafish larvae after 48 hours (3-5dpf) exposure. Magnified histological images at x400 of zebrafish larvae liver after water exposure to triptolide at the concentrations indicated. Three representative fish are presented for each dose. Note the presence of dose dependent increase in hepatocyte vacuolation (A), necrosis (with nuclei breaking down (B) and karyolysis (C)) and the presence of disarray (red lines). The latter two features are absent from the control group. Scale bar = 20μm.

Supplementary Figure 2. Histological images of adult zebrafish after exposure to triptolide (1.6 μM) for 10 hours. (A) Subgross view. Liver is indicated by the red arrow. The area displaying hepatic necrosis is indicated by the circle. (B) Arrows denote lesions consistent with hepatic necrosis after triptolide exposure. (C) Control adult zebrafish after exposure to vehicle control. Normal liver, with no areas of necrosis.

Supplementary Table 1. Significantly enriched GO terms in response to triptolide in zebrafish larvae (with $P < 0.001$ cutoff).

Funding information

Author ADBV was supported by an NC3Rs PhD Studentship (NC/K001485/1). Author JWD acknowledges the support of NHS Research Scotland (NRS) through NHS Lothian and a BHF Centre of Research Excellence Award.

References

Attia, S. M. (2010). Deleterious effects of reactive metabolites. *Oxidative Medicine and Cellular Longevity* **3**(4), 238-53.

Barnes, P. M., Powell-Griner, E., McFann, K., and Nahin, R. L. (2004). Complementary and alternative medicine use among adults: United States, 2002. *Advance Data*(343), 1-19.

Bent, S. (2008). Herbal medicine in the United States: review of efficacy, safety, and regulation: grand rounds at University of California, San Francisco Medical Center. *Journal of General Internal Medicine* **23**(6), 854-9.

Bunchorntavakul, C., and Reddy, K. R. (2013). Review article: herbal and dietary supplement hepatotoxicity. *Alimentary Pharmacology & Therapeutics* **37**(1), 3-17.

Chen, B. J. (2001). Triptolide, a novel immunosuppressive and anti-inflammatory agent purified from a Chinese herb Tripterygium wilfordii Hook F. *Leukemia & Lymphoma* **42**(3), 253-65.

Du, F., Liu, Z., Li, X., and Xing, J. (2014). Metabolic pathways leading to detoxification of triptolide, a major active component of the herbal medicine Tripterygium wilfordii. *Journal of Applied Toxicology* **34**(8), 878-84.

Fu, Q., Huang, X., Shu, B., Xue, M., Zhang, P., Wang, T., Liu, L., Jiang, Z., and Zhang, L. (2011). Inhibition of mitochondrial respiratory chain is involved in triptolide-induced liver injury. *Fitoterapia* **82**(8), 1241-8.

Her, G. M., Chiang, C. C., Chen, W. Y., and Wu, J. L. (2003). In vivo studies of liver-type fatty acid binding protein (L-FABP) gene expression in liver of transgenic zebrafish (Danio rerio). *FEBS letters* **538**(1-3), 125-33.

Hinson, J. A., Bucci, T. J., Irwin, L. K., Michael, S. L., and Mayeux, P. R. (2002). Effect of inhibitors of nitric oxide synthase on acetaminophen-induced hepatotoxicity in mice. *Nitric Oxide : biology and chemistry* **6**(2), 160-7.

Huisken, J., and Stainier, D. Y. (2009). Selective plane illumination microscopy techniques in developmental biology. *Development (Cambridge, England)* **136**(12), 1963-75.

Ju, C., and Reilly, T. (2012). Role of immune reactions in drug-induced liver injury (DILI). *Drug Metabolism Reviews* **44**(1), 107-15.

Kaufmann, A., Mickoleit, M., Weber, M., and Huisken, J. (2012). Multilayer mounting enables long-term imaging of zebrafish development in a light sheet microscope. *Development (Cambridge, England)* **139**(17), 3242-7.

Kim, Y. M., Bergonia, H., and Lancaster, J. R., Jr. (1995). Nitrogen oxide-induced autoprotection in isolated rat hepatocytes. *FEBS letters* **374**(2), 228-32.

Kitzen, J. J., de Jonge, M. J., Lamers, C. H., Eskens, F. A., van der Biessen, D., van Doorn, L., Ter Steeg, J., Brandely, M., Puozzo, C., and Verweij, J. (2009). Phase I dose-escalation study of F60008, a novel apoptosis inducer, in patients with advanced solid tumours. *European Journal of Cancer (Oxford, England : 1990)* **45**(10), 1764-72.

Kupchan, S. M., Court, W. A., Dailey, R. G., Jr., Gilmore, C. J., and Bryan, R. F. (1972). Triptolide and tripdiolide, novel antileukemic diterpenoid triepoxides from Tripterygium wilfordii. *Journal of the American Chemical Society* **94**(20), 7194-5.

Langmead, B., and Salzberg, S. L. (2012). Fast gapped-read alignment with Bowtie 2. *Nature Methods* **9**(4), 357-9.

Lepiller, S., Franche, N., Solary, E., Chluba, J., and Laurens, V. (2009). Comparative analysis of zebrafish nos2a and nos2b genes. *Gene* **445**(1-2), 58-65.

Li, W., Liu, Y., He, Y. Q., Zhang, J. W., Gao, Y., Ge, G. B., Liu, H. X., Huo, H., Liu, H. T., Wang, L. M., *et al.* (2008). Characterization of triptolide hydroxylation by cytochrome P450 in human and rat liver microsomes. *Xenobiotica; the fate of foreign compounds in biological systems* **38**(12), 1551-65.

Li, X. J., Jiang, Z. Z., and Zhang, L. Y. (2014). Triptolide: progress on research in pharmacodynamics and toxicology. *Journal of Ethnopharmacology* **155**(1), 67-79.

Lieschke, G. J., and Currie, P. D. (2007). Animal models of human disease: zebrafish swim into view. *Nature Reviews. Genetics* **8**(5), 353-67.

Liu, Q. (2011). Triptolide and its expanding multiple pharmacological functions. *International Immunopharmacology* **11**(3), 377-83.

McGrath, P., and Li, C. Q. (2008). Zebrafish: a predictive model for assessing drug-induced toxicity. *Drug Discovery Today* **13**(9-10), 394-401.

Mickoleit, M., Schmid, B., Weber, M., Fahrbach, F. O., Hombach, S., Reischauer, S., and Huisken, J. (2014). High-resolution reconstruction of the beating zebrafish heart. *Nat Methods* **11**(9), 919-22.

Nanji, A. A., Greenberg, S. S., Tahan, S. R., Fogt, F., Loscalzo, J., Sadrzadeh, S. M., Xie, J., and Stamler, J. S. (1995). Nitric oxide production in experimental alcoholic liver disease in the rat: role in protection from injury. *Gastroenterology* **109**(3), 899-907.

Panier, T., Romano, S. A., Olive, R., Pietri, T., Sumbre, G., Candelier, R., and Debregeas, G. (2013). Fast functional imaging of multiple brain regions in intact zebrafish larvae using selective plane illumination microscopy. *Frontiers in Neural Circuits* **7**, 65.

Parveen, A., Parveen, B., Parveen, R., and Ahmad, S. (2015). Challenges and guidelines for clinical trial of herbal drugs. *Journal of Pharmacy & Bioallied Sciences* **7**(4), 329-33.

Ritchie, M. E., Phipson, B., Wu, D., Hu, Y., Law, C. W., Shi, W., and Smyth, G. K. (2015). limma powers differential expression analyses for RNA-sequencing and microarray studies. *Nucleic acids research* **43**(7), e47.

Robinson, M. M., and Zhang, X. The World Medicines Situation 2011 - Traditional Medicines: Global Situation, Issues and Challenges.

Sabaliauskas, N. A., Foutz, C. A., Mest, J. R., Budgeon, L. R., Sidor, A. T., Gershenson, J. A., Joshi, S. B., and Cheng, K. C. (2006). High-throughput zebrafish histology. *Methods (San Diego, Calif.)* **39**(3), 246-54.

Shao, F., Wang, G., Xie, H., Zhu, X., Sun, J., and A, J. (2007). Pharmacokinetic study of triptolide, a constituent of immunosuppressive chinese herb medicine, in rats. *Biol Pharm Bull* **30**(4), 702-7.

Smedley, D., Haider, S., Durinck, S., Pandini, L., Provero, P., Allen, J., Arnaiz, O., Awedh, M. H., Baldock, R., Barbiera, G., *et al.* (2015). The BioMart community portal: an innovative alternative to large, centralized data repositories. *Nucleic acids research* **43**(W1), W589-98.

Taylor, J. M., Girkin, J. M., and Love, G. D. (2012). High-resolution 3D optical microscopy inside the beating zebrafish heart using prospective optical gating. *Biomedical optics express* **3**(12), 3043-53.

Teschke, R., Wolff, A., Frenzel, C., Schulze, J., and Eickhoff, A. (2012). Herbal hepatotoxicity: a tabular compilation of reported cases. *Liver international* **32**(10), 1543-56.

Titov, D. V., Gilman, B., He, Q. L., Bhat, S., Low, W. K., Dang, Y., Smeaton, M., Demain, A. L., Miller, P. S., Kugel, J. F., *et al.* (2011). XPB, a subunit of TFIIH, is a target of the natural product triptolide. *Nature Chemical Biology* **7**(3), 182-8.

Vispe, S., DeVries, L., Creancier, L., Besse, J., Breand, S., Hobson, D. J., Svejstrup, J. Q., Annereau, J. P., Cussac, D., Dumontet, C., *et al.* (2009). Triptolide is an inhibitor of RNA polymerase I and II-dependent transcription leading predominantly to down-regulation of short-lived mRNA. *Molecular Cancer Therapeutics* **8**(10), 2780-90.

Vliegenthart, A. D., Shaffer, J. M., Clarke, J. I., Peeters, L. E., Caporali, A., Bateman, D. N., Wood, D. M., Dargan, P. I., Craig, D. G., Moore, J. K., *et al.* (2015). Comprehensive microRNA profiling in acetaminophen toxicity identifies novel circulating biomarkers for human liver and kidney injury. *Scientific Reports* **5**, 15501.

Vliegenthart, A. D., Starkey Lewis, P., Tucker, C. S., Del Pozo, J., Rider, S., Antoine, D. J., Dubost, V., Westphal, M., Moulin, P., Bailey, M. A., *et al.* (2014a). Retro-orbital blood acquisition facilitates circulating microRNA measurement in zebrafish with paracetamol hepatotoxicity. *Zebrafish* **11**(3), 219-26.

Vliegenthart, A. D., Tucker, C. S., Del Pozo, J., and Dear, J. W. (2014b). Zebrafish as model organisms for studying drug-induced liver injury. *British journal of Clinical Pharmacology* **78**(6), 1217-27.

Wang, X., Jiang, Z., Cao, W., Yuan, Z., Sun, L., and Zhang, L. (2014). Th17/Treg imbalance in triptolide-induced liver injury. *Fitoterapia* **93**, 245-51.

Weber, M., and Huisken, J. (2011). Light sheet microscopy for real-time developmental biology. *Current opinion in genetics & development* **21**(5), 566-72.

Westerfield, M. (2007). *The Zebrafish Book: A Guide for the Laboratory Use of Zebrafish (Danio Rerio)*. University of Oregon Press.

Wittmann, C., Reischl, M., Shah, A. H., Kronfuss, E., Mikut, R., Liebel, U., and Grabher, C. (2015). A Zebrafish Drug-Repurposing Screen Reveals sGC-Dependent and sGC-Independent Pro-Inflammatory Activities of Nitric Oxide. *PloS One* **10**(10), e0137286.

Xue, M., Zhao, Y., Li, X. J., Jiang, Z. Z., Zhang, L., Liu, S. H., Li, X. M., Zhang, L. Y., and Yang, S. Y. (2012). Comparison of toxicokinetic and tissue distribution of triptolide-loaded solid lipid nanoparticles vs free triptolide in rats. *European Journal of Pharmaceutical Sciences* **47**(4), 713-7.

Xue, X., Gong, L., Qi, X., Wu, Y., Xing, G., Yao, J., Luan, Y., Xiao, Y., Li, Y., Wu, X., *et al.* (2011). Knockout of hepatic P450 reductase aggravates triptolide-induced toxicity. *Toxicology letters* **205**(1), 47-54.

Yao, J., Zhang, L., Zhao, X., Hu, L., and Jiang, Z. (2006). Simultaneous determination of triptolide, wilforlide A and triptonide in human plasma by high-performance liquid chromatography-electrospray ionization mass spectrometry. *Biol Pharm Bull* **29**(7), 1483-6.

Ye, X., Li, W., Yan, Y., Mao, C., Cai, R., Xu, H., and Yang, X. (2010). Effects of cytochrome P4503A inducer dexamethasone on the metabolism and toxicity of triptolide in rat. *Toxicology letters* **192**(2), 212-20.

Zhang, L., Yan, J., Liu, X., Ye, Z., Yang, X., Meyboom, R., Chan, K., Shaw, D., and Duez, P. (2012). Pharmacovigilance practice and risk control of Traditional Chinese Medicine drugs in China: current status and future perspective. *Journal of ethnopharmacology* **140**(3), 519-25.

Zheng, Y., Zhang, W. J., and Wang, X. M. (2013). Triptolide with potential medicinal value for diseases of the central nervous system. *CNS neuroscience & therapeutics* **19**(2), 76-82.

Zhu, W., and Fung, P. C. (2000). The roles played by crucial free radicals like lipid free radicals, nitric oxide, and enzymes NOS and NADPH in CCl(4)-induced acute liver injury of mice. *Free radical biology & medicine* **29**(9), 870-80.

Ziaei, S., and Halaby, R. (2016). Immunosuppressive, anti-inflammatory and anti-cancer properties of triptolide: A mini review. *Avicenna journal of phytomedicine* **6**(2), 149-64.

Zon, L. I., and Peterson, R. T. (2005). In vivo drug discovery in the zebrafish. *Nature Reviews. Drug Discovery* **4**(1), 35-44.

Figures

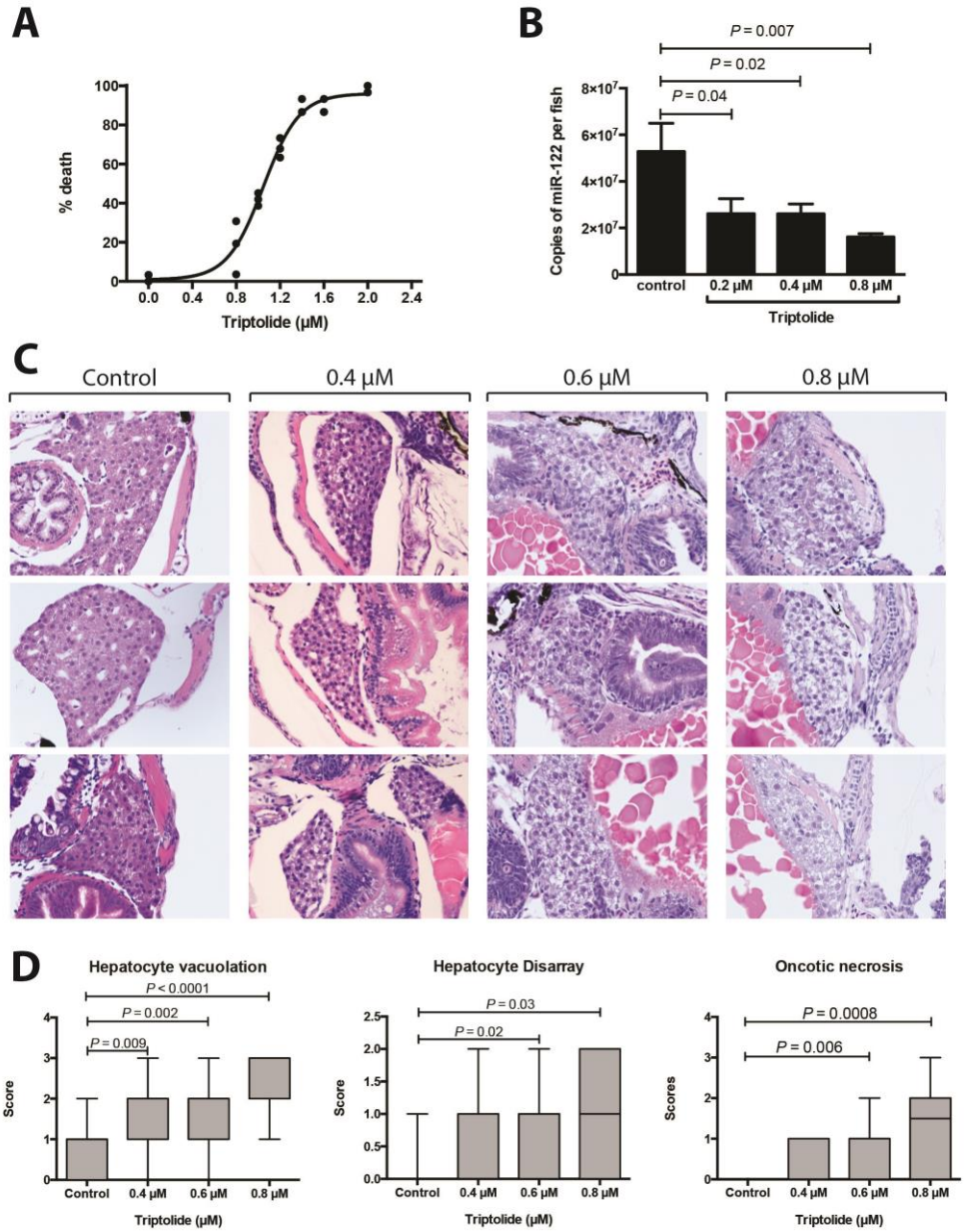

Figure 1. Effect of triptolide on zebrafish larvae after 48 hours (3-5dpf) exposure. (A) Survival of zebrafish larvae after TP exposure at the concentrations indicated. Each dot represents mean mortality of 30 larvae. (B) Copies of miR-122 per larva after 48 hours of exposure at the concentrations indicated (from 3-5 dpf). (C) Histological images of zebrafish larvae after exposures of the TP concentrations indicated. 3 representative fish are presented per TP dose. (D) Box plots (min to max) of histology scores for hepatocyte vacuolation, hepatocyte disarray and oncotic necrosis after TP exposure at the concentrations indicated (control N=12, 0.4 μM N=20, 0.6 μM =18 and 0.8 μM N=18).

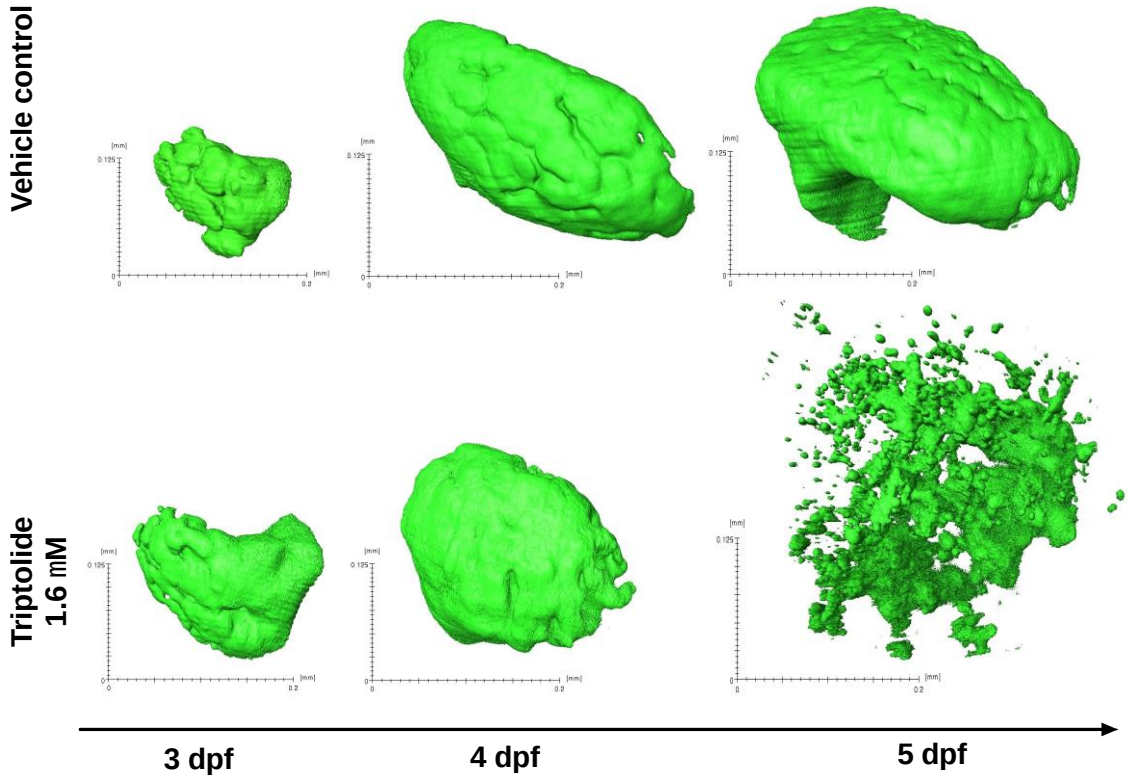

Figure 2. 3D images of livers captured by SPIM. 3dpf zebrafish larvae were exposed to 1.6µM triptolide or vehicle control. After 6 hours of exposure the first image was captured and subsequent images were taken at 4 and 5 dpf.

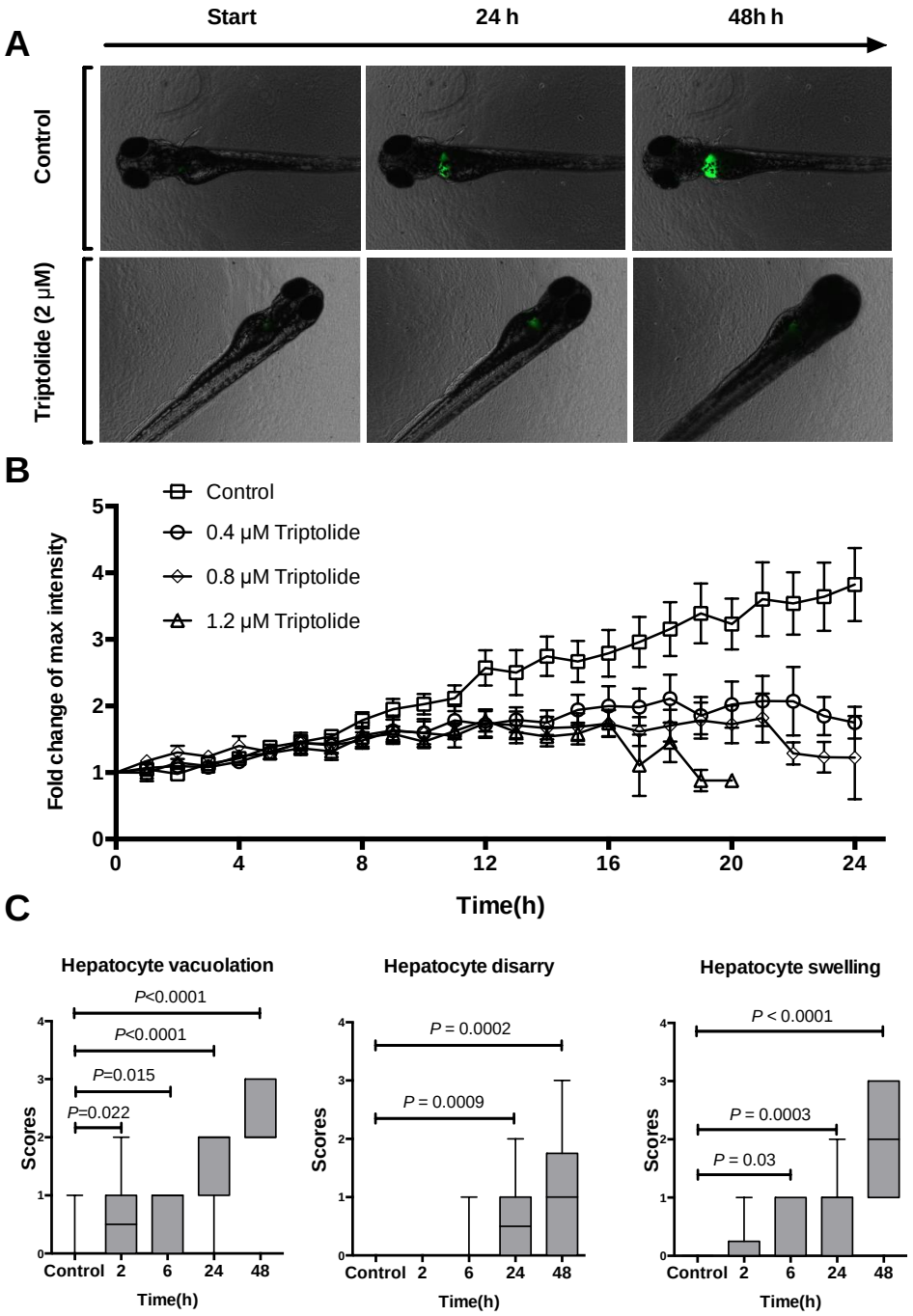

Figure 3. Time-course of triptolide-induced liver injury. (A) Fluorescent images of control and TP exposed fish obtained during time-lapse experiments at the indicated time from start of exposure. (B) Relative fold change of fluorescent intensity from baseline during TP exposure with the doses indicated. (N=15 larvae for each dose) (C) Box plots (min to max) of histology scores of hepatocyte vacuolation, hepatocyte disarray and hepatocyte swelling during exposure to TP (0.8 μM) for the time durations indicated (control N=17, 2h N=10, 6h N=9, 24h N=16, 48 h N=20).

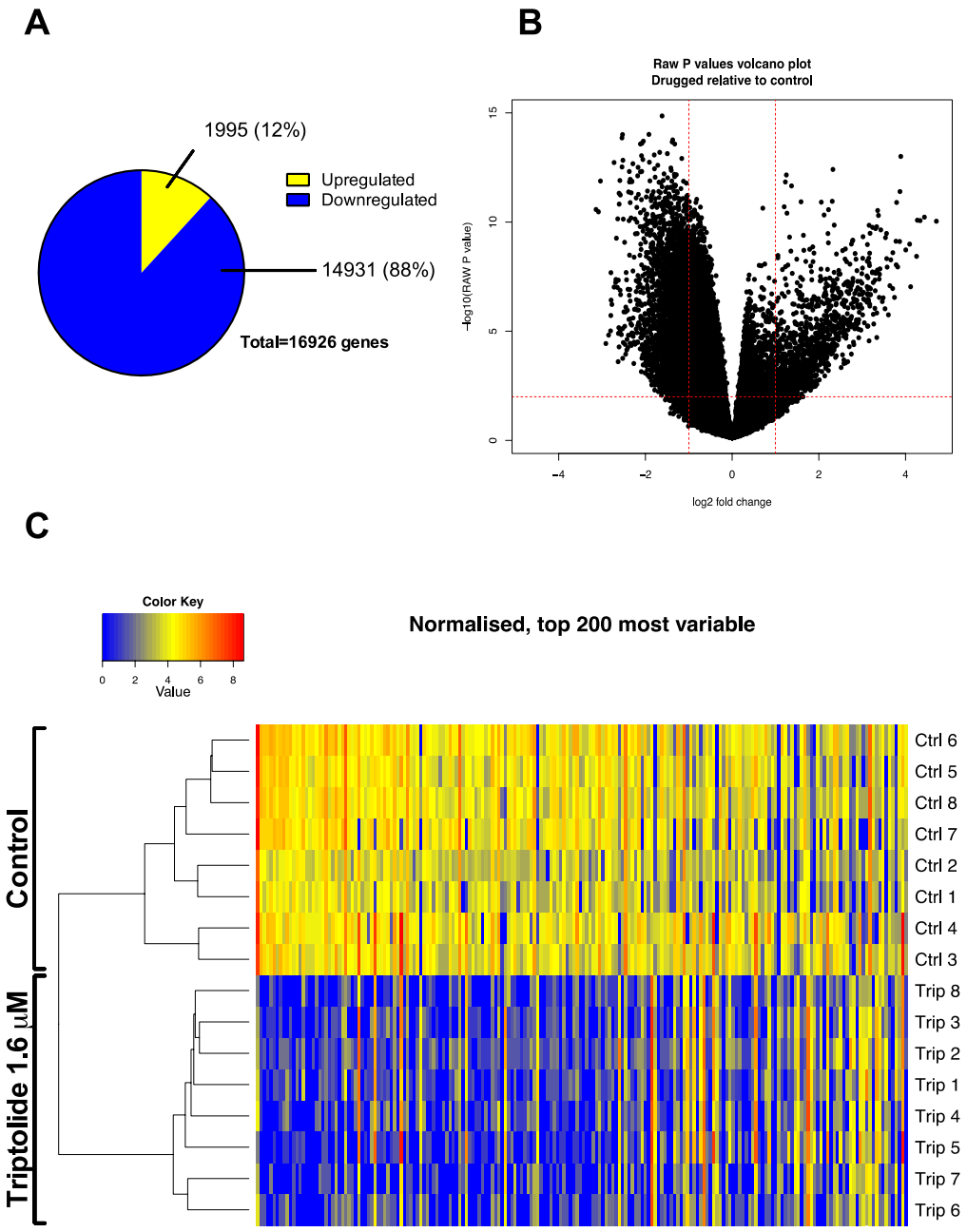

Figure 4. RNA-sequencing of zebrafish larvae exposed to triptolide. RNA-seq was performed on 5 dpf larvae after exposure to triptolide (1.6μM) for 6 hours. A total of 16 sequencing experiments were performed (control N=8 and treatment N=8). Each individual experiment consisted of 30 pooled larvae, therefore 480 larvae were included in total. (A) Proportion of down-regulated and up-regulated genes. (B) Volcano plot of adjusted p value versus log2 fold change of triptolide treated fish versus control. (C) Clustered heatmap with the top 200 most variable genes.

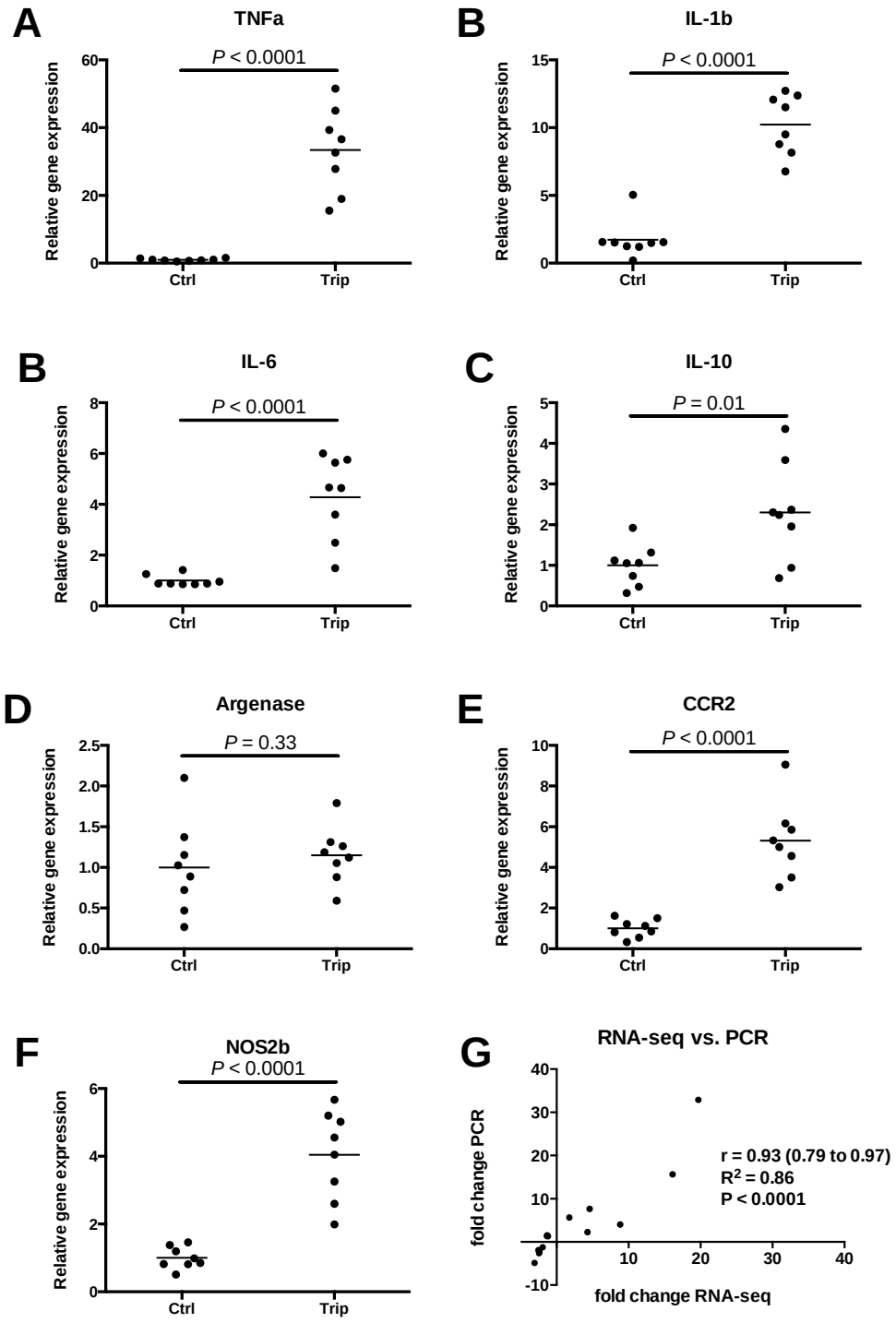

Figure 5. Inflammatory gene expression in zebrafish larvae treated with triptolide (1.6μM) for 6 hours. A-F, Relative gene expression of various inflammatory associated genes measured by PCR. (N=8 pooled sample of 30 larvae for each group, each dot represents one pooled sample and line represents mean). G, correlation between fold change of 14 genes obtained by RNA-seq versus PCR. All genes measured by PCR were normalised by MRPS18B.

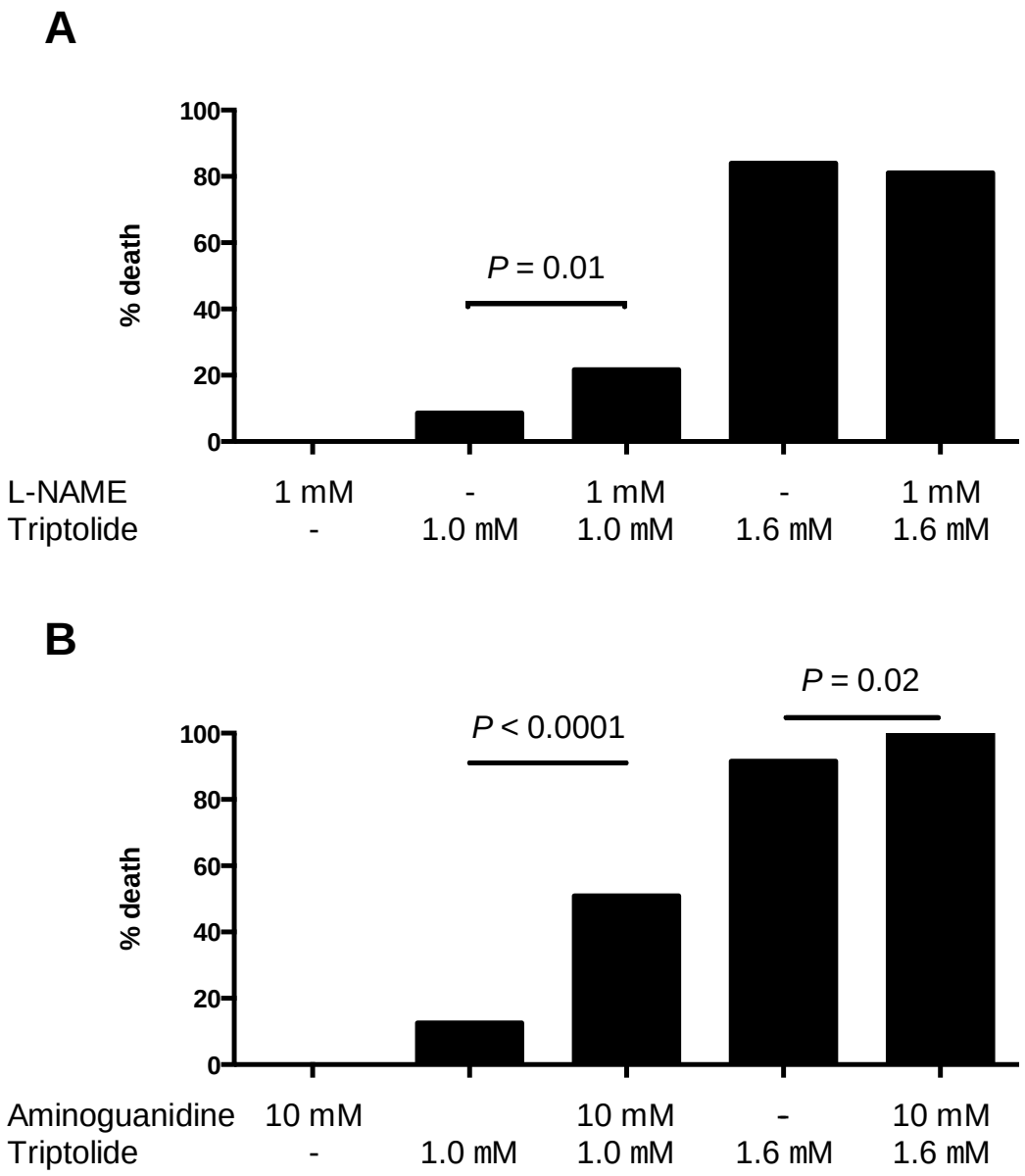

Figure 6. Effect on mortality of co-treatment with (A) L-NAME or (B) aminoguanidine. 3dpf old larvae were exposed for 24h to triptolide and/or the NOS inhibitor indicated. Each dose was tested on at least 60 larvae. Mortality was assessed blinded to the treatment groups. Fisher's exact test was used for statistical differences between groups.

Table 1. Top 10 most up regulated and down regulated genes. RNA-sequencing of zebrafish larvae exposed to triptolide (1.6μM) for 6 hours compared to vehicle control.

ID	Symbol	Fold change	Adjusted *P* value
ENSDART00000128835	NA	26.2	$2.39*10^{-8}$
ENSDART00000154981	wu:fi47d06	21.7	$1.80*10^{-8}$
ENSDART00000103858	LOC557782	20.3	$2.29*10^{-8}$
ENSDART00000025847	TNF-α	19.3	$2.24*10^{-8}$
ENSDART00000037557	admp	19.0	$3.16*10^{-7}$
ENSDART00000062715	NA	17.4	$3.17*10^{-06}$
ENSDART00000157090	LOC557782	17.0	$1.30*10^{-7}$
ENSDART00000129697	ifnphi3	16.1	$1.97*10^{-7}$
ENSDART00000146927	LOC100330560	14.8	$3.74*10^{-10}$
ENSDART00000019296	gdf9	14.6	$3.33*10^{-09}$
ENSDART00000145976	hsp47	-6.8	$1.28*10^{-05}$
ENSDART00000138941	shox2	-6.9	$9.08*10^{-06}$
ENSDART00000048182	v2rh32	-7.0	$1.07*10^{-06}$
ENSDART00000134215	grik1a	-7.0	$3.09*10^{-05}$
ENSDART00000169378	mmp13a	-7.0	0.0001
ENSDART00000101289	zgc:153395	-7.2	0.0002
ENSDART00000054588	spon2b	-7.5	0.0003
ENSDART00000132490	NA	-8.2	$1.65*10^{-09}$
ENSDART00000082333	LOC792903	-8.5	$1.22*10^{-8}$
ENSDART00000078154	npas4	-8.8	$1.03*10^{-8}$

Table 2 KEGG pathways. RNA-sequencing of zebrafish larvae exposed to triptolide (1.6μM) for 6 hours compared to vehicle control.

Up/Down (trip vs Ctrl)	Pathway Description	P-Value
Up	Ribosome	1.87E-86
Up	Cardiac muscle contraction	8.01E-07
Up	Oxidative phosphorylation	0.002544
Up	Steroid hormone biosynthesis	0.006209
Down	Spliceosome	4.19E-08
Down	Notch signaling pathway	0.000845
Down	Progesterone-mediated oocyte maturation	0.004103
Down	Ubiquitin mediated proteolysis	0.005622
Down	Gap junction	0.00651

6.4 Discussion

The purpose of the studies described in this chapter was to characterize TP induced toxicity in zebrafish larvae. Larvae died with a dose-response relationship in the micromolar range and histological examination revealed that TP-induced highly reproducible hepatic necrosis without affecting other organs. This is the first study confirming that TP-induced hepatotoxicity can be modelled in zebrafish larvae. The administration of TP is straightforward and the resultant liver injury is reproducible and tractable. This is in contrast to paracetamol, an archetypal compound used to induce hepatocyte necrosis, which is variable with regard to histological liver injury in larvae and requires millimolar water concentrations for an effect. The enhanced ability of TP to induce liver toxicity is likely due to a combination of its pharmacokinetics and its ability to induce injury without need for metabolism. It is proposed that the data from these studies with triptolide confirm the benefits of zebrafish as a model organism to screen for DILI.

In previous chapters it was reported that upon DILI, miR-122-5p is released from the liver and increases in the circulation of humans and adult zebrafish. The present study reports that the number of copies miR-122-5p per zebrafish larva is decreased with TP-induced DILI, indicating that miR-122-5p can also be utilised as a biomarker for DILI in whole zebrafish larvae.

By exploiting the optical transparency of the zebrafish larvae, in combination with the liver specific fluorescent reporter transgenic fish line, Tg(-*2.8lfabp*:GFP)^{as3}, I captured 3D images by using SPIM of the fish liver. This confirmed that the liver volume was substantially reduced with injury. Fluorescent time-lapse microscopy allowed the characterisation of the time course of injury and identified an early time point for RNA sequencing, which demonstrated that TP has similar effects on RNA transcription as in vitro models (251). PCR confirmed that multiple inflammatory markers were increased in the TP treated fish compared to control, with the cytokine TNF-α being increased 32.9 fold. This suggests that besides a general down regulation of transcription, inflammation potentially has a role in TP-induced DILI. Various

models for inflammation indicate that the zebrafish nitric oxide synthase 2b (NOS2b) is involved in inflammation and has a protective role in the liver (252, 253). NOS2b was upregulated with TP induced toxicity and chemically blocking NOS2b increased TP toxicity.

In conclusion, TP induces hepatic necrosis in zebrafish larvae and inhibits RNA synthesis in line with previous published data. The hepatocyte necrosis induces a protective inflammatory response. TP is a model compound for studying DILI in zebrafish.

6.5 Copyright

Not applicable.

Chapter 7: General Conclusions

The studies presented in first part of this thesis aimed to identify the circulating miRNAs that are most sensitive at detecting paracetamol induced liver injury in humans. Subsequently the leading miRNA candidate was taken forward to further qualify in clinically-relevant scenarios.

Circulating miR-122-5p was the most sensitive miRNA for detecting and predicting liver injury in patients after paracetamol overdose at first presentation at the hospital.

In healthy volunteers, ethanol ingestion led to a significant but not clinically relevant rise in circulating miR-122-5p of 2.2 fold. The circulating miR-122-5p concentration was reduced in patients with ESRD but not in patients with CKD when comparing to healthy volunteers. Circulating miR-122-5p increased after dialysis to healthy levels. These conclusions need to be considered when interpreting liver injury using miR-122-5p in patients with ESRD because a lower baseline concentration might conceal the signal.

Furthermore, it was determined that the lead miRNA, miR-122-5p, measured in capillary blood obtained from a finger prick yielded sufficient miR-122-5p for robust quantification and faithfully reflected the concentration in venous blood and plasma. Capillary miR-122-5p reported paracetamol induced ALI with high sensitivity and specificity and a comparable dynamic range as observed in chapter 2. This leads to the conclusion that miR-122-5p measured in capillary blood obtained from a finger prick can be used as biomarker for DILI.

Besides identifying a circulating miRNA that can be used as a sensitive biomarker for liver injury, the toxicokinetics of circulating paracetamol metabolites were explored to determine if they could be used to quantify the toxic burden and so further refine patient risk stratification.

The results of chapter 4 show that in patients presenting at the hospital after paracetamol overdose, the relative fraction of toxic paracetamol metabolites formed

by P450 (CYP%) was higher in patients that subsequently developed liver injury. In these patients, the ratio of APAP-Cys and APAP-Sul (APAP-Cys/APAP-Sul) had the most sensitivity for predicting subsequent liver injury. This leads to the conclusion that paracetamol metabolites could further refine risk assessment at the front door and guide requirement for NAC treatment.

In the second part of this thesis a new blood letting method was developed that allowed for the measurement of circulating miR-122-5p in adult zebrafish. Subsequently it was tested if circulating miR-122-5p is increased with paracetamol induced liver injury in zebrafish. In paracetamol exposed zebrafish, there was a clear, dose-response elevation in circulating miR-122-5p. The conclusions from this chapter adds zebrafish to the list of species that report hepatotoxicity by elevation in circulating miR-122-5p.

The next aim was to develop a hepatotoxicity model in zebrafish larvae for which TP, a hepatotoxic compound popular in traditional medicine, was used. The administration of TP to zebrafish larvae induced highly reproducible liver injury. This indicates that TP could be used as a model compound to further develop tools for studying DILI in zebrafish larvae.

Future work

The findings of the studies in this thesis have raised further questions that need to be addressed.

For novel markers for which new assays are being developed and validated, normal reference limits need to be determined. These reference limits need to be generated in healthy reference samples from which the lower 2.5th and upper 97.5th percentile cut points must be determined to define abnormality. Approximately 200 individuals is a reasonable sample size to obtain the lower 2.5th and upper 97.5th percentile cut points with high confidence per reference group (254). Results in chapter 3 indicated that ESRD patients on HD have a lower concentration of circulating miR-122-5p. For this reason, reference ranges should also be determined for patients with reduced renal function. When determining the reference range, samples should be measured by a validated assay complying with Good Clinical Laboratory practice standards (255).

In chapter 2 and 4, it was reported that miR-122-5p and paracetamol metabolites were able to predict the onset of ALI determined by an ALT rise. Besides using these markers to determine who is at high risk for developing DILI, they could also be utilised to identify a low risk group who do not need treatment. This would improve patient care by reducing over treatment and it would reduce healthcare costs. The limitation of the studies that measured miR-122-5p at the front door as risk assessment for developing DILI is that each patient received NAC treatment (231). Some patients with a miR-122-5p concentration that is perceived as low risk could have developed DILI if no NAC treatment was given. A clinical study is needed to determine if miR-122-5p could be used to identify patients at low risk that do not need treatment. In this study I suggest that only patients that have a plasma paracetamol concentration within the nomograms “100 mg l^{-l}” and the “200 mg l^{-l}” line receive NAC if their miR-122-5p concentration indicates high risk for developing DILI. All other patients should receive placebo during which they are monitored for developing DILI and receive NAC if DILI occurs during placebo treatment. A power calculation using historical data on determining how many patients develop DILI with

an initial plasma paracetamol concentration within the nomograms "100 mg l^{-1}" and the "200 mg l^{-1}" line needs to determine how many patients would need to be included to test the hypothesis that miR-122-5p can be used to determine which patients require NAC treatment or not. The limitation of this study is that a point of care test needs to be available.

It also needs to be assessed whether these markers are able to predict which patients will need a liver transplant to avoid death. In a previous report, circulating miR-122-5p concentration, on the first day of patient admission, was 2 fold higher in patients reaching KCC compared to those who did not satisfy KCC, however this did not reach statistical significance (77). In order to test whether miR-122-5p and paracetamol metabolites fulfil the TBP attributes of quantitative relationship with disease severity and if they could distinguish benign and clinical relevant increase in ALT, studies need to be performed with a higher number of patients reaching serum ALT of ≥ 1000 IU/L and patients reaching Kings College Criteria (KCC) despite NAC treatment. In the studies performed in this thesis only a small number of patients reached an ALT of ≥ 1000 IU/L and none reached KCC. Being able to stratify patients as early as possible with regard to clinical outcome would assist clinical management of paracetamol poisoning and improve the decision making with regard to liver transplantation. If these markers could predict severe DILI, they would also allow clinical trials of new therapeutics in a group enriched for people with a poor clinical outcome.

Certain medications have been demonstrated to have an effect on specific circulating miRNA concentrations (256). Regular use of medications is common in patients with paracetamol overdose, predominantly benzodiazepines, antidepressants, neuroleptics, paracetamol, oral contraceptives, beta-agonists, opioid analgesic and anticonvulsants (257). Also, concomitant overdosing of other drugs than paracetamol is common of which benzodiazepines, opioid analgesics, acetylsalicylic acid and NSAIDs predominate (258). There are no data regarding the effect of these drug classes on miR-122-5p. In order to further qualify miR-122-5p as biomarker, the effects of these drug classes need to be investigated. However, it should be noted that miR-122-5p retains its sensitivity and specificity for predicting ALI across a range of mixed overdoses.

Future studies should investigate the clearance mechanisms of miR-122-5p when combined with its circulating carrier, Ago2. Such studies would include defining the contribution of the kidney. The results from chapter B demonstrated that the Ago2 bound form of miR-122-5p is substantially reduced in patients with ESRD. Mechanisms that underlie this are yet to be defined but may include reduced production of microRNA. However, if this were the case, the extra-cellular vesicle (ECV) bound fraction would also be expected to fall. Neal et al. have reported that ESRD is associated with increased circulating RNAse activity (235). The Ago2 bound form of miR-122-5p may be more sensitive to enzymatic digestion compared with ECV encapsulated miR-122-5p. *A priori* it could be hypothesised that the ECV fraction would differ between patients with ESRD and healthy controls because as it has clearly demonstrated that systemically injected ECVs are excreted in urine (259, 260). This would suggest that their clearance may be altered in ESRD. However, the miR-122-5p concentration in this fraction did not change. Defining the kinetics of miR-122 will be a priority if it is to be adopted into clinical practice and drug development.

The results from this thesis amongst other publications suggest that zebrafish could potentially be used as an effective economical method for early hepatotoxicity screening in drug development (205). In order to confirm this and make it useful in drug development, an automated assay needs to be developed that can test a high number of compounds in a high throughput fashion. The VAST (Vertebrate Automated Screening Technology) BioImager platform could be an ideal platform. The VAST system allows for fast automatic loading of larvae from multiwall plates in a capillary tube after which it is automatically oriented along the desired axis from which it is imaged (261). This system in combination with the fluorescent reporter Tg(*-2.8lfabp*:GFP)^{as3} that was able to track TP induced hepatotoxicity by liver volume and fluorescent intensity might be an effective system for screening compound libraries for DILI at an early stage during drug development. This system will need to be benchmarked and compared to the currently used high content screens used in drug development that primarily uses cell lines (205), by testing a wide variety of known hepatotoxic and non-hepatotoxic compounds.

The results in this thesis report that TP can induce specific and reproducible hepatotoxicity in zebrafish larvae. In the future it should be tested if there is a dosing regimen that can induce hepatotoxicity in zebrafish larvae from which they can recover. Zebrafish exhibit a strong regenerative capacity (262), with for instance the heart being able to fully regenerate within 2 months after 20% ventricular resection (263). Some models for liver regeneration in zebrafish exist such as partial hepatectomy by removal of one lobe (264) and liver ablation by using bacterial nitro reductase (NTR) in transgenic zebrafish with a liver specific promotor for NTR (265). However, these models have limitations due to their complexity and low throughput. If a dosing regimen with TP could be found that results in liver injury in a short time by simply adding drug to the water after which it can recover in clean system water it would offer useful system in the area of screening compounds and drugs for their effects upon liver regeneration (266).

The development of circulating miRNAs as biomarkers in DILI is an exciting and valuable field to focus research efforts on. Exploiting these small RNA molecules has a great potential to improve paracetamol overdose management and the detection of DILI in clinical drug development. The work presented in this thesis confirmed that miR-122-5p was the optimum circulating miRNA for predicting the onset of DILI at first presentation to the hospital. The work presented in this thesis has highlighted the limitations and challenges related to the development and qualification required in biomarker research and have addressed this by exploring specific clinical scenarios. In conclusion, miRNAs can be used as specific markers for hepatotoxicity in humans and zebrafish. Zebrafish can be used as a pre-clinical model for drug induced liver injury.

REFERENCES

1. Trey C, Davidson CS. The management of fulminant hepatic failure. Prog Liver Dis 1970;3:282-298.
2. Wlodzimirow KA, Eslami S, Abu-Hanna A, Nieuwoudt M, Chamuleau RA. Systematic review: acute liver failure - one disease, more than 40 definitions. Aliment Pharmacol Ther 2012;35:1245-1256.
3. O'Grady JG, Schalm SW, Williams R. Acute liver failure: redefining the syndromes. Lancet 1993;342:273-275.
4. Bernuau J, Rueff B, Benhamou JP. Fulminant and subfulminant liver failure: definitions and causes. Semin Liver Dis 1986;6:97-106.
5. Escorsell A, Mas A, de la Mata M. Acute liver failure in Spain: analysis of 267 cases. Liver Transpl 2007;13:1389-1395.
6. Bower WA, Johns M, Margolis HS, Williams IT, Bell BP. Population-based surveillance for acute liver failure. Am J Gastroenterol 2007;102:2459-2463.
7. Kumar R, Bhatia V, Khanal S, Sreenivas V, Gupta SD, Panda SK, Acharya SK. Antituberculosis therapy-induced acute liver failure: magnitude, profile, prognosis, and predictors of outcome. Hepatology 2010;51:1665-1674.
8. Rakela J, Lange SM, Ludwig J, Baldus WP. Fulminant hepatitis: Mayo Clinic experience with 34 cases. Mayo Clin Proc 1985;60:289-292.
9. Ostapowicz G, Fontana RJ, Schiodt FV, Larson A, Davern TJ, Han SH, McCashland TM, Shakil AO, Hay JE, Hynan L, Crippin JS, Blei AT, Samuel G, Reisch J, Lee WM. Results of a prospective study of acute liver failure at 17 tertiary care centers in the United States. Ann Intern Med 2002;137:947-954.
10. O'Grady JG, Alexander GJ, Hayllar KM, Williams R. Early indicators of prognosis in fulminant hepatic failure. Gastroenterology 1989;97:439-445.
11. McPhail MJ, Wendon JA, Bernal W. Meta-analysis of performance of Kings's College Hospital Criteria in prediction of outcome in non-paracetamol-induced acute liver failure. J Hepatol 2010;53:492-499.
12. Bernal W, Auzinger G, Dhawan A, Wendon J. Acute liver failure. Lancet 2010;376:190-201.

13. Acharya SK, Batra Y, Hazari S, Choudhury V, Panda SK, Dattagupta S. Etiopathogenesis of acute hepatic failure: Eastern versus Western countries. J Gastroenterol Hepatol 2002;17 Suppl 3:S268-273.

14. Kaplowitz N. Idiosyncratic drug hepatotoxicity. Nat Rev Drug Discov 2005;4:489-499.

15. Iorga A, Dara L, Kaplowitz N. Drug-Induced Liver Injury: Cascade of Events Leading to Cell Death, Apoptosis or Necrosis. Int J Mol Sci 2017;18.

16. Farrell GC, Liddle C. Drugs and the liver updated, 2002. Semin Liver Dis 2002;22:109-113.

17. Navarro VJ, Senior JR. Drug-related hepatotoxicity. N Engl J Med 2006;354:731-739.

18. Chalasani NP, Hayashi PH, Bonkovsky HL, Navarro VJ, Lee WM, Fontana RJ. ACG Clinical Guideline: the diagnosis and management of idiosyncratic drug-induced liver injury. Am J Gastroenterol 2014;109:950-966; quiz 967.

19. McDonnell ME, Braverman LE. Drug-related hepatotoxicity. N Engl J Med 2006;354:2191-2193; author reply 2191-2193.

20. Bernal W, Auzinger G, Wendon J. Prognostic utility of the bilirubin lactate and etiology score. Clin Gastroenterol Hepatol 2009;7:249; author reply 249.

21. Reuben A, Koch DG, Lee WM. Drug-induced acute liver failure: results of a U.S. multicenter, prospective study. Hepatology 2010;52:2065-2076.

22. Bateman DN, Carroll R, Pettie J, Yamamoto T, Elamin ME, Peart L, Dow M, Coyle J, Cranfield KR, Hook C, Sandilands EA, Veiraiah A, Webb D, Gray A, Dargan PI, Wood DM, Thomas SH, Dear JW, Eddleston M. Effect of the UK's revised paracetamol poisoning management guidelines on admissions, adverse reactions and costs of treatment. Br J Clin Pharmacol 2014;78:610-618.

23. NHS. A&E Attendances and Emergency Admissions. In; 2016.

24. Raucy JL, Lasker JM, Lieber CS, Black M. Acetaminophen activation by human liver cytochromes P450IIE1 and P450IA2. Arch Biochem Biophys 1989;271:270-283.

25. Snawder JE, Roe AL, Benson RW, Roberts DW. Loss of CYP2E1 and CYP1A2 activity as a function of acetaminophen dose: relation to toxicity. Biochem Biophys Res Commun 1994;203:532-539.

26. Thummel KE, Lee CA, Kunze KL, Nelson SD, Slattery JT. Oxidation of acetaminophen to N-acetyl-p-aminobenzoquinone imine by human CYP3A4. Biochem Pharmacol 1993;45:1563-1569.

27. Ferner RE, Dear JW, Bateman DN. Management of paracetamol poisoning. Bmj 2011;342:d2218.

28. Smilkstein MJ, Knapp GL, Kulig KW, Rumack BH. Efficacy of oral N-acetylcysteine in the treatment of acetaminophen overdose. Analysis of the national multicenter study (1976 to 1985). N Engl J Med 1988;319:1557-1562.

29. Waring WS. Criteria for acetylcysteine treatment and clinical outcomes after paracetamol poisoning. Expert Rev Clin Pharmacol 2012;5:311-318.

30. Senior JR. Alanine aminotransferase: a clinical and regulatory tool for detecting liver injury-past, present, and future. Clin Pharmacol Ther 2012;92:332-339.

31. Prescott K, Stratton R, Freyer A, Hall I, Le Jeune I. Detailed analyses of self-poisoning episodes presenting to a large regional teaching hospital in the UK. Br J Clin Pharmacol 2009;68:260-268.

32. NPIS. TOXBASE. In.

33. Al-Hourani K, Mansi R, Pettie J, Dow M, Bateman DN, Dear JW. The predictive value of hospital admission serum alanine transaminase activity in patients treated for paracetamol overdose. Qjm 2013;106:541-546.

34. Ozer J, Ratner M, Shaw M, Bailey W, Schomaker S. The current state of serum biomarkers of hepatotoxicity. Toxicology 2008;245:194-205.

35. Rumack BH, Peterson RC, Koch GG, Amara IA. Acetaminophen overdose. 662 cases with evaluation of oral acetylcysteine treatment. Arch Intern Med 1981;141:380-385.

36. Prescott LF, Roscoe P, Wright N, Brown SS. Plasma-paracetamol half-life and hepatic necrosis in patients with paracetamol overdosage. Lancet 1971;1:519-522.

37. Beringer RM, Thompson JP, Parry S, Stoddart PA. Intravenous paracetamol overdose: two case reports and a change to national treatment guidelines. Arch Dis Child 2011;96:307-308.

38. MHRA. Benefit risk profile of acetylcysteine in the management of paracetamol overdose. . In; 2012.

39. FDA. Draft guidance for industry and review staff, target product profile—a strategic development process tool. In. http://www.fda.gov/cder/guidance/index.htm: FDA; 2007.

40. Watkins PB, Merz M, Avigan MI, Kaplowitz N, Regev A, Senior JR. The clinical liver safety assessment best practices workshop: rationale, goals, accomplishments and the future. Drug Saf 2014;37 Suppl 1:S1-7.

41. Muller-Bardorff M, Rauscher T, Kampmann M, Schoolmann S, Laufenberg F, Mangold D, Zerback R, Remppis A, Katus HA. Quantitative bedside assay for cardiac troponin T: a complementary method to centralized laboratory testing. Clin Chem 1999;45:1002-1008.

42. Hawkins RC. Laboratory turnaround time. Clin Biochem Rev 2007;28:179-194.

43. Pollock NR, Rolland JP, Kumar S, Beattie PD, Jain S, Noubary F, Wong VL, Pohlmann RA, Ryan US, Whitesides GM. A paper-based multiplexed transaminase test for low-cost, point-of-care liver function testing. Sci Transl Med 2012;4:152ra129.

44. Prescott LF, Illingworth RN, Critchley JA, Stewart MJ, Adam RD, Proudfoot AT. Intravenous N-acetylcystine: the treatment of choice for paracetamol poisoning. Br Med J 1979;2:1097-1100.

45. Thygesen K, Mair J, Katus H, Plebani M, Venge P, Collinson P, Lindahl B, Giannitsis E, Hasin Y, Galvani M, Tubaro M, Alpert JS, Biasucci LM, Koenig W, Mueller C, Huber K, Hamm C, Jaffe AS. Recommendations for the use of cardiac troponin measurement in acute cardiac care. Eur Heart J 2010;31:2197-2204.

46. Lo Re V, 3rd, Haynes K, Forde KA, Goldberg DS, Lewis JD, Carbonari DM, Leidl KB, Reddy KR, Nezamzadeh MS, Roy J, Sha D, Marks AR, De Boer J, Schneider JL, Strom BL, Corley DA. Risk of Acute Liver Failure in Patients With Drug-Induced Liver Injury: Evaluation of Hy's Law and a New Prognostic Model. Clin Gastroenterol Hepatol 2015;13:2360-2368.

47. Reuben A. Hy's law. Hepatology 2004;39:574-578.

48. Temple R. Hy's law: predicting serious hepatotoxicity. Pharmacoepidemiol Drug Saf 2006;15:241-243.

49. Vliegenthart AD, Antoine DJ, Dear JW. Target biomarker profile for the clinical management of paracetamol overdose. Br J Clin Pharmacol 2015;80:351-362.

50. Ardekani AM, Naeini MM. The Role of MicroRNAs in Human Diseases. Avicenna J Med Biotechnol 2010;2:161-179.

51. Kozomara A, Griffiths-Jones S. miRBase: annotating high confidence microRNAs using deep sequencing data. Nucleic Acids Res 2014;42:D68-73.

52. Altuvia Y, Landgraf P, Lithwick G, Elefant N, Pfeffer S, Aravin A, Brownstein MJ, Tuschl T, Margalit H. Clustering and conservation patterns of human microRNAs. Nucleic Acids Res 2005;33:2697-2706.

53. Lee Y, Kim M, Han J, Yeom KH, Lee S, Baek SH, Kim VN. MicroRNA genes are transcribed by RNA polymerase II. Embo j 2004;23:4051-4060.

54. Borchert GM, Lanier W, Davidson BL. RNA polymerase III transcribes human microRNAs. Nat Struct Mol Biol 2006;13:1097-1101.

55. Cai X, Hagedorn CH, Cullen BR. Human microRNAs are processed from capped, polyadenylated transcripts that can also function as mRNAs. Rna 2004;10:1957-1966.

56. Han J, Lee Y, Yeom KH, Kim YK, Jin H, Kim VN. The Drosha-DGCR8 complex in primary microRNA processing. Genes Dev 2004;18:3016-3027.

57. Han J, Lee Y, Yeom KH, Nam JW, Heo I, Rhee JK, Sohn SY, Cho Y, Zhang BT, Kim VN. Molecular basis for the recognition of primary microRNAs by the Drosha-DGCR8 complex. Cell 2006;125:887-901.

58. Yi R, Qin Y, Macara IG, Cullen BR. Exportin-5 mediates the nuclear export of pre-microRNAs and short hairpin RNAs. Genes Dev 2003;17:3011-3016.

59. Chendrimada TP, Gregory RI, Kumaraswamy E, Norman J, Cooch N, Nishikura K, Shiekhattar R. TRBP recruits the Dicer complex to Ago2 for microRNA processing and gene silencing. Nature 2005;436:740-744.

60. Gregory RI, Chendrimada TP, Cooch N, Shiekhattar R. Human RISC couples microRNA biogenesis and posttranscriptional gene silencing. Cell 2005;123:631-640.

61. Lee Y, Hur I, Park SY, Kim YK, Suh MR, Kim VN. The role of PACT in the RNA silencing pathway. Embo j 2006;25:522-532.

62. Moxon S, Jing R, Szittya G, Schwach F, Rusholme Pilcher RL, Moulton V, Dalmay T. Deep sequencing of tomato short RNAs identifies microRNAs targeting genes involved in fruit ripening. Genome Res 2008;18:1602-1609.

63. Bartel DP. MicroRNAs: target recognition and regulatory functions. Cell 2009;136:215-233.

64. Winter J, Jung S, Keller S, Gregory RI, Diederichs S. Many roads to maturity: microRNA biogenesis pathways and their regulation. Nat Cell Biol 2009;11:228-234.

65. Hunter MP, Ismail N, Zhang X, Aguda BD, Lee EJ, Yu L, Xiao T, Schafer J, Lee ML, Schmittgen TD, Nana-Sinkam SP, Jarjoura D, Marsh CB. Detection of microRNA expression in human peripheral blood microvesicles. PLoS One 2008;3:e3694.

66. Arroyo JD, Chevillet JR, Kroh EM, Ruf IK, Pritchard CC, Gibson DF, Mitchell PS, Bennett CF, Pogosova-Agadjanyan EL, Stirewalt DL, Tait JF, Tewari M. Argonaute2 complexes carry a population of circulating microRNAs independent of vesicles in human plasma. Proc Natl Acad Sci U S A 2011;108:5003-5008.

67. Liang Y, Ridzon D, Wong L, Chen C. Characterization of microRNA expression profiles in normal human tissues. BMC Genomics 2007;8:166.

68. Bhattacharyya SN, Habermacher R, Martine U, Closs EI, Filipowicz W. Relief of microRNA-mediated translational repression in human cells subjected to stress. Cell 2006;125:1111-1124.

69. Esau C, Davis S, Murray SF, Yu XX, Pandey SK, Pear M, Watts L, Booten SL, Graham M, McKay R, Subramaniam A, Propp S, Lollo BA, Freier S, Bennett CF, Bhanot S, Monia BP. miR-122 regulation of lipid metabolism revealed by in vivo antisense targeting. Cell Metab 2006;3:87-98.

70. Krutzfeldt J, Rajewsky N, Braich R, Rajeev KG, Tuschl T, Manoharan M, Stoffel M. Silencing of microRNAs in vivo with 'antagomirs'. Nature 2005;438:685-689.

71. Tsai WC, Hsu SD, Hsu CS, Lai TC, Chen SJ, Shen R, Huang Y, Chen HC, Lee CH, Tsai TF, Hsu MT, Wu JC, Huang HD, Shiao MS, Hsiao M, Tsou AP. MicroRNA-122 plays a critical role in liver homeostasis and hepatocarcinogenesis. J Clin Invest 2012;122:2884-2897.

72. Wang K, Zhang S, Marzolf B, Troisch P, Brightman A, Hu Z, Hood LE, Galas DJ. Circulating microRNAs, potential biomarkers for drug-induced liver injury. Proc Natl Acad Sci U S A 2009;106:4402-4407.

73. Su YW, Chen X, Jiang ZZ, Wang T, Wang C, Zhang Y, Wen J, Xue M, Zhu D, Zhang Y, Su YJ, Xing TY, Zhang CY, Zhang LY. A panel of serum microRNAs as specific biomarkers for diagnosis of compound- and herb-induced liver injury in rats. PLoS One 2012;7:e37395.

74. Harrill AH, Eaddy JS, Rose K, Cullen JM, Ramanathan L, Wanaski S, Collins S, Ho Y, Watkins PB, Lecluyse EL. Liver biomarker and in vitro assessment confirm the hepatic origin of aminotransferase elevations lacking histopathological correlate in beagle dogs treated with GABAA receptor antagonist NP260. Toxicol Appl Pharmacol 2014;277:131-137.

75. Vliegenthart AD, Starkey Lewis P, Tucker CS, Del Pozo J, Rider S, Antoine DJ, Dubost V, Westphal M, Moulin P, Bailey MA, Moggs JG, Goldring CE, Park BK, Dear JW. Retro-orbital blood acquisition facilitates circulating microRNA measurement in zebrafish with paracetamol hepatotoxicity. Zebrafish 2014;11:219-226.

76. Andersson P, Gidlof O, Braun OO, Gotberg M, van der Pals J, Olde B, Erlinge D. Plasma levels of liver-specific miR-122 is massively increased in a porcine cardiogenic shock model and attenuated by hypothermia. Shock 2012;37:234-238.

77. Starkey Lewis PJ, Dear J, Platt V, Simpson KJ, Craig DG, Antoine DJ, French NS, Dhaun N, Webb DJ, Costello EM, Neoptolemos JP, Moggs J, Goldring CE, Park BK. Circulating microRNAs as potential markers of human drug-induced liver injury. Hepatology 2011;54:1767-1776.

78. Yang X, Salminen WF, Shi Q, Greenhaw J, Gill PS, Bhattacharyya S, Beger RD, Mendrick DL, Mattes WB, James LP. Potential of extracellular microRNAs as biomarkers of acetaminophen toxicity in children. Toxicol Appl Pharmacol 2015;284:180-187.

79. Antoine DJ, Dear JW, Lewis PS, Platt V, Coyle J, Masson M, Thanacoody RH, Gray AJ, Webb DJ, Moggs JG, Bateman DN, Goldring CE, Park BK. Mechanistic biomarkers provide early and sensitive detection of acetaminophen-induced acute liver injury at first presentation to hospital. Hepatology 2013;58:777-787.

80. Omary MB, Ku NO, Tao GZ, Toivola DM, Liao J. "Heads and tails" of intermediate filament phosphorylation: multiple sites and functional insights. Trends Biochem Sci 2006;31:383-394.

81. Vijayaraj P, Sohl G, Magin TM. Keratin transgenic and knockout mice: functional analysis and validation of disease-causing mutations. Methods Mol Biol 2007;360:203-251.

82. Ku NO, Zhou X, Toivola DM, Omary MB. The cytoskeleton of digestive epithelia in health and disease. Am J Physiol 1999;277:G1108-1137.

83. Schutte B, Henfling M, Kolgen W, Bouman M, Meex S, Leers MP, Nap M, Bjorklund V, Bjorklund P, Bjorklund B, Lane EB, Omary MB, Jornvall H, Ramaekers FC. Keratin 8/18 breakdown and reorganization during apoptosis. Exp Cell Res 2004;297:11-26.

84. Cummings J, Hodgkinson C, Odedra R, Sini P, Heaton SP, Mundt KE, Ward TH, Wilkinson RW, Growcott J, Hughes A, Dive C. Preclinical evaluation of M30 and M65 ELISAs as biomarkers of drug induced tumor cell death and antitumor activity. Mol Cancer Ther 2008;7:455-463.

85. Kramer G, Schwarz S, Hagg M, Havelka AM, Linder S. Docetaxel induces apoptosis in hormone refractory prostate carcinomas during multiple treatment cycles. Br J Cancer 2006;94:1592-1598.

86. Williams CD, Antoine DJ, Shaw PJ, Benson C, Farhood A, Williams DP, Kanneganti TD, Park BK, Jaeschke H. Role of the Nalp3 inflammasome in acetaminophen-induced sterile inflammation and liver injury. Toxicol Appl Pharmacol 2011;252:289-297.

87. Antoine DJ, Jenkins RE, Dear JW, Williams DP, McGill MR, Sharpe MR, Craig DG, Simpson KJ, Jaeschke H, Park BK. Molecular forms of HMGB1 and keratin-18 as mechanistic biomarkers for mode of cell death and prognosis during clinical acetaminophen hepatotoxicity. J Hepatol 2012;56:1070-1079.

88. Possamai LA, McPhail MJ, Quaglia A, Zingarelli V, Abeles RD, Tidswell R, Puthucheary Z, Rawal J, Karvellas CJ, Leslie EM, Hughes RD, Ma Y, Jassem W, Shawcross DL, Bernal W, Dharwan A, Heaton ND, Thursz M, Wendon JA, Mitry RR, Antoniades CG. Character and temporal evolution of apoptosis in acetaminophen-induced acute liver failure*. Crit Care Med 2013;41:2543-2550.

89. Gujral JS, Knight TR, Farhood A, Bajt ML, Jaeschke H. Mode of cell death after acetaminophen overdose in mice: apoptosis or oncotic necrosis? Toxicol Sci 2002;67:322-328.

90. Scaffidi P, Misteli T, Bianchi ME. Release of chromatin protein HMGB1 by necrotic cells triggers inflammation. Nature 2002;418:191-195.
91. Lotze MT, Tracey KJ. High-mobility group box 1 protein (HMGB1): nuclear weapon in the immune arsenal. Nat Rev Immunol 2005;5:331-342.
92. Bianchi ME, Manfredi AA. High-mobility group box 1 (HMGB1) protein at the crossroads between innate and adaptive immunity. Immunol Rev 2007;220:35-46.
93. Hori O, Brett J, Slattery T, Cao R, Zhang J, Chen JX, Nagashima M, Lundh ER, Vijay S, Nitecki D, et al. The receptor for advanced glycation end products (RAGE) is a cellular binding site for amphoterin. Mediation of neurite outgrowth and co-expression of rage and amphoterin in the developing nervous system. J Biol Chem 1995;270:25752-25761.
94. Park JS, Svetkauskaite D, He Q, Kim JY, Strassheim D, Ishizaka A, Abraham E. Involvement of toll-like receptors 2 and 4 in cellular activation by high mobility group box 1 protein. J Biol Chem 2004;279:7370-7377.
95. Yang H, Antoine DJ, Andersson U, Tracey KJ. The many faces of HMGB1: molecular structure-functional activity in inflammation, apoptosis, and chemotaxis. J Leukoc Biol 2013;93:865-873.
96. Bonaldi T, Talamo F, Scaffidi P, Ferrera D, Porto A, Bachi A, Rubartelli A, Agresti A, Bianchi ME. Monocytic cells hyperacetylate chromatin protein HMGB1 to redirect it towards secretion. Embo j 2003;22:5551-5560.
97. Yang H, Lundback P, Ottosson L, Erlandsson-Harris H, Venereau E, Bianchi ME, Al-Abed Y, Andersson U, Tracey KJ, Antoine DJ. Redox modification of cysteine residues regulates the cytokine activity of high mobility group box-1 (HMGB1). Mol Med 2012;18:250-259.
98. Wang H, Bloom O, Zhang M, Vishnubhakat JM, Ombrellino M, Che J, Frazier A, Yang H, Ivanova S, Borovikova L, Manogue KR, Faist E, Abraham E, Andersson J, Andersson U, Molina PE, Abumrad NN, Sama A, Tracey KJ. HMG-1 as a late mediator of endotoxin lethality in mice. Science 1999;285:248-251.
99. Yasuda T, Ueda T, Takeyama Y, Shinzeki M, Sawa H, Nakajima T, Ajiki T, Fujino Y, Suzuki Y, Kuroda Y. Significant increase of serum high-mobility group box chromosomal protein 1 levels in patients with severe acute pancreatitis. Pancreas 2006;33:359-363.

100. Taniguchi N, Kawahara K, Yone K, Hashiguchi T, Yamakuchi M, Goto M, Inoue K, Yamada S, Ijiri K, Matsunaga S, Nakajima T, Komiya S, Maruyama I. High mobility group box chromosomal protein 1 plays a role in the pathogenesis of rheumatoid arthritis as a novel cytokine. Arthritis Rheum 2003;48:971-981.

101. Antoine DJ, Williams DP, Kipar A, Jenkins RE, Regan SL, Sathish JG, Kitteringham NR, Park BK. High-mobility group box-1 protein and keratin-18, circulating serum proteins informative of acetaminophen-induced necrosis and apoptosis in vivo. Toxicol Sci 2009;112:521-531.

102. Huebener P, Pradere JP, Hernandez C, Gwak GY, Caviglia JM, Mu X, Loike JD, Jenkins RE, Antoine DJ, Schwabe RF. The HMGB1/RAGE axis triggers neutrophil-mediated injury amplification following necrosis. J Clin Invest 2015;125:539-550.

103. Antoine DJ, Williams DP, Kipar A, Laverty H, Park BK. Diet restriction inhibits apoptosis and HMGB1 oxidation and promotes inflammatory cell recruitment during acetaminophen hepatotoxicity. Mol Med 2010;16:479-490.

104. Lundback P, Lea JD, Sowinska A, Ottosson L, Furst CM, Steen J, Aulin C, Clarke JI, Kipar A, Klevenvall L, Yang H, Palmblad K, Park BK, Tracey KJ, Blom AM, Andersson U, Antoine DJ, Erlandsson Harris H. A novel high mobility group box 1 neutralizing chimeric antibody attenuates drug-induced liver injury and postinjury inflammation in mice. Hepatology 2016.

105. Fang J, Hsu BY, MacMullen CM, Poncz M, Smith TJ, Stanley CA. Expression, purification and characterization of human glutamate dehydrogenase (GDH) allosteric regulatory mutations. Biochem J 2002;363:81-87.

106. Jaeschke H, McGill MR. Serum glutamate dehydrogenase--biomarker for liver cell death or mitochondrial dysfunction? Toxicol Sci 2013;134:221-222.

107. Wong SG, Card JW, Racz WJ. The role of mitochondrial injury in bromobenzene and furosemide induced hepatotoxicity. Toxicol Lett 2000;116:171-181.

108. McGill MR, Sharpe MR, Williams CD, Taha M, Curry SC, Jaeschke H. The mechanism underlying acetaminophen-induced hepatotoxicity in humans and mice involves mitochondrial damage and nuclear DNA fragmentation. J Clin Invest 2012;122:1574-1583.

109. Krysko DV, Agostinis P, Krysko O, Garg AD, Bachert C, Lambrecht BN, Vandenabeele P. Emerging role of damage-associated molecular patterns derived from mitochondria in inflammation. Trends Immunol 2011;32:157-164.
110. Zhang Q, Raoof M, Chen Y, Sumi Y, Sursal T, Junger W, Brohi K, Itagaki K, Hauser CJ. Circulating mitochondrial DAMPs cause inflammatory responses to injury. Nature 2010;464:104-107.
111. Simmons JD, Lee YL, Mulekar S, Kuck JL, Brevard SB, Gonzalez RP, Gillespie MN, Richards WO. Elevated levels of plasma mitochondrial DNA DAMPs are linked to clinical outcome in severely injured human subjects. Ann Surg 2013;258:591-598.
112. Nakahira K, Kyung SY, Rogers AJ, Gazourian L, Youn S, Massaro AF, Quintana C, Osorio JC, Wang Z, Zhao Y, Lawler LA, Christie JD, Meyer NJ, Mc Causland FR, Waikar SS, Waxman AB, Chung RT, Bueno R, Rosas IO, Fredenburgh LE, Baron RM, Christiani DC, Hunninghake GM, Choi AM. Circulating mitochondrial DNA in patients in the ICU as a marker of mortality: derivation and validation. PLoS Med 2013;10:e1001577; discussion e1001577.
113. Vaidya VS, Ozer JS, Dieterle F, Collings FB, Ramirez V, Troth S, Muniappa N, Thudium D, Gerhold D, Holder DJ, Bobadilla NA, Marrer E, Perentes E, Cordier A, Vonderscher J, Maurer G, Goering PL, Sistare FD, Bonventre JV. Kidney injury molecule-1 outperforms traditional biomarkers of kidney injury in preclinical biomarker qualification studies. Nat Biotechnol 2010;28:478-485.
114. McWilliam SJ, Antoine DJ, Sabbisetti V, Turner MA, Farragher T, Bonventre JV, Park BK, Smyth RL, Pirmohamed M. Mechanism-based urinary biomarkers to identify the potential for aminoglycoside-induced nephrotoxicity in premature neonates: a proof-of-concept study. PLoS One 2012;7:e43809.
115. Sabbisetti VS, Waikar SS, Antoine DJ, Smiles A, Wang C, Ravisankar A, Ito K, Sharma S, Ramadesikan S, Lee M, Briskin R, De Jager PL, Ngo TT, Radlinski M, Dear JW, Park KB, Betensky R, Krolewski AS, Bonventre JV. Blood kidney injury molecule-1 is a biomarker of acute and chronic kidney injury and predicts progression to ESRD in type I diabetes. J Am Soc Nephrol 2014;25:2177-2186.
116. Antoine DJ, Sabbisetti VS, Francis B, Jorgensen AL, Craig DG, Simpson KJ, Bonventre JV, Park BK, Dear JW. Circulating kidney injury molecule-1 predicts

prognosis and poor outcome in patients with acetaminophen-induced liver injury. Hepatology 2015.

117. Streeter AJ, Dahlin DC, Nelson SD, Baillie TA. The covalent binding of acetaminophen to protein. Evidence for cysteine residues as major sites of arylation in vitro. Chem Biol Interact 1984;48:349-366.

118. Roberts DW, Bucci TJ, Benson RW, Warbritton AR, McRae TA, Pumford NR, Hinson JA. Immunohistochemical localization and quantification of the 3-(cystein-S-yl)-acetaminophen protein adduct in acetaminophen hepatotoxicity. Am J Pathol 1991;138:359-371.

119. Pumford NR, Hinson JA, Potter DW, Rowland KL, Benson RW, Roberts DW. Immunochemical quantitation of 3-(cystein-S-yl)acetaminophen adducts in serum and liver proteins of acetaminophen-treated mice. J Pharmacol Exp Ther 1989;248:190-196.

120. Muldrew KL, James LP, Coop L, McCullough SS, Hendrickson HP, Hinson JA, Mayeux PR. Determination of acetaminophen-protein adducts in mouse liver and serum and human serum after hepatotoxic doses of acetaminophen using high-performance liquid chromatography with electrochemical detection. Drug Metab Dispos 2002;30:446-451.

121. Davern TJ, 2nd, James LP, Hinson JA, Polson J, Larson AM, Fontana RJ, Lalani E, Munoz S, Shakil AO, Lee WM. Measurement of serum acetaminophen-protein adducts in patients with acute liver failure. Gastroenterology 2006;130:687-694.

122. James LP, Alonso EM, Hynan LS, Hinson JA, Davern TJ, Lee WM, Squires RH. Detection of acetaminophen protein adducts in children with acute liver failure of indeterminate cause. Pediatrics 2006;118:e676-681.

123. Alonso EM, James LP, Zhang S, Squires RH. Acetaminophen Adducts Detected in Serum of Pediatric Patients with Acute Liver Failure. J Pediatr Gastroenterol Nutr 2015.

124. James LP, Letzig L, Simpson PM, Capparelli E, Roberts DW, Hinson JA, Davern TJ, Lee WM. Pharmacokinetics of acetaminophen-protein adducts in adults with acetaminophen overdose and acute liver failure. Drug Metab Dispos 2009;37:1779-1784.

125. James LP, Capparelli EV, Simpson PM, Letzig L, Roberts D, Hinson JA, Kearns GL, Blumer JL, Sullivan JE. Acetaminophen-associated hepatic injury: evaluation of acetaminophen protein adducts in children and adolescents with acetaminophen overdose. Clin Pharmacol Ther 2008;84:684-690.

126. Prescott LF. Kinetics and metabolism of paracetamol and phenacetin. Br J Clin Pharmacol 1980;10 Suppl 2:291s-298s.

127. Roberts DW, Lee WM, Hinson JA, Bai S, Swearingen CJ, Stravitz RT, Reuben A, Letzig L, Simpson PM, Rule J, Fontana RJ, Ganger D, Reddy KR, Liou I, Fix O, James LP. An Immunoassay to Rapidly Measure Acetaminophen Protein Adducts Accurately Identifies Patients with Acute Liver Injury or Failure. Clin Gastroenterol Hepatol 2016.

128. McShane LM. Statistical challenges in the development and evaluation of marker-based clinical tests. BMC Med 2012;10:52.

129. Terblanche J, Hickman R. Animal models of fulminant hepatic failure. Dig Dis Sci 1991;36:770-774.

130. Maes M, Vinken M, Jaeschke H. Experimental models of hepatotoxicity related to acute liver failure. Toxicol Appl Pharmacol 2016;290:86-97.

131. Belanger M, Butterworth RF. Acute liver failure: a critical appraisal of available animal models. Metab Brain Dis 2005;20:409-423.

132. McGill MR, Williams CD, Xie Y, Ramachandran A, Jaeschke H. Acetaminophen-induced liver injury in rats and mice: comparison of protein adducts, mitochondrial dysfunction, and oxidative stress in the mechanism of toxicity. Toxicol Appl Pharmacol 2012;264:387-394.

133. Mitchell JR, Jollow DJ, Potter WZ, Gillette JR, Brodie BB. Acetaminophen-induced hepatic necrosis. IV. Protective role of glutathione. J Pharmacol Exp Ther 1973;187:211-217.

134. Prescott LF, Park J, Ballantyne A, Adriaenssens P, Proudfoot AT. Treatment of paracetamol (acetaminophen) poisoning with N-acetylcysteine. Lancet 1977;2:432-434.

135. Elferink MG, Olinga P, van Leeuwen EM, Bauerschmidt S, Polman J, Schoonen WG, Heisterkamp SH, Groothuis GM. Gene expression analysis of

precision-cut human liver slices indicates stable expression of ADME-Tox related genes. Toxicol Appl Pharmacol 2011;253:57-69.

136. Soldatow VY, Lecluyse EL, Griffith LG, Rusyn I. In vitro models for liver toxicity testing. Toxicol Res (Camb) 2013;2:23-39.

137. Guguen-Guillouzo C, Guillouzo A. General review on in vitro hepatocyte models and their applications. Methods Mol Biol 2010;640:1-40.

138. Guguen-Guillouzo C, Corlu A, Guillouzo A. Stem cell-derived hepatocytes and their use in toxicology. Toxicology 2010;270:3-9.

139. Aninat C, Piton A, Glaise D, Le Charpentier T, Langouet S, Morel F, Guguen-Guillouzo C, Guillouzo A. Expression of cytochromes P450, conjugating enzymes and nuclear receptors in human hepatoma HepaRG cells. Drug Metab Dispos 2006;34:75-83.

140. Hewitt NJ, Lechon MJ, Houston JB, Hallifax D, Brown HS, Maurel P, Kenna JG, Gustavsson L, Lohmann C, Skonberg C, Guillouzo A, Tuschl G, Li AP, LeCluyse E, Groothuis GM, Hengstler JG. Primary hepatocytes: current understanding of the regulation of metabolic enzymes and transporter proteins, and pharmaceutical practice for the use of hepatocytes in metabolism, enzyme induction, transporter, clearance, and hepatotoxicity studies. Drug Metab Rev 2007;39:159-234.

141. Beigel J, Fella K, Kramer PJ, Kroeger M, Hewitt P. Genomics and proteomics analysis of cultured primary rat hepatocytes. Toxicol In Vitro 2008;22:171-181.

142. Godoy P, Hengstler JG, Ilkavets I, Meyer C, Bachmann A, Muller A, Tuschl G, Mueller SO, Dooley S. Extracellular matrix modulates sensitivity of hepatocytes to fibroblastoid dedifferentiation and transforming growth factor beta-induced apoptosis. Hepatology 2009;49:2031-2043.

143. Tuschl G, Hrach J, Walter Y, Hewitt PG, Mueller SO. Serum-free collagen sandwich cultures of adult rat hepatocytes maintain liver-like properties long term: a valuable model for in vitro toxicity and drug-drug interaction studies. Chem Biol Interact 2009;181:124-137.

144. Kienhuis AS, Wortelboer HM, Maas WJ, van Herwijnen M, Kleinjans JC, van Delft JH, Stierum RH. A sandwich-cultured rat hepatocyte system with increased metabolic competence evaluated by gene expression profiling. Toxicol In Vitro 2007;21:892-901.

145. Grattagliano I, Bonfrate L, Diogo CV, Wang HH, Wang DQ, Portincasa P. Biochemical mechanisms in drug-induced liver injury: certainties and doubts. World J Gastroenterol 2009;15:4865-4876.
146. Rivera CA, Adegboyega P, van Rooijen N, Tagalicud A, Allman M, Wallace M. Toll-like receptor-4 signaling and Kupffer cells play pivotal roles in the pathogenesis of non-alcoholic steatohepatitis. J Hepatol 2007;47:571-579.
147. De Kanter R, De Jager MH, Draaisma AL, Jurva JU, Olinga P, Meijer DK, Groothuis GM. Drug-metabolizing activity of human and rat liver, lung, kidney and intestine slices. Xenobiotica 2002;32:349-362.
148. van Midwoud PM, Merema MT, Verpoorte E, Groothuis GM. A microfluidic approach for in vitro assessment of interorgan interactions in drug metabolism using intestinal and liver slices. Lab Chip 2010;10:2778-2786.
149. Vickers AE, Fisher R, Olinga P, Dial S. Repair pathways evident in human liver organ slices. Toxicol In Vitro 2011;25:1485-1492.
150. Lieschke GJ, Currie PD. Animal models of human disease: zebrafish swim into view. Nat Rev Genet 2007;8:353-367.
151. McGrath P, Li CQ. Zebrafish: a predictive model for assessing drug-induced toxicity. Drug Discov Today 2008;13:394-401.
152. Barros TP, Alderton WK, Reynolds HM, Roach AG, Berghmans S. Zebrafish: an emerging technology for in vivo pharmacological assessment to identify potential safety liabilities in early drug discovery. Br J Pharmacol 2008;154:1400-1413.
153. Lerche-Langrand C, Toutain HJ. Precision-cut liver slices: characteristics and use for in vitro pharmaco-toxicology. Toxicology 2000;153:221-253.
154. LeCluyse EL. Human hepatocyte culture systems for the in vitro evaluation of cytochrome P450 expression and regulation. Eur J Pharm Sci 2001;13:343-368.
155. Schoonen WG, Westerink WM, de Roos JA, Debiton E. Cytotoxic effects of 100 reference compounds on Hep G2 and HeLa cells and of 60 compounds on ECC-1 and CHO cells. I mechanistic assays on ROS, glutathione depletion and calcein uptake. Toxicol In Vitro 2005;19:505-516.
156. Boess F, Kamber M, Romer S, Gasser R, Muller D, Albertini S, Suter L. Gene expression in two hepatic cell lines, cultured primary hepatocytes, and liver slices

compared to the in vivo liver gene expression in rats: possible implications for toxicogenomics use of in vitro systems. Toxicol Sci 2003;73:386-402.

157. O'Brien PJ, Irwin W, Diaz D, Howard-Cofield E, Krejsa CM, Slaughter MR, Gao B, Kaludercic N, Angeline A, Bernardi P, Brain P, Hougham C. High concordance of drug-induced human hepatotoxicity with in vitro cytotoxicity measured in a novel cell-based model using high content screening. Arch Toxicol 2006;80:580-604.

158. Chen JN, Haffter P, Odenthal J, Vogelsang E, Brand M, van Eeden FJ, Furutani-Seiki M, Granato M, Hammerschmidt M, Heisenberg CP, Jiang YJ, Kane DA, Kelsh RN, Mullins MC, Nusslein-Volhard C. Mutations affecting the cardiovascular system and other internal organs in zebrafish. Development 1996;123:293-302.

159. Howe K, Clark MD, Torroja CF, Torrance J, Berthelot C, Muffato M, Collins JE, Humphray S, McLaren K, Matthews L, McLaren S, Sealy I, Caccamo M, Churcher C, Scott C, Barrett JC, Koch R, Rauch GJ, White S, Chow W, Kilian B, Quintais LT, Guerra-Assuncao JA, Zhou Y, Gu Y, Yen J, Vogel JH, Eyre T, Redmond S, Banerjee R, Chi J, Fu B, Langley E, Maguire SF, Laird GK, Lloyd D, Kenyon E, Donaldson S, Sehra H, Almeida-King J, Loveland J, Trevanion S, Jones M, Quail M, Willey D, Hunt A, Burton J, Sims S, McLay K, Plumb B, Davis J, Clee C, Oliver K, Clark R, Riddle C, Elliot D, Threadgold G, Harden G, Ware D, Mortimore B, Kerry G, Heath P, Phillimore B, Tracey A, Corby N, Dunn M, Johnson C, Wood J, Clark S, Pelan S, Griffiths G, Smith M, Glithero R, Howden P, Barker N, Stevens C, Harley J, Holt K, Panagiotidis G, Lovell J, Beasley H, Henderson C, Gordon D, Auger K, Wright D, Collins J, Raisen C, Dyer L, Leung K, Robertson L, Ambridge K, Leongamornlert D, McGuire S, Gilderthorp R, Griffiths C, Manthravadi D, Nichol S, Barker G, Whitehead S, Kay M, Brown J, Murnane C, Gray E, Humphries M, Sycamore N, Barker D, Saunders D, Wallis J, Babbage A, Hammond S, Mashreghi-Mohammadi M, Barr L, Martin S, Wray P, Ellington A, Matthews N, Ellwood M, Woodmansey R, Clark G, Cooper J, Tromans A, Grafham D, Skuce C, Pandian R, Andrews R, Harrison E, Kimberley A, Garnett J, Fosker N, Hall R, Garner P, Kelly D, Bird C, Palmer S, Gehring I, Berger A, Dooley CM, Ersan-Urun Z, Eser C, Geiger H, Geisler M, Karotki L, Kirn A, Konantz J, Konantz M, Oberlander M, Rudolph-Geiger S, Teucke M, Osoegawa K, Zhu B, Rapp A, Widaa S, Langford C, Yang F, Carter NP, Harrow J, Ning Z, Herrero J, Searle SM, Enright A, Geisler R, Plasterk RH, Lee C, Westerfield M, de Jong PJ, Zon LI, Postlethwait JH,

Nusslein-Volhard C, Hubbard TJ, Roest Crollius H, Rogers J, Stemple DL, Begum S, Lloyd C, Lanz C, Raddatz G, Schuster SC. The zebrafish reference genome sequence and its relationship to the human genome. Nature 2013;496:498-503.

160. Briggs JP. The zebrafish: a new model organism for integrative physiology. Am J Physiol Regul Integr Comp Physiol 2002;282:R3-9.

161. Santoriello C, Zon LI. Hooked! Modeling human disease in zebrafish. J Clin Invest 2012;122:2337-2343.

162. Seth A, Stemple DL, Barroso I. The emerging use of zebrafish to model metabolic disease. Dis Model Mech 2013;6:1080-1088.

163. Menke AL, Spitsbergen JM, Wolterbeek AP, Woutersen RA. Normal anatomy and histology of the adult zebrafish. Toxicol Pathol 2011;39:759-775.

164. Tao T, Peng J. Liver development in zebrafish (Danio rerio). J Genet Genomics 2009;36:325-334.

165. Isogai S, Horiguchi M, Weinstein BM. The vascular anatomy of the developing zebrafish: an atlas of embryonic and early larval development. Dev Biol 2001;230:278-301.

166. Zhao R, Duncan SA. Embryonic development of the liver. Hepatology 2005;41:956-967.

167. Lorent K, Yeo SY, Oda T, Chandrasekharappa S, Chitnis A, Matthews RP, Pack M. Inhibition of Jagged-mediated Notch signaling disrupts zebrafish biliary development and generates multi-organ defects compatible with an Alagille syndrome phenocopy. Development 2004;131:5753-5766.

168. Goldstone JV, McArthur AG, Kubota A, Zanette J, Parente T, Jonsson ME, Nelson DR, Stegeman JJ. Identification and developmental expression of the full complement of Cytochrome P450 genes in Zebrafish. BMC Genomics 2010;11:643.

169. Nebert DW, Dalton TP. The role of cytochrome P450 enzymes in endogenous signalling pathways and environmental carcinogenesis. Nat Rev Cancer 2006;6:947-960.

170. Williams RT. The metabolism of certain drugs and food chemicals in man. Ann N Y Acad Sci 1971;179:141-154.

171. Park BK, Boobis A, Clarke S, Goldring CE, Jones D, Kenna JG, Lambert C, Laverty HG, Naisbitt DJ, Nelson S, Nicoll-Griffith DA, Obach RS, Routledge P, Smith

DA, Tweedie DJ, Vermeulen N, Williams DP, Wilson ID, Baillie TA. Managing the challenge of chemically reactive metabolites in drug development. Nat Rev Drug Discov 2011;10:292-306.

172. Adams SS, Bough RG, Cliffe EE, Lessel B, Mills RF. Absorption, distribution and toxicity of ibuprofen. Toxicol Appl Pharmacol 1969;15:310-330.

173. Smith HS, Voss B. Pharmacokinetics of intravenous ibuprofen: implications of time of infusion in the treatment of pain and fever. Drugs 2012;72:327-337.

174. Kepp DR, Sidelmann UG, Tjornelund J, Hansen SH. Simultaneous quantitative determination of the major phase I and II metabolites of ibuprofen in biological fluids by high-performance liquid chromatography on dynamically modified silica. J Chromatogr B Biomed Sci Appl 1997;696:235-241.

175. Brown CM, Reisfeld B, Mayeno AN. Cytochromes P450: a structure-based summary of biotransformations using representative substrates. Drug Metab Rev 2008;40:1-100.

176. Jones HS, Trollope HT, Hutchinson TH, Panter GH, Chipman JK. Metabolism of ibuprofen in zebrafish larvae. Xenobiotica 2012;42:1069-1075.

177. Dahlin DC, Miwa GT, Lu AY, Nelson SD. N-acetyl-p-benzoquinone imine: a cytochrome P-450-mediated oxidation product of acetaminophen. Proc Natl Acad Sci U S A 1984;81:1327-1331.

178. Laine JE, Auriola S, Pasanen M, Juvonen RO. Acetaminophen bioactivation by human cytochrome P450 enzymes and animal microsomes. Xenobiotica 2009;39:11-21.

179. Jemnitz K, Veres Z, Monostory K, Kobori L, Vereczkey L. Interspecies differences in acetaminophen sensitivity of human, rat, and mouse primary hepatocytes. Toxicol In Vitro 2008;22:961-967.

180. Chng HT, Ho HK, Yap CW, Lam SH, Chan EC. An investigation of the bioactivation potential and metabolism profile of Zebrafish versus human. J Biomol Screen 2012;17:974-986.

181. Alderton W, Berghmans S, Butler P, Chassaing H, Fleming A, Golder Z, Richards F, Gardner I. Accumulation and metabolism of drugs and CYP probe substrates in zebrafish larvae. Xenobiotica 2010;40:547-557.

182. Reimers MJ, Flockton AR, Tanguay RL. Ethanol- and acetaldehyde-mediated developmental toxicity in zebrafish. Neurotoxicol Teratol 2004;26:769-781.
183. Meuldermans W, Van Peer A, Hendrickx J, Lauwers W, Swysen E, Bockx M, Woestenborghs R, Heykants J. Excretion and biotransformation of cisapride in dogs and humans after oral administration. Drug Metab Dispos 1988;16:403-409.
184. Eichelbaum M, Ende M, Remberg G, Schomerus M, Dengler HJ. The metabolism of DL-[14C]verapamil in man. Drug Metab Dispos 1979;7:145-148.
185. Mani S, Dou W, Redinbo MR. PXR antagonists and implication in drug metabolism. Drug Metab Rev 2013;45:60-72.
186. Li F, Lu J, Cheng J, Wang L, Matsubara T, Csanaky IL, Klaassen CD, Gonzalez FJ, Ma X. Human PXR modulates hepatotoxicity associated with rifampicin and isoniazid co-therapy. Nat Med 2013;19:418-420.
187. Bresolin T, de Freitas Rebelo M, Celso Dias Bainy A. Expression of PXR, CYP3A and MDR1 genes in liver of zebrafish. Comp Biochem Physiol C Toxicol Pharmacol 2005;140:403-407.
188. Moore LB, Maglich JM, McKee DD, Wisely B, Willson TM, Kliewer SA, Lambert MH, Moore JT. Pregnane X receptor (PXR), constitutive androstane receptor (CAR), and benzoate X receptor (BXR) define three pharmacologically distinct classes of nuclear receptors. Mol Endocrinol 2002;16:977-986.
189. Tseng HP, Hseu TH, Buhler DR, Wang WD, Hu CH. Constitutive and xenobiotics-induced expression of a novel CYP3A gene from zebrafish larva. Toxicol Appl Pharmacol 2005;205:247-258.
190. Xu C, Li CY, Kong AN. Induction of phase I, II and III drug metabolism/transport by xenobiotics. Arch Pharm Res 2005;28:249-268.
191. Rowlands JC, Gustafsson JA. Aryl hydrocarbon receptor-mediated signal transduction. Crit Rev Toxicol 1997;27:109-134.
192. Poellinger L, Gottlicher M, Gustafsson JA. The dioxin and peroxisome proliferator-activated receptors: nuclear receptors in search of endogenous ligands. Trends Pharmacol Sci 1992;13:241-245.
193. Tian Z, Chen Y, Gao B. Natural killer cells in liver disease. Hepatology 2013;57:1654-1662.

194. Jaeschke H, Williams CD, Ramachandran A, Bajt ML. Acetaminophen hepatotoxicity and repair: the role of sterile inflammation and innate immunity. Liver Int 2012;32:8-20.

195. Ju C, Reilly T. Role of immune reactions in drug-induced liver injury (DILI). Drug Metab Rev 2012;44:107-115.

196. Wilke RA, Lin DW, Roden DM, Watkins PB, Flockhart D, Zineh I, Giacomini KM, Krauss RM. Identifying genetic risk factors for serious adverse drug reactions: current progress and challenges. Nat Rev Drug Discov 2007;6:904-916.

197. Uetrecht J. Idiosyncratic drug reactions: current understanding. Annu Rev Pharmacol Toxicol 2007;47:513-539.

198. Daly AK, Donaldson PT, Bhatnagar P, Shen Y, Pe'er I, Floratos A, Daly MJ, Goldstein DB, John S, Nelson MR, Graham J, Park BK, Dillon JF, Bernal W, Cordell HJ, Pirmohamed M, Aithal GP, Day CP. HLA-B*5701 genotype is a major determinant of drug-induced liver injury due to flucloxacillin. Nat Genet 2009;41:816-819.

199. Donaldson PT, Daly AK, Henderson J, Graham J, Pirmohamed M, Bernal W, Day CP, Aithal GP. Human leucocyte antigen class II genotype in susceptibility and resistance to co-amoxiclav-induced liver injury. J Hepatol 2010;53:1049-1053.

200. Martin AM, Nolan D, Gaudieri S, Almeida CA, Nolan R, James I, Carvalho F, Phillips E, Christiansen FT, Purcell AW, McCluskey J, Mallal S. Predisposition to abacavir hypersensitivity conferred by HLA-B*5701 and a haplotypic Hsp70-Hom variant. Proc Natl Acad Sci U S A 2004;101:4180-4185.

201. Mallal S, Nolan D, Witt C, Masel G, Martin AM, Moore C, Sayer D, Castley A, Mamotte C, Maxwell D, James I, Christiansen FT. Association between presence of HLA-B*5701, HLA-DR7, and HLA-DQ3 and hypersensitivity to HIV-1 reverse-transcriptase inhibitor abacavir. Lancet 2002;359:727-732.

202. Berman J, Hsu K, Look AT. Zebrafish as a model organism for blood diseases. Br J Haematol 2003;123:568-576.

203. Bajoghli B. Evolution and function of chemokine receptors in the immune system of lower vertebrates. Eur J Immunol 2013;43:1686-1692.

204. Jones M, Ball JS, Dodd A, Hill AJ. Comparison between zebrafish and Hep G2 assays for the predictive identification of hepatotoxins. Toxicology 2009;262:13-14.

205. Hill A, Mesens N, Steemans M, Xu JJ, Aleo MD. Comparisons between in vitro whole cell imaging and in vivo zebrafish-based approaches for identifying potential human hepatotoxicants earlier in pharmaceutical development. Drug Metab Rev 2012;44:127-140.

206. He JH, Guo SY, Zhu F, Zhu JJ, Chen YX, Huang CJ, Gao JM, Dong QX, Xuan YX, Li CQ. A zebrafish phenotypic assay for assessing drug-induced hepatotoxicity. J Pharmacol Toxicol Methods 2013;67:25-32.

207. Zhang X, Li C, Gong Z. Development of a Convenient In Vivo Hepatotoxin Assay Using a Transgenic Zebrafish Line with Liver-Specific DsRed Expression. PLoS One 2014;9:e91874.

208. Nadanaciva S, Aleo MD, Strock CJ, Stedman DB, Wang H, Will Y. Toxicity assessments of nonsteroidal anti-inflammatory drugs in isolated mitochondria, rat hepatocytes, and zebrafish show good concordance across chemical classes. Toxicol Appl Pharmacol 2013;272:272-280.

209. North TE, Babu IR, Vedder LM, Lord AM, Wishnok JS, Tannenbaum SR, Zon LI, Goessling W. PGE2-regulated wnt signaling and N-acetylcysteine are synergistically hepatoprotective in zebrafish acetaminophen injury. Proc Natl Acad Sci U S A 2010;107:17315-17320.

210. Braunbeck T, Gorge G, Storch V, Nagel R. Hepatic steatosis in zebra fish (Brachydanio rerio) induced by long-term exposure to gamma-hexachlorocyclohexane. Ecotoxicol Environ Saf 1990;19:355-374.

211. Amali AA, Rekha RD, Lin CJ, Wang WL, Gong HY, Her GM, Wu JL. Thioacetamide induced liver damage in zebrafish embryo as a disease model for steatohepatitis. J Biomed Sci 2006;13:225-232.

212. Passeri MJ, Cinaroglu A, Gao C, Sadler KC. Hepatic steatosis in response to acute alcohol exposure in zebrafish requires sterol regulatory element binding protein activation. Hepatology 2009;49:443-452.

213. Murtha JM, Qi W, Keller ET. Hematologic and serum biochemical values for zebrafish (Danio rerio). Comp Med 2003;53:37-41.

214. Rumack BH, Bateman DN. Acetaminophen and acetylcysteine dose and duration: past, present and future. Clin Toxicol (Phila) 2012;50:91-98.

215. Cox AG, Saunders DC, Kelsey PB, Jr., Conway AA, Tesmenitsky Y, Marchini JF, Brown KK, Stamler JS, Colagiovanni DB, Rosenthal GJ, Croce KJ, North TE, Goessling W. S-nitrosothiol signaling regulates liver development and improves outcome following toxic liver injury. Cell Rep 2014;6:56-69.

216. Burns CG, Milan DJ, Grande EJ, Rottbauer W, MacRae CA, Fishman MC. High-throughput assay for small molecules that modulate zebrafish embryonic heart rate. Nat Chem Biol 2005;1:263-264.

217. Berghmans S, Butler P, Goldsmith P, Waldron G, Gardner I, Golder Z, Richards FM, Kimber G, Roach A, Alderton W, Fleming A. Zebrafish based assays for the assessment of cardiac, visual and gut function--potential safety screens for early drug discovery. J Pharmacol Toxicol Methods 2008;58:59-68.

218. Langheinrich U. Zebrafish: a new model on the pharmaceutical catwalk. Bioessays 2003;25:904-912.

219. Doshna C, Benbow J, Depasquale M, Okerberg C, Turnquist S, Stedman D, Chapin R, Sivaraman L, Waldron G, Navetta K, Brady J, Banker M, Casimiro-Garcia A, Hill A, Jones M, Ball J, Aleo M. Multi-phase analysis of uptake and toxicity in Zebrafish: Relationship to compound physical-chemical properties. Toxicol Sci 2009;108.

220. Van den Bulck K, Hill A, Mesens N, Diekman H, De Schaepdrijver L, Lammens L. Zebrafish developmental toxicity assay: A fishy solution to reproductive toxicity screening, or just a red herring? Reprod Toxicol 2011;32:213-219.

221. Diekmann H, Hill A. ADMETox in zebrafish. Drug Discovery Today: Disease Models 2013;10:e31-e35.

222. Kantae V, Krekels EH, Ordas A, Gonzalez O, van Wijk RC, Harms AC, Racz PI, van der Graaf PH, Spaink HP, Hankemeier T. Pharmacokinetic Modeling of Paracetamol Uptake and Clearance in Zebrafish Larvae: Expanding the Allometric Scale in Vertebrates with Five Orders of Magnitude. Zebrafish 2016;13:504-510.

223. Babaei F, Ramalingam R, Tavendale A, Liang Y, Yan LS, Ajuh P, Cheng SH, Lam YW. Novel Blood Collection Method Allows Plasma Proteome Analysis from Single Zebrafish. J Proteome Res 2013.

224. Jagadeeswaran P, Sheehan JP, Craig FE, Troyer D. Identification and characterization of zebrafish thrombocytes. Br J Haematol 1999;107:731-738.

225. Eames SC, Philipson LH, Prince VE, Kinkel MD. Blood sugar measurement in zebrafish reveals dynamics of glucose homeostasis. Zebrafish 2010;7:205-213.
226. Pedroso GL, Hammes TO, Escobar TD, Fracasso LB, Forgiarini LF, da Silveira TR. Blood collection for biochemical analysis in adult zebrafish. J Vis Exp 2012:e3865.
227. Zang L, Shimada Y, Nishimura Y, Tanaka T, Nishimura N. A novel, reliable method for repeated blood collection from aquarium fish. Zebrafish 2013;10:425-432.
228. Ando H, Yanagihara H, Sugimoto K, Hayashi Y, Tsuruoka S, Takamura T, Kaneko S, Fujimura A. Daily rhythms of P-glycoprotein expression in mice. Chronobiol Int 2005;22:655-665.
229. Ward J, Kanchagar C, Veksler-Lublinsky I, Lee RC, McGill MR, Jaeschke H, Curry SC, Ambros VR. Circulating microRNA profiles in human patients with acetaminophen hepatotoxicity or ischemic hepatitis. Proc Natl Acad Sci U S A 2014;111:12169-12174.
230. Krauskopf J, Caiment F, Claessen SM, Johnson KJ, Warner RL, Schomaker SJ, Burt DA, Aubrecht J, Kleinjans JC. Application of high-throughput sequencing to circulating microRNAs reveals novel biomarkers for drug-induced liver injury. Toxicol Sci 2015;143:268-276.
231. Vliegenthart AD, Shaffer JM, Clarke JI, Peeters LE, Caporali A, Bateman DN, Wood DM, Dargan PI, Craig DG, Moore JK, Thompson AI, Henderson NC, Webb DJ, Sharkey J, Antoine DJ, Park BK, Bailey MA, Lader E, Simpson KJ, Dear JW. Comprehensive microRNA profiling in acetaminophen toxicity identifies novel circulating biomarkers for human liver and kidney injury. Sci Rep 2015;5:15501.
232. Waring WS, Stephen AF, Malkowska AM, Robinson OD. Acute ethanol coingestion confers a lower risk of hepatotoxicity after deliberate acetaminophen overdose. Acad Emerg Med 2008;15:54-58.
233. Teo AI, Cooper JG. The epidemiology and management of adult poisonings admitted to the short-stay ward of a large Scottish emergency department. Scott Med J 2013;58:149-153.

234. McCrae JC, Sharkey N, Webb DJ, Vliegenthart AD, Dear JW. Ethanol consumption produces a small increase in circulating miR-122 in healthy individuals. Clin Toxicol (Phila) 2016;54:53-55.

235. Neal CS, Michael MZ, Pimlott LK, Yong TY, Li JY, Gleadle JM. Circulating microRNA expression is reduced in chronic kidney disease. Nephrol Dial Transplant 2011;26:3794-3802.

236. Rivoli L, Vliegenthart AD, de Potter CM, van Bragt JJ, Tzoumas N, Gallacher P, Farrah TE, Dhaun N, Dear JW. The effect of renal dysfunction and haemodialysis on circulating liver specific miR-122. Br J Clin Pharmacol 2016.

237. Jones M, Nunez M. Liver toxicity of antiretroviral drugs. Semin Liver Dis 2012;32:167-176.

238. Vliegenthart AD, Berends C, Potter CM, Kersaudy-Kerhoas M, Dear JW. MicroRNA-122 can be measured in capillary blood which facilitates point-of-care testing for drug-induced liver injury. Br J Clin Pharmacol 2017.

239. Campuzano S, Pedrero M, Pingarron JM. Electrochemical genosensors for the detection of cancer-related miRNAs. Anal Bioanal Chem 2014;406:27-33.

240. Zhang J, Cui D. Nanoparticle-based Optical Detection of MicroRNA. Nano Biomedicine & Engineering 2013;5.

241. Ding X, Yan Y, Li S, Zhang Y, Cheng W, Cheng Q, Ding S. Surface plasmon resonance biosensor for highly sensitive detection of microRNA based on DNA super-sandwich assemblies and streptavidin signal amplification. Anal Chim Acta 2015;874:59-65.

242. Li X, Cheng W, Li D, Wu J, Ding X, Cheng Q, Ding S. A novel surface plasmon resonance biosensor for enzyme-free and highly sensitive detection of microRNA based on multi component nucleic acid enzyme (MNAzyme)-mediated catalyzed hairpin assembly. Biosens Bioelectron 2016;80:98-104.

243. Ishihara R, Hasegawa K, Hosokawa K, Maeda M. Multiplex MicroRNA Detection on a Power-free Microfluidic Chip with Laminar Flow-assisted Dendritic Amplification. Anal Sci 2015;31:573-576.

244. Arata H, Hosokawa K, Maeda M. Rapid sub-attomole microRNA detection on a portable microfluidic chip. Anal Sci 2014;30:129-135.

245. Critchley JA, Nimmo GR, Gregson CA, Woolhouse NM, Prescott LF. Inter-subject and ethnic differences in paracetamol metabolism. Br J Clin Pharmacol 1986;22:649-657.
246. Patel M, Tang BK, Kalow W. Variability of acetaminophen metabolism in Caucasians and Orientals. Pharmacogenetics 1992;2:38-45.
247. Bateman DN, Dear JW, Thanacoody HK, Thomas SH, Eddleston M, Sandilands EA, Coyle J, Cooper JG, Rodriguez A, Butcher I, Lewis SC, Vliegenthart AD, Veiraiah A, Webb DJ, Gray A. Reduction of adverse effects from intravenous acetylcysteine treatment for paracetamol poisoning: a randomised controlled trial. Lancet 2014;383:697-704.
248. Chen BJ. Triptolide, a novel immunosuppressive and anti-inflammatory agent purified from a Chinese herb Tripterygium wilfordii Hook F. Leuk Lymphoma 2001;42:253-265.
249. Liu Q. Triptolide and its expanding multiple pharmacological functions. Int Immunopharmacol 2011;11:377-383.
250. Li XJ, Jiang ZZ, Zhang LY. Triptolide: progress on research in pharmacodynamics and toxicology. J Ethnopharmacol 2014;155:67-79.
251. Vispe S, DeVries L, Creancier L, Besse J, Breand S, Hobson DJ, Svejstrup JQ, Annereau JP, Cussac D, Dumontet C, Guilbaud N, Barret JM, Bailly C. Triptolide is an inhibitor of RNA polymerase I and II-dependent transcription leading predominantly to down-regulation of short-lived mRNA. Mol Cancer Ther 2009;8:2780-2790.
252. Wittmann C, Reischl M, Shah AH, Kronfuss E, Mikut R, Liebel U, Grabher C. A Zebrafish Drug-Repurposing Screen Reveals sGC-Dependent and sGC-Independent Pro-Inflammatory Activities of Nitric Oxide. PLoS One 2015;10:e0137286.
253. Hinson JA, Bucci TJ, Irwin LK, Michael SL, Mayeux PR. Effect of inhibitors of nitric oxide synthase on acetaminophen-induced hepatotoxicity in mice. Nitric Oxide 2002;6:160-167.
254. Lott JA, Mitchell LC, Moeschberger ML, Sutherland DE. Estimation of reference ranges: how many subjects are needed? Clin Chem 1992;38:648-650.
255. Ezzelle J, Rodriguez-Chavez IR, Darden JM, Stirewalt M, Kunwar N, Hitchcock R, Walter T, D'Souza MP. Guidelines on good clinical laboratory practice: bridging

operations between research and clinical research laboratories. J Pharm Biomed Anal 2008;46:18-29.

256. Willeit P, Zampetaki A, Dudek K, Kaudewitz D, King A, Kirkby NS, Crosby-Nwaobi R, Prokopi M, Drozdov I, Langley SR, Sivaprasad S, Markus HS, Mitchell JA, Warner TD, Kiechl S, Mayr M. Circulating microRNAs as novel biomarkers for platelet activation. Circ Res 2013;112:595-600.

257. Schmidt LE, Dalhoff K. The effect of regular medication on the outcome of paracetamol poisoning. Aliment Pharmacol Ther 2002;16:1539-1545.

258. Schmidt LE, Dalhoff K. Concomitant overdosing of other drugs in patients with paracetamol poisoning. Br J Clin Pharmacol 2002;53:535-541.

259. Oosthuyzen W, Scullion KM, Ivy JR, Morrison EE, Hunter RW, Starkey Lewis PJ, O'Duibhir E, Street JM, Caporali A, Gregory CD, Forbes SJ, Webb DJ, Bailey MA, Dear JW. Vasopressin Regulates Extracellular Vesicle Uptake by Kidney Collecting Duct Cells. J Am Soc Nephrol 2016.

260. Cheng Y, Wang X, Yang J, Duan X, Yao Y, Shi X, Chen Z, Fan Z, Liu X, Qin S, Tang X, Zhang C. A translational study of urine miRNAs in acute myocardial infarction. J Mol Cell Cardiol 2012;53:668-676.

261. Tamplin OJ, Zon LI. Fishing at the cellular level. Nat Methods 2010;7:600-601.

262. Major RJ, Poss KD. Zebrafish Heart Regeneration as a Model for Cardiac Tissue Repair. Drug Discov Today Dis Models 2007;4:219-225.

263. Poss KD, Wilson LG, Keating MT. Heart regeneration in zebrafish. Science 2002;298:2188-2190.

264. Sadler KC, Krahn KN, Gaur NA, Ukomadu C. Liver growth in the embryo and during liver regeneration in zebrafish requires the cell cycle regulator, uhrf1. Proc Natl Acad Sci U S A 2007;104:1570-1575.

265. Curado S, Stainier DY, Anderson RM. Nitroreductase-mediated cell/tissue ablation in zebrafish: a spatially and temporally controlled ablation method with applications in developmental and regeneration studies. Nat Protoc 2008;3:948-954.

266. Forbes SJ, Newsome PN. Liver regeneration - mechanisms and models to clinical application. Nat Rev Gastroenterol Hepatol 2016;13:473-485.

APPENDICES

Appendix 1 (Paper 1)

Comprehensive microRNA profiling in acetaminophen toxicity identifies novel circulating biomarkers for human liver and kidney injury

A D B Vliegenthart, J M Shaffer, J I Clarke, L E J Peeters, A Caporali, D N Bateman, D M Wood,

P I Dargan, D G Craig, J K Moore, A I Thompson, N C Henderson, D J Webb, J Sharkey, D J Antoine, B K Park, M A Bailey, E Lader, K J Simpson, J W Dear

Supplementary Tables

Supplementary Table 1. Patient demographics and clinical chemistry results in the training and test set.

	Training set		**Test set**	
	APAP-TOX	**APAP-no TOX**	**APAP-TOX**	**APAP-no TOX**
Number	27	27	41	40
Sex (male:female)	10:17	11:16	13:28	15:25
Age years (IQR)	39 (26-54)	38 (25-55)	39 (31-49)	38 (29-49)
ALT IU/l (IQR)	2150 (487-4444)	16 (13-26)	3661 (2454-6306)	20 (12-25)
INR (IQR)	1.5 (1.3-2.1)	1.1 (1.0-1.2)	3.4 (2.3-6.2)	1.1 (1.0-1.1)
Creatinine μmol/L (IQR)	66 (58-170)	62 (55-80)	157 (66-230)	64 (56-69)
Creatinine >110 μmol/L (number)	8	0	22	0

ALT, alanine aminotransferase; INR, International Normalized Ratio. Data are presented as median values.

Supplementary Table 2. Patient demographics and clinical chemistry results in patients with acetaminophen induced liver injury with normal renal function (APAP-ALI no AKI) and with abnormal renal function (APAP-ALI with AKI)

	APAP-ALI no AKI	APAP-ALI with AKI
Number	38	30
Sex (male:female)	(14:24)	(14:16)
Age years (IQR)	40 (27-58)	41 (31-49)
ALT IU/l (IQR)	2307 (651-3455)	4083 (2920-7398)
INR (IQR)	1.9 (1.4-2.8)	3.4 (2.1-6.1)
Creatinine µmol/L (IQR)	61 (56-73)	209 (120-286)

ALT, alanine aminotransferase (ALT); INR, International Normalized Ratio. Data are presented as median values. *** $P < 0.0001$; ** $P < 0.001$ (Mann Whitney test).

Supplementary Table 3. Normfinder assessment of 50 most stable expressed microRNA, including stability value.

microRNA	Stability value
hsa-miR-1287	0.000012
hsa-miR-4289	0.000013
hsa-miR-1913	0.000015
hsa-miR-5194	0.000016
hsa-miR-671-3p	0.000017
hsa-miR-1260a	0.000018
hsa-miR-324-3p	0.000018
hsa-miR-423-5p	0.000018
hsa-miR-572	0.000019
hsa-miR-195-5p	0.000019
hsa-miR-718	0.000019
hsa-miR-23b-3p	0.000020
hsa-miR-505-3p	0.000020
hsa-miR-151a-5p	0.000020
hsa-miR-21-5p	0.000020
hsa-miR-874	0.000021
hsa-let-7b-5p	0.000021
hsa-miR-375	0.000021
hsa-miR-564	0.000021
hsa-miR-101-3p	0.000021
hsa-miR-766-3p	0.000021
hsa-miR-421	0.000022
hsa-miR-30e-5p	0.000022
hsa-miR-433	0.000022
hsa-miR-30d-5p	0.000022
hsa-miR-30a-5p	0.000022
hsa-miR-4291	0.000022
hsa-let-7d-3p	0.000022
hsa-miR-193b-3p	0.000023
hsa-miR-19a-3p	0.000023
hsa-let-7b-3p	0.000023
hsa-miR-4286	0.000023
hsa-miR-15b-3p	0.000024
hsa-miR-1307-3p	0.000024
hsa-miR-3663-3p	0.000027
hsa-miR-92a-3p	0.000028
hsa-miR-3689a-5p // hsa-miR-3689b-5p // hsa-miR-3689e	0.000033
hsa-miR-1260b	0.000038
hsa-miR-29a-3p	0.000042
hsa-miR-19b-3p	0.000042
hsa-miR-181b-5p	0.000047
hsa-let-7c	0.000049
hsa-miR-3187-3p	0.000050
hsa-miR-29b-1-5p	0.000055
hsa-miR-25-3p	0.000069
hsa-miR-4695-5p	0.000073
hsa-miR-484	0.000076
hsa-miR-486-5p	0.000116
hsa-miR-1238-3p	0.000166
hsa-miR-3183	0.000169

Supplementary Table 4. Patient demographics of the early acetaminophen overdose patient cohort.

Number	67
Sex (male:female)	34:33
Age years	39 (26-49)
Amount of acetaminophen ingested g	16 (12-30)
Time from ingestion to first blood sample hr	6 (4-16)
Admission acetaminophen concentration mg/L	101 (24-139)
Admission serum creatinine µmol/L	66 (56-77)
Admission billirubin µmol/L	6 (4-11)
Admission ALT activity IU/L	20 (14-34)
Admission ALP activity IU/L	72 (56-89)
Admission GGT activity IU/L	31 (20-73)
Admission INR	1.0 (1.0-1.1)
Number with admission ALT<ULN	58
Number with peak ALT > 3x ULN	13
Number with peak ALT > 1000 IU/L	5
Number with admission INR > 1.5	1
Number with peak INR > 1.5	6

ALT, alanine aminotransferase; ALP, alkaline phosphatase; GGT, gamma glutamyl transpeptidase; INR, International Normalized Ratio; ULN, upper limit of normal. Data are presented as median values with IQR.

Supplementary Table 5. miRNA biomarker profiles

miRNA species	Change with APAP	Reports non-APAP ALI	Reports APAP-ALI in mice	Change with kidney injury	Ago2 bound	More sensitive than ALT for early injury
miR-122-5p	Increase	Yes	Yes	No	Yes	Yes
miR-885-5p	Increase	Yes	No	No	Yes	No
miR-151a-3p	Increase	Yes	Yes	No	No	No
miR-382-5p	Decrease	Yes	Yes	No	Yes	No

Supplementary Figures

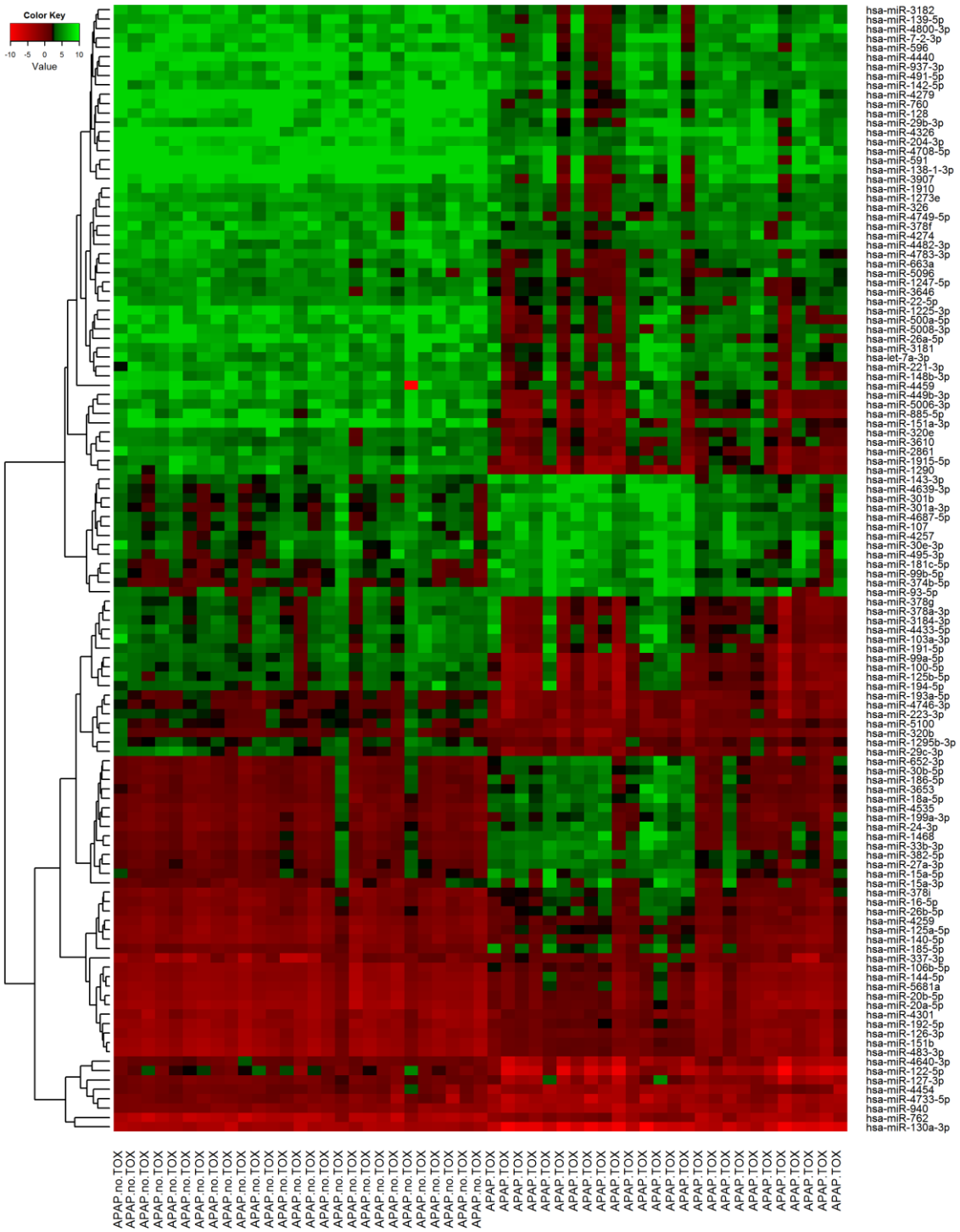

Supplementary Fig. 1. Heatmap displaying cluster analysis of >3-fold increased/decreased circulating miRNAs in acetaminophen no toxicity (APAP-no TOX) and acetaminophen toxicity (APAP-TOX) patients from the training set. Each row represents a miRNA, and each column represents a patient sample.

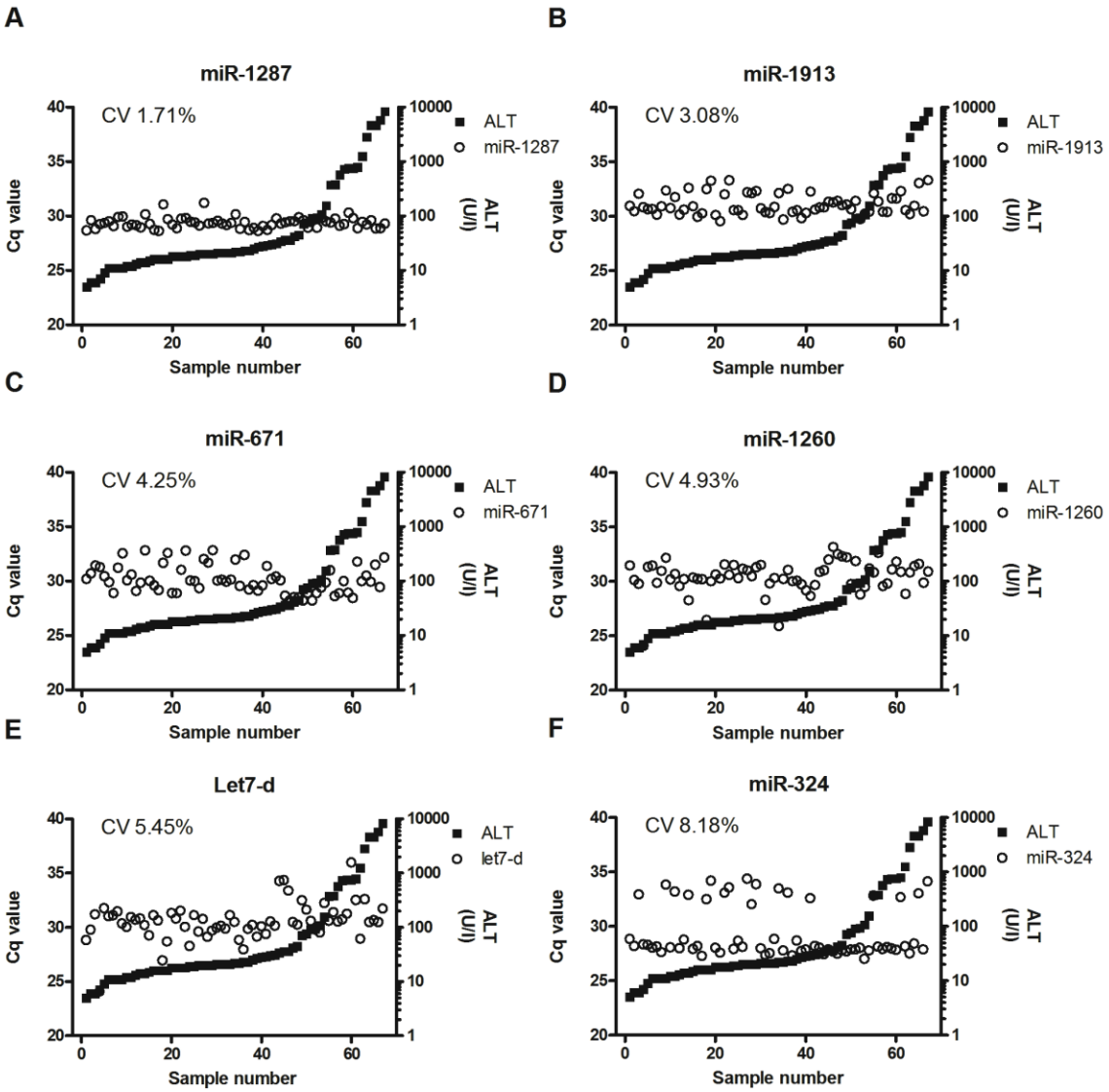

Supplemental Fig 2. Graphical representations of the Ct values of 6 endogenous normalizers and ALT. Samples are from the APAP-early cohort. The coefficient of variation (CV) is recorded on each graph.

Supplementary methods

MicroRNA profiling

miRNA PCR RNA isolation and Sample Quality Control

RNA was isolated from 200 µl plasma samples using the miRNeasy Serum/Plasma Kit (Qiagen, Venlo, Netherlands). RNA was eluted in a fixed volume of 14 µl and stored at -80^{0}C. Samples were evaluated for suitability by using the miScript PCR System (Qiagen, Venlo, Netherlands). Briefly, 1.5 µl of each eluate was reverse transcribed into cDNA using the miScript II RT Kit with miScript HiSpec Buffer. The reactions were incubated for 60 minutes at 37°C followed by a heat inactivation step for 5 minute at 95°C. One µl of each 10 µl cDNA synthesis was then diluted eleven-fold and assessed for a) the presence of common miRNA and for the absence of RT-PCR inhibitors using the miScript SYBR Green PCR Kit and the miScript miRNA QC PCR Array. Real-time PCR was performed on an ABI-7900HT (Applied Biosystems, Foster City, CA) using the recommended miScript cycling parameters.

Phase I: Determine Expressed miRNAs

A collection of 18 randomly chosen training set APAP no TOX samples and 18 randomly chosen training set APAP-TOX samples were combined into two control pools and two liver injury sample pools, respectively, with each pool containing RNA from 9 samples. cDNA synthesis and real-time PCR were performed using the miScript PCR System. Briefly, 7.5 µl of total RNA eluate from each of the four

pooled samples was reverse transcribed into cDNA using the miScript II RT Kit with miScript HiSpec Buffer. Each cDNA synthesis was diluted to a final volume of 550 µl using RNase-free water. For real-time PCR analysis of miRNA expression, diluted cDNA (1 µl per 4 wells) was analyzed using the miScript SYBR Green PCR Kit and the Human miRNome miScript miRNA PCR Array (miRBase V18, 1809 miScript Primer Assays). Real-time PCR was performed on an ABI-7900HT (Applied Biosystems, Foster City, CA) using the miScript cycling program. A miRNA was deemed to be expressed if its C_t value was less than 35 with a single, sharp melt peak in at least one of the four pools. A total of 356 miScript Primer Assays (or roughly 20% of the miRNome) were selected for Phase II screening.

Phase II: Determine Differentially Expressed miRNAs

cDNA synthesis, cDNA preamplification, and real-time PCR were performed as described earlier for each of the 54 samples. Each cDNA synthesis was diluted 5-fold and one-tenth was preamplified using the miScript Microfluidics PreAMP Kit in combination with a Custom miScript PreAMP Primer Mix containing the 356 miScript Primer Assays identified as 'expressed' in Phase I. Twelve cycles of preamplification was performed using the manufacturer recommended 384-plex preamplification protocol. Amplified cDNA was diluted to a final volume of 125 µl using RNase-free water and assessed in real-time PCR using the miScript Microfluidics PCR Kit and a Custom miScript miRNA PCR Array containing the 356 expressed assays from Phase I. Real-time PCR was performed on a Fluidigm BioMark HD (Fluidigm, San Francisco, US) using the miScript cycling program for the Fluidigm BioMark, which consists of an initial thermal mix stage (50°C for 2

minutes, 70°C for 30 minutes, and 25°C for 10 minutes) followed by a hot start at 95°C for 15 minutes and 40 cycles of 94°C for 15 seconds, 55°C for 30 seconds, and 70°C for 30 seconds. For data processing, C_t values were calibrated for RNA recovery using the cel-miR-39-3p assay (which detects a synthetic miRNA spiked in to each sample during sample prep), and any miRNA assay with a $C_t > 23$ was deemed to be not expressed. For data analysis, the $\Delta\Delta C_t$ method of relative quantification was used. The C_t values used for calculating the fold changes were normalized using the Global C_t mean. The miRNAs included in the C_t mean were expressed in all samples at a $C_t < 23$. The C_t values used for the random forest analysis were normalized using invariant miRNAs.

Random forest analysis of profiling test set data

Classifier training was performed using APAP-no TOX (27 samples) versus APAP-TOX (26 samples). The random forest classification method was used for two independent steps: (1) selection of the most predictive 16 miRNAs from the full set of experimentally selected 92 miRNAs and 1 snoRNA, and (2) training a final 16-miRNA classification model.

Step 1: selection of 16 miRNAs. To select 16 miRNAs from the 93 measured without feature selection bias, we drew 250 bootstrap subsamples of the full training set, without replacement. The subsamples were chosen to contain about 80% of the smaller TOX class and an equal number of no-TOX samples. This gave 20 APAP-noTOX versus 20 APAP-TOX. For each subsample, random forest classifier was trained, saved by the gene importance rank (by sorting according to the marginal

decrease in out-of-bag prediction accuracy when the gene's expression measurements are scrambled), saved by predictions on the left-out samples and then the random forest model was discarded. After all 250 iterations were complete, 93 genes were sorted by their median importance rank across all 250 bootstrap trainings, and the top 16 genes were selected. In addition to using the 250 bootstrap subsamples to obtain the 16 potentially most predictive genes, we also used the samples left out of training in each subsample to assess class separation magnitude and model error.

Step 2: final classifier training. Using the final 16 genes only, we trained a new random forest classifier using all training set samples, and saved this for use in class prediction on new samples. The performance of this final 16 gene classifier was tested using our independent test set samples. The classifier gives the probability that each sample is APAP-TOX. This classification was performed blind to the true sample grouping.

MicroRNA measurement by PCR

miRNA timecourse, miRNA in Ago2 fraction and miRNA in mice

RNA was isolated from 50 µl plasma samples using the miRNeasy Serum/Plasma Kit (Qiagen, Venlo, Netherlands). RNA was eluted in a fixed volume of 14 µl, after which 2 µl was reverse transcribed using the TaqMan MicroRNA Reverse Transcription Kit using stem-loop primers (Applied Biosystems, Foster City, CA) for each target miRNA species following the manufacturer's instructions. Then, 1.33 µL of cDNA was used in the PCR mixture using the specific PCR probes (Applied Biosystems, Foster City, CA). Levels of miRNAs were measured using the Light Cycler 480 (Roche, Basel, Switzerland).

miRNA measurement - APAP - early

RNA was isolated from 50 µl plasma samples using the miRNeasy Serum/Plasma Kit (Qiagen, Venlo, Netherlands). RNA was eluted in a fixed volume of 14 µl, after which 5 µl of each eluate was reverse transcribed into cDNA using the miScript II RT Kit (Qiagen, Venlo, Netherlands) following manufacturers instructions. The synthesized cDNA was ten-fold diluted and used for cDNA template in combination with the miScript SYBR Green PCR Kit (Qiagen, Venlo, Netherlands) using the specific miScript assays (Qiagen, Venlo, Netherlands). Real-time PCR was performed on a Light Cycler 480 (Roche, Basel, Switzerland) using the recommended miScript cycling parameters. Ct values greater than 35 were considered to be negative for that miRNA.

Appendix 2 (Paper 3)

Supplemental Figure 1.

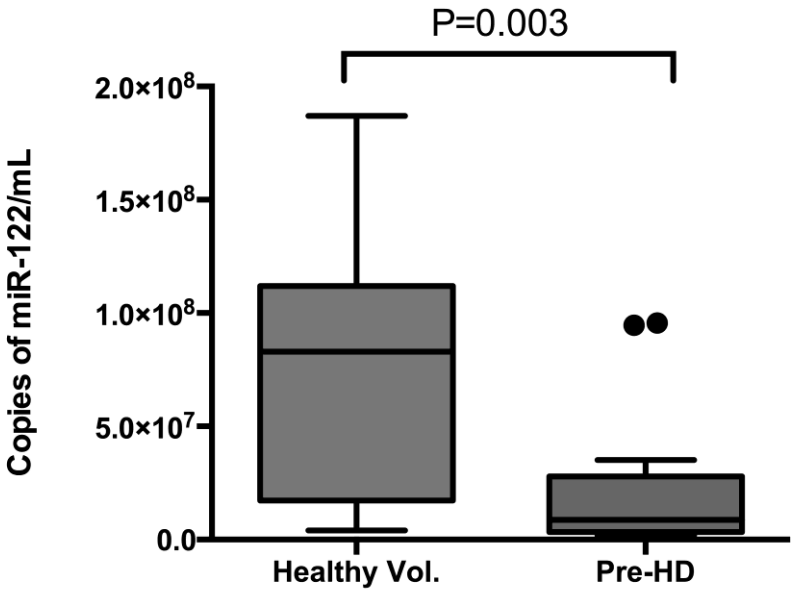

Appendix 3 (Paper 5)

Supplementary material legends

Supplementary Figure 1. Discovery cohort. (A) Correlation between plasma APAP concentration (APAP) measured by LC-MS/MS and measured in the clinical chemistry laboratory as part of routine clinical care. Correlation coefficient (95% confidence interval), R squared and P value are given. N=116 (B) In patients recruited to SNAP trial the time course of the mean plasma concentration of each APAP metabolite. Error bars represent standard deviation. N=116.

Supplementary Figure 2. APAP metabolite concentrations in patients with no acute liver injury (ALI) and ALI, in discovery (N=116) and validation cohorts (N=150). (A) APAP-CYS, (B) APAP-Mer, and (C) APAP-GSH represent the concentration of CYP mediated metabolites. (D) APAP-Glu and (E) APAP-Sul represent the concentrations of non CYP mediated metabolites. Boxes show median±IQR, whiskers represent range. Mann Whitney test was used to calculate statistical differences.

Supplementary Figure 3. Predictive accuracy of current and new biomarkers. Example ROC curves for the most sensitive and specific APAP metabolites in the discovery (A) and validation (B) cohorts. ROC curves for APAP parent drug are presented for the discovery (C) and validation (D) cohorts. (E) Correlation between the APAP-Cys/APAP-Sul metabolite ratio at hospital presentation in the discovery cohort and peak hospital stay serum alanine transaminase (ALT) activity (N=116). (F) At hospital presentation in the validation cohort.

Metabolites formed by CYP enzyme activity are expressed as a proportion of total circulating metabolites (CYP/total (%)) in liver injury (ALI) (N=19) and non-liver injury (No ALI) patients (N=131). Boxes show median±IQR, whiskers represent range.

Supplementary Table 1. Discovery cohort patient characteristics divided by SNAP treatment groups. †according to the British National Formulary 2009. *p=0.02 ondansetron vs. placebo. No patients were taking enzyme-inducing drugs. Statistical significance was tested by Mann Whitney test or Chi-square test.

	Placebo/ modified NAC	Ondansetron/ modified NAC	Placebo/ conventional NAC	Ondansetron/ conventional NAC
Number	34	30	25	27
Median (IQR) age (years)	38.5 (25.3-51.8)	31 (21-48)	36.5 (28.6-46)	29 (23.5-42.5)
Median (IQR) weight (kg)	69 (62-79.3)	64.5 (54-82)	71 (60.8-79.5)	68 (61.5-79.5)
Number of females	22 (65%)	16 (55%)	15 (58%)	20 (74%)
Median (IQR) time from ingestion to treatment	8.1 (7.3-10.1)	7.7 (6.8-12.2)	7.5 (6.3-8.8)	8 (6.7-10.1)
Number with ingestion to treatment <8hr	20 (59%)	17 (59%)	18 (69%)	18 (67%)
Median (IQR) ingested APAP (mg/kg)	234 (172-304)	167 (145-311)	238 (162-364)	239 (199-325)
Number who ingested APAP ≥16g	17 (50%)	10 (34%)	12 (46%)	14 (52%)
Alcohol ingested	14 (41%)	15 (52%)	15 (58%)	16 (59%)
Other drugs ingested	20 (59%)	17 (59%)	19 (73%)	20 (74%)
Opioids	3	3	7	4
Anti-histamines	1	1	1	0
Nutritional deficiency	7 (21%)	6 (21%)	2 (8%)	4 (15%)
Debilitating disease	1 (3%)	1 (3%)	0 (0%)	0 (0%)
Chronic alcohol use	12 (35%)	10 (34%)	13 (50%)	9 (33%)
Identified as high risk†	17 (50%)	16 (55%)	14 (54%)	12 (44%)
Median (IQR) admission alanine aminotransferase (U/L)	18.5 (13.3-24.3)	20 (13-36)	18 (13-28)	22 (17-28.5)
Number with acute liver injury (>50% ALT rise)	2 (6%)*	5 (17%)*	1 (4%)*	6 (22%)*

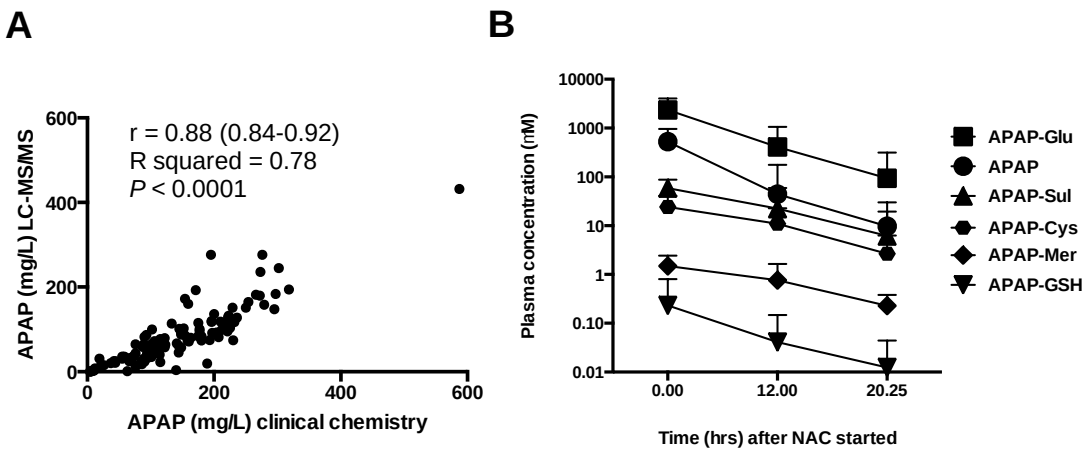

Supplementary figure 1.

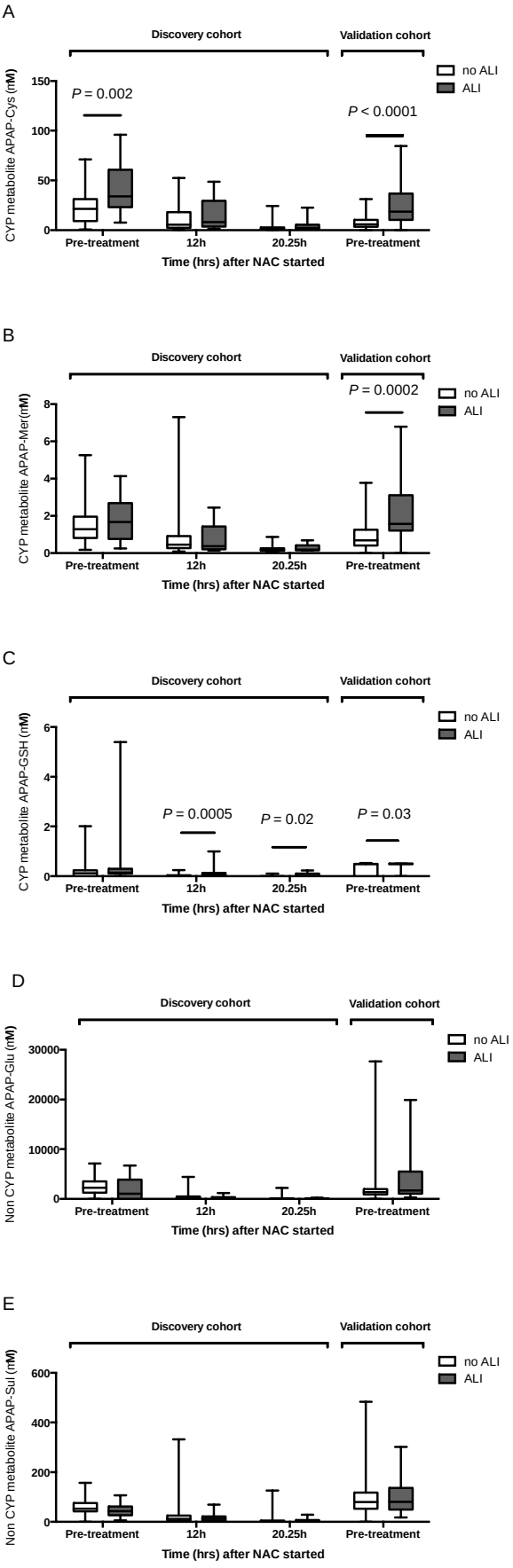

Supplementary figure 2.

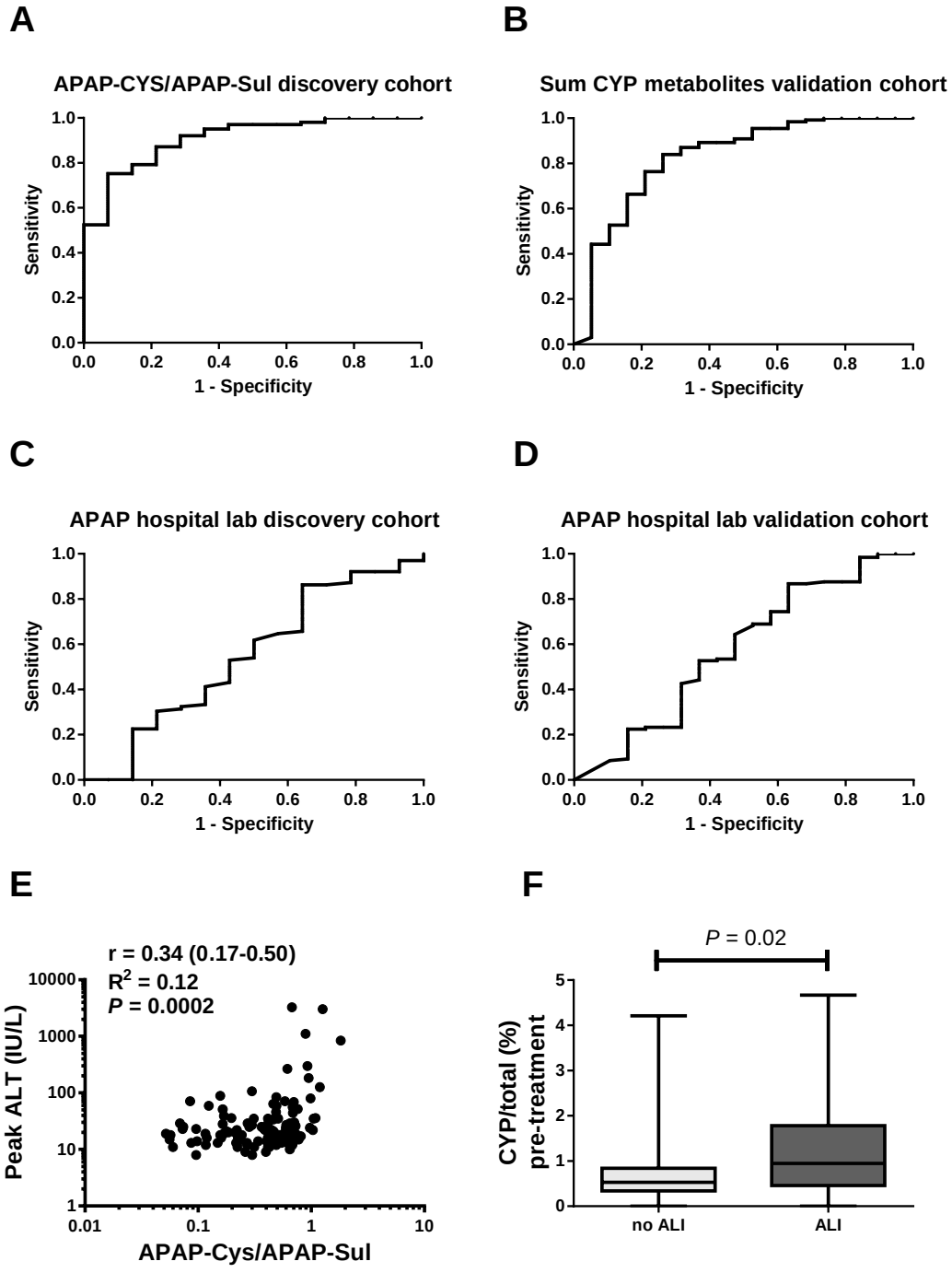

Supplementary figure 3.

Appendix 4 (Paper 7)

Characterization of triptolide-induced hepatotoxicity by imaging and transcriptomics in a novel zebrafish model

AD Bastiaan Vliegenthart, Chunmin Wei, Charlotte Buckley, Cécile Berends, Carmelita MJ de Potter, Sarah Schneemann, Jorge Del Pozo, Carl Tucker, John J Mullins, David J Webb, James W Dear

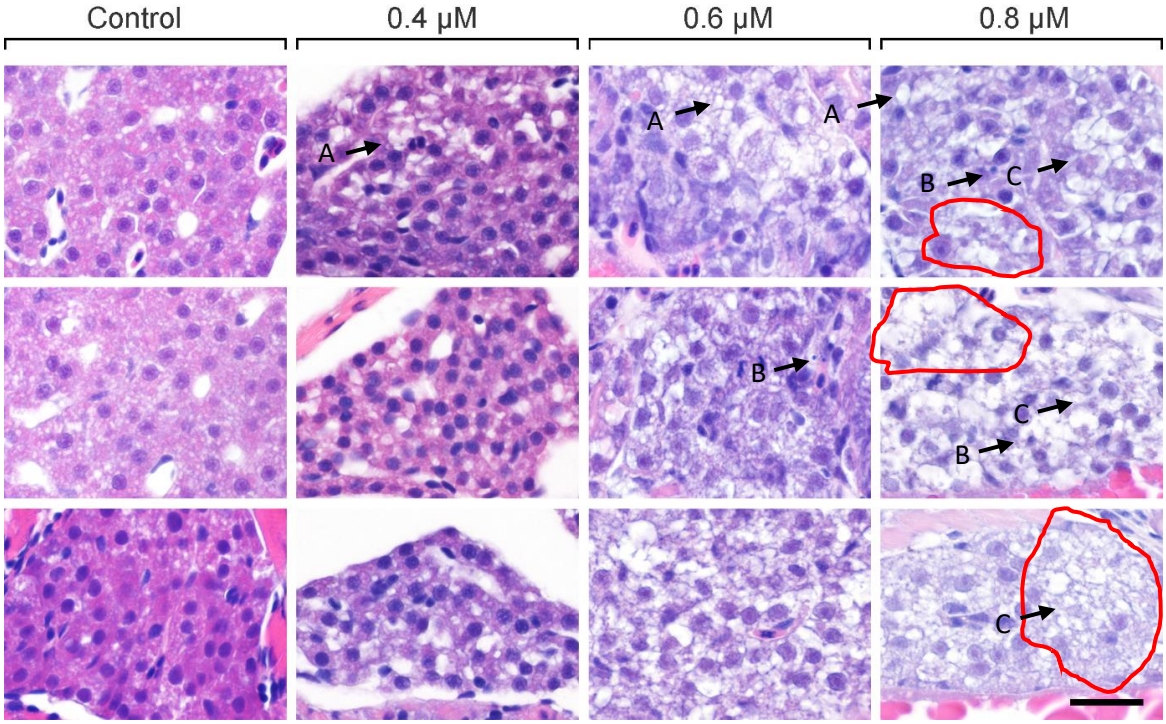

Supplementary Figure 1. Effect of triptolide on zebrafish larvae after 48 hours (3-5dpf) exposure. Magnified histological images at x400 of zebrafish larvae liver after water exposure to triptolide at the concentrations indicated. Three representative fish are presented for each dose. Note the presence of dose dependent increase in hepatocyte vacuolation (A), necrosis (with nuclei breaking down (B) and karyolysis (C)) and the presence of disarray (red lines). The latter two features are absent from the control group. Scale bar = 20µm.

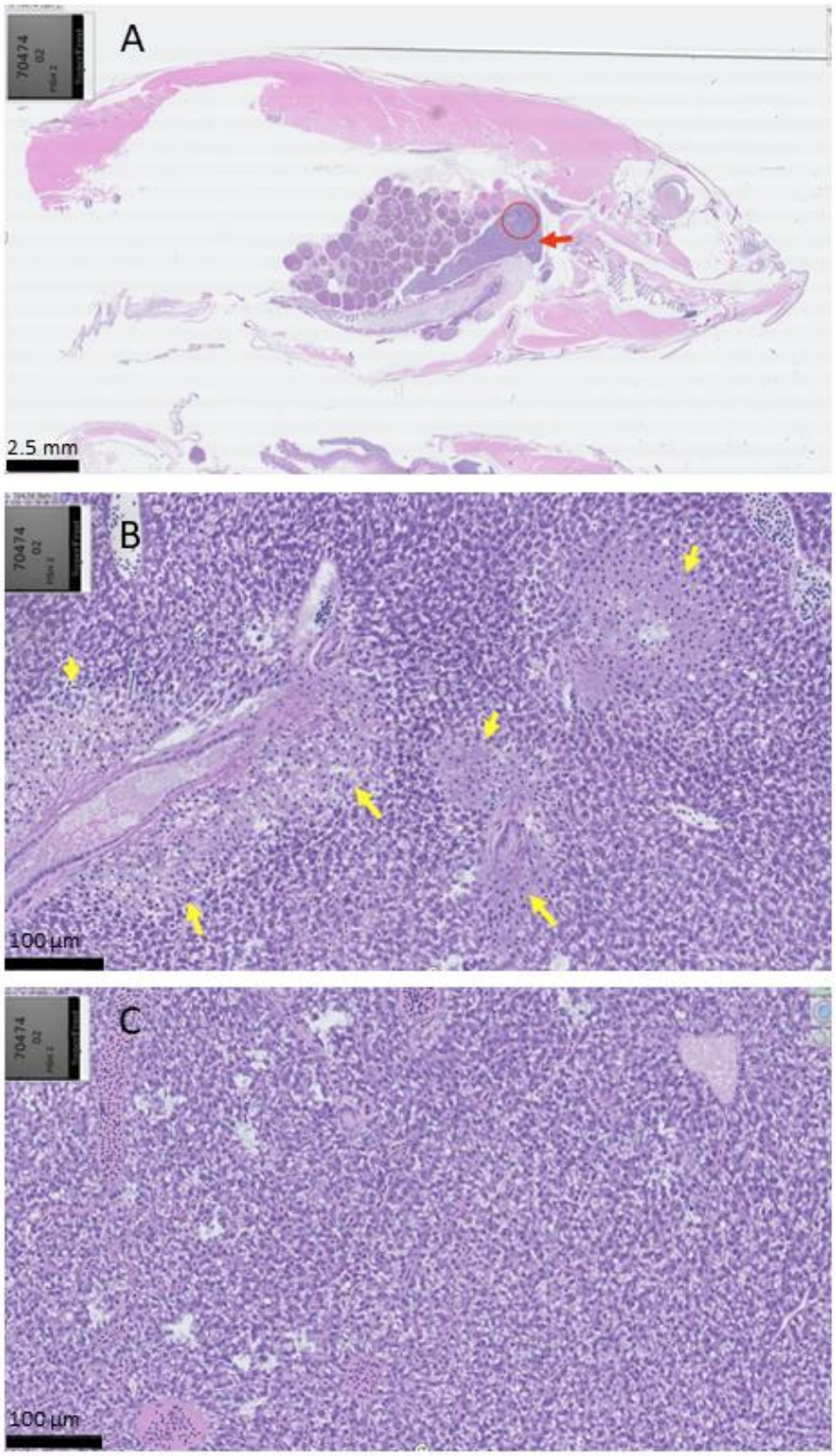

Supplementary figure 2. Histological images of adult zebrafish after exposure to triptolide (1.6 µM) during 10 hours. (A) Subgross view. Liver is indicated by the red arrow. The area whith hepatic necrosis is indicated by the circle. (B) Arrows denote lesions consistent with hepatic necrosis after triptolide exposure. (C) Control adult zebrafish after exposure to vehicle control. Normal liver, with no areas of necrosis.

Supplementary Table 1. Significantly enriched GO terms in response to triptolide in zebrafish larvae (with $P < 0.001$ cutoff).

	GO Term	Up/ Down	PValux10
Biological Process	translation	Up	4.35×10^{-51}
	cellular protein metabolic process	Up	2.31×10^{-13}
	protein metabolic process	Up	1.56×10^{-12}
	cellular biosynthetic process	Up	7.93×10^{-12}
	biosynthetic process	Up	8.50×10^{-12}
	macromolecule biosynthetic process	Up	4.12×10^{-10}
	cellular macromolecule biosynthetic process	Up	5.81×10^{-10}
	gene expression	Up	5.19×10^{-08}
	generation of precursor metabolites and energy	Up	5.81×10^{-07}
	immune response	Up	2.35×10^{-06}
	regulation of cell cycle	Up	2.41×10^{-06}
	translational elongation	Up	2.58×10^{-06}
	defense response	Up	9.92×10^{-06}
	primary metabolic process	Up	1.24×10^{-05}
	response to other organism	Up	1.83×10^{-05}
	multi-organism process	Up	2.69×10^{-05}
	immune system process	Up	5.92×10^{-05}
	cellular metabolic process	Up	9.07×10^{-05}
	response to biotic stimulus	Up	0.0001
	embryo development	Up	0.0002
	carbohydrate catabolic process	Up	0.0002
	hormone biosynthetic process	Up	0.0003
	energy derivation by oxidation of organic compounds	Up	0.0004
	metabolic process	Up	0.0005
	glycolysis	Up	0.0005
	glucose metabolic process	Up	0.0006
	cellular carbohydrate catabolic process	Up	0.0006
	alcohol catabolic process	Up	0.0006
	respiratory electron transport chain	Up	0.0006
	purine nucleotide biosynthetic process	Up	0.0006
	response to virus	Up	0.0009
	response to lipopolysaccharide	Up	0.0009
	nucleic acid metabolic process	Down	4.83×10^{-27}
	cellular nitrogen compound metabolic process	Down	2.61×10^{-23}

	nucleobase, nucleoside, nucleotide and nucleic acid metabolic process	Down	$3.95x10^{-23}$
	transcription	Down	$4.01x10^{-23}$
	regulation of transcription	Down	$2.65x10^{-22}$
	nitrogen compound metabolic process	Down	$4.84x10^{-22}$
	regulation of nucleobase, nucleoside, nucleotide and nucleic acid metabolic process	Down	$3.00x10^{-21}$
	regulation of gene expression	Down	$4.36x10^{-21}$
	regulation of nitrogen compound metabolic process	Down	$5.67x10^{-21}$
	regulation of macromolecule biosynthetic process	Down	$1.24x10^{-20}$
	regulation of biosynthetic process	Down	$1.35x10^{-20}$
	regulation of cellular biosynthetic process	Down	$1.80x10^{-20}$
	regulation of cellular metabolic process	Down	$1.18x10^{-19}$
	RNA metabolic process	Down	$5.84x10^{-19}$
	regulation of primary metabolic process	Down	$4.89x10^{-18}$
	regulation of macromolecule metabolic process	Down	$6.20x10^{-18}$
	gene expression	Down	$8.92x10^{-18}$
	regulation of metabolic process	Down	$1.99x10^{-17}$
	cellular macromolecule metabolic process	Down	$6.59x10^{-14}$
	regulation of RNA metabolic process	Down	$6.65x10^{-12}$
	regulation of transcription, DNA-dependent	Down	$8.54x10^{-12}$
	transcription, DNA-dependent	Down	$1.22x10^{-11}$
	nervous system development	Down	$1.52x10^{-11}$
	multicellular organismal development	Down	$1.82x10^{-11}$
	system development	Down	$2.66x10^{-11}$
	RNA biosynthetic process	Down	$2.68x10^{-11}$
	RNA processing	Down	$8.40x10^{-11}$
	multicellular organismal process	Down	$2.38x10^{-10}$
	developmental process	Down	$3.65x10^{-10}$
	macromolecule metabolic process	Down	$1.51x10^{-09}$
	regulation of cellular process	Down	$1.76x10^{-09}$
	anatomical structure development	Down	$2.51x10^{-09}$
	regulation of biological process	Down	$1.07x10^{-08}$
	cellular macromolecule biosynthetic process	Down	$2.01x10^{-08}$
	brain development	Down	$4.16x10^{-08}$
	organ development	Down	$4.46x10^{-08}$
	central nervous system development	Down	$5.35x10^{-08}$
	macromolecule biosynthetic process	Down	$5.73x10^{-08}$
	neurogenesis	Down	$2.13x10^{-07}$

	cellular metabolic process	Down	$5.09x10^{-07}$
	generation of neurons	Down	$7.20x10^{-07}$
	biological regulation	Down	$1.09x10^{-06}$
	skeletal system development	Down	$1.15x10^{-06}$
	forebrain development	Down	$1.23x10^{-06}$
	neuron differentiation	Down	$1.32x10^{-06}$
	cellular developmental process	Down	$2.33x10^{-06}$
	cartilage development	Down	$2.83x10^{-06}$
	embryo development ending in birth or egg hatching	Down	$3.57x10^{-06}$
	chordate embryonic development	Down	$3.57x10^{-06}$
	cellular biosynthetic process	Down	$8.45x10^{-06}$
	cell fate commitment	Down	$9.71x10^{-06}$
	cell differentiation	Down	$1.36x10^{-05}$
	biosynthetic process	Down	$2.24x10^{-05}$
	cellular process	Down	$2.74x10^{-05}$
	cell fate specification	Down	$2.84x10^{-05}$
	mRNA processing	Down	$3.09x10^{-05}$
	sensory organ development	Down	$3.52x10^{-05}$
	ncRNA processing	Down	$4.28x10^{-05}$
	cellular component organization	Down	$4.66x10^{-05}$
	skeletal system morphogenesis	Down	$5.29x10^{-05}$
	ribosome biogenesis	Down	$8.59x10^{-05}$
	primary metabolic process	Down	0.0001
	ribonucleoprotein complex biogenesis	Down	0.0001
	embryonic skeletal system development	Down	0.0001
	anatomical structure morphogenesis	Down	0.0001
	regulation of signaling pathway	Down	0.0001
	rRNA processing	Down	0.0002
	ncRNA metabolic process	Down	0.0002
	embryonic skeletal system morphogenesis	Down	0.0002
	camera-type eye development	Down	0.0002
	hindbrain development	Down	0.0003
	eye development	Down	0.0003
	mRNA metabolic process	Down	0.0003
	neuron development	Down	0.0003
	embryonic cranial skeleton morphogenesis	Down	0.0004
	cellular response to stimulus	Down	0.0004
	rRNA metabolic process	Down	0.0004
	RNA modification	Down	0.0005
	cellular membrane organization	Down	0.0005
	membrane organization	Down	0.0005

	embryonic organ morphogenesis	Down	0.0005
	generation of neurons in the forebrain	Down	0.0005
	forebrain neuron differentiation	Down	0.0005
	chromatin organization	Down	0.0006
	neural crest cell differentiation	Down	0.0006
	anterior/posterior pattern formation	Down	0.0007
	peroxisome organization	Down	0.0008
	cardioblast differentiation	Down	0.0008
	regionalization	Down	0.0008
	RNA splicing	Down	0.0009
	neural crest cell development	Down	0.0009
	pattern specification process	Down	0.0009
	chromosome organization	Down	0.0009
Molecular Function	structural constituent of ribosome	Up	$3.13x10^{-64}$
	structural molecule activity	Up	$2.09x10^{-41}$
	rRNA binding	Up	$6.47x10^{-08}$
	hydrogen ion transmembrane transporter activity	Up	$4.97x10^{-06}$
	actin binding	Up	$1.26x10^{-05}$
	monovalent inorganic cation transmembrane transporter activity	Up	$8.25x10^{-05}$
	inorganic cation transmembrane transporter activity	Up	0.0002
	cytoskeletal protein binding	Up	0.0002
	cytochrome-c oxidase activity	Up	0.0004
	heme-copper terminal oxidase activity	Up	0.0004
	oxidoreductase activity, acting on heme group of donors	Up	0.0004
	oxidoreductase activity, acting on heme group of donors, oxygen as acceptor	Up	0.0004
	cytokine receptor binding	Up	0.0004
	cation transmembrane transporter activity	Up	0.0004
	substrate-specific transmembrane transporter activity	Up	0.0007
	ion transmembrane transporter activity	Up	0.0009
	nucleic acid binding	Down	$7.69x10^{-22}$
	transcription regulator activity	Down	$1.36x10^{-16}$
	DNA binding	Down	$1.63x10^{-14}$
	sequence-specific DNA binding transcription factor activity	Down	$4.96x10^{-13}$
	sequence-specific DNA binding	Down	$1.28x10^{-09}$
	binding	Down	$1.71x10^{-08}$
	zinc ion binding	Down	$7.20x10^{-06}$
	ubiquitin thiolesterase activity	Down	0.0002
	transferase activity, transferring phosphorus-containing groups	Down	0.0005

	transition metal ion binding	Down	0.0006
Cellular Component	ribosome	Up	9.09×10^{-61}
	ribonucleoprotein complex	Up	3.48×10^{-46}
	non-membrane-bounded organelle	Up	7.41×10^{-33}
	intracellular non-membrane-bounded organelle	Up	7.41×10^{-33}
	macromolecular complex	Up	1.67×10^{-24}
	cytoplasmic part	Up	4.73×10^{-24}
	cytoplasm	Up	1.01×10^{-17}
	ribosomal subunit	Up	1.08×10^{-10}
	small ribosomal subunit	Up	4.86×10^{-08}
	intracellular part	Up	6.25×10^{-08}
	intracellular organelle	Up	3.82×10^{-07}
	organelle	Up	3.92×10^{-07}
	eukaryotic translation elongation factor 1 complex	Up	4.66×10^{-06}
	intracellular	Up	0.0002
	large ribosomal subunit	Up	0.0005
	myosin filament	Up	0.0008
	proton-transporting ATP synthase complex, catalytic core F(1)	Up	0.0009
	nucleus	Down	2.45×10^{-30}
	membrane-bounded organelle	Down	4.74×10^{-18}
	intracellular membrane-bounded organelle	Down	4.74×10^{-18}
	intracellular	Down	7.22×10^{-12}
	intracellular organelle	Down	8.23×10^{-12}
	organelle	Down	9.53×10^{-12}
	intracellular part	Down	4.24×10^{-09}